REPORT NO. FRA/ORD—79/10 PB

MECHANICAL IMPEDANCE EVALUATIONS OF THE KANSAS TEST TRACK: PRETRAFFIC AND POST TRAFFIC TESTS

NOVEMBER 1979
FINAL REPORT

Document is available to the public through the
National Technical Information Service,
Springfield, Virginia 22161.

Prepared for

U.S. DEPARTMENT OF TRANSPORTATION
FEDERAL RAILROAD ADMINISTRATION
Office of Research and Development
Washington, D.C. 20590

NOTICES

This document is disseminated under the sponsorship of the Department of Transportation in the interest of information exchange. The United States Government assumes no liability for its contents or use thereof.

The United States Government does not endorse products or manufacturers. Trade or manufacturers' names appear herein solely because they are considered essential to the object of this report.

Technical Report Documentation Page

1. Report No.	2. Government Accession No.	3. Recipient's Catalog No.
FRA/ORD-79/10		

4. Title and Subtitle

MECHANICAL IMPEDANCE EVALUATIONS OF THE KANSAS TEST TRACK: PRETRAFFIC AND POSTTRAFFIC TESTS

5. Report Date
November 1979

6. Performing Organization Code

8. Performing Organization Report No.

7. Author(s)
Stafford S. Cooper

9. Performing Organization Name and Address

U. S. Army Engineer Waterways Experiment Station
Geotechnical Laboratory
P. O. Box 631, Vicksburg, Miss. 39180

10. Work Unit No. (TRAIS)

11. Contract or Grant No.
DOT AR-30025

12. Sponsoring Agency Name and Address
U. S. Department of Transportation
Federal Railroad Administration
Office of Rail Safety Research
Washington, D. C. 20590

13. Type of Report and Period Covered
Final Report
6/1/73 - 6/1/75

14. Sponsoring Agency Code
RRD-32

15. Supplementary Notes

16. Abstract

The Kansas Test Track (KTT) was comprised of nine different track systems whose dynamic response was measured in two series of impedance tests. Pretraffic impedance testing was done in 1973, before the KTT was opened to traffic, and a second (posttraffic) test series was carried out in 1975 after the KTT had experienced premature failure in service.

Results of these tests, presented in the form of impedance and velocity transfer ratio plots, have been used to characterize the various KTT track systems according to their initial dynamic stiffness and component behavior. Known limitations of the test apparatus precluded a detailed analysis; however, a linear idealization was developed to grossly model track system response. These results illustrate the feasibility of an impedance approach to the structure-ballast-interaction processes which govern track system performance.

17. Key Words	18. Distribution Statement
Mechanical Impedance, Velocity Transfer Ratio, Linear Idealization, Performance Comparisons, Track Structure Response	Report is available through the National Technical Information Service, Springfield, Va. 22161

19. Security Classif. (of this report)	20. Security Classif. (of this page)	21. No. of Pages	22. Price
Unclassified	Unclassified	167	

Form DOT F 1700.7 (8-72) Reproduction of completed page authorized

SUMMARY

This report is primarily directed to the railroad research community, and documents the results of mechanical impedance tests performed by the U. S. Army Engineer Waterways Experiment Station (WES) on the Kansas Test Track (KTT). The KTT was build and operated under joint sponsorship of the Department of Transportation (DOT) Federal Railroad Administration (FRA) and the Atchison, Topeka and Sante Fe Railroad. Impedance testing consisted of a pretraffic test series in 1973, just before KTT was first opened to traffic, and a posttraffic test series performed in 1975, after KTT had experienced premature failure.

The original objectives for the study were as follows:

1. To demonstrate that mechanical impedance techniques could be used to determine the comparative pretraffic dynamic response of the nine track sections which comprised KTT.
2. To provide dynamic forces of known magnitude for pretraffic calibrations of KTT instrumentation installed by other investigators.
3. To periodically retest KTT track sections for purposes of performance evaluations, providing meaningful results were obtained in pretraffic testing.

With the consent of DOT, item 1 above was later eliminated as being impractical. Premature failure of KTT prompted further revisions to the original objectives. Because KTT failure was attributed to problems with the subgrade, as evidenced by severe pumping under traffic, the DOT wanted to conduct posttraffic tests under pumping conditions. The KTT operations were terminated in June 1975, and posttraffic tests could not be conducted before October 1975, so it was decided to try to recreate pumping conditions by watering each test location and subjecting it to repeated passes of a captive train. Impedance testing would then follow. Pumping was achieved only at the test locations in Track Sections 1, 2, and 3, despite the application of up to 16,000 gal of water and up to 600 train passes over the other test locations. Posttraffic testing was confined to Track Sections 1 through 5, 8,

and 9, in accordance with DOT requirements.

Time and funding constraints precluded the adaption of a state-of-the-art electrohydraulic actuator for this study; instead, an eccentric mass vibrator was used as an expedient means of exciting the track structures. Although this expediency complicated interpretation of the data, results of considerable significance were obtained. These results include:

1. A ranking of KTT track sections according to their initial dynamic stiffness, as measured under pretraffic and posttraffic test conditions.
2. Selection of a parallel three-element linear idealization which grossly models the observed dynamic response and which facilitates interpretation of the results.
3. Use of velocity transfer plots to rationalize track system component behavior.
4. Comparisons which indicate that impedance results are generally comparable to results obtained under live train loadings.

It was concluded that impedance methods provide a viable means of determining track system dynamic response and the structure-ballast-subgrade interaction processes which govern track performance. Future applications of the technique could be directed to (1) determining the dynamic stiffness of existing trackage, (2) developing a performance criteria for track stiffness, and (3) performing interaction studies, which could provide the basis for improved track design and/or remedial treatments of existing trackage.

PREFACE

This study was authorized by the Department of Transportation (DOT) Federal Railroad Administration (FRA) under Interagency Agreement AR 30025, dated 12 December 1972, and Amendment 1 thereto, dated 13 March 1973. The work was performed by personnel of the Geotechnical Laboratory (GL), U. S. Army Engineer Waterways Experiment Station (WES), P. O. Box 631, Vicksburg, Mississippi 39180. Dr. R. M. McCafferty of the Office of Rail Safety Research, FRA, monitored the project.

Pretraffic and posttraffic field investigations were carried out by Messrs. J. R. Curro and S. S. Cooper, respectively, of the Geodynamics Branch (GDB), Earthquake Engineering and Vibrations Division (EE&VD), GL. Mr. H. C. Greer III provided technical assistance in the data acquisition and reduction phases of the work. Mr. S. S. Cooper prepared this report under the supervision and with the assistance of Mr. R. F. Ballard, Chief, GDB, and Messrs. P. F. Hadala and F. G. McLean, Chief and former Chief, respectively, of the EE&VD. The work was performed under the general supervision of Mr. J. P. Sale, Chief, GL.

COL G. H. Hilt, CE, and COL J. L. Cannon, CE, were Directors of the WES during the conduct of this study. Mr. F. R. Brown was Technical Director.

METRIC CONVERSION FACTORS

Approximate Conversions to Metric Measures

Symbol	When You Know	Multiply by	To Find	Symbol
	LENGTH			
in	inches	*2.5	centimeters	cm
ft	feet	30	centimeters	cm
yd	yards	0.9	meters	m
mi	miles	1.6	kilometers	km
	AREA			
in^2	square inches	6.5	square centimeters	cm^2
ft^2	square feet	0.09	square meters	m^2
yd^2	square yards	0.8	square meters	m^2
mi^2	square miles	2.6	square kilometers	km^2
	acres	0.4	hectares	ha
	MASS (weight)			
oz	ounces	28	grams	g
lb	pounds	0.45	kilograms	kg
	short tons (2000 lb)	0.9	tonnes	t
	VOLUME			
tsp	teaspoons	5	milliliters	ml
Tbsp	tablespoons	15	milliliters	ml
fl oz	fluid ounces	30	milliliters	ml
c	cups	0.24	liters	l
pt	pints	0.47	liters	l
qt	quarts	0.95	liters	l
gal	gallons	3.8	liters	l
ft^3	cubic feet	0.03	cubic meters	m^3
yd^3	cubic yards	0.76	cubic meters	m^3
	TEMPERATURE (exact)			
°F	Fahrenheit temperature	5/9 (after subtracting 32)	Celsius temperature	°C

*1 in = 2.54 (exactly). For other exact conversions and more detailed tables, see NBS Misc. Publ. 286, Units of Weights and Measures, Price $2.25, SD Catalog No. C13.10:286.

Approximate Conversions from Metric Measures

Symbol	When You Know	Multiply by	To Find	Symbol
	LENGTH			
mm	millimeters	0.04	inches	in
cm	centimeters	0.4	inches	in
m	meters	3.3	feet	ft
m	meters	1.1	yards	yd
km	kilometers	0.6	miles	mi
	AREA			
cm^2	square centimeters	0.16	square inches	in^2
m^2	square meters	1.2	square yards	yd^2
km^2	square kilometers	0.4	square miles	mi^2
ha	hectares (10,000 m^2)	2.5	acres	
	MASS (weight)			
g	grams	0.035	ounces	oz
kg	kilograms	2.2	pounds	lb
t	tonnes (1000 kg)	1.1	short tons	
	VOLUME			
ml	milliliters	0.03	fluid ounces	fl oz
l	liters	2.1	pints	pt
l	liters	1.06	quarts	qt
l	liters	0.26	gallons	gal
m^3	cubic meters	35	cubic feet	ft^3
m^3	cubic meters	1.3	cubic yards	yd^3
	TEMPERATURE (exact)			
°C	Celsius temperature	9/5 (then add 32)	Fahrenheit temperature	°F

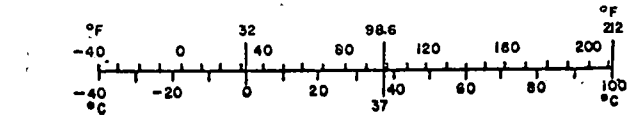

TABLE OF CONTENTS

LIST OF TABLES

LIST OF FIGURES

MECHANICAL IMPEDANCE EVALUATIONS OF THE KANSAS TEST TRACK: PRETRAFFIC AND POSTTRAFFIC TESTS

INTRODUCTION

Background

The Atchison, Topeka and Sante Fe Railroad (ATSF), in joint sponsorship with the Department of Transportation (DOT),[1,2,3] constructed approximately two miles* of test track adjacent to the existing ATSF main line near Aikman, Kansas. Figure 1 is a site location map. The Kansas Test Track (KTT) was offset approximately 30 ft from the ATSF mainline and was composed of nine different track support systems founded on a specially designed embankment.[4,5] The embankment was constructed under rigid controls in order to achieve the maximum possible degree of subgrade uniformity.[6] Prior to construction of the track systems, the U. S. Army Engineer Waterways Experiment Station (WES) had conducted a vibroseismic survey to determine in situ elastic properties of the constructed embankment.[7]

The embankment was built using mixed residual clays, and a 6-in.-thick, 3 percent lime stabilized surface layer was used to protect the embankment from softening over one winter season.[6] Additional protective measures consisted of a sprayed (thin) asphalt membrane and a 6-in.-thick covering of slag ballast.[6] The slag, in varying thicknesses, was also used for ballast of the track structures, which were installed later.

The nine test sections were grouped into two general categories, consisting of tie systems (including both concrete and wood) and non-conventional continuous reinforced concrete systems. Several variations of tie spacing and ballast depths, or treatments, were utilized for

---

* A table of factors for converting units of measurement is presented on page vi.

purposes of performance comparisons with the tie group. The reinforced concrete systems consisted of continuous twin beams and slabs. Two types of construction procedures were used for the twin beams. Track Sections 1, 2, and 3; Sections 2 and 8; Sections 4, 5, and 7; and Sections 6 and 9 were subgroupings on a comparative basis. Section 9 is a control section built approximately to Santa Fe standards for the region. The design variables for the nine sections are summarized in Table 1.

Scope and Authority

The scope of the present study encompasses both pretraffic and posttraffic mechanical impedance studies of the KTT track systems. Included herein are descriptions of the adaption of a counterrotating mass vibrator to mount on the track, performance of field tests, data reduction, and analysis of results.

Authority for this study was granted by the DOT Federal Railroad Administration (FRA) under Interagency Reimbursable Agreement AR 30025, dated 12 December 1972, and Amendment 1 thereto, dated 13 March 1973.

Objectives

The original objectives of the pretraffic investigation were to study responses of the track systems and components through the use of forced vibrations and velocity measurements (mechanical impedance methods) and to supply dynamic forces of known magnitude to provide some measure of calibration to instrumentation arrays, which have previously been installed in the track structures by other investigators. This latter objective was secondary and, because of low excitation levels and malfunctions of several instrumented ties within the arrays, was discarded early in the program. Plans had also been developed for periodic retesting of the various track sections in order to assess traffic-induced changes in performance during the service life of KTT. However, premature failure of KTT led to the suspension of rail traffic in June 1975 after about six months of operation. Both the scope and intent of the posttraffic testing were revised to conform with these

developments. One series of posttraffic impedance tests was conducted in October 1975 in conjunction with a postmortem investigation of KTT.

In these investigations, mechanical impedance methods were to be used to derive transfer ratios which describe the responses of the various components of the track support systems and to derive representative impedance measurements for each of the track systems tested. A description of the equipment, test procedures, and data reduction methods employed for the purpose are presented herein. Analyses and comparisons of response on a test section-to-test-section basis are developed in this report for both the pretraffic and posttraffic test conditions.

MECHANICAL IMPEDANCE TESTING

Electrical engineers have for some time been utilizing the relationship between an applied sinusoidal voltage and the resulting current for the analysis of linear circuits. Such analyses have been termed impedance methods and have subsequently been adapted to other fields through the use of analogies. The use of impedance methods for the study of mechanical systems has developed significantly in recent years as improvements in loading systems and instrumentation have prompted a broader application of the technique.

Mechanical impedance may be defined as a quantitative measure of structural response to a defined vibratory input force.[8] In the WES impedance test, a vibrator is used to excite a structure at a preselected location with a sinusoidal force, and structural response at the same or another point is measured with velocity transducers. While vibration can be described in terms of either acceleration or displacement, velocity measurements are usually preferred since dynamic stresses are believed to be more closely related to particle velocity.[8,9]

The sinusoidal force acting on a single degree of freedom system can be represented as a counterclockwise rotating phasor on the complex plane as shown in Figure 2(a). The complex representation of the force F is thus

$$F = F_o \cos \omega t + j F_o \sin \omega t \qquad (1)$$

The force F can also be expressed in terms of magnitude and phase angle as

$$F = F_o e^{j\omega t} \qquad (2)$$

where

F_o = phase force magnitude (or vector length)

$e = 2.718$ = base of Naperian logarithms from the identity $e^{jz} = \cos z + j \sin z$

$j = \sqrt{-1}$

ω = angular velocity in radians/sec

t = time

Similarly, when the force F is taken as the phase reference, the velocity V is described by the complex notation

$$V = V_o e^{j\phi} \tag{3}$$

In this notation ϕ is the phase angle between force and particle velocity and equals the impedance angel θ. If the particle velocity V is measured at the point of application of the driving force F, then the ratio of force to velocity is mechanical driving-point impedance Z from

$$Z = \frac{F_0}{V_0} \tag{4}$$

where

F_0 = applied force

V_0 = resultant particle velocity in the direction of the force at the point of force application

The ratio of the driving force to the resulting velocity at other points in the system may also be expresses as a mechanical transfer impedance Z_{0-2} in the equation

$$Z_{0-2} = \frac{F_0}{V_2} \tag{5}$$

where

F_0 = force applied at Point "0"

V_2 = resultant particle velocity at another point in the system (in this example, Point 2)

Similarly, velocity transfer functions may conveniently be used to determine component behavior. In this method, the absolute magnitude

of peak particle velocities are measured at any two points of interest in the system. If these two points are designated as Point 1 and Point 2, where Point 2 is further from the excitation source, then the velocity transfer R_{1-2} between the two points is simply

$$R_{1-2} = \frac{V_2}{V_1} \tag{6}$$

where

V_2 = absolute magnitude of particle velocity at Point 2

V_1 = absolute magnitude of particle velocity at Point 1

If impedance (Equation 4) and transfer ratios (Equations 5 and 6) are plotted versus frequency, then the resulting curves may be used as indices of attenuation, resonance, etc.

Thus, the most direct approach to determining dynamic response is to drive a system at a given frequency with a known sinusoidal force and measure the resulting vibration velocity at points of interest. This procedure is repeated over a range of frequencies until the response of the system has been adequately defined in terms of Z, Z_{i-j}, and/or R_{i-j} versus frequency. The impedance value Z obtained in this way is the absolute magnitude of impedance, given by the equation

$$|Z| = Z\, e^{j\theta} = R(Z) + j\, I(Z) \tag{7}$$

where

$|Z|$ = the absolute value of impedance

$R(Z)$ = real part of impedance

$I(Z)$ = imaginary part of impedance

θ = impedance angle

A diagrammatic representation of impedance in the complex plane is shown in Figure 2(b). The real part of impedance can be thought of as relating the applied force to the component of velocity that is in phase with it and the imaginary component of impedance as relating the force

to the component of velocity that is in quadrature with it. The impedance angel θ, which is equal to the angle ϕ depicted in Figure 2(a), is the phase angle between the force and velocity, using force as a reference.

An impedance analysis of this type can be performed on each part of a physical system; however, the method is adaptable to systems which are so complex that a detailed analysis is neither practical nor desirable. In many instances, measurements at a few points of interest will suffice, and the physical properties of a linear system can conveniently be described in terms of idealized elements having lumped constants. Idealized inertial, elastic, and damping elements are conventionally represented as masses, springs, and dashpots, which are usually identified with the symbols m, k, and c, respectively. These elements may be used in various combinations to represent the physical characteristics of the system and/or subsystems of interest. A more detailed discussion of the properties of each element and their impedance characteristics is beyond the scope of this report but is available from the literature.[8,9]

In the case of tests involving a rocking mode, by analogy, the impedance Z_r can be defined as

$$Z_r = \frac{M_o}{\alpha'} \tag{8}$$

where

$\alpha' = \frac{2V_1}{D}$ = angular frequency, rad/sec

V_1 = peak particle velocity at north railhead, in./sec

D = distance between rails, C-C, in.

$M_o = DF$ = applied moment, in.-lb

F = force applied to either rail, lb

Then,

$$Z_r = \frac{D^2F}{2V_1} = 1740\,\frac{F_o}{V_1} \text{ in.-lb-sec/rad} \tag{9}$$

Thus rocking impedance Z_r is proportional to F_0/V_1 when both F_0 and V_1 are measured in the rocking mode test. For convenience, the rocking mode impedance data in this report will be plotted in terms of F_0/V_1.

The practical value of an impedance study is that the data serves not only to define the system response but also to evaluate the effects of system variations, whether these be controlled or uncontrolled. For example, a controlled variation might consist of adding mass to the system; and uncontrolled variation might result from system degradation due to wear, weathering, or other causes. The change in system response resulting from such variations can be determined or predicted from impedance analyses.

FIELD INVESTIGATIONS

General

Field work for the pretraffic investigation was completed in the period 13-25 April 1973. The WES field party engaged in this work consisted of a project engineer, an instrumentation technician, and a civil engineering technician. Immediately after the departure of the WES field crew, KTT was opened to traffic.

Posttraffic impedance testing was conducted from 27 October to 8 November 1975 by a similar WES field party. The test track had been closed to traffic since June 1975, but DOT/FRA wanted WES to conduct the posttraffic tests under track conditions as close as possible to those existing at the time of failure. Of primary interest was the "pumping" condition which had been present in varying degrees of severity throughout the test track at the time traffic was suspended. Posttraffic test locations were selected both to facilitate comparisons with pretraffic results and to typify either "good" or "poor" performance in service. Performance judgments were based on visual inspections conducted during two reconnaissance trips and from Santa Fe maintenance records. In order to recreate the pumping problem, the selected test locations were repeatedly wetted and subjected to multiple passes by a captive train. Also, the posttraffic testing was reduced in scope because of scheduling and funding limitations as well as other considerations. For example, the ballast stabilization treatment used in Track Section 6 was believed to be a primary cause of this section's poor performance; hence the DOT/FRA decided not to test in Track Section 6. As a means to reduce costs, it was decided not to conduct posttraffic impedance tests on Track Section 7 because its physical properties and response in pretraffic testing were generally similar to that of Track Section 4, which was to be tested. A further time and cost saving measure was to reduce the number of data channels and omit the rocking mode tests conducted in the pretraffic testing. The pretraffic rocking mode and vertical mode test results were generally so similar there was a minimal

sacrifice of the data base available for comparisons, and the cost savings were substantial.

Vibratory Equipment

Impedance tests of KTT track systems were carried out using the hydraulically operated, counterrotating eccentric weight vibrator shown in Figures 3 and 4. The vibrator hydraulic system was driven by a gasoline-powered variable displacement pump. The variable displacement feature served to provide frequency control. This vibrator had been modified from its previous usage by adapting it to a 2-in.-thick steel base plate which spanned both rails of the test track. A clamping mechanism, consisting of the butt-block and wedge arrangement shown in Figure 5, was provided at each corner of the base plate so that the vibrator apparatus could be securely fastened to the railhead at four points. The total weight of the vibrator with base plate attached is 2865 lb, and the vibrator can produce dynamic forces of up to 4000 lb in the frequency range of 5 to about 50 Hz. The vibrator may be operated in either the vertical or rocking mode simply by changing positions of the eccentric weights, as shown in Figure 6. Four identical eccentric weights are actually used on the vibrator; however, the total effective eccentric weight is significant in terms of vibrator force output. So, eccentric weight, as used in this report, refers to the total effective eccentric weight. Force applied to the track section was measured with quartz load washers (Figure 5) which were located at the four corners of the base plate. Prior to testing, the cells were clamped (preloaded) between the base plate and railhead, as shown in Figure 5.

In preparation for field testing, a short section of wood crosstie track was installed at WES for preliminary calibration and shakedown testing of the WES vibrator. Procedures for attaching the vibrator to the rails and other operating techniques were developed at this time. The WES also intended to verify the vibrator's response characteristics by attaching it to an "infinite" mass and sweeping the frequency range

of interest. Unfortunately, this testing was not accomplished because of the time and money constraints previously mentioned.

Pretraffic Test Procedures

Vertical particle velocities at various points on the track support system and on the embankment were measured with the instrumentation array shown in Figure 7. The transducer locations shown in Figure 7 are all referenced to the center line of the vibrator, as shown in Figure 8. Note that the velocity transducers were all located on the north side of the track system; none of the transducers were located beneath the center of load application (Point "0") which is a point midway between the rails at the level of the top of the rails (i.e. a point in air). The transducer locations were selected to exemplify the vertical and longitudinal response of the track and embankment. With the vibrator and instrumentation array in place, vertical mode testing was begun by sweeping the frequency range from 1 to 50 Hz with 3.5 lb of eccentric weight on the vibrator. Next, the frequency range from 1 to 15 Hz was swept using 40 pounds of eccentric weight. The same pattern was followed for testing in the rocking mode (i.e. rocking normal to the track center line, about Point "0"). All of the data were recorded simultaneously on broad band analog magnetic tape. In vertical mode testing, the force output signals from all four load cells were monitored individually before being summed to give the total force (F_0) applied to the system. In rocking mode testing, the force output signals from the pair of cells on the north rail were summed separately.

The impedance test procedure outlined was dictated primarily by the frequency and force output limitations of the vibrator employed, i.e., at low frequency it was necessary to substitute larger weights in order to achieve the force output necessary to excite the track system. Also, the vibrator could not be driven to frequencies higher than about 50 Hz, because it had been decided to limit the force output of the vibrator to 4000 lb so as not to apply large negative (upward) accelerations to the track structures. These and other limitations of

the vibratory system used were recognized prior to embarking on the test program; however, initial time and funding constraints precluded further refinements and/or additions to the test apparatus.

Posttraffic Test Procedures

The same equipment and procedures used in pretraffic testing were, with a few notable exceptions, also used in posttraffic testing. A list of these exceptions is as follows:

1. The posttraffic test locations had been watered and repeatedly loaded by a captive train just prior to testing.
2. In addition to the 40- and 3.5-lb vibrator eccentric weights, 80- and 19-lb weights were also used.
3. No posttraffic rocking mode tests were made.
4. Velocity pickups 4, 7, and 9 (see Figure 7) were omitted from the typical instrumentation array, shown in Figure 8, in all test sections except Track Sections 4 and 5. In these two sections, pickups 4 and 7 were omitted.

The attempt to stimulate pumping was only partially successful since pumping was achieved only at the test locations in Track Sections 1, 2, and 3. In these sections, pumping occurred after about 8000 gal of water had been applied to each test location (an area of about 9 by 30 ft) and after approximately 150 passes of the captive train. The captive train consisted of an engine, two ballast cars, and a way car (caboose). Up to 16,000 gal of water and 600 train passes were applied to the test locations in Track Sections 4, 5, and 7. However, pumping was never achieved in Track Sections 4-9, although slight traces of muddy water were sometimes seen at the test location in Track Section 5.

In Track Sections 1 and 2, 80-lb eccentric mass weight was used to increase the vibrator's force output at low frequency. Since this only resulted in extending the low-frequency response by about 1-2 Hz, the use of the 80-lb weight was discontinued. The bulk of the post-traffic testing was done using 40-, 19-, and 3.5-lb eccentric mass

weights. The 19-lb weight was used primarily in hopes of securing a more continuous impedance curve to facilitate interpretation.

Data Acquisition

Pretraffic data acquisition was begun with testing in Track Section 9. Initially, it was desired to validate response of the built-in instrumentation arrays by means of the impedance vibrations. For this reason, testing in Track Sections 8 and 9 was conducted at the main instrumentation array location. Malfunctions of several instruments within these arrays (subsequent checks of the remaining arrays revealed similar problems) prevented data acquisition. Consequently, testing in the remaining track sections was conducted at a location approximately 100 ft east of the main instrumentation array so that "near vicinity" information could be obtained at a location undisturbed by the presence of subsurface instruments. In the course of pretraffic testing, data were acquired at the following locations:

	Pretraffic
Track Section	Station
1	8524+68
2	8534+67
3	8542+16
4	8551+36
5	8559+36
6	8566+80
7	8575+41
8	8587+33 (Main Inst Array)
9	8559+33 (Main Inst Array)

Beginning with Track Section 1, posttraffic impedance testing was conducted at the following locations:

Posttraffic		
Track Section	Designation of Test Location	Station
1	1	8524+75
2	2A	8531+62
	2B	8535+16
3	3A	8540+20
	3B	8542+49
4	4	8553+85
5	5	8558+25
6		Not tested
7		Not tested
8	8	8571+00
9	9	8595+33

DATA REDUCTION

General

The measurement parameters of interest for an impedance study are driving force, particle velocity, and frequency. Impedance curves derived from these data are typically presented in log-log scaled plots because this format facilitates interpretation of the results. Impedance results in this report are presented in this way.

Equipment

A block diagram of the WES data reduction system is shown in Figure 9. Of primary importance to this and similar systems is the excitation frequency since all other data channels are synchronized to it. Excitation frequency was measured with a sine potentiometer which was driven from the output shaft of the vibrator. Signal output from the sine pot was fed to a low-pass filter to achieve the best possible sinusoidal wave shape. The frequency signal was fed simultaneously to a master tracking filter and to a frequency log converter. Output from the log converter was a DC signal with magnitude proportional to the log of frequency. This signal was the frequency reference for the log-log plots described earlier. The frequency signal supplied to the master tracking filter also served to synchronized the other data channels through a filter tuning system and slave tracking filter.

Output from the velocity pickups was enhanced with amplifiers. The amplified velocity signals were fed to the master tracking filter, which converted the input to a DC signal with magnitude proportional to the log of velocity. This signal was fed to a WES-designed subtracter network (subtracting logarithms performs the division process) for further conditioning. The master tracking filter also provided velocity phase information to a phasemeter in the form of a modulated 100-kHz signal.

Force output signals from the four load cells were sent to charge amplifiers. Output from the amplifiers was fed to a WES-designed

summing network and was monitored simultaneously on a four-channel oscilloscope. During data acquisition, this network summed the load cell force output signals according to the excitation mode, i.e., vertical or rocking. The summed force signal was fed to the slave tracking filter for conversion to a DC signal with magnitude proportional to the log of force. The DC signal from the slave tracking filter was sent to a WES-designed subtracter network for the F/V division process. Force-phase information, in the form of a modulated 100-kHz signal, was also sent from the slave tracking filter to the phasemeter for comparison with similarly derived velocity phase information from the master tracking filter.

Final division of the force and velocity signals was performed in the WES-designed subtractor. Output from the subtracter was a DC signal proportional to the log of force divided by velocity. This signal provided the impedance information for plotting purposes.

Final conditioning of the phase information was performed with the phasemeter. Output from this meter was a DC signal proportional to the phase angle between force and velocity, using force as the reference.

The various DC signals described above were fed to an X-Y plotter. The final products were plots of mechanical impedance or phase angle versus frequency.

Velocity transfer ratios were also derived using the system described above. For the transfer ratio derivation, one amplified velocity signal was fed directly to the slave tracking filter instead of the force output signal from the force summary network. The other velocity signal, needed to derive the transfer ratio, was fed to the system in the normal way. In this configuration, the final output from the subtracter was a DC signal proportional to the $\log V_2/V_1$, or $\log V_5/V_2$, etc. This signal was applied to the ordinate scale of the X-Y plotter so that plots of velocity transfer ratio versus frequency were obtained.

Quick-look impedance (F_0/V_1) curves and oscillograph playbacks of the recorded signals were made in the field as a check on data quality. The bulk of the data was reduced after the recording and signal conditioning equipment had been returned to WES. In the course of the

data reduction procedures at WES, additional quality control checks were performed on each of the data channels recorded. Results of these tests, as well as other pertinent information, are presented in the analysis section of this report.

ANALYSIS OF RESULTS

General

In the following analyses, pretraffic and posttraffic results are first considered separately. Then, performance comparisons are made based on pretraffic and posttraffic test results from Track Sections 1-5, 8, and 9.

Since an eccentric mass vibrator was used in this study, some consideration must be given to its limitations for impedance applications. The WES has made extensive use of intermediate and high force output electrohydraulic shakers in other impedance work. Such systems have the capability of providing a selected constant force output throughout the frequency range of interest. This is a particularly important consideration when testing materials whose response is nonlinear and/or force level dependent. Unfortunately, time and money constraints precluded adapting a state-of-the-art electrohydraulic system for this investigation, so an eccentric mass vibrator was used as an expedient alternative.

The primary characteristic and chief limitation of the eccentric mass vibrator is that its force output, F , increases with frequency according to the formula

$$F = me\omega^2 \tag{10}$$

where

m = mass, lb-sec^2/in.

e = eccentricity (4.0 in., in this instance)

ω = angular velocity, rad/sec = $2\pi f$

f = frequency, Hz

Calculated force output versus frequency curves for the various eccentric weights used in this study are plotted to log-log scale in Figure 10. Measurements of actual force output versus frequency were made during testing, and these data are generally comparable to the

calculated values. From Figure 10, it is apparent that force output varies widely for different eccentric weights rotated at the same frequency. For example, at a frequency of 10 Hz the vibrator delivers about 1900-lb force with 40-lb eccentric weight but only 140-lb force with 3.5-lb eccentric weight. And, at low frequencies, force output diminishes rapidly with any of the available weights.

The effect of these limitations is to restrict the usable frequency range for each eccentric weight. Referring to Figure 10, a dashed line defines the approximate upper bound force limit established in the current study. The upper bound limit of 4000-lb force was arbitrarily selected so that negative accelerations of the track structure should not exceed 1 g, i.e. the vibrator weight (2855 lb) plus the minimum weight of track structure to which the vibrator would be fastened could safely be assumed to exceed 4000 lb. It was also necessary to define low-level force limits based on response characteristics of the structures and signal conditioning equipment. As it turned out, accurate force measurements could be made even at very low force levels. However, at these very low force levels the resulting particle velocities could not be accurately measured, i.e. velocity signals were so small as to be within the noise level of the signal conditioning equipment. Under these conditions erroneous impedance and transfer ratio results were derived. In the case of the impedance data, the F/V calculation resulted in anomalously high values of impedance at low force levels (where the apparent value of V trended to zero). Valid data were obtained when force levels exceeded a lower limit defined from data quality checks as follows:

1. Unfiltered oscillograph records had been obtained for each test run. These records were examined to determine the signal level recorded for each data channel as well as the relative response of all channels in the frequency domain from 0-50 Hz. The signals were also evaluated in terms of their signal-to-noise ratio, instrumentation system sensitivity, and sinusoidal response characteristics.
2. Comparisons of response were made for various vibrator force

levels and frequencies to determine approximate threshold excitation values.

3. Signal output from the tracking filters was examined on an oscilloscope to determine wave shape and phase characteristics.

Results of these checks indicated that valid data were obtained when force levels exceeded 500-1000 lb, depending on the track structure and eccentric weight used. Accordingly, lower bound frequency limits have been identified with a "tick" mark, where appropriate, on the curves in the data plots. The foregoing qualifications were necessary because a continuous impedance and/or transfer ratio curve could not be obtained with the eccentric mass vibrator, for reasons which have been discussed.

Pretraffic Tests

Pretraffic test data are presented in Figures 11-64. The data for each track section are presented in six figures, as follows:

Track Section	Figures
1	11-16
2	17-22
3	23-28
4	29-34
5	35-40
6	41-46
7	47-52
8	53-58
9	59-64

Each set of six figures includes a vertical mode impedance plot, rocking mode impedance (in terms of F_0/V_a) plot, and four plots of vertical mode transfer ratios for Points 1, 2, and 5; Points 5, 6, and 7; Points 1, 3, and 4; and Points 5, 8, and 9 in the typical instrumentation array shown in Figure 7.

The impedance curves serve to define the dynamic response of the various track structures measured at the railhead. Transfer ratio curves were used as a convenient means to assess the interaction between selected components of the track support system. Since the intent of this study was to demonstrate the feasibility of such an approach, a detailed analysis of component behavior will not be attempted. However, some general vertical mode response comparisons of track sections having similar physical characteristics will be made.

To this end, a characterization of the dynamic response of the track systems has been developed from the vertical mode impedance plots. This characterization was based on idealized elements having lumped constants, arranged in a parallel three-element system as shown in Figure 65. Idealized inertial, elastic, and damping elements are conventionally represented as masses, springs, and dashpots, using the symbols m, k, and c, respectively. It should be stressed that while this idealization is reasonably consistent with the data, it only represents a gross approximation to actual system response. It has been adopted to facilitate comparisons among the various track support systems, but it is not considered to be a unique or rigorous characterization because a gross idealization of this type does not adequately account for the known nonlinear behavior of materials such as the embankment soil. Also, the responses measured in this study were certainly affected to some degree by using an eccentric mass, i.e. variable force level vibrator to excite such nonlinear (force level sensitive) systems. One effect worth noting is that the adoption of upper and lower bound frequency limits in pretraffic analyses tended to minimize or eliminate data in the 10- to 20-Hz frequency domain. Although the eliminated data are not meaningful, the net result is a data discontinuity which complicates interpretation of the results.

For the parallel three-element system shown in Figure 65a, the impedance at the driving point (railhead) is given by

$$Z = c + j\left(2\pi fm - \frac{k}{2\pi f}\right) \qquad (11)$$

where

c = damping resistance

$j = -1$

f = frequency = $\omega/2\pi$

m = participating mass

k = spring constant

In this expression, c represents the real part of impedance, and the term $j\,(2\pi fm - k/2\pi f)$ represents the imaginary part of impedance.

The absolute magnitude of impedance $|Z|$ and the impedance angle θ are given by

$$Z = \sqrt{c^2 + \left(2\pi fm - \frac{k}{2\pi f}\right)^2} \qquad (12)$$

$$\theta = \tan^{-1} \frac{2\pi fm - \frac{K}{2\pi f}}{c} \qquad (13)$$

Graphic representations of Z and θ for a parallel three-element system are shown in Figures 65b and 65c, respectively. From Figure 65, it can be seen that at low frequencies Z approaches the spring value k, and the system is said to be "stiffness controlled." At high frequencies Z approaches the mass value m, and the system is said to be "mass controlled." At resonance (the frequency f_r where the impedance angle $\theta = 0$, as illustrated in Figure 11c) the impedance is real and equal to the damping value c.

Using this model, the idealized dynamic properties of each track section were determined as shown in Table 2. The impedance vertical and rocking mode impedance plots show the way in which the values of initial (vertical) stiffness k were determined. The rocking mode impedance plots were derived by dividing the total force F (applied to the north rail) by the resulting peak particle velocity V (at the railhead). These results are proportional to rocking mode impedance and were used to facilitate comparisons between vertical and rocking mode impedance test results. However, the correct units for rocking mode impedance Z_r are inch-pound-seconds per radian from the expression

$$Z_r = \frac{M}{\alpha'} = \frac{D}{2V} \cdot DF = \frac{D^2F}{2V} \qquad (14)$$

where

M = DF = applied moment, in.-lb

α' = 2V/D = angular velocity, rad/sec

D = distance between rails, C-C, in.

V = peak particle velocity at north railhead, in./sec

F = force applied to north rail, lb

Table 2 presents both the k_r (convenience units) and k (actual units) initial stiffness values for each rocking mode test conducted. The values of k and f_r from the vertical mode impedance plots were used to calculate the corresponding value of m the participating system mass (expressed as weight in pounds). This value is separate from (i.e. does not include) the mass of the vibrator). Only the initial stiffness values are given for Track Sections 7 and 8 because f_r could not be determined with confidence from the data. Since the relative stiffness of the various track sections is a matter of primary interest, the k values were used to construct the plot shown in Figure 66. Corresponding Young's E moduli values for the upper 4 ft of the embankment, determined in earlier WES tests, are also shown in Figure 66. These earlier test results show that the nonconventional track structure later installed in Track Section 7 was founded on the stiffest part of the embankment. Track Section 7 also had the stiffest response measured in impedance testing.

The results shown in Figure 12 are in good agreement with intuition regarding the effect of structure and ballast thickness variations on relative stiffness of the various track systems. These results may be summarized as follows:

Track Section	Variable	Effect on Measured Stiffness
1, 2, 3	Tie spacing, 1 > 2 > 3	Stiffness increases as tie spacing decreases

(Continued)

Track Section	Variable	Effect on Measured Stiffness
4, 5, 7	Method of construction (structures designed to have same stiffness)	Track Section 7 slightly stiffer than Sections 4 and 5. Stiffness difference is attributed to higher embankment strength in Track Section 7
2, 8	Ballast thickness, 8 > 2	Stiffness increases with ballast thickness
6, 9	Ballast treatment	Ballast treatment of the type used on Section 6 apparently tends to degrade vertical stiffness (Note: treatment was not completed at time these tests were run. Also, the intent of the treatment was ballast stabilization rather than enhancing stiffness)

In all cases the vertical resonant frequencies lie between 30 and 45 Hz. Conventional (tie) structures typically resonated near 30 Hz while the nonconventional structures resonated near 40 Hz.

The transfer ratio plots contained herein may be useful for purposes which are beyond the scope of this investigation. The data plots have been presented for such usage. The transfer ratio data may conveniently be summarized in terms of a maximum transfer ratio and the frequency or frequency range in which this ratio applies, as shown in Table 3.

Typically, concrete tie Track Sections 1, 2, 3, and 8 had a V_2/V_1 ratio of 1, indicating that the tie and rail moved in concert. From this we may conclude that the rail fasteners on the concrete tie functioned as an essentially rigid connection. The wood crosstie Track Sections 6 and 9 had a V_2/V_1 ratio less than 1, indicating that spikes do not behave as a rigid connection between the rail and the crosstie. The rail fasteners of the nonconventional track structures in Track Sections 4, 5, and 7 also had V_2/V_1 ratio less than 1, principally in the frequency range from 15-30 Hz. This response is attributed to special

nonconventional fastener characteristics or possibly to loose anchor bolts. In those instances where the V_2/V_1 transfer ratio was 1 or nearly so, the V_5/V_1 and V_5/V_2 transfer ratio curves were virtually identical, as they should be. Where the V_2/V_1 transfer ratio varied, the V_5/V_1 and V_5/V_2 ratios were different, since there was energy loss (attenuation) through the fastener.

The V_5/V_2 ratios are an index of signal attenuation (or conversely, energy transmission) through the ballast. From the data contained in Table 3, it is apparent that the tie structures in Track Sections 1, 2, 3, 6, 8, and 9 behaved similarly in terms of signal attenuation through the ballast (maximum V_5/V_2 values ranging from 0.095 to 0.16). Of course, these ratios were determined at frequencies which ranged from 21 Hz (Section 9) to 42 Hz (Section 1). There was, however, considerable variation in the V_5/V_2 values derived for the nonconventional track structures. Track Section 4, for example, had a maximum V_5/V_2 ratio of 0.8 at 31 Hz. A possible explanation for this behavior is that the ballast layer beneath the structure was relatively thin (less than the 6-in. thickness specified) and as a result did not effectively attenuate (or distribute) structural loadings. The corresponding V_5/V_2 values for Track Sections 5 and 7 of 0.31 and 0.20, respectively, indicate a much higher level of signal attenuation in these ballast layers.

Similar attenuation characteristics are evident from the V_6/V_5 and V_7/V_5 transfer ratio summaries and from the curves shown in the figures. These data, summarized in Table 3, indicate that considerable signal attenuation occurs in the embankment under the crosstie sections, and much less signal attenuation occurs in the embankment beneath the nonconventional structures. Considering the physical size and mass of the nonconventional structures, this behavior is not surprising. But, Track Section 4 is again noted as the section having least signal attenuation.

Posttraffic Tests

Posttraffic testing was done as a part of the KTT postmortem

investigation by WES. For reasons previously discussed, only Track Sections 1, 2, 3, 4, 5, 8, and 9 were tested. The posttraffic test locations were selected primarily to typify performance in service based on a WES evaluation of KTT track maintenance records furnished by ATSF. According to the rationale developed by WES, performance of the various test locations was typified as follows:

Section	Designation of Test Location	Station	System Performance Under Traffic
1	1	8524+75	Poor
2	2A	8531+62	Poor
	2B	8535+16	Good
3	3A	8540+20	Good
	3B	8542+49	Poor
4	4	8553+85	Poor
5	5	8558+25	Poor
8	8	8571+00	Good
9	9	8595+33	Good

The criterion for a "poor" performance designation was simply that ATSF maintenance records indicated pumping at that location as well as relatively frequent maintenance in most instances. The reverse was true for locations designated as having "good" performance. The reason for testing two locations in Track Sections 2 and 3 was to establish the approximate variation in dynamic properties associated with the "poor" or "good" performance designations. Also, DOT desired a comparison with pretraffic results which could be done with greater confidence if posttraffic performance judgments were validated by the test results. Results of the testing are presented in the following order:

Track Section	Test Location	Figures
1	1	67-71
2	2A	72-76
	2B	77-81

(Continued)

Track Section	Test Location	Figures
3	3A	82-86
	3B	87-91
4	4	92-97
5	5	98-103
8	8	104-108
9	9	109-113

Similar procedures were used in pretraffic and posttraffic testing, except that in the posttraffic testing additional eccentric weights were used. One concern with the pretraffic results was the lack of meaningful data in the 10- to 20-Hz frequency domain. Using more closely graded eccentric weights would, it was hoped, remove this concern and also provide better data continuity.

Applying a parallel three-element idealization to the posttraffic data yields the results shown in Table 4. It can be seen from Table 4 that only the initial dynamic stiffness values have been developed for Test Location 3A (Track Section 3) and Track Section 8. This is because the resonant frequency f_r cannot be established with reasonable confidence from these data; hence the remaining parameters were not derived. A ranking of the various track systems according to their initial dynamic stiffness is shown in Figure 114. These results are in generally good agreement with the performance judgments made from Santa Fe maintenance data. An exception is the posttraffic response of Track Sections 1 and 4. This will be discussed in the comparisons to follow.

The data obtained from Points 1, 2, 5, and 6 in the typical instrumentation array, shown in Figure 7, may be used to exemplify the vertical mode behavior of the rail, structure, ballast, and embankment. These data are summarized, in terms of a maximum transfer ratio and the frequency or frequency range in which this ratio applies, in Table 5.

From the V_2/V_1 transfer ratio results in Table 5, it is apparent that all of the fasteners tested, except those in Track Section 9,

behaved as an essentially rigid connection between the rail and the tie or structure. In the case of Track Section 9, WES field records noted that numerous spikes had backed out of the wood ties at the test location. This condition is evidenced by the V_2/V_1 transfer ratio curve for Track Section 9, which never exceeds a maximum value of 0.2 in the frequency domain from 7-50 Hz. Had the rail and ties in Track Section 9 moved in concert, then the V_2/V_1 ratio would have been approximately 1, as in the case of the other track sections tested.

There is more data scatter in the V_5/V_2 transfer ratios (an index of signal attenuation through the ballast) recorded for each track section. However, Track Sections 4 and 5 had minimum V_5/V_2 ratios of 0.3 and 0.7, respectively, indicating appreciably less signal attenuation occurred in the ballast of these sections than in the tie sections.

The V_6/V_5 maximum transfer ratio data exhibit considerable scatter. For example, the V_6/V_5 values derived for Track Section 1 and Test Location 2A in Track Section 2 appear to be abnormally high in comparison with results from the other test locations. The test geometry employed and/or embankment conditions existing at the time of testing may account for most of the observed scatter. The WES posttraffic field notes indicate that the flanks of the embankment were very soft and wet in most of the test areas partly because of the water applied to the test sections to stimulate pumping.

Comparison of Pretraffic and Posttraffic Test Results

Comparisons of pretraffic and posttraffic test results will be developed for the following purposes:

1. To demonstrate that an impedance approach of this type is capable of detecting changes in track system response due to traffic or other service life related parameters.
2. To relate, if possible, these changes in dynamic response to track system performance.

Because this test program was performed primarily as a feasibility study, and since the vibratory apparatus used was relatively crude in

terms of state-of-the-art capabilities, the comparative analyses to follow will necessarily be general in nature.

Posttraffic testing was conducted only on Track Sections 1-5, 8, and 9, and comparisons will be made only for these sections. Although track conditions existing at the time of testing have already been described, a brief chronology of KTT events will help to put the comparisons in proper perspective, as follows:

1. Pretraffic impedance tests were conducted in April 1973 just prior to opening the test track for slow speed shakedown traffic.
2. The test track was closed from 3 May 1974 until 31 October 1974 for replacement of fastener anchor bolts in the nonconventional track sections. A number of these had experienced early failure, so the entire complement was replaced.
3. Rapid deterioration of the subgrade began in October 1974 when mainline ATSF freight traffic was diverted onto KTT.
4. Mid-chord offset tests were run in December 1974 when subgrade deterioration was well underway.
5. Track operations were suspended in April 1975 because of severe pumping and resulting maintenance problems. Closure of the track followed in June 1975.
6. After June 1975, moisture contents in the ballast and top few inches of the embankment decreased under the drying action of the Kansas summer weather. Only dried traces of pumped material were visible in October 1975 when the WES field crew arrived at the KTT site to begin posttraffic testing.
7. The WES field crew attempted to recreate pumping conditions in October 1975 at selected locations along the embankment. Surface indications of pumping were achieved at the test locations in Track Sections 1-3, and traces of the onset of pumping were observed in Track Section 5 but not in Track Section 4 (Track Sections 8 and 9 did not visibly pump under rail traffic). Hense, the WES attempt to recreate pumping conditions was only partly successful.

Since the initial dynamic stiffness of the various track systems is of primary interest, Figure 115 compares these results of the pretraffic and posttraffic impedance tests. The posttraffic results show a general degradation in stiffness of Track Sections 2-5, 8, and 9, as expected, and the initial stiffness values derived for Test Locations 2A, 2B, 3A, and 3B are in good agreement with WES performance judgments made prior to posttraffic testing. A particularly surprising result was the anomalously high stiffness recorded for the test location in Track Section 1, which had been judged to show "poor" performance and had been expected to have a low stiffness. A detailed recheck of the calibration, data acquisition, and reduction procedures used for Track Section 1 did not reveal any discrepancies. However, the posttraffic initial dynamic stiffness value recorded for Track Section 1 is clearly not related to its performance under traffic from December 1974 to April 1975. The most plausible explanation is that WES attempts to recreate pumping conditions were only marginally successful, i.e., the subgrade in Track Section 1 was not softened to the extent it was during actual rail traffic, if at all. Similar reservations probably apply to the posttraffic initial dynamic stiffness value derived for Track Section 4, because a greater decrease in stiffness was expected based on pretest performance judgments. The WES attempts to recreate operational conditions were apparently more successful at Test Locations 2A and 2B (Track Section 2), Locations 3A and 3B (Track Section 3), and Location 9 (Track Section 9). Posttraffic impedance results from these locations typically show a much lower resonant frequency than in pretraffic tests, which is consistent with a pronounced decrease in stiffness. Only a slight decrease in resonant frequency was noted for Track Sections 1, 4, and 5; however, Track Section 5 had not been expected to show a large decrease in either stiffness or resonant frequency.

Data recorded by other investigators[10,11] in the traffic period from December 1974 to April 1975 provide some insight into subgrade conditions existing at that time. Figure 116 presents a relative stiffness ranking of KTT track sections which was derived by the ENSCO

Corporation,[10] a Department of Transportation contractor organization using a specially equipped railway test car. Comparing Figures 115 and 116 shows that the ENSCO, Inc. and WES posttraffic impedance results are in generally good agreement, except in Track Sections 1 and 4. And, with the exception of Track Section 4, ENSCO and WES pretraffic results show the same general trends in stiffness. The differences between WES posttraffic and ENSCO results are believed to stem from differences in the methods of testing and from time-dependent variations in subgrade conditions. For example, ENSCO results were based on response averaged over an entire track section,[10] while WES results were derived from tests at discrete locations. More than 11 months (5 months after KTT traffic was suspended) elapsed before WES attempted to recreate pumping conditions, and the track had certainly dried out to some extent by that time. As noted, WES efforts to recreate pumping were only partly successful. Hence, there probably were significant time-related variations in subgrade conditions.

A comparison of pretraffic and posttraffic transfer ratio results, summarized in Tables 3 and 5, respectively, shows that there was a marked increase in the rigidity of the special rail fasteners used in the nonconventional track sections. Contrary to the V_2/V_1 transfer ratio results obtained in pretraffic testing, the posttraffic V_2/V_1 ratios for the nonconventional fasteners typically have unity values throughout the frequency range tested. It will be recalled that the anchor bolts of the nonconventional fasteners were replaced after pretraffic testing was completed. The replacement bolts functioned well in service and the posttraffic V_2/V_1 transfer ratio curves reflect the modification as an increase in fastener stiffness.

The remaining transfer ratio curves, i.e., V_5/V_2 , V_5/V_6 , V_5/V_8 , V_5/V_9 , were all derived from various points on the top shoulder and flank of the embankment. Comparison of these data for the pretraffic and posttraffic condition indicates that traffic-related changes in dynamic response did occur.

CONCLUSIONS AND RECOMMENDATIONS

In this study, results were obtained that clearly demonstrate the feasibility of an impedance approach to track response measurements. Initial stiffness values were determined for each track section under pretraffic and posttraffic conditions, and the data have also been used to explain and/or rank the behavior of selected track components. WES attempted to recreate pumping of the subgrade as a precondition for posttraffic testing; however, this effort was apparently successful only in Track Sections 2, 3, 5, 8, and 9. Impedance results from these sections correlate fairly well with performance judgments based on ATSF maintenance records and test results obtained from December 1974 to April 1975 (the period of KTT traffic) by other investigators.[10,11] However, impedance results on Track Sections 1 and 4 do not correlate well with the other data. This is attributed primarily to different subgrade conditions at the time of testing and to a lesser degree to the method of testing used.

It was recognized that the eccentric mass vibrator used in this study does not represent state-of-the-art capability for impedance testing. The presence of these limitations made an analysis to determine data validity necessary and also complicated interpretation of the results. Although meaningful data were obtained, employment of an improved apparatus for future testing is still needed.

It should be stressed that track system response measured at the railhead is influenced by all track components, including the foundation soil. Soil typically behaves as a nonlinear, hysteretic material. It follows that track system dynamic response will vary to some degree with the magnitude of the vertical forces applied. For example, if the tests in this study had been conducted at force levels equivalent to live train loadings, then the resulting impedance curves would generally be similar in character to the curves presented herein. However, the curves for higher force levels would undoubtedly shift to lower absolute values of initial stiffness and resonant frequency because of the influence of the foundation soil. Preliminary results of other railway

impedance studies, now underway at WES, support this argument. An important conclusion is that impedance values derived in the current study are not unique. They are directly related only to the stress levels at which the tests were conducted. Future impedance tests should be conducted at force levels equivalent to live train loadings.

It is concluded that an impedance approach of the type used in this study is a viable method of measuring track system response, and future applications of impedance techniques can provide information of considerable value to the railroad community. Such applications might include evaluations of in-service trackage, expedient remedial treatments, performance predictions, and input to the design of improved track structures. Impedance testing clearly provides a powerful tool for achieving a better understanding of track structure-ballast-subgrade interaction and track structure component behavior. Computer programs can be used to advantage for detailed analyses of impedance data.[12]

Based on results obtained in the current study, the following recommendations are offered:

1. A high-output constant force actuator, such as the 50-kip electrohydraulic unit now in use at WES, should be used in any future impedance studies.
2. Since track system performance is governed primarily by structure-ballast-subgrade interaction processes, which are only partially understood, and since these processes can be adequately defined using impedance techniques, it is recommended that the current study be expanded into a targeted research project.
3. Consideration should also be given to other applications of impedance techniques, such as evaluating stiffness variations in existing trackage, development of a trackage rating index based on stiffness measurements, assessing the effects of improvements to trackage, or other related uses.

REFERENCES

1. Staff, Rail Technical Division, "Kansas Test Track," Progress Report, Report No. FRA-RT-72-08, Oct 1971, Federal Railway Administration, Washington, D. C.

2. Meacham, H. C. et al., "Study of New Track Structure Design: Phase I," Report No. FRA-RT-72-12, Sep 1966, prepared for the U. S. Department of Transportation, Federal Rail Administration, Office of High Speed Ground Transportation, Washington, D. C., by the Batelle Memorial Institute.

3. Meacham, H. C. et al., "Study of New Track Structure Design: Phase II," Report No. FRA-RT-72-15, Aug 1968, prepared for the U. S. Department of Transportation, Federal Rail Administraion, Office of High Speed Ground Transportation, Washington, D. C., by the Batelle Memorial Institute.

4. Dietrich, R. J. and Salley, J. R., "Embankment Support for a Railroad Test Track: Design Studies," Report No. FRA-RT-72-7, Aug 1971, prepared for the U. S. Department of Transportation, Federal Rail Administration, Office of High Speed Ground Transportation, Washington, D. C., by Shannon and Wilson, Inc.

5. McLean, F. G. et al., "Kansas Test Track: Nonconventional Track Structures, Design Report," Sep 1974, Westenhoff and Novick, Inc., Chicago, Ill.

6. Dietrich, R. J. and Salley, J. R., "Embankment Support for a Railroad Test Track, Construction Report," Final Report, Apr 1972, prepared for Department of Transportation, Federal Railway Administration, Office of Research, Development, and Demonstrations, Washington, D. C., by Shannon and Wilson, Inc.

7. Curro, J. R., "Vibroseismic Survey, Railroad Test Embankment, Aikman, Kansas," Miscellaneous Paper No. S-72-36, June 1972, U. S. Army Engineer Waterways Experiment Station, CE, Vicksburg, Miss.

8. Harris, C. M. and Crede, C. E., Shock and Vibration Handbook, Vol 1, McGraw-Hill Co., New York, 1961.

9. Plunkett, R., "Measurement of Mobility," Trans., Journal of Applied Mechanics, American Society of Mechanical Engineers, Vol 21, No. 3, Sep 1954, pp 250-256.

10. Talapatra, D. C. and Corbin, J. C., "A Feasibility Study of Method for Observing Track Stiffness from Mid-Chord Offset and Profilometer Measurements," IEEE Industry Application Society Tenth Annual Meeting Conference Record, Institute of Electrical and Electronic Engineers, Inc., Oct 1975, New York, N. Y., pp 312-517.

11. Dietrich, R. J. and Salley, J. R., "Embankment Support for Kansas Test Track, Analysis of Embankment Instrument Data," Report

No. FRA-ORD-76-258, Feb 1976, prepared for the Department of Transportation, Federal Rail Administration, Office of High Speed Ground Transportation, Washington, D. C., by Shannon and Wilson, Inc.

12. Safford, F. B. (Agbabian Associates) and Walker, R. E., "Hardness Program Non-EMP In-Place Testing of Shock-Isolation Systems for Safeguard TSE Ground Facilities," WES, HND SP-75-346-ED-R, prepared for the U. S. Army Engineer Division, Huntsville, by the U. S. Army Engineer Waterways Experiment Station, CE, Vicksburg, Miss.

TABLE 1. TRACK TEST SECTION CONFIGURATION

Track Section	System Type	Ballast Depth	Remarks
1	Concrete ties, 30-in. C-C	10 in.	
2	Concrete ties, 27-in. C-C	10 in.	
3	Concrete ties, 24-in. C-C	10 in.	
4	Continuous concrete beams	6 in.	Cast in place structure
5	Continuous concrete slab	6 in.	Cast in place structure
6	Wood ties, 19.5-in. C-C	10 in.	6-in. stabilized ballast layer on subgrade
7	Continuous concrete beams	6 in.	Precase beams, installed and field joined
8	Concrete ties, 27-in. C-C	15 in.	
9	Wood ties, 19.5-in. C-C	10 in.	Control section (standard Santa Fe)

TABLE 2. PRETRAFFIC IDEALIZED DYNAMIC PROPERTIES
(Derived From a Parallel Three-Element Characterization)

Track Section	Vertical Mode Initial Stiffness k, lb/in.	Rocking Mode Initial Stiffness		Vertical Mode Resonant Frequency f_r, Hz	Vertical Mode Damping at Resonance c, lb sec/in.	Calculated Vertical Mode Participating Mass** m, lb	Approximate Vertical Force Level at f_r lb
		Convenience Units k_r, lb/in.	Actual Units* k, in.-lb-sec/rad				
1	3×10^5	4×10^5	6.96×10^8	33	640	2,700	1,700
2	4×10^5	5×10^5	8.70×10^8	31	1,000	4,000	1,300
3	1×10^6	1×10^6	1.74×10^9	30	1,050	11,000	1,200
4	2.5×10^6	1.5×10^6	2.61×10^9	43	3,500	13,000	2,800
5	2.5×10^6	2.5×10^6	4.35×10^9	42	6,000	14,000	2,700
6	2.6×10^5	4.0×10^5	6.96×10^8	35	500	2,100	1,800
7	3.0×10^6	1.6×10^6	2.78×10^9	35-45†	---	---	---
8	1.5×10^6	1.0×10^6	1.74×10^9	30-42†	---	---	---
9	5.2×10^5	5.2×10^5	9.05×10^8	30	1,050	5,600	1,200

* $k = 1740\ k_r$.

** $m = k/4\pi^2 f_r^2$.

† The apparent resonant frequency of these track sections lies within the ranges but cannot be determined with reasonable confidence from the available data.

TABLE 3. PRETRAFFIC APPROXIMATE MAXIMUM VERTICAL MODE TRANSFER RATIO AND FREQUENCY(S)

Track Section	$\frac{V_2}{V_1}$	$\frac{V_5}{V_1}$	$\frac{V_5}{V_2}$	$\frac{V_6}{V_5}$	$\frac{V_7}{V_5}$
1	1 (6-50 Hz)	0.15 (37 Hz)	0.15 (37 Hz)	0.39 (43 Hz)	0.07 (40 Hz)
2	1 (6-50 Hz)	0.095 (40 Hz)	0.095 (40 Hz)	0.48 (35 Hz)	0.07 (40 Hz)
3	1 (9-50 Hz)	0.12 (35 Hz)	0.12 (35 Hz)	0.24 (35 Hz)	0.09 (40 Hz)
4	Varies, 0.75-1.0 (9-50 Hz)	0.7 (31 Hz)	0.8 (31 Hz)	1.4 (35 Hz)	1.0 (50 Hz)
5	Varies, 0.7-1.2 (15-50 Hz)	0.29 (34 Hz)	0.31 (34 Hz)	Data considered to be unreliable	
6	0.6 (26 Hz)	0.03 (37 Hz)	0.10 (34 Hz)	0.63 (30 Hz)	0.024 (38 Hz)
7	Varies, 0.6-1.0 (8-43 Hz)	0.15 (42 Hz)	0.20 (40 Hz)	0.75 (20,37 Hz)	0.22 (43 Hz)
8	1 (20-50 Hz)	0.16 (28 Hz)	0.16 (28 Hz)	0.75 (41 Hz)	0.15 (41 Hz)
9	Varies, 0.8-1.0 (7-50 Hz)	0.15 (21, 38 Hz)	0.15 (21, 38 Hz)	0.4 (32 Hz)	0.095 (32 Hz)

Note: See Figure 7 for location of Points 1, 2, 5, 6, and 7.

TABLE 4. POSTTRAFFIC IDEALIZED DYNAMIC PROPERTIES
(Derived From a Parallel Three-Element Characterization)

Track Section	Designation of Test Location	Vertical Mode Initial Dynamic Stiffness k, lb/in.	Resonant Frequency f_r, Hz	Damping At Resonance c, lb sec/in.	Calculated Participating Mass m, lb	Approximate Vertical Force Level at f_r, lb
1	1	5×10^5	30	2,100	5,500	1,300
2	2A	6×10^4	13	400	3,500	3,000
	2B	1×10^5	15	900	4,500	4,000
3	3A	3.5×10^5	--*	---	---	---
	3B	1.5×10^5	20 (est.)	900	3,700	3,000
4	4	1.5×10^6	40	3,500	9,000	2,300
5	5	1.0×10^6	30	4,000	11,000	1,300
8	8	4.0×10^5	--*	---	---	---
9	9	1.2×10^5	18	450	3,600	2,500

* The resonant frequency of these track sections could not be determined with reasonable confidence from the available data.

TABLE 5. POSTTRAFFIC APPROXIMATE MAXIMUM VERTICAL MODE TRANSFER RATIO AND FREQUENCY(S)

Track Section	$\frac{V_2}{V_1}$	$\frac{V_5}{V_1}$	$\frac{V_5}{V_2}$	$\frac{V_6}{V_5}$
1	0.9-1.0 (8-50 Hz)	0.2 (50 Hz)	0.2 (50 Hz)	2.8 (27 Hz)
2 (Location 2A)	1.0 (5-50 Hz)	0.02 (40 Hz)	0.02 (40 Hz)	1.7 (34 Hz)
2 (Location 2B)	1.0 (5-50 Hz)	0.11 (43 Hz)	0.11 (43 Hz)	0.70 (35 Hz)
3 (Location 3A)	1.0 (8-50 Hz)	0.17 (40 Hz)	0.17 (40 Hz)	0.64 (30 Hz)
3 (Location 3B)	1.0 (9-50 Hz)	0.16 (33 Hz)	0.16 (33 Hz)	0.75 (37 Hz)
4	1.0 (9-50 Hz)	0.30 (21 Hz)	0.30 (21 Hz)	2.0 (33 Hz)
5	0.9 (12-50 Hz)	0.70 (50 Hz)	0.70 (50 Hz)	0.90 (21 Hz)
6		Not Tested		
7		Not Tested		
8	1.0 (7-50 Hz)	0.17 (40 Hz)	0.17 (40 Hz)	0.90 (30 Hz)
9	Varies, 0.1-0.2 (7-50 Hz)	0.009 (37 Hz)	0.075 (40 Hz)	1.0 (50 Hz)

Note: See Figure 7 for location of Points 1, 2, 5, and 6.

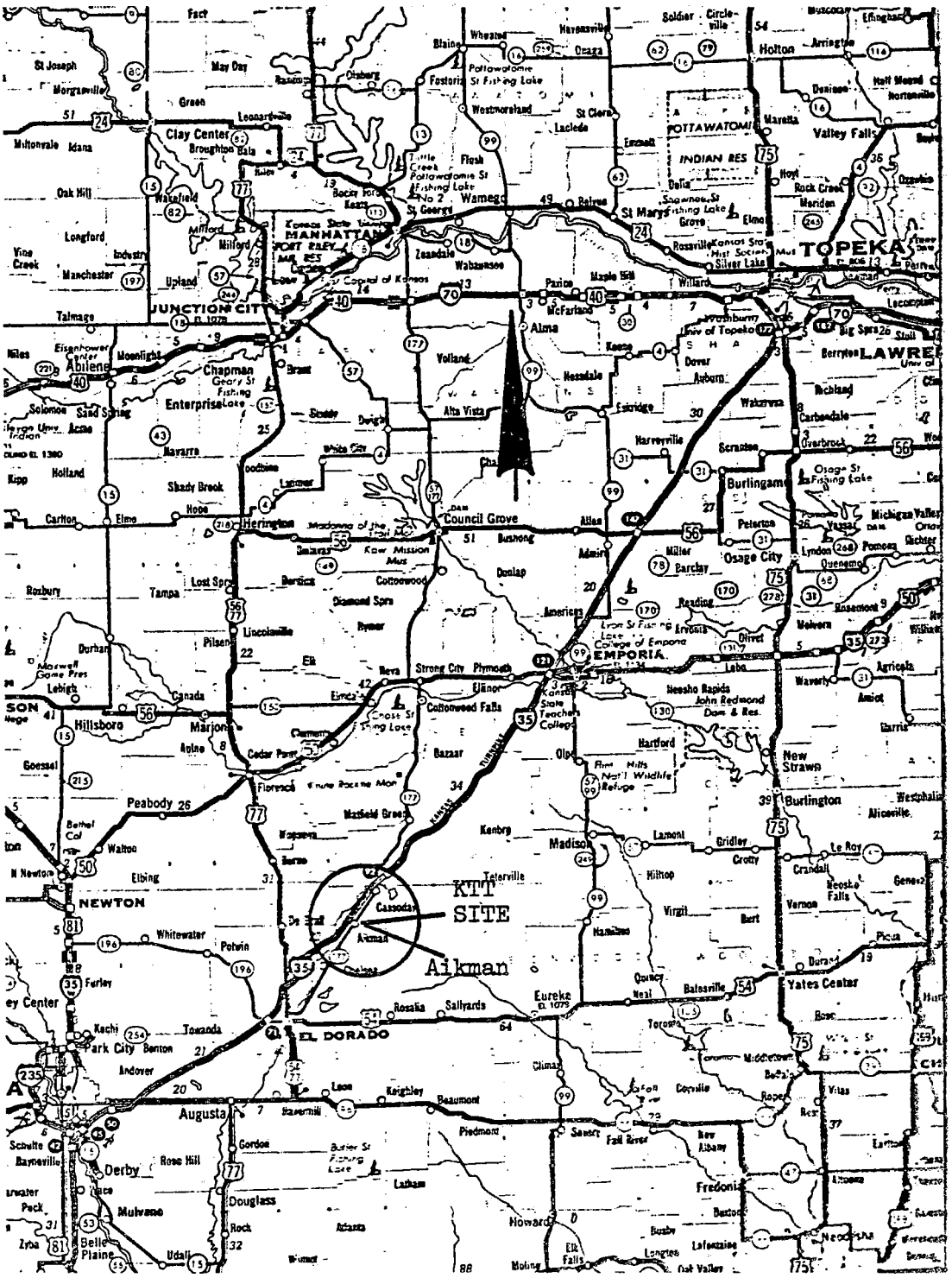

FIGURE 1. LOCATION OF KTT TEST SITE

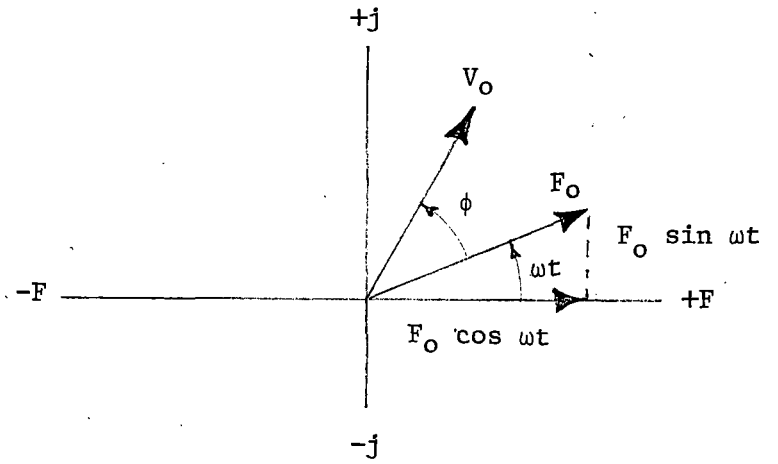

(a) Force phasor

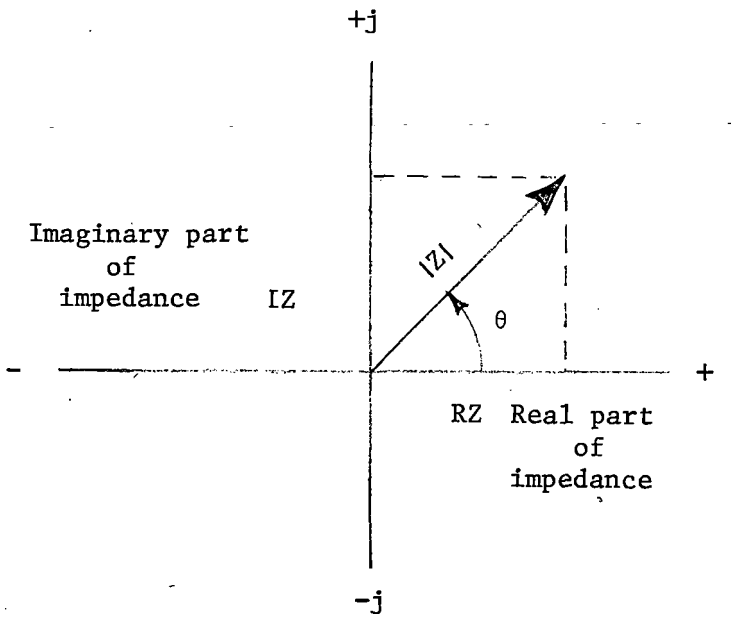

(b) Impedance phasor

FIGURE 2. PHASOR REPRESENTATIONS OF FORCE AND VELOCITY IN THE COMPLEX PLANE

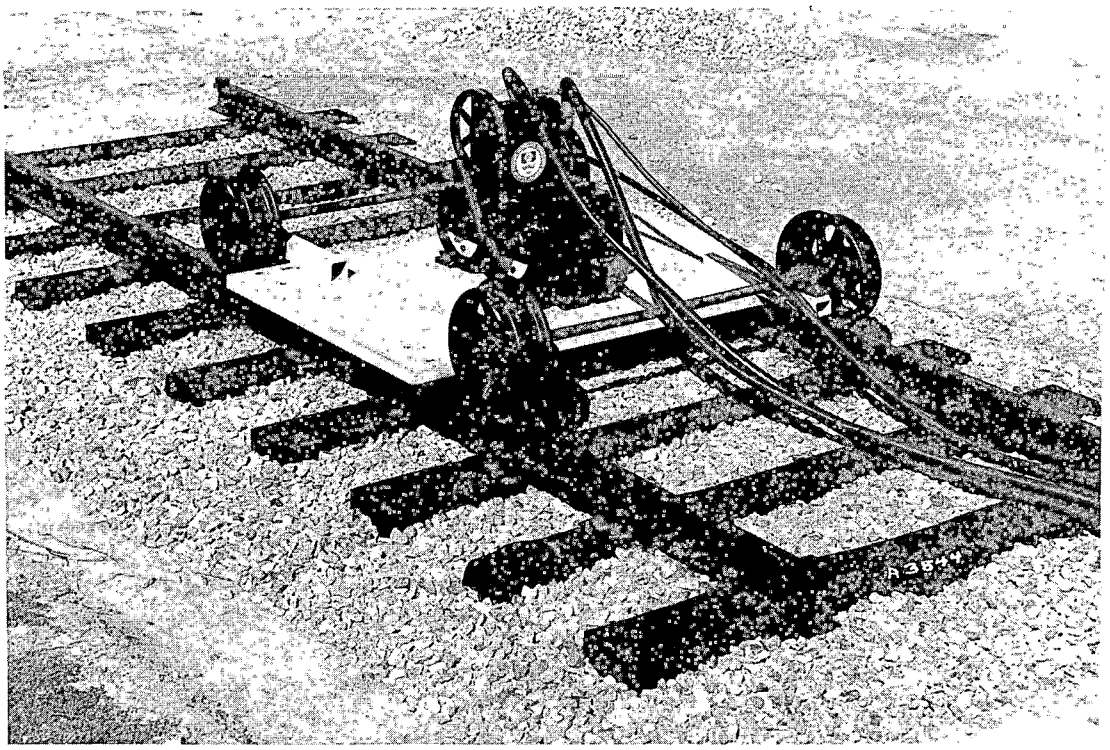

FIGURE 3. VIBRATORY APPARATUS USED FOR IMPEDANCE TESTING

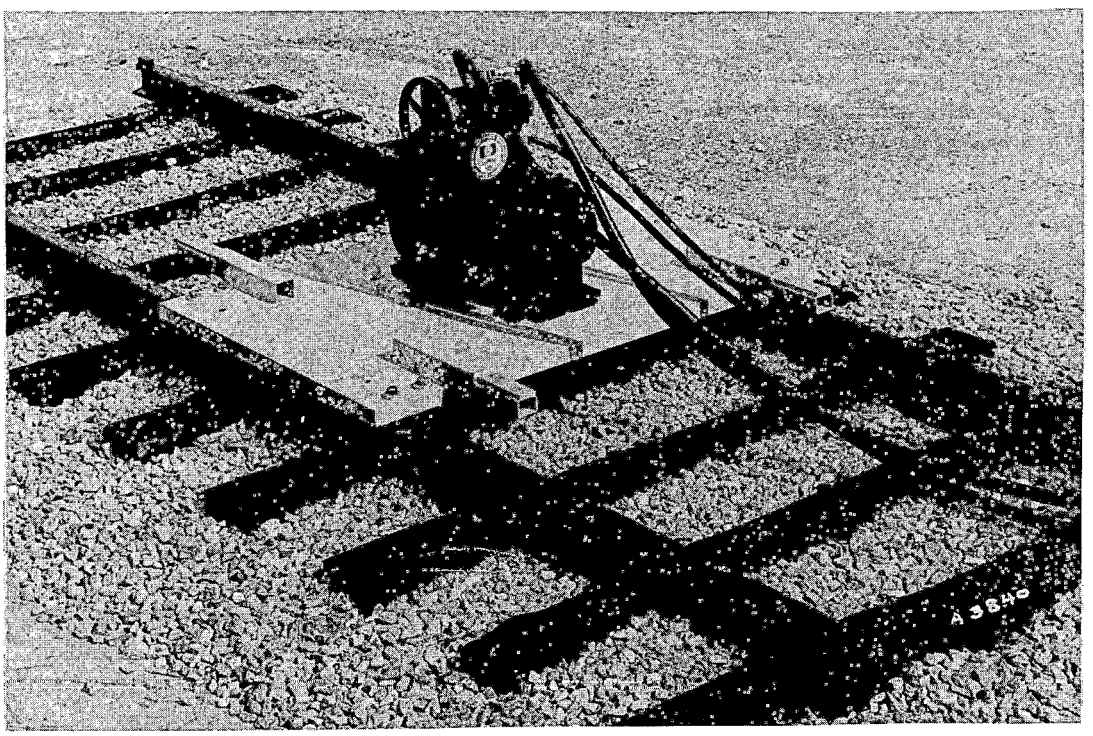

FIGURE 4. VIBRATOR FASTENED TO RAILHEADS AND CONFIGURED FOR TESTING

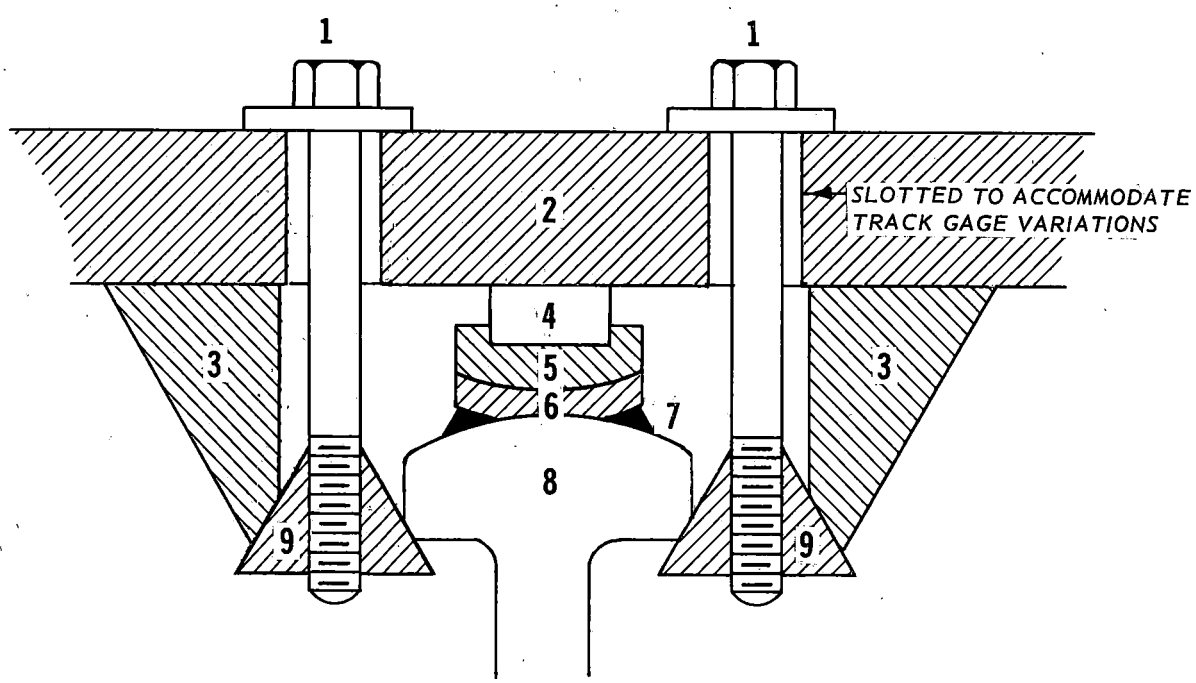

1. Clamping Bolts
2. 2-in.-Thick Steel Vibrator Baseplate
3. Steel Butt Blocks
4. Quartz Load Washer For Force Measurement
5. Upper Cell Housing
6. Lower Cell Housing

} Lubricated Spherical Mating Surface

7. Lower Cell Housing Epoxied To Railhead
8. Railhead
9. Steel Clamping Wedges

FIGURE 5. VIBRATOR CLAMPING MECHANISM

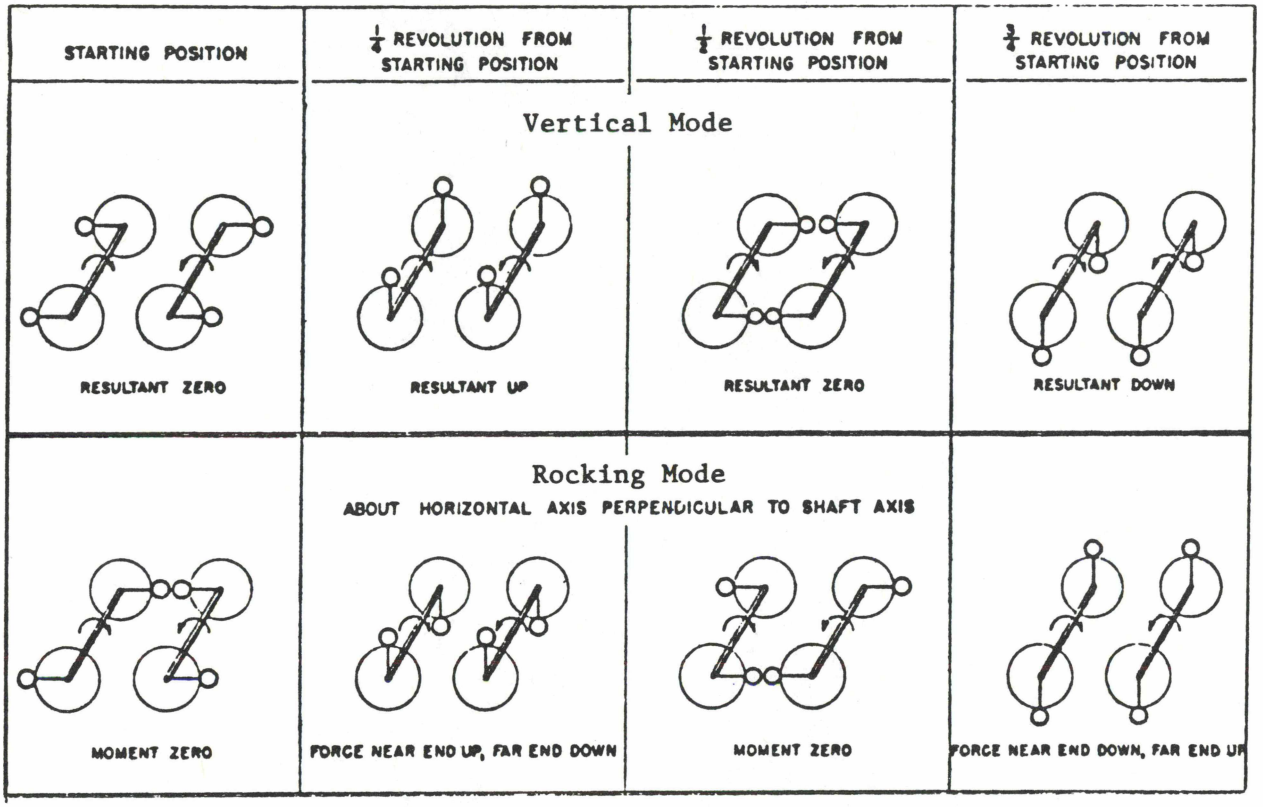

FIGURE 6. ECCENTRIC WEIGHT CONFIGURATIONS FOR VERTICAL AND ROCKING MODES OF EXCITATION

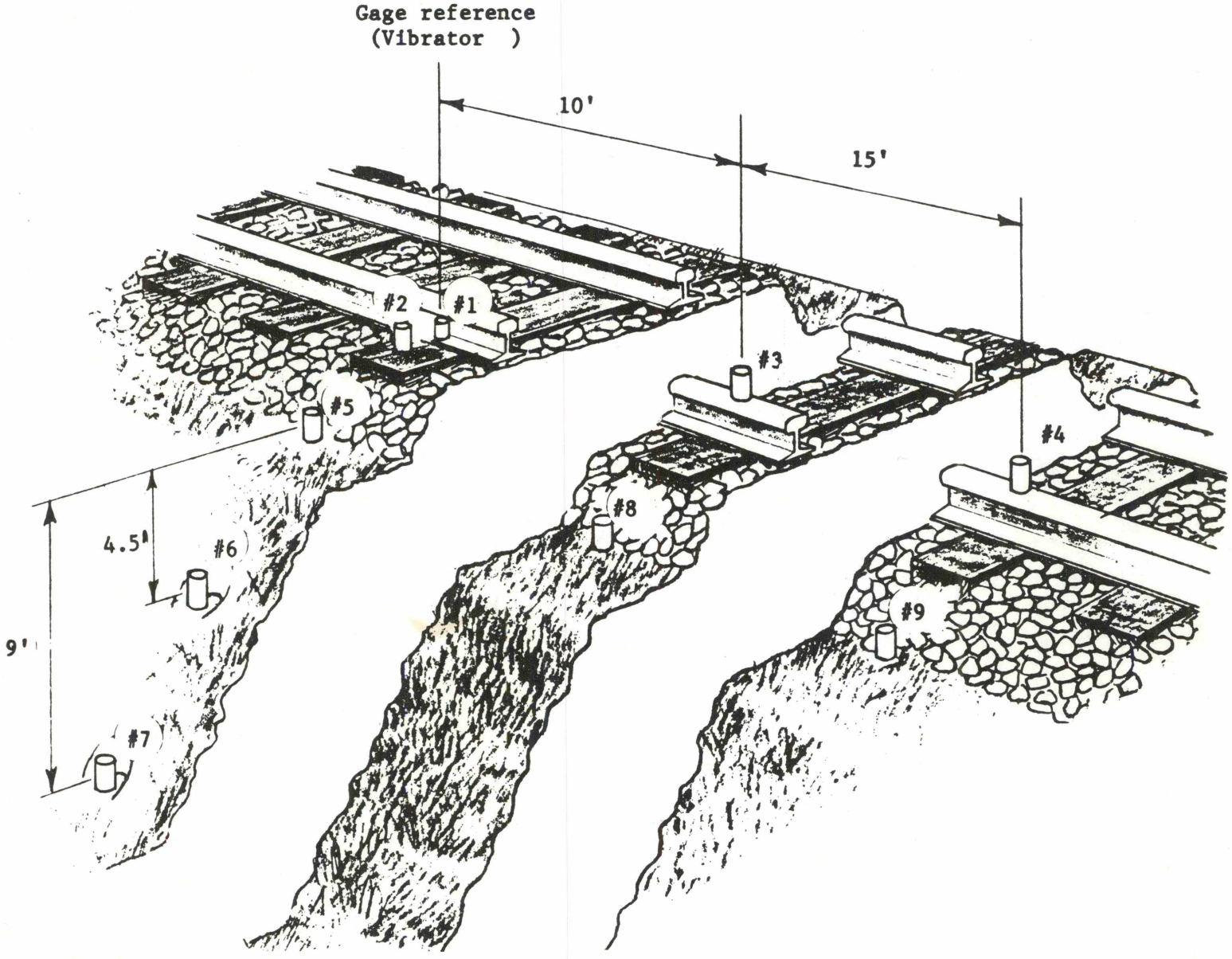

FIGURE 7. TYPICAL INSTRUMENTATION ARRAY

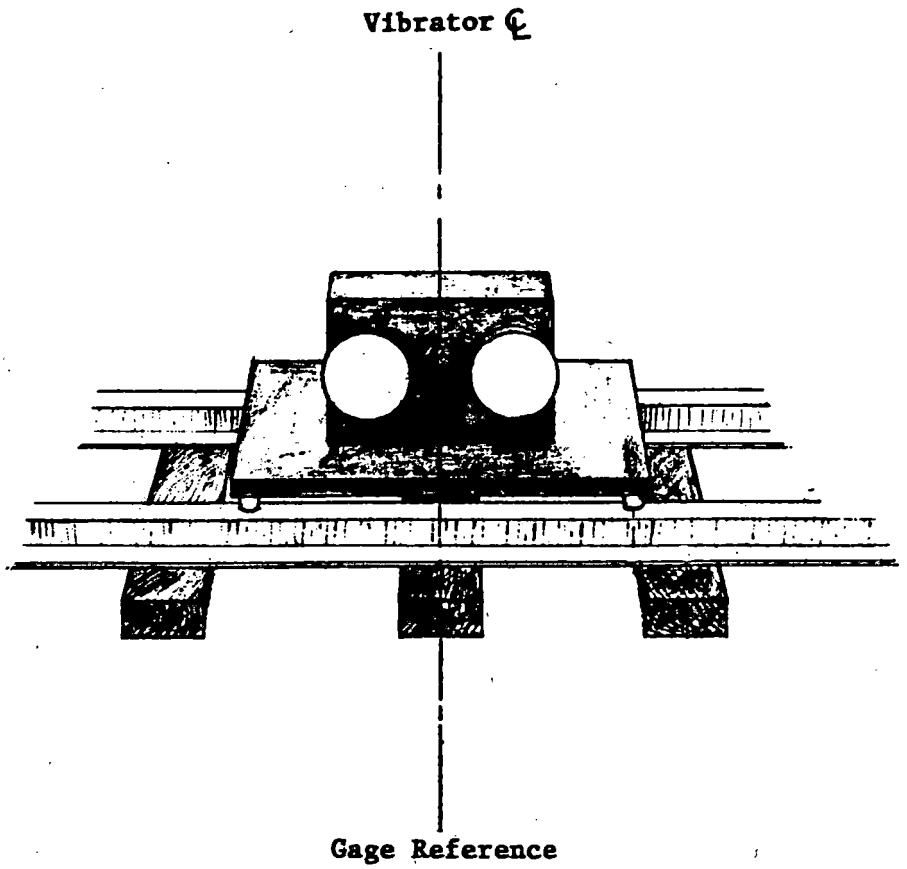

FIGURE 8. REFERENCE LINE FOR INSTRUMENTATION ARRAY

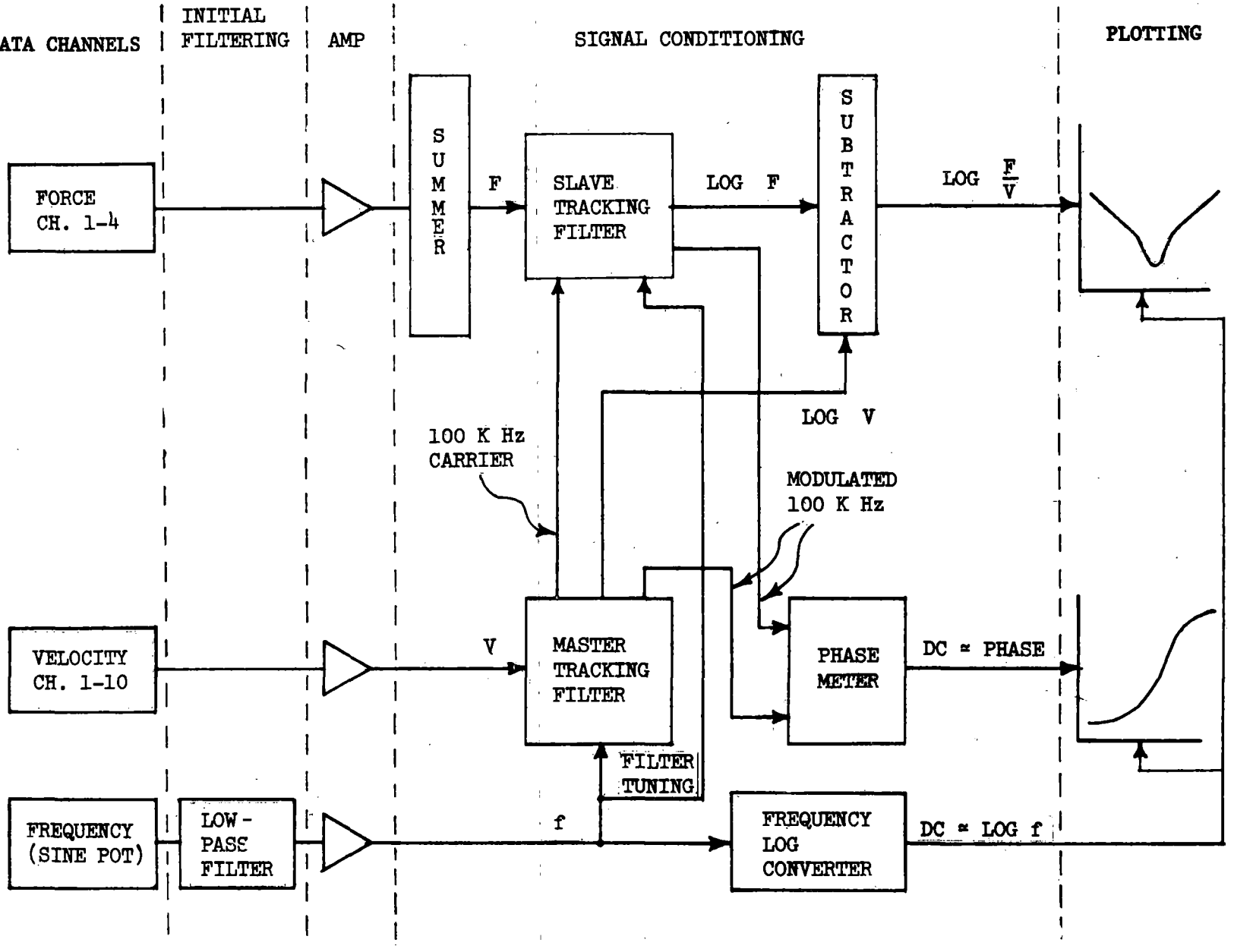

FIGURE 9. INSTRUMENTATION BLOCK DIAGRAM

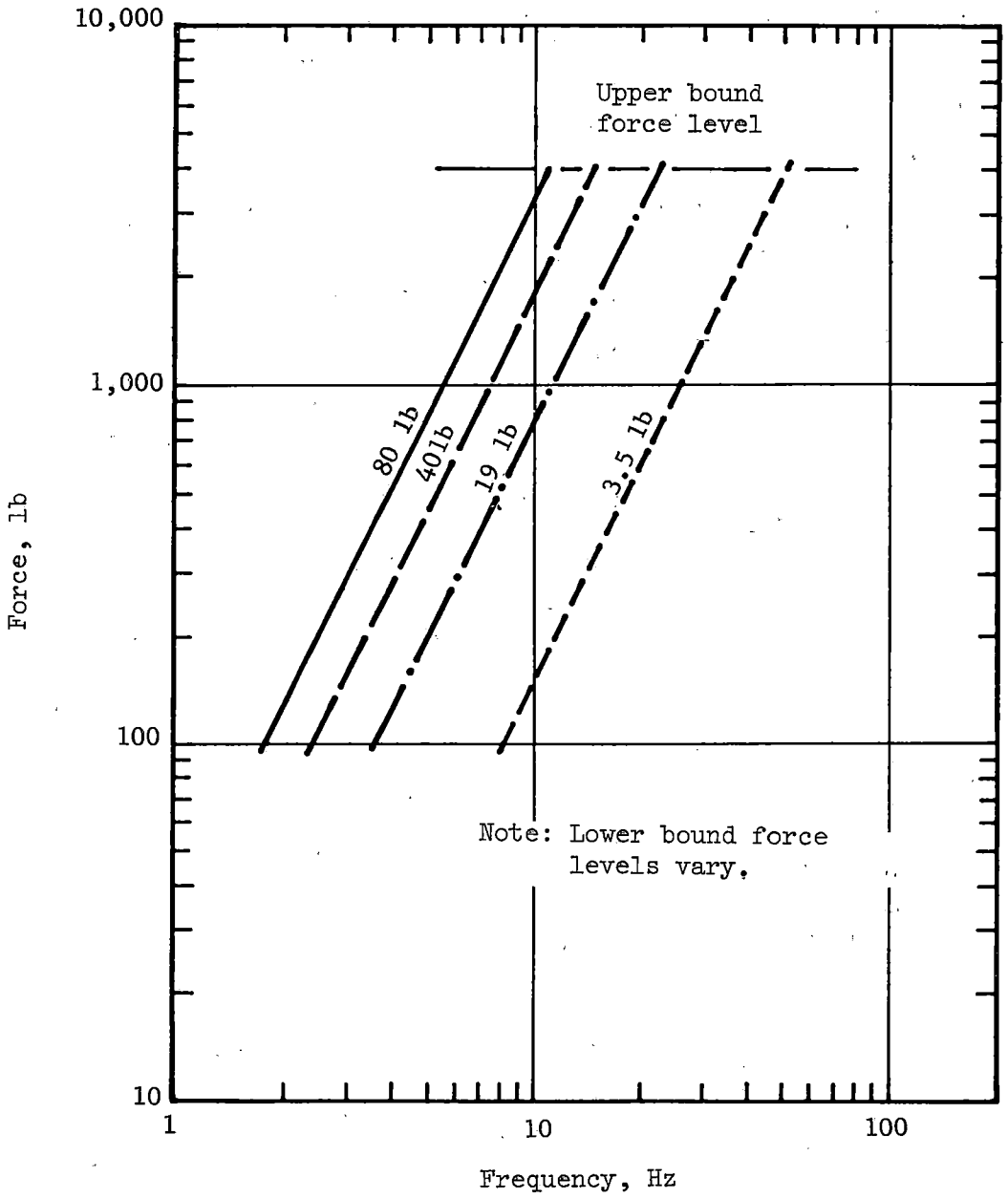

FIGURE 10. CALCULATED VIBRATOR FORCE OUTPUT VERSUS FREQUENCY CURVES FOR THE VARIOUS ECCENTRIC WEIGHTS USED IN THIS STUDY

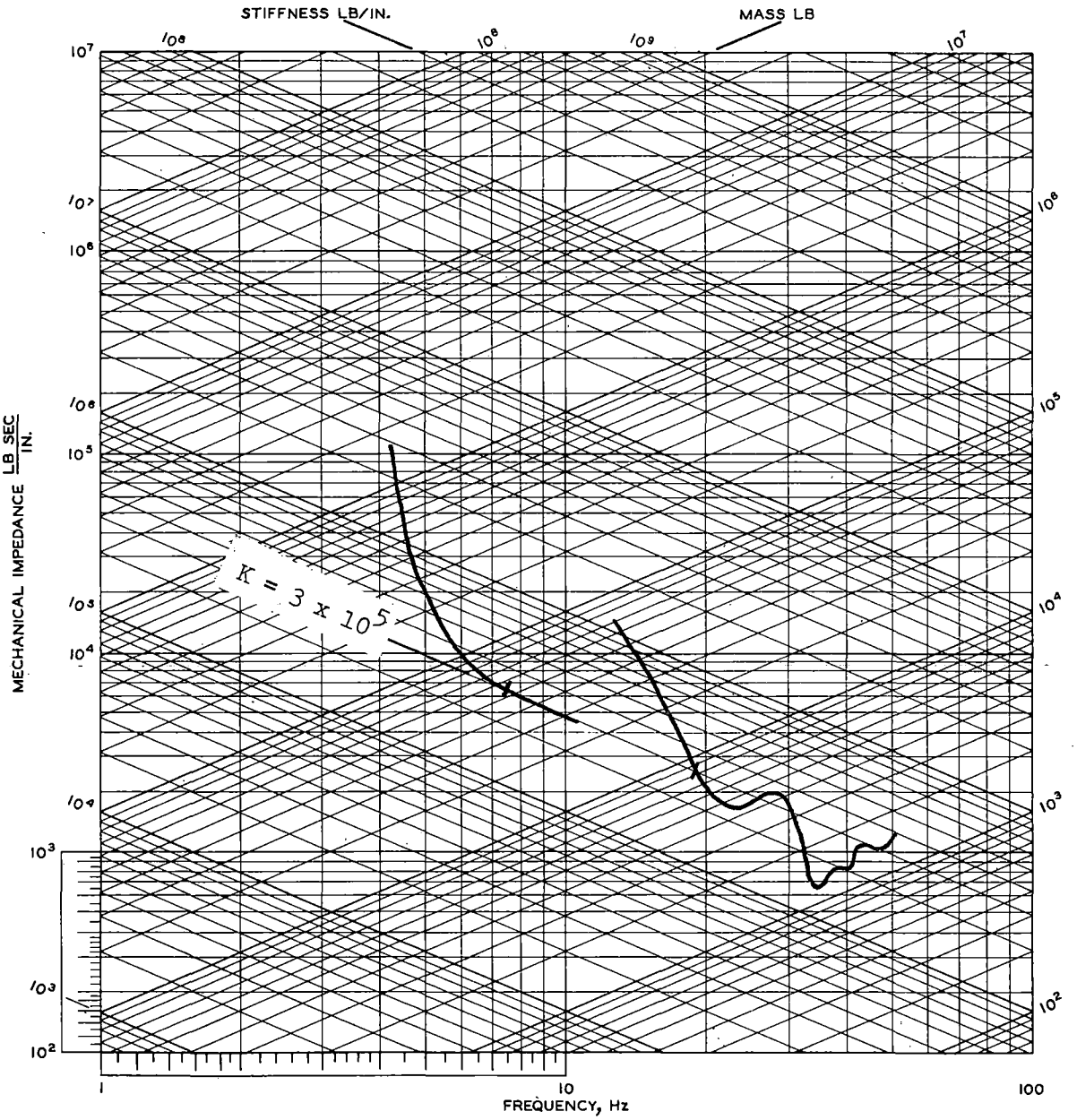

FIGURE 11. PRETRAFFIC MECHANICAL IMPEDANCE RESULTS, TRACK SECTION 1, VERTICAL MODE, POINT 1

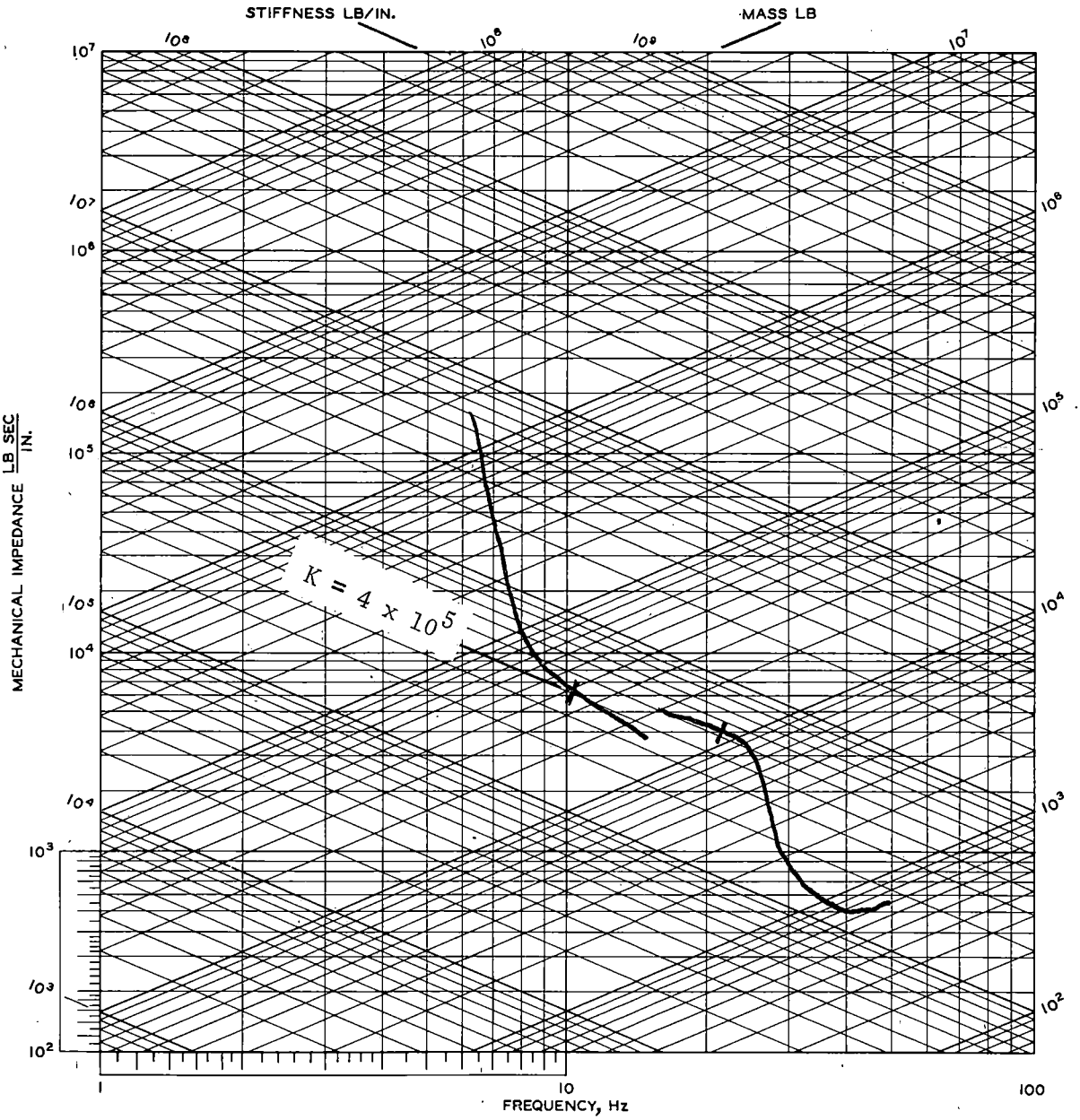

FIGURE 12. PRETRAFFIC MECHANICAL IMPEDANCE RESULTS, TRACK SECTION 1, ROCKING MODE, POINT 1

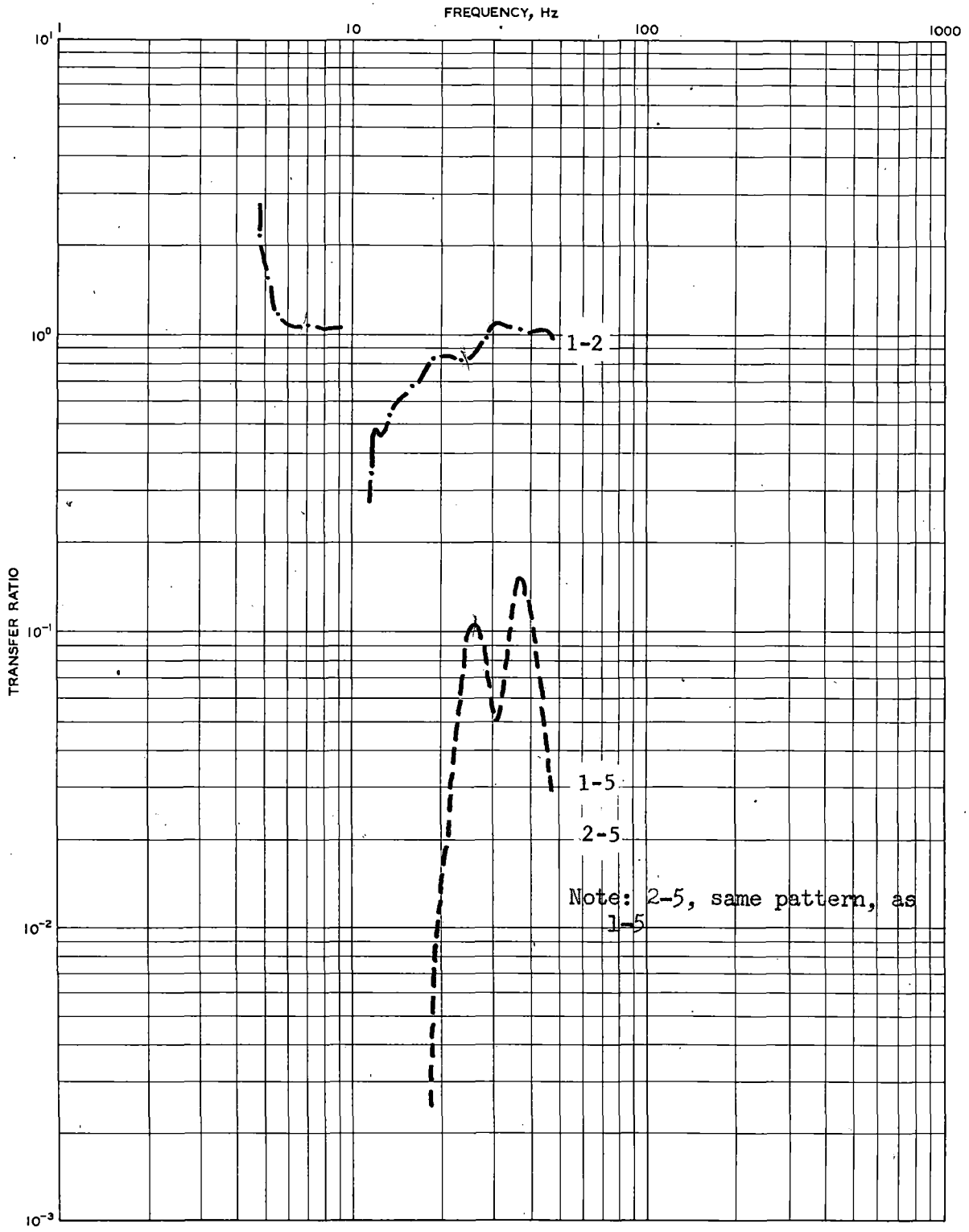

FIGURE 13. PRETRAFFIC TRANSFER RATIO RESULTS, TRACK SECTION 1, VERTICAL MODE, POINTS 1-2, 1-5, 2-5

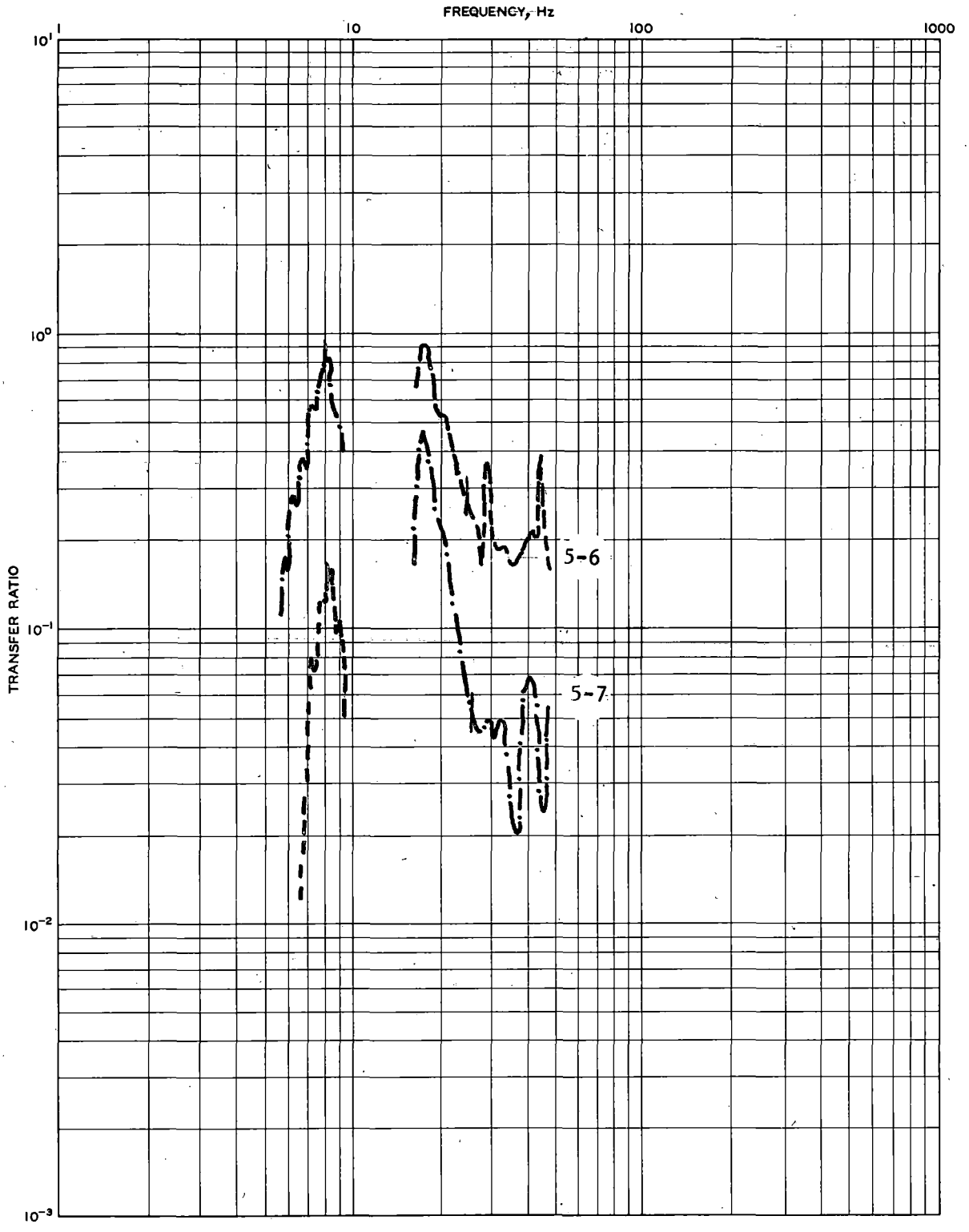

FIGURE 14. PRETRAFFIC TRANSFER RATIO RESULTS, TRACK SECTION 1, VERTICAL MODE, POINTS 5-6, 5-7

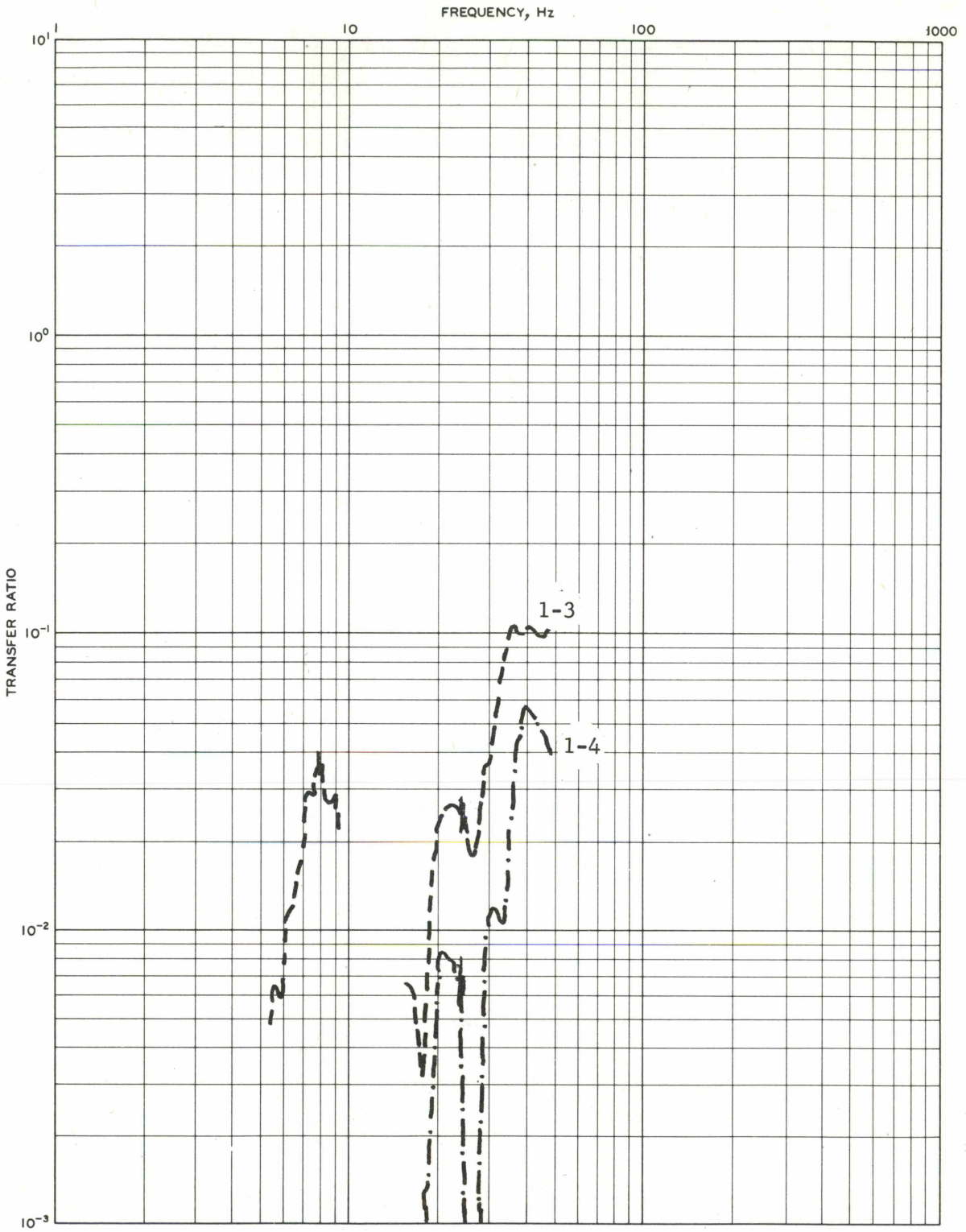

FIGURE 15. PRETRAFFIC TRANSFER RATIO RESULTS, TRACK SECTION 1, VERTICAL MODE, POINTS 1-3, 1-4

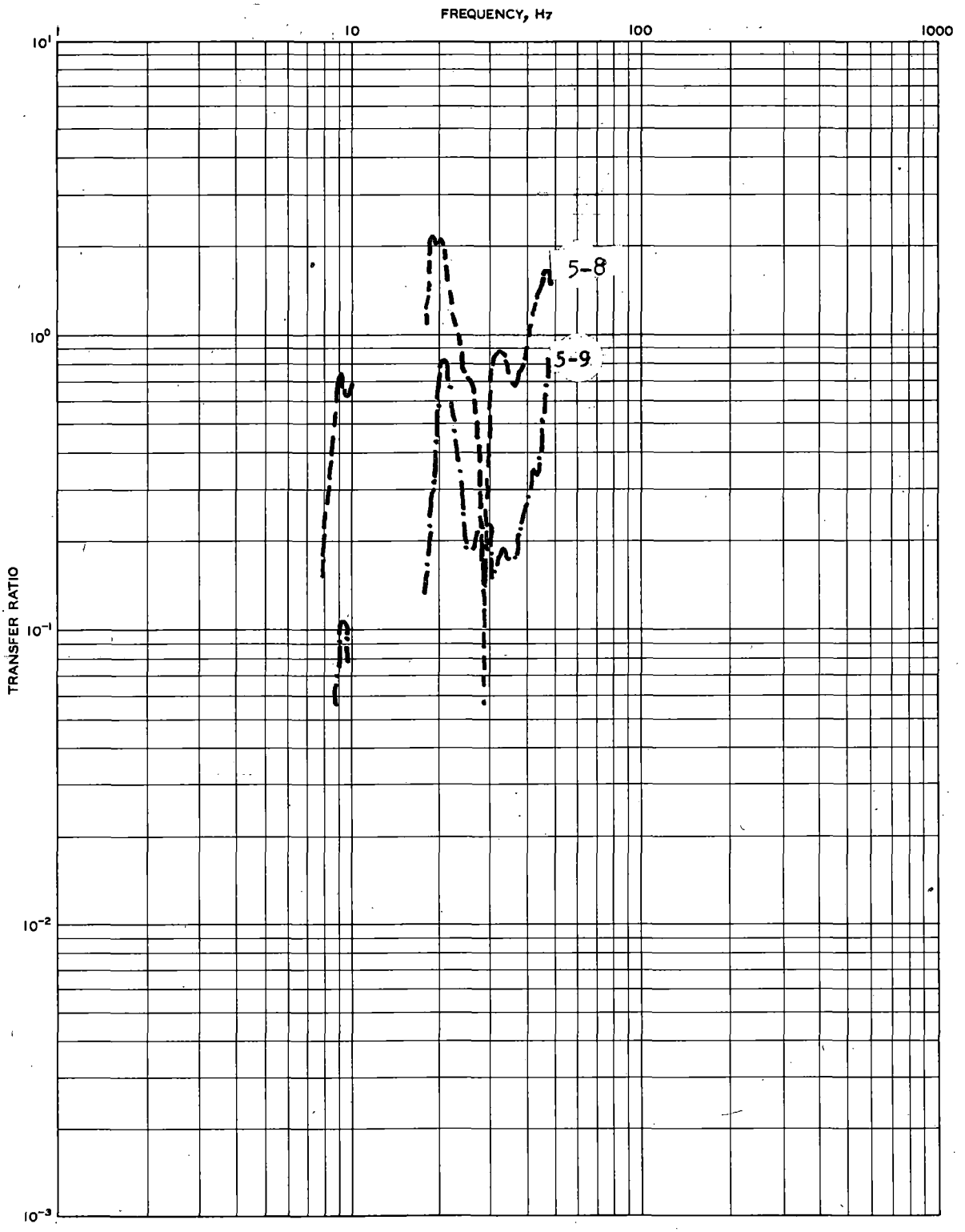

FIGURE 16. PRETRAFFIC TRANSFER RATIO RESULTS, TRACK SECTION 1, VERTICAL MODE, POINTS 5-8, 5-9

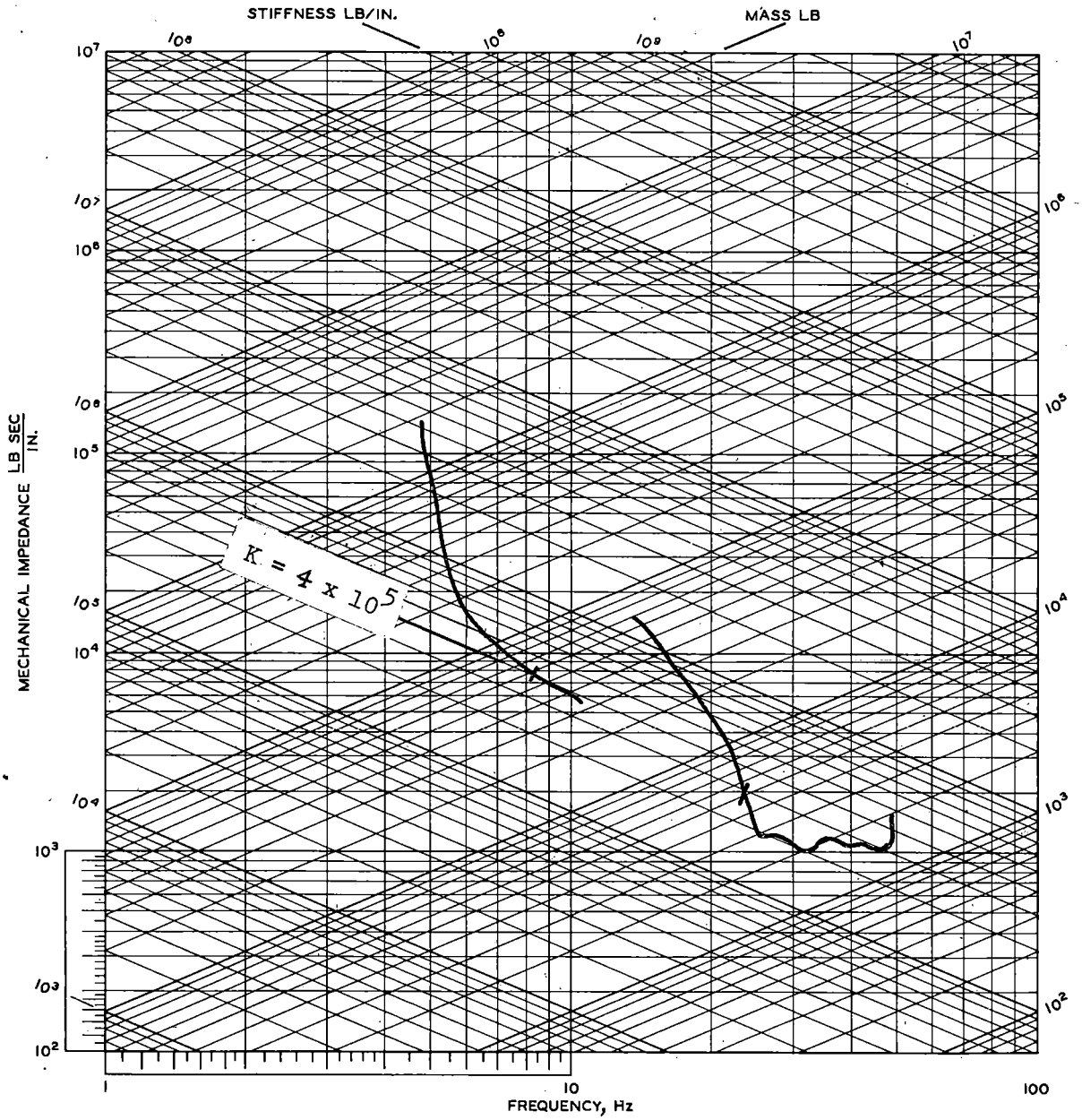

FIGURE 17. PRETRAFFIC MECHANICAL IMPEDANCE RESULTS, TRACK SECTION 2, VERTICAL MODE, POINT 1

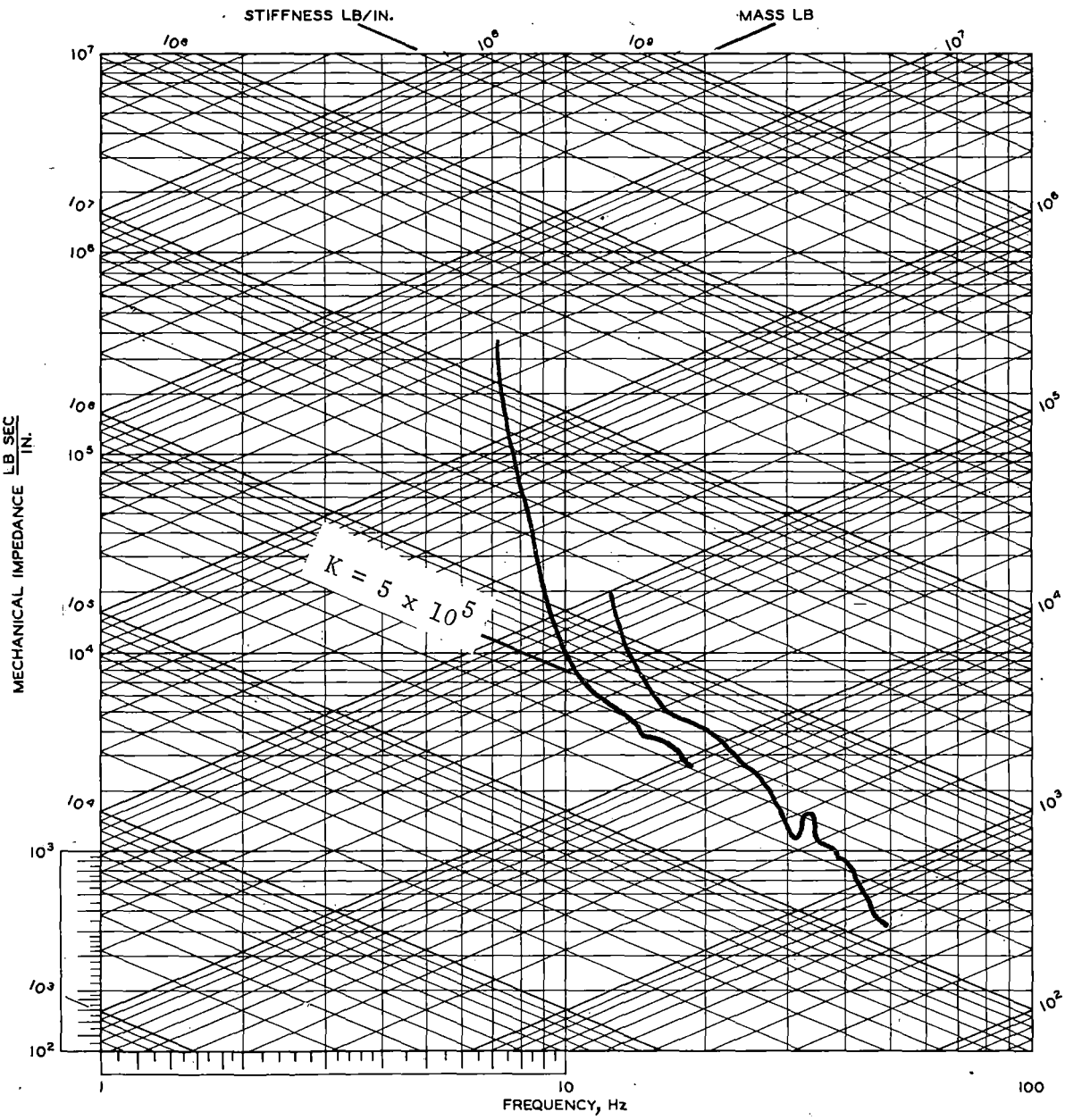

FIGURE 18. PRETRAFFIC MECHANICAL IMPEDANCE RESULTS, TRACK SECTION 2, ROCKING MODE, POINT 1

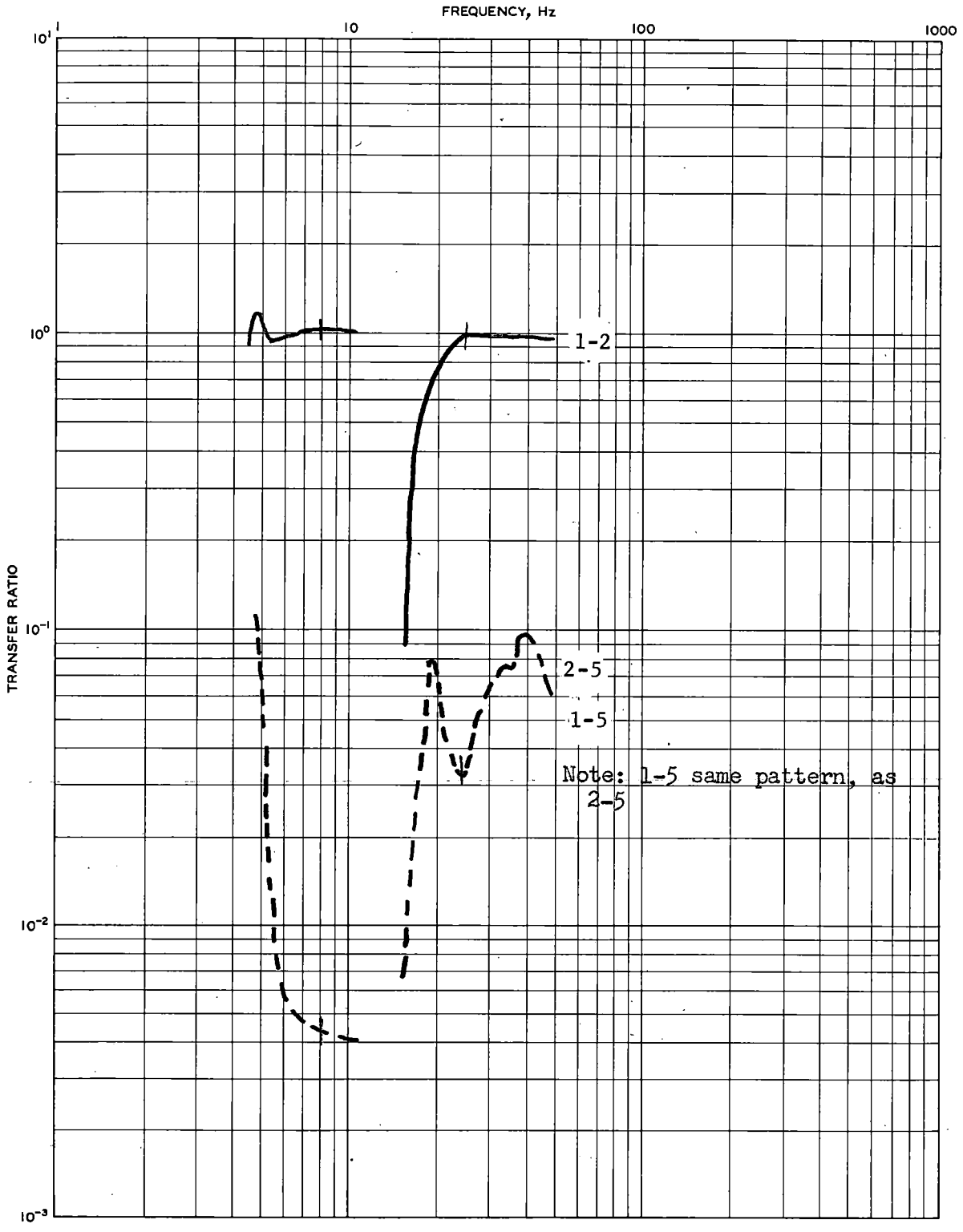

FIGURE 19. PRETRAFFIC TRANSFER RATIO RESULTS, TRACK SECTION 2, VERTICAL MODE, POINTS 1-2, 1-5, 2-5

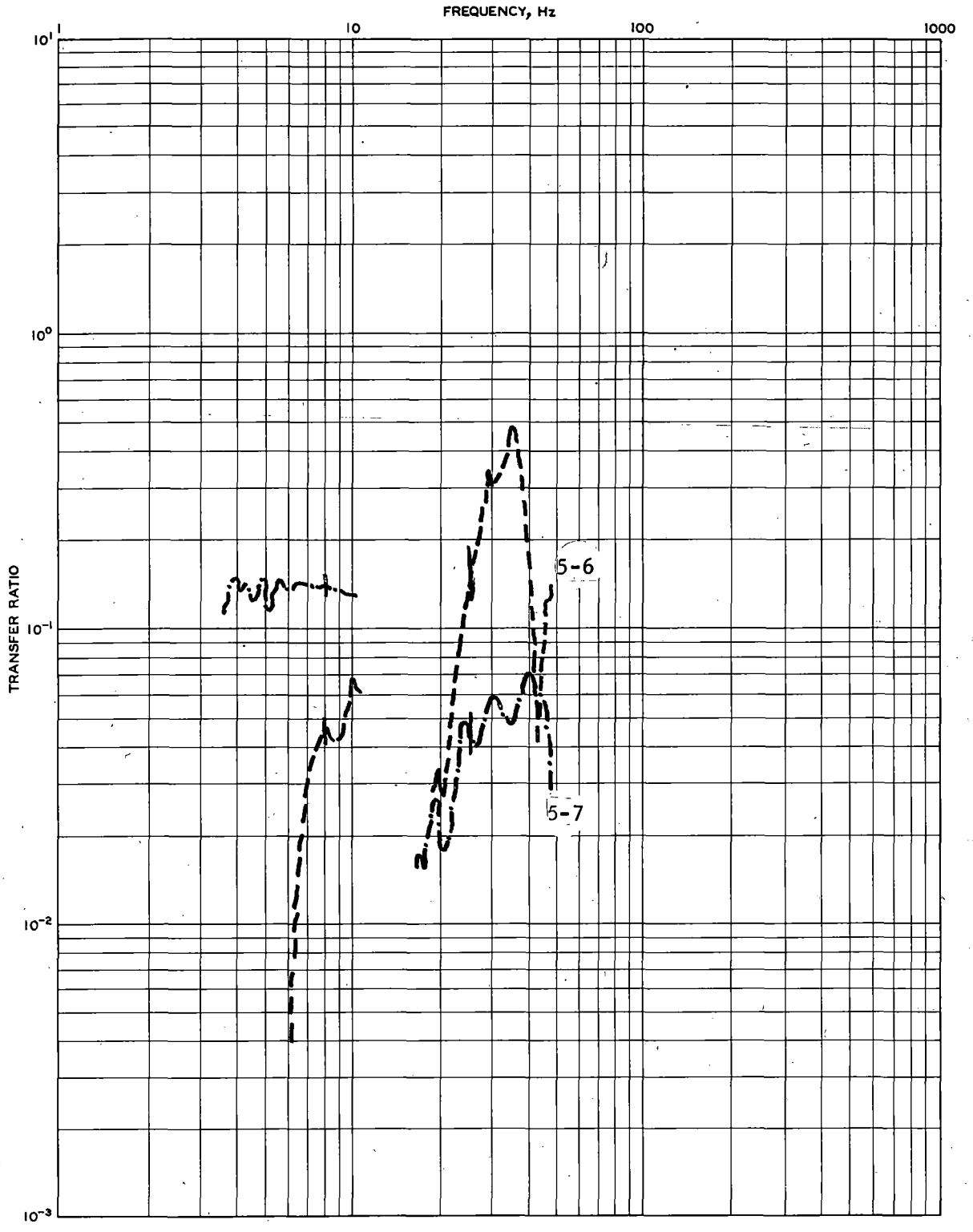

FIGURE 20. PRETRAFFIC TRANSFER RATIO RESULTS, TRACK SECTION 2, VERTICAL MODE, POINTS 5-6, 5-7

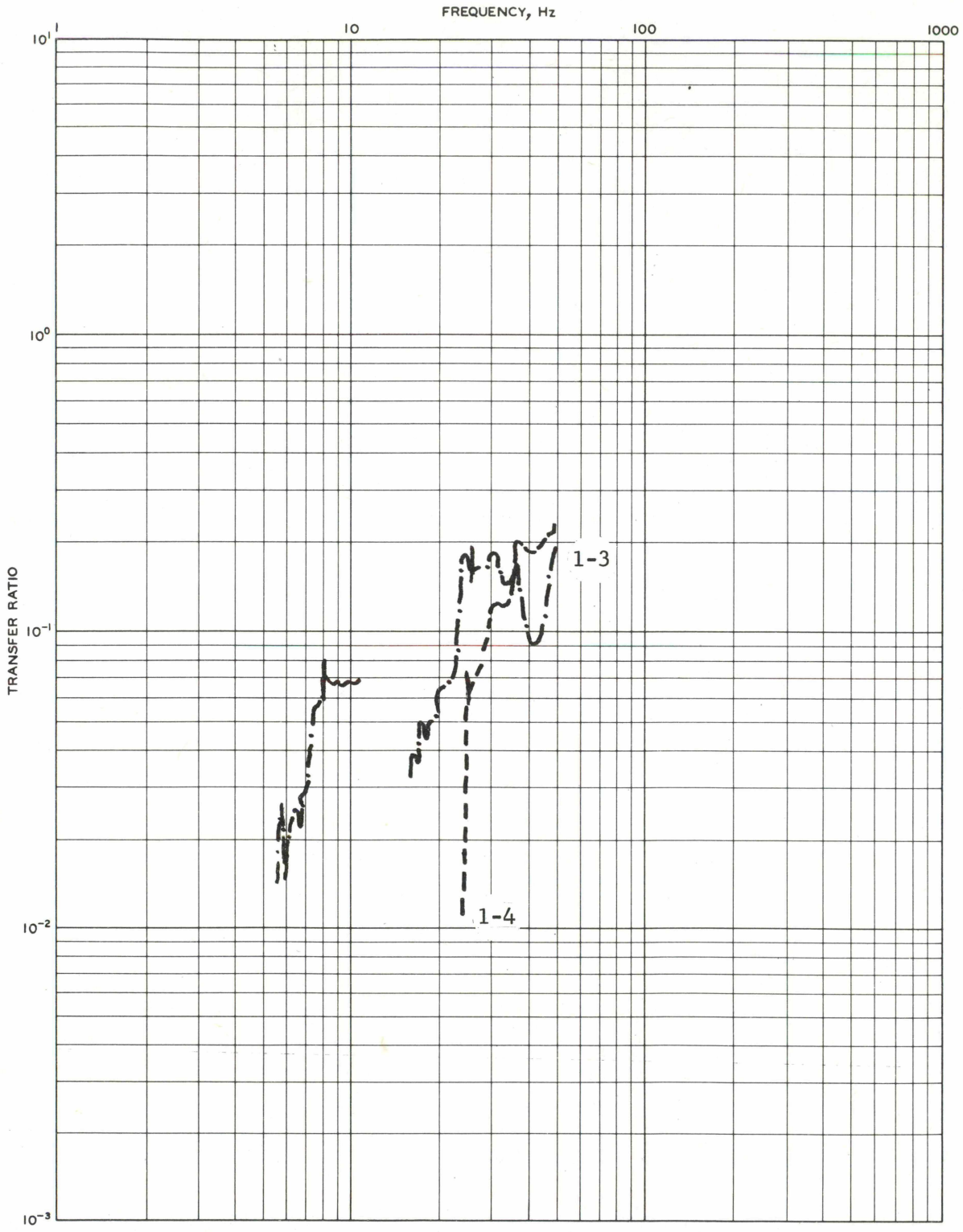

FIGURE 21. PRETRAFFIC TRANSFER RATIO RESULTS, TRACK SECTION 2, VERTICAL MODE, POINTS 1-3, 1-4

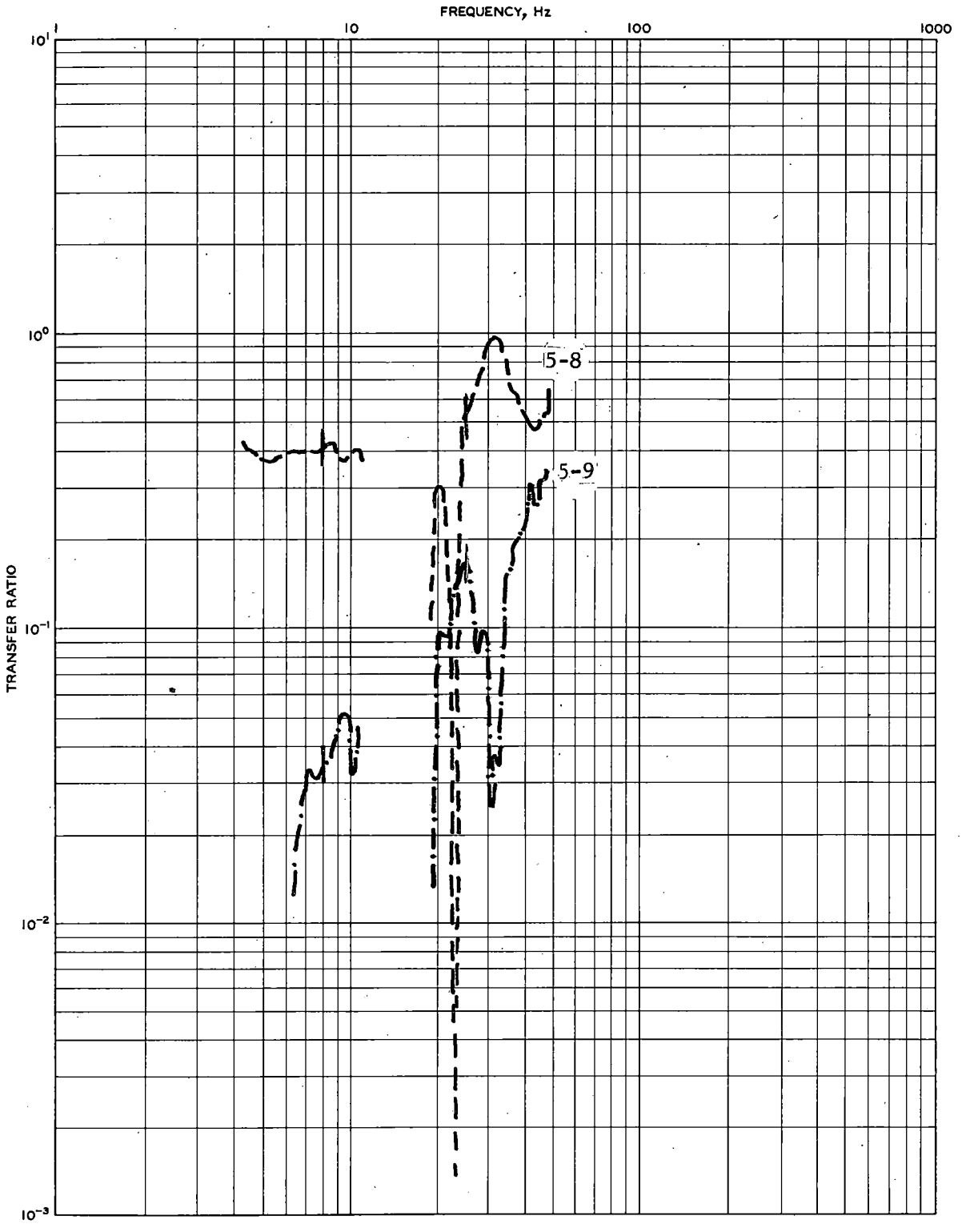

FIGURE 22. PRETRAFFIC TRANSFER RATIO RESULTS, TRACK SECTION-2, VERTICAL MODE, POINTS 5-8, 5-9

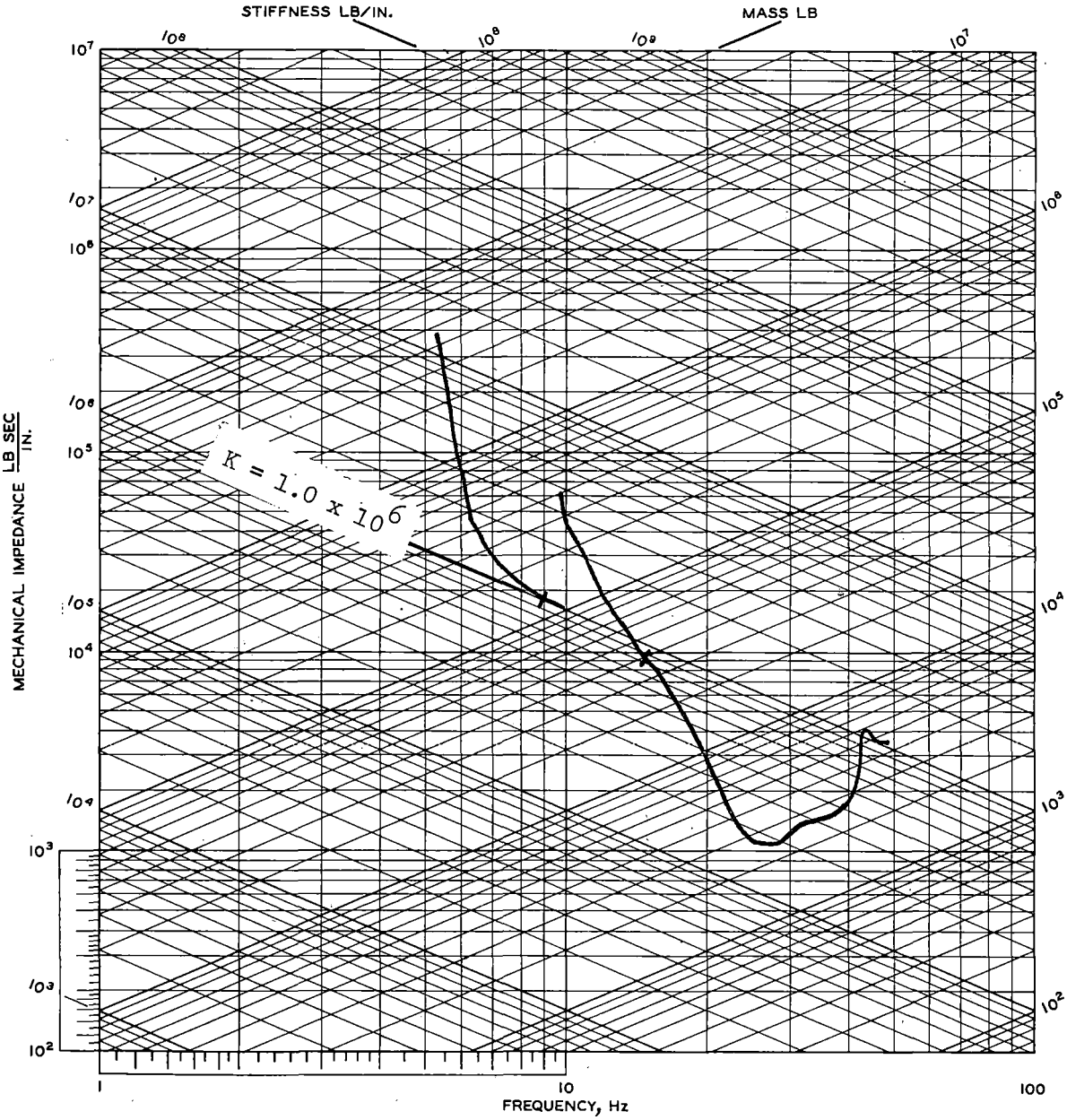

FIGURE 23. PRETRAFFIC MECHANICAL IMPEDANCE RESULTS, TRACK SECTION 3, VERTICAL MODE, POINT 1

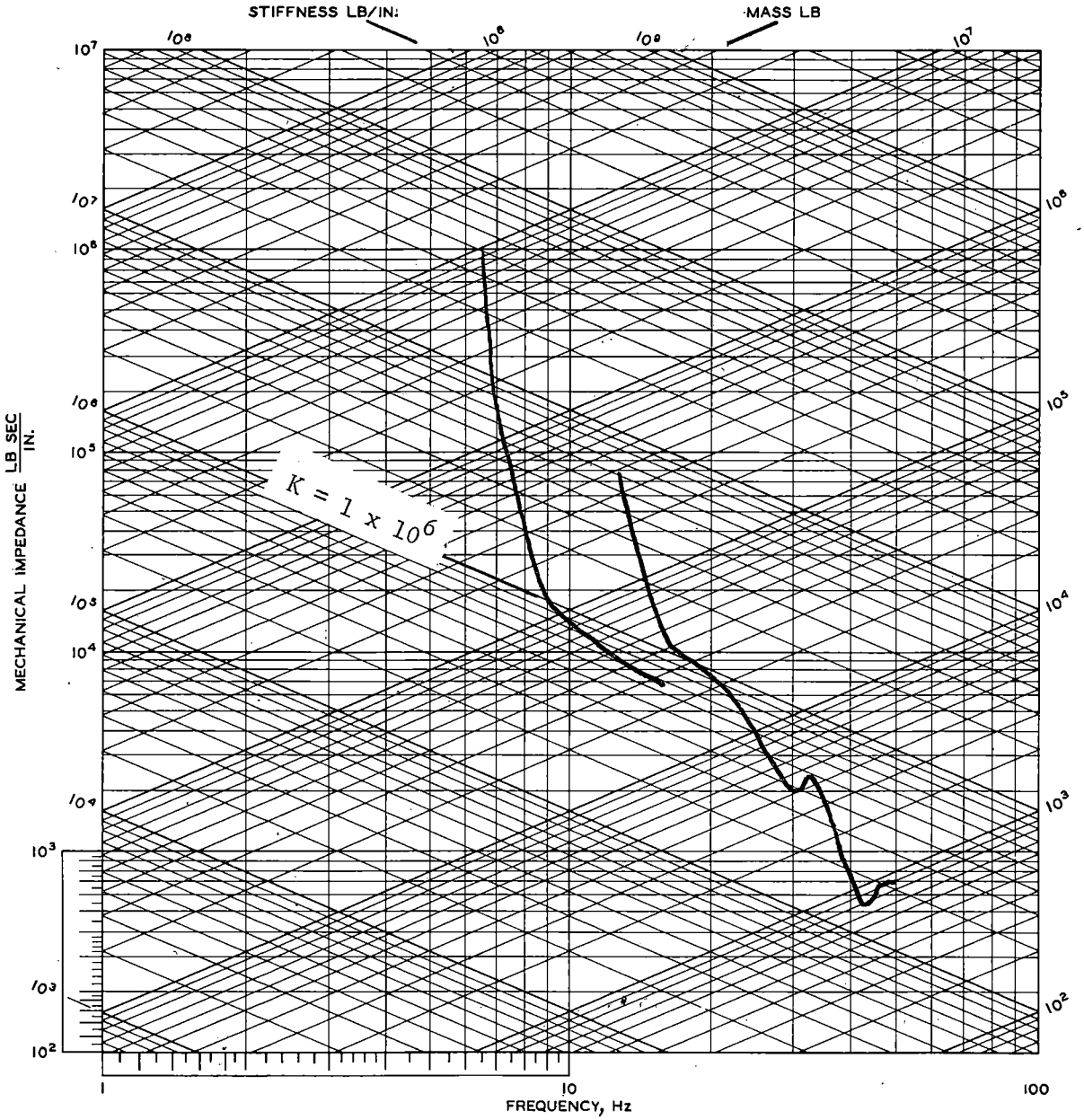

FIGURE 24. PRETRAFFIC MECHANICAL IMPEDANCE RESULTS, TRACK SECTION 3, ROCKING MODE, POINT 1

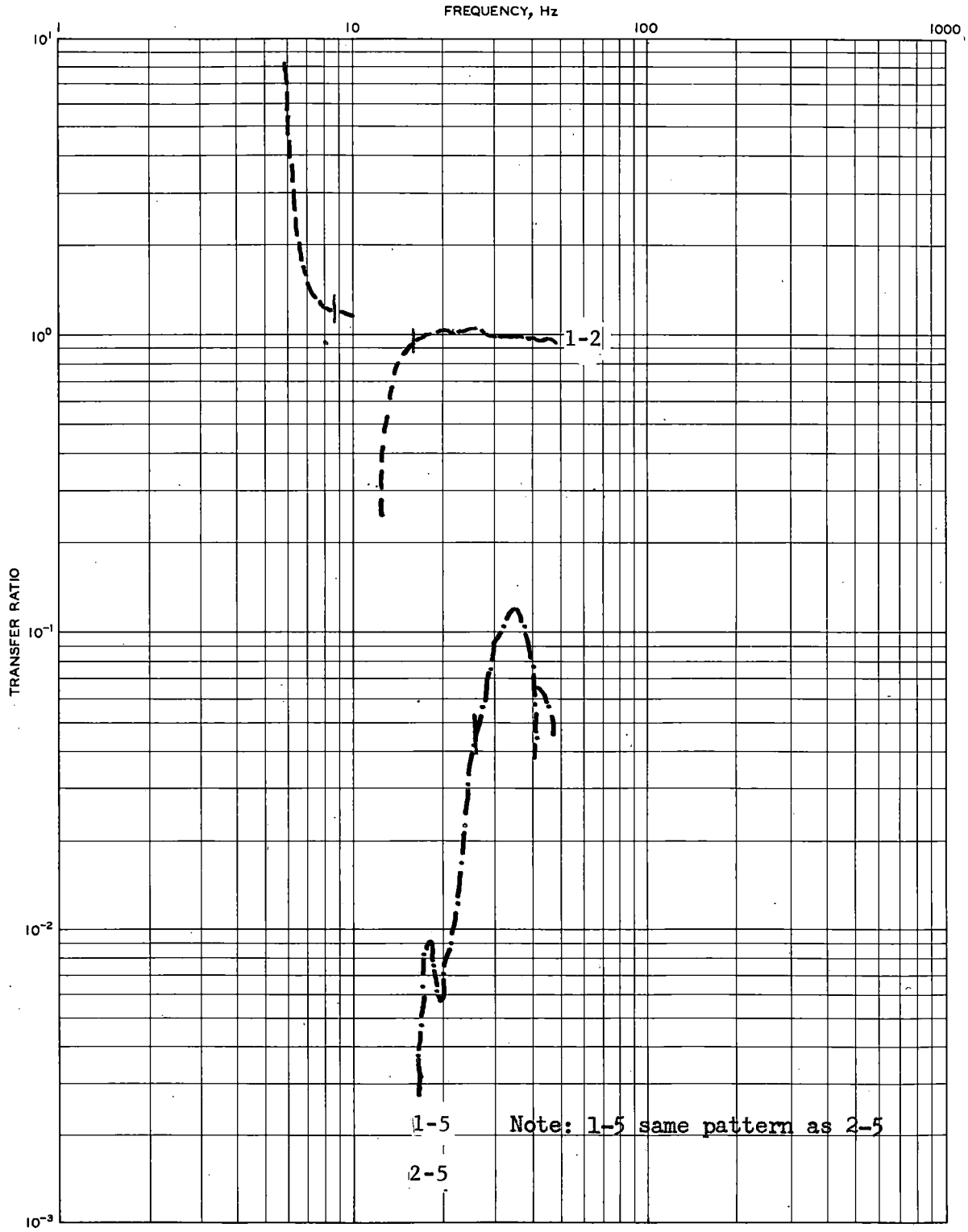

FIGURE 25. PRETRAFFIC TRANSFER RATIO RESULTS, TRACK SECTION 3, VERTICAL MODE, POINTS 1-2, 2-5, 1-5

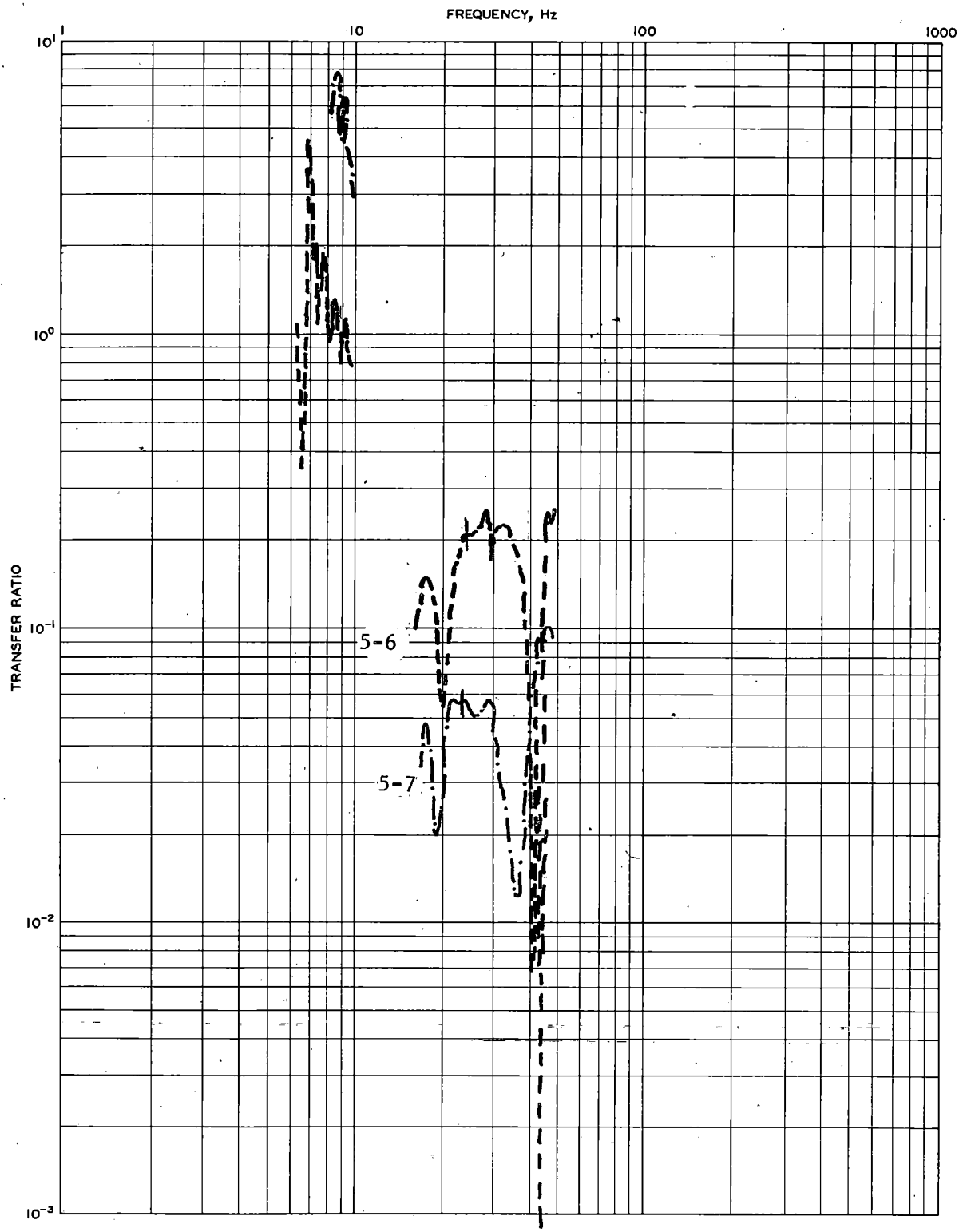

FIGURE 26. PRETRAFFIC TRANSFER RATIO RESULTS, TRACK SECTION 3, VERTICAL MODE, POINTS 5-6, 5-7

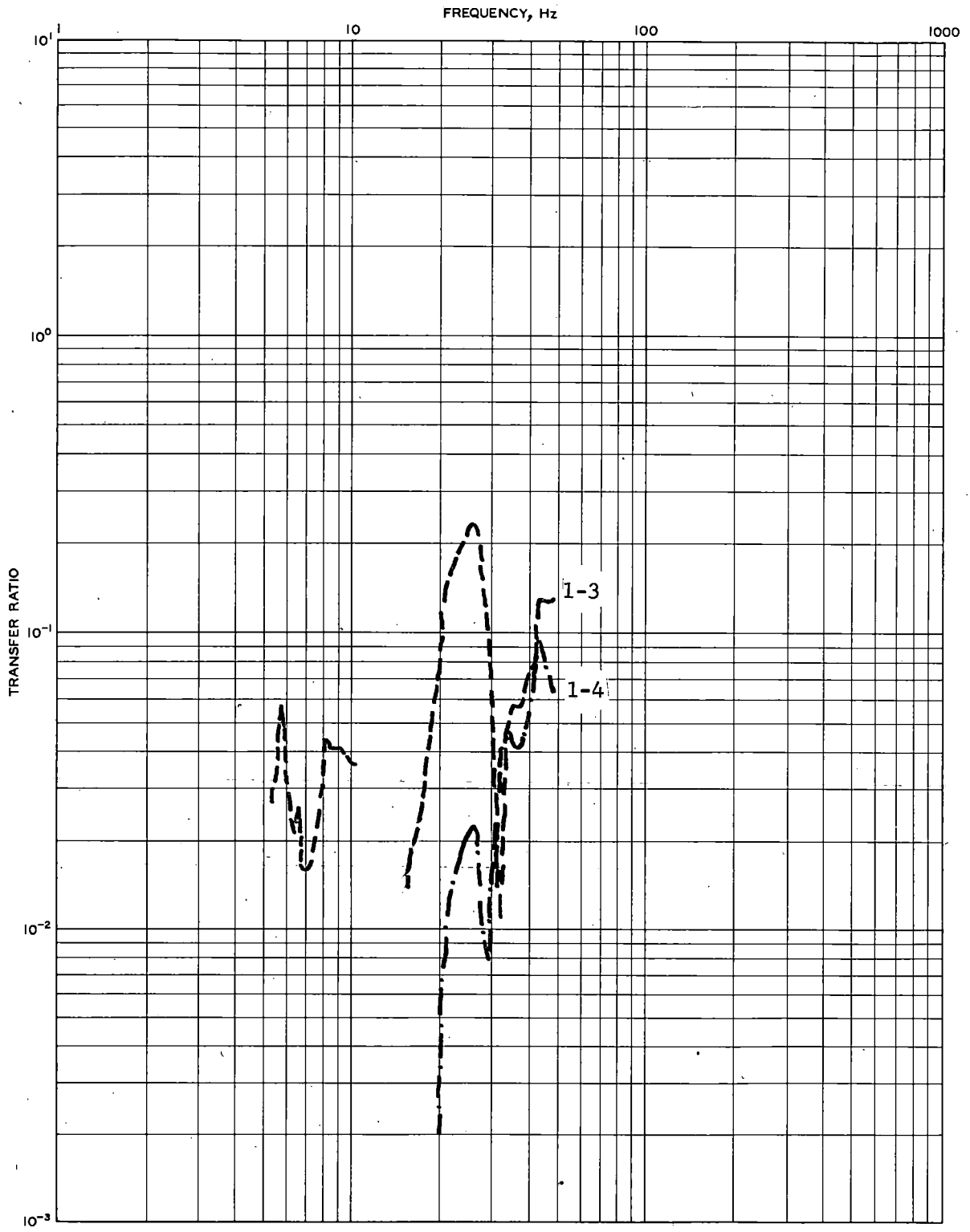

FIGURE 27. PRETRAFFIC TRANSFER RATIO RESULTS, TRACK SECTION 3, VERTICAL MODE, POINTS 1-3, 1-4

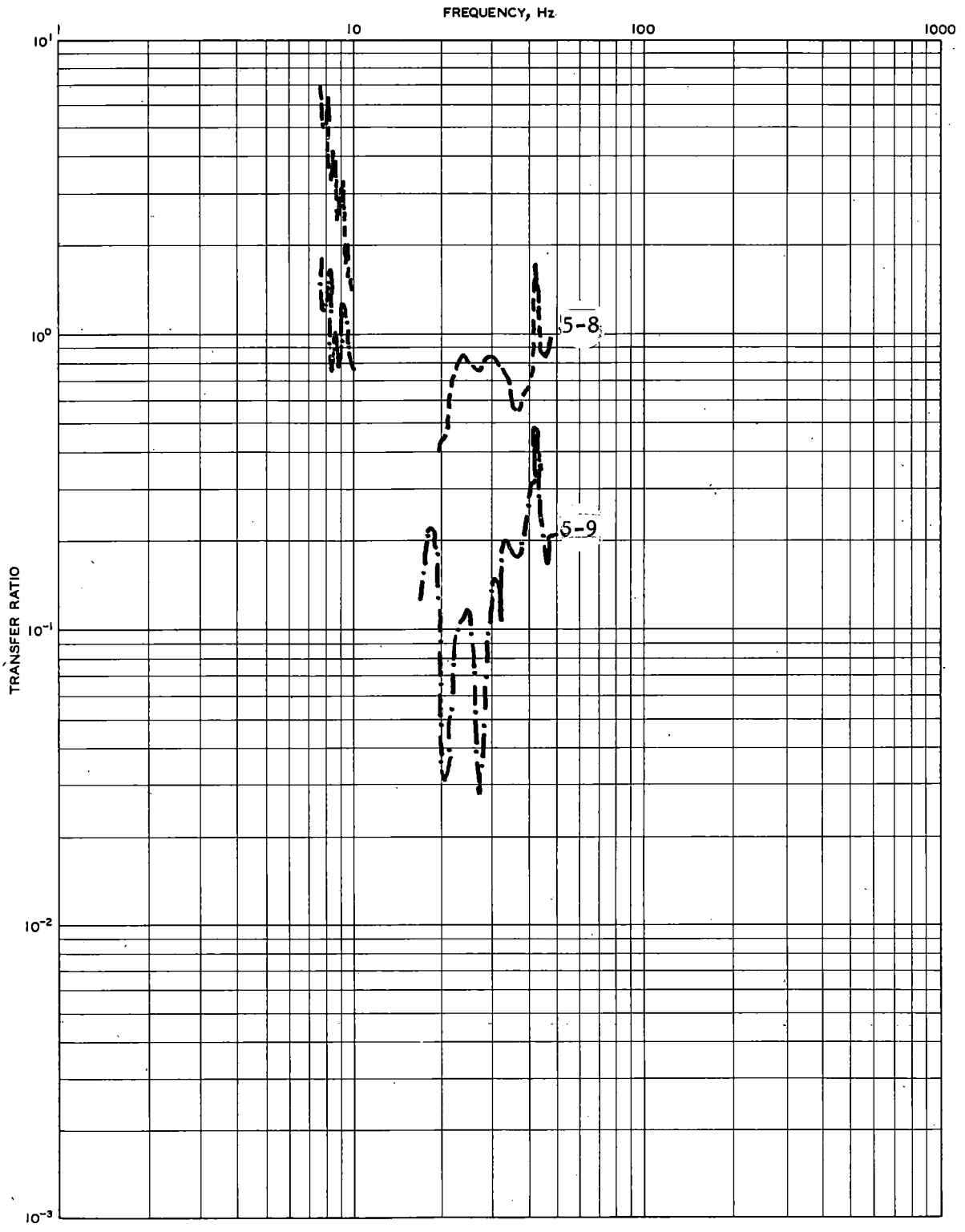

FIGURE 28. PRETRAFFIC TRANSFER RATIO RESULTS, TRACK SECTION 3, VERTICAL MODE, POINTS 5-8, 5-9

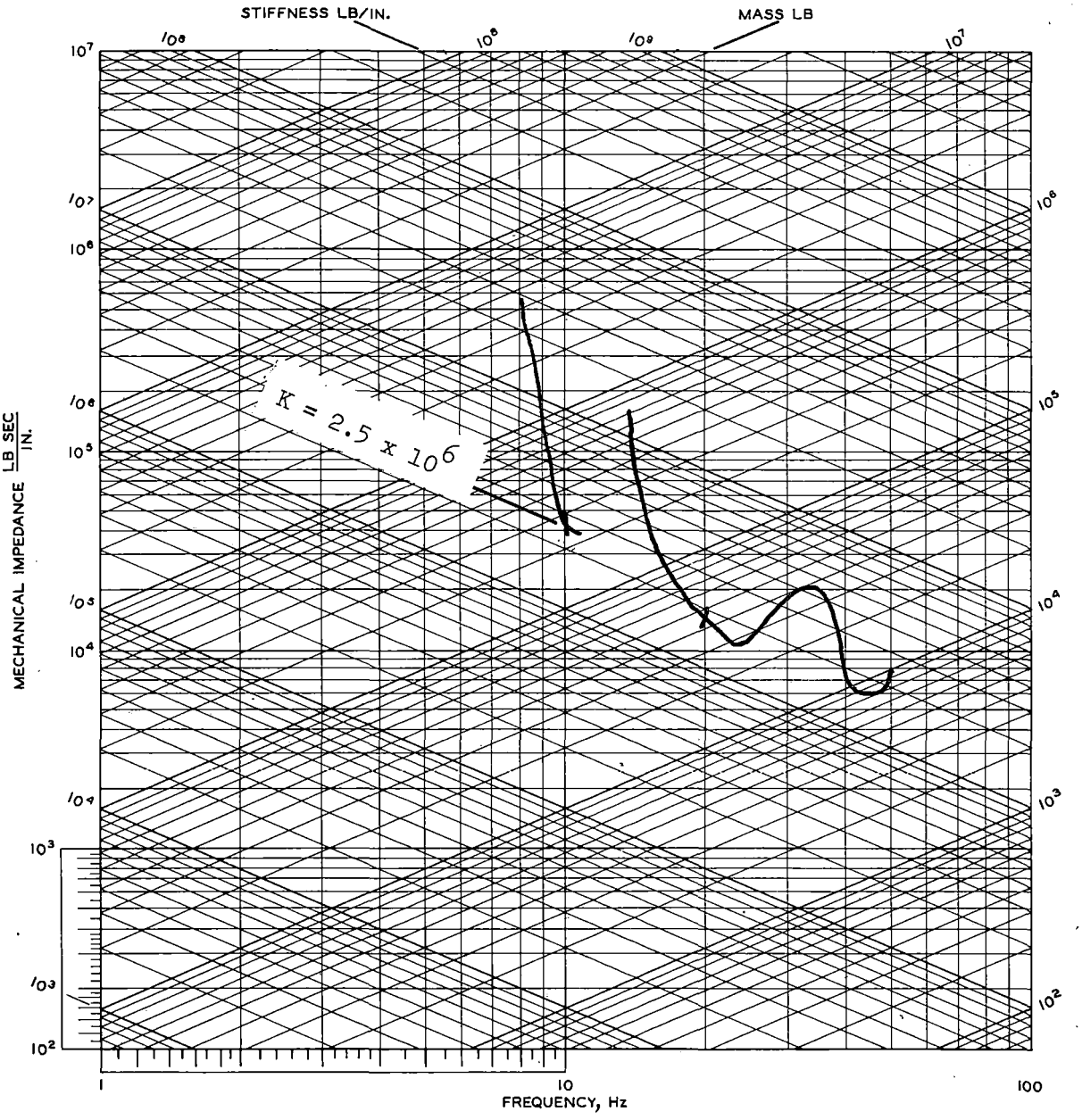

FIGURE 29. PRETRAFFIC MECHANICAL IMPEDANCE RESULTS, TRACK SECTION 4, VERTICAL MODE, POINT 1

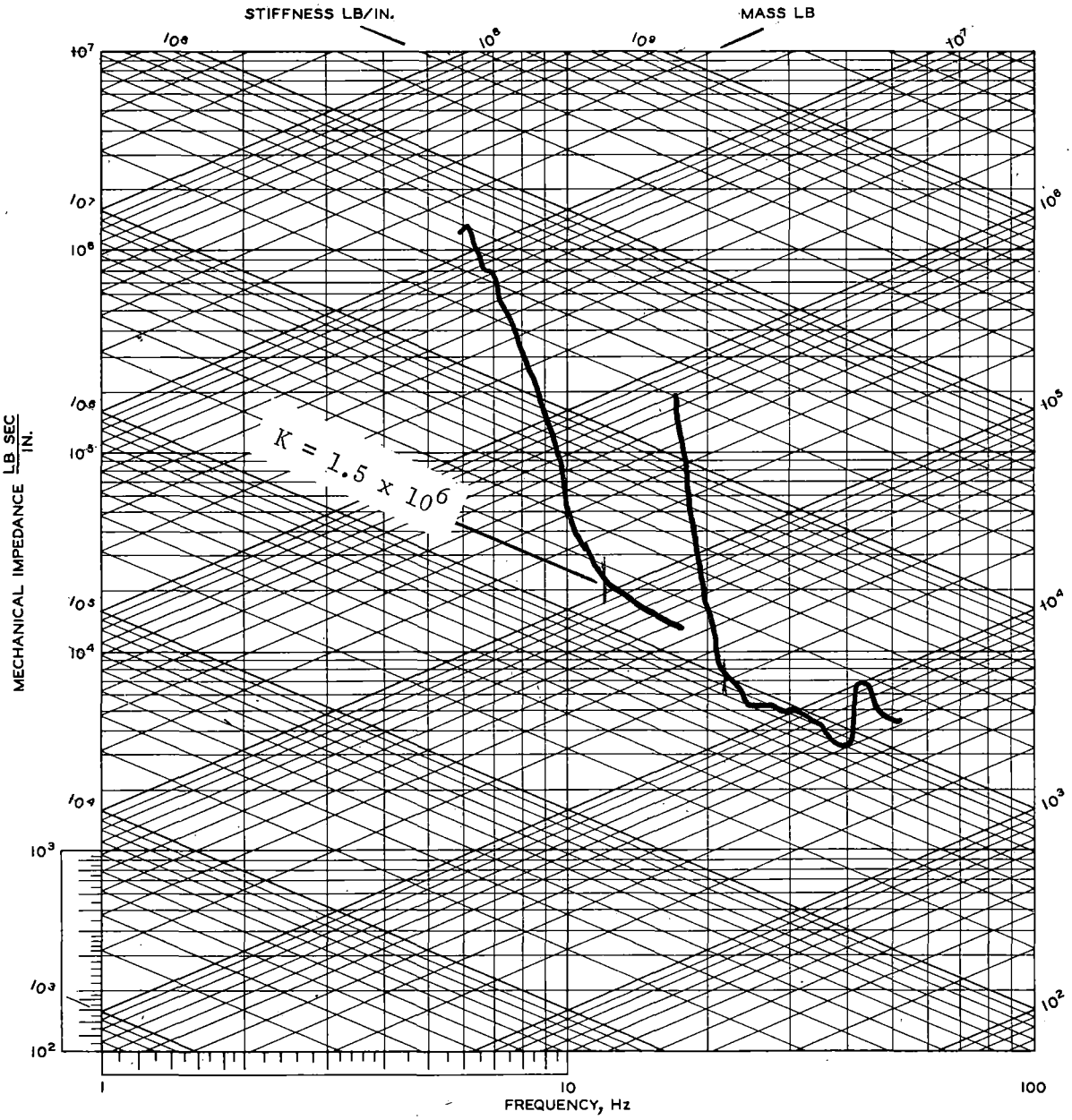

FIGURE 30. PRETRAFFIC MECHANICAL IMPEDANCE RESULTS, TRACK SECTION 4, ROCKING MODE, POINT 1

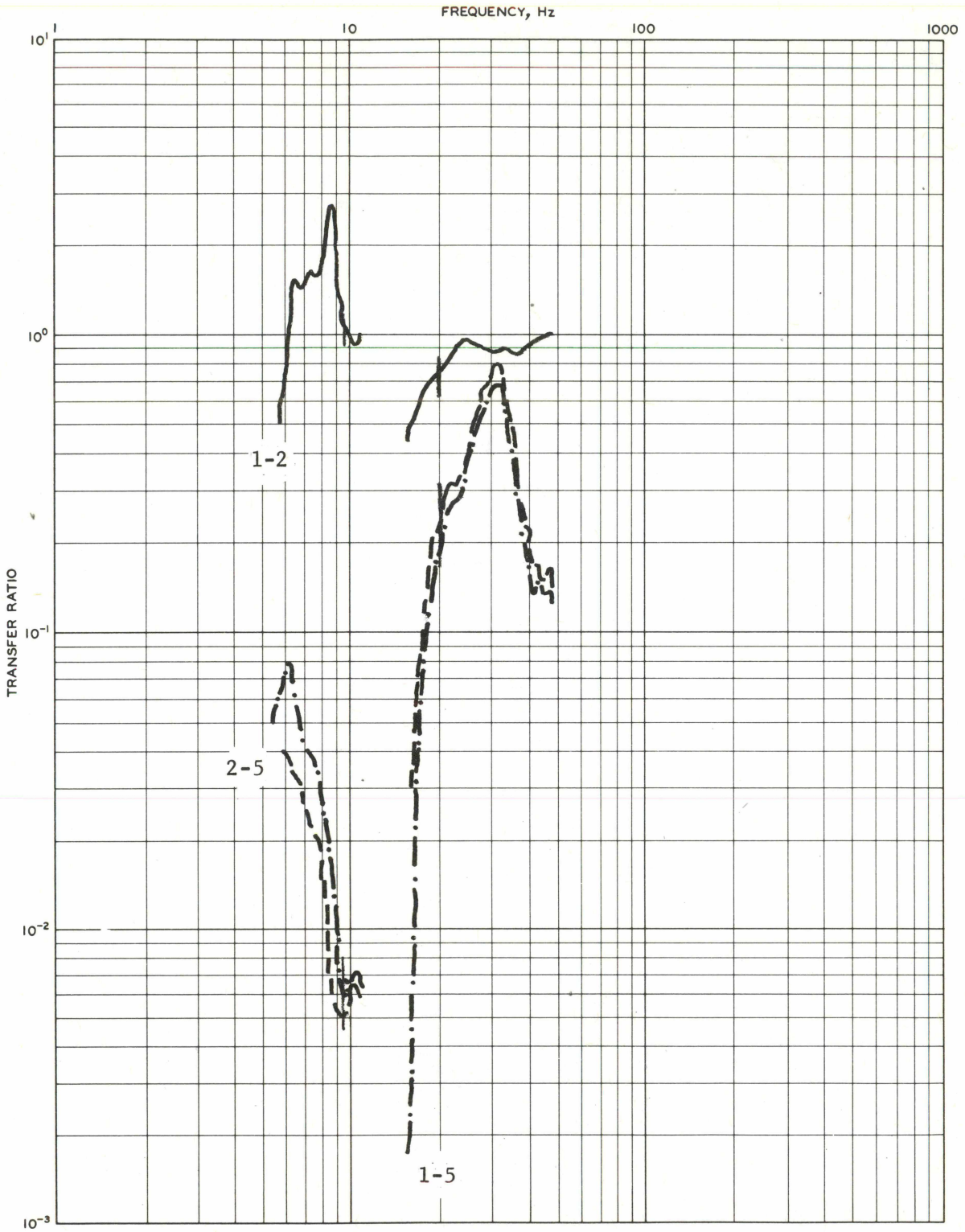

FIGURE 31. PRETRAFFIC TRANSFER RATIO RESULTS, TRACK SECTION 4, VERTICAL MODE, POINTS 1-2, 2-5, 1-5

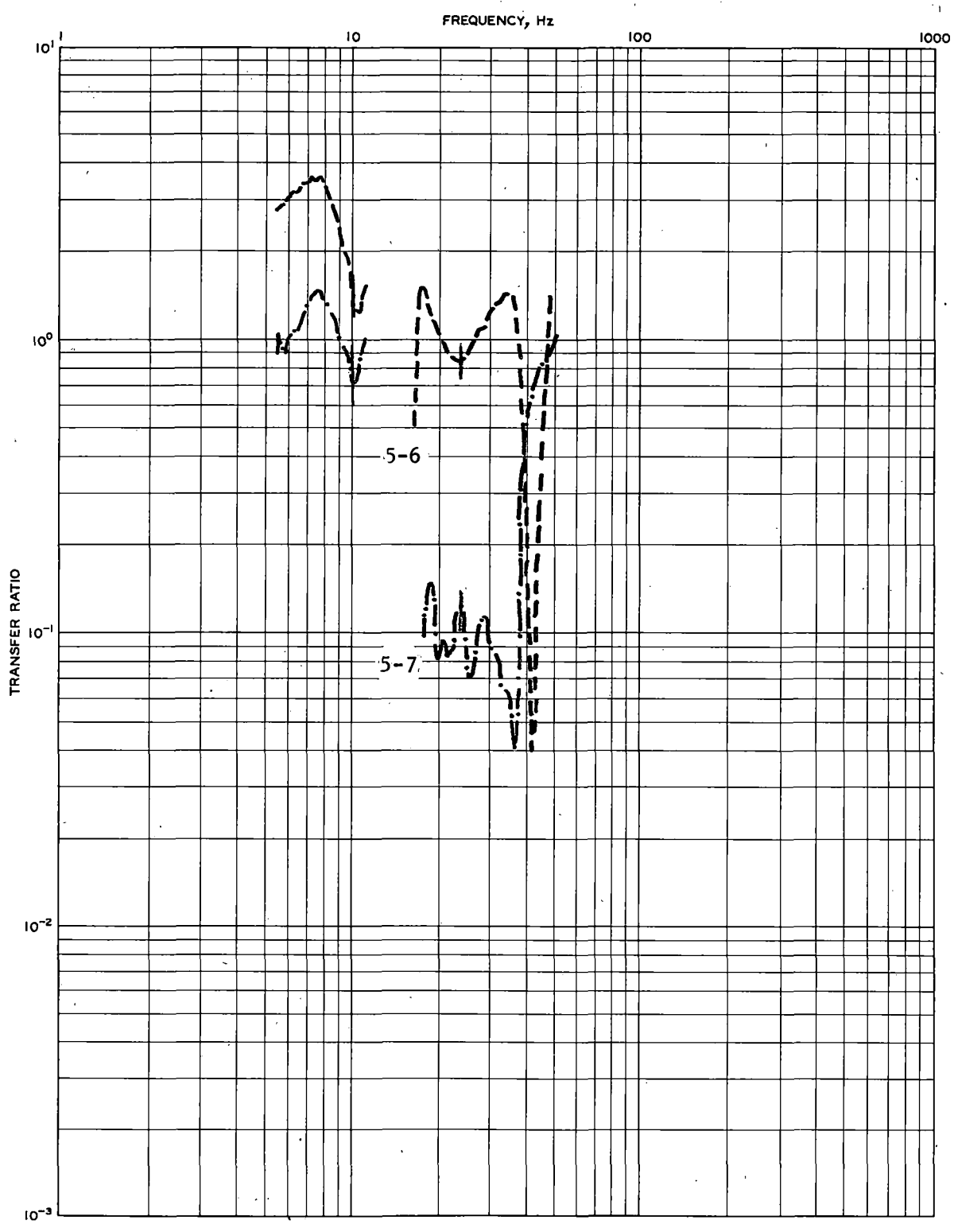

FIGURE 32. PRETRAFFIC TRANSFER RATIO RESULTS, TRACK SECTION 4, VERTICAL MODE, POINTS 5-6, 5-7

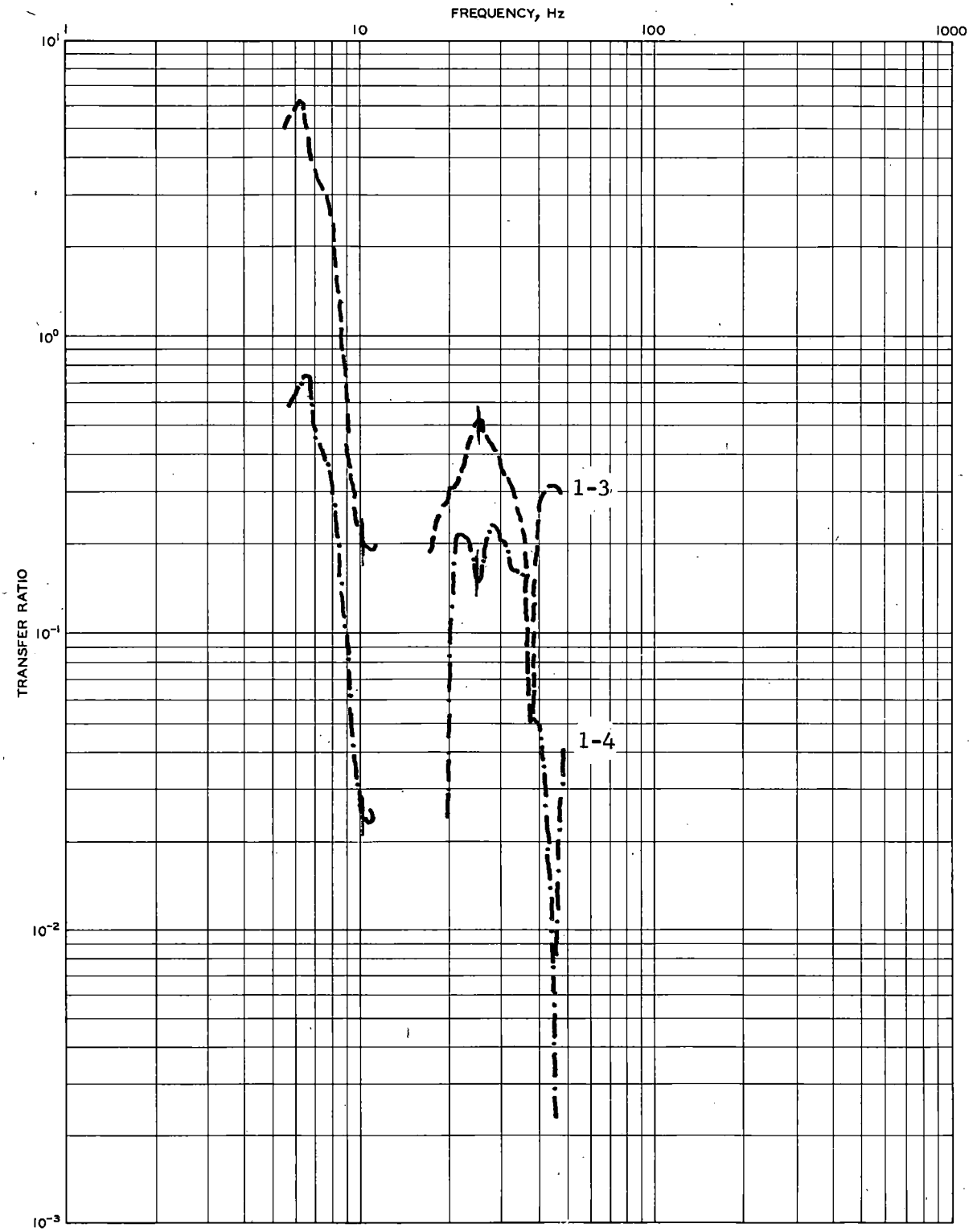

FIGURE 33. PRETRAFFIC TRANSFER RATIO RESULTS, TRACK SECTION 4, VERTICAL MODE, POINTS 1-3, 1-4

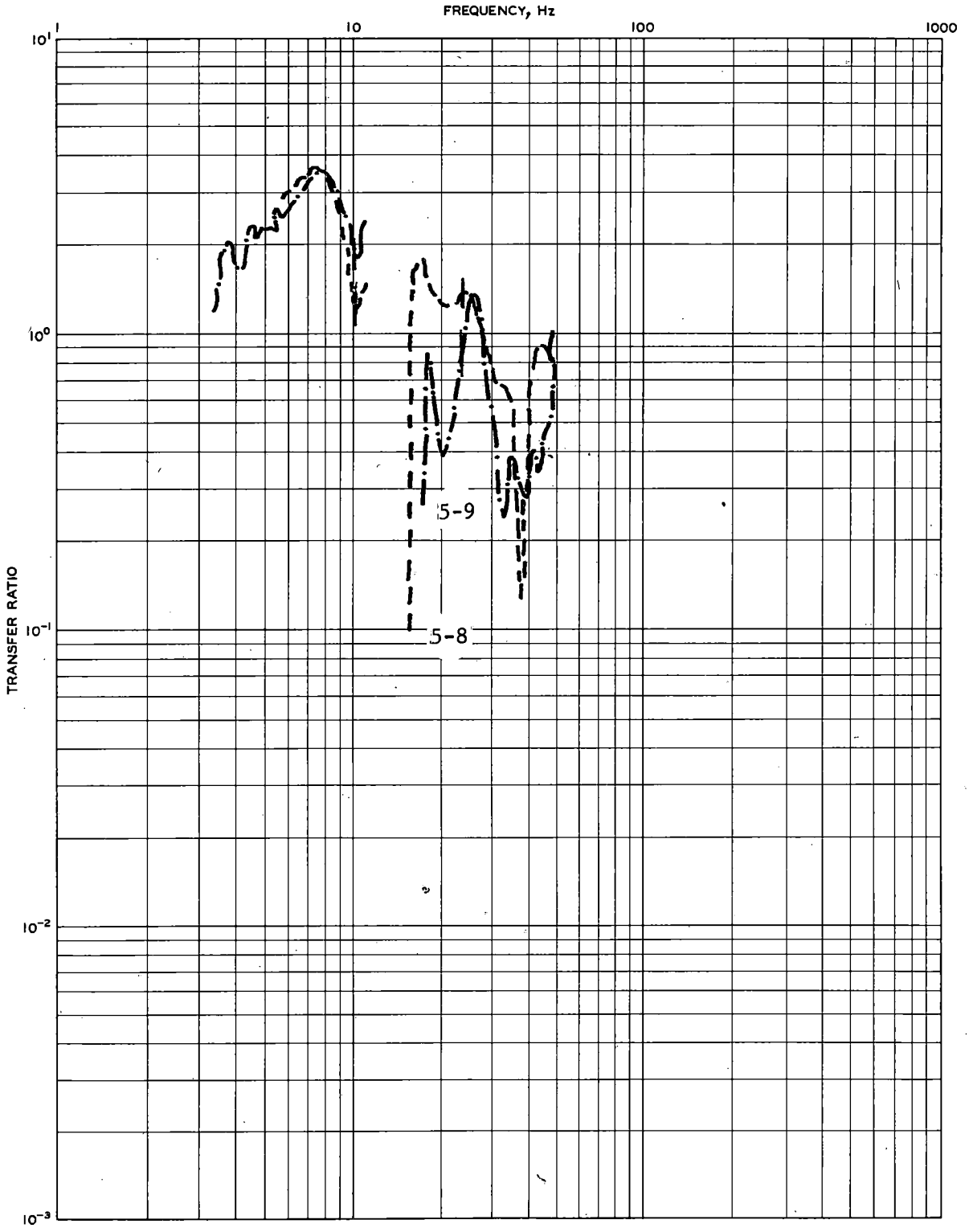

FIGURE 34. PRETRAFFIC TRANSFER RATIO RESULTS, TRACK SECTION 4, VERTICAL MODE, POINTS 5-8, 5-9

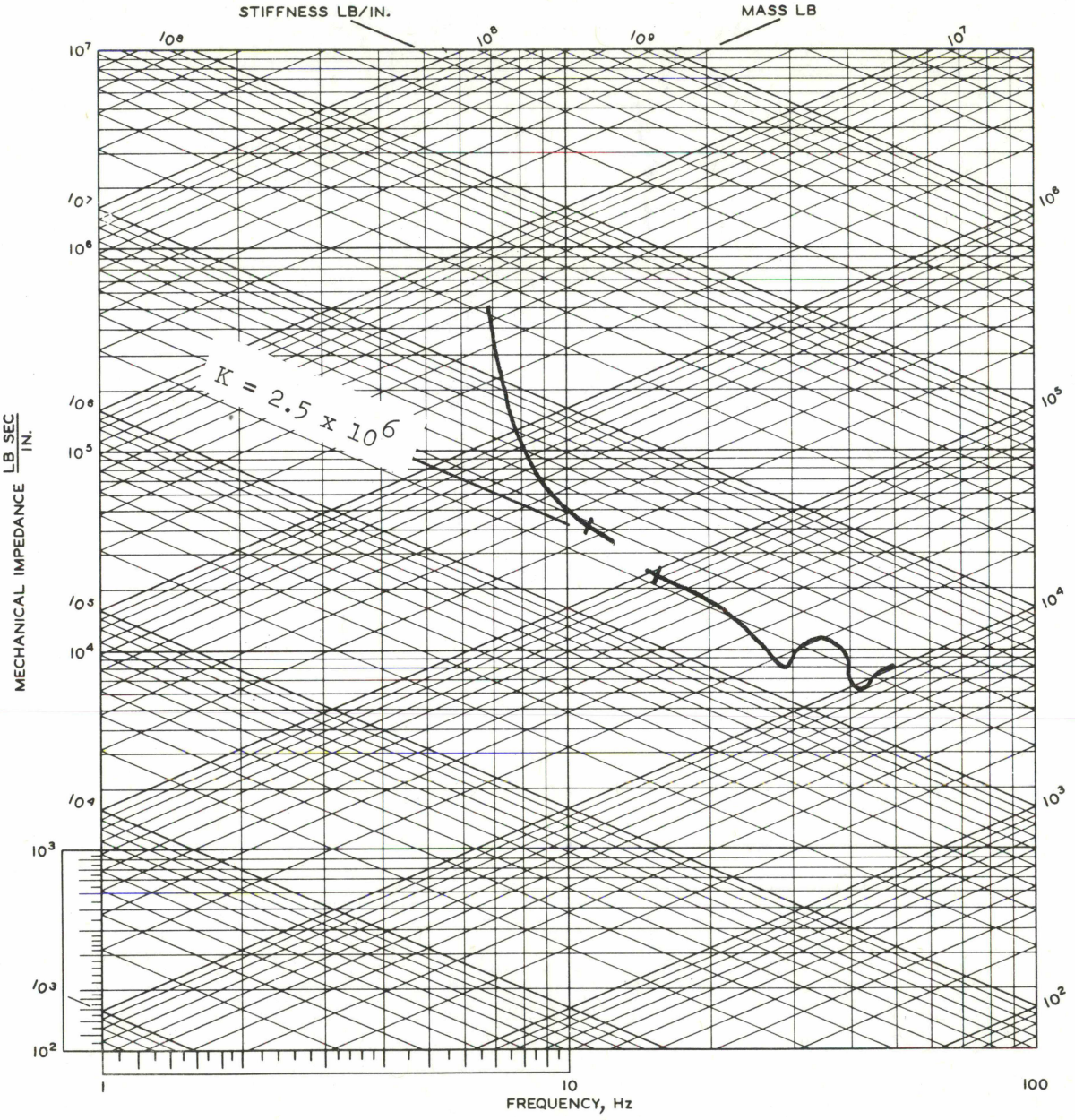

FIGURE 35. PRETRAFFIC MECHANICAL IMPEDANCE RESULTS, TRACK SECTION 5, VERTICAL MODE, POINT 1

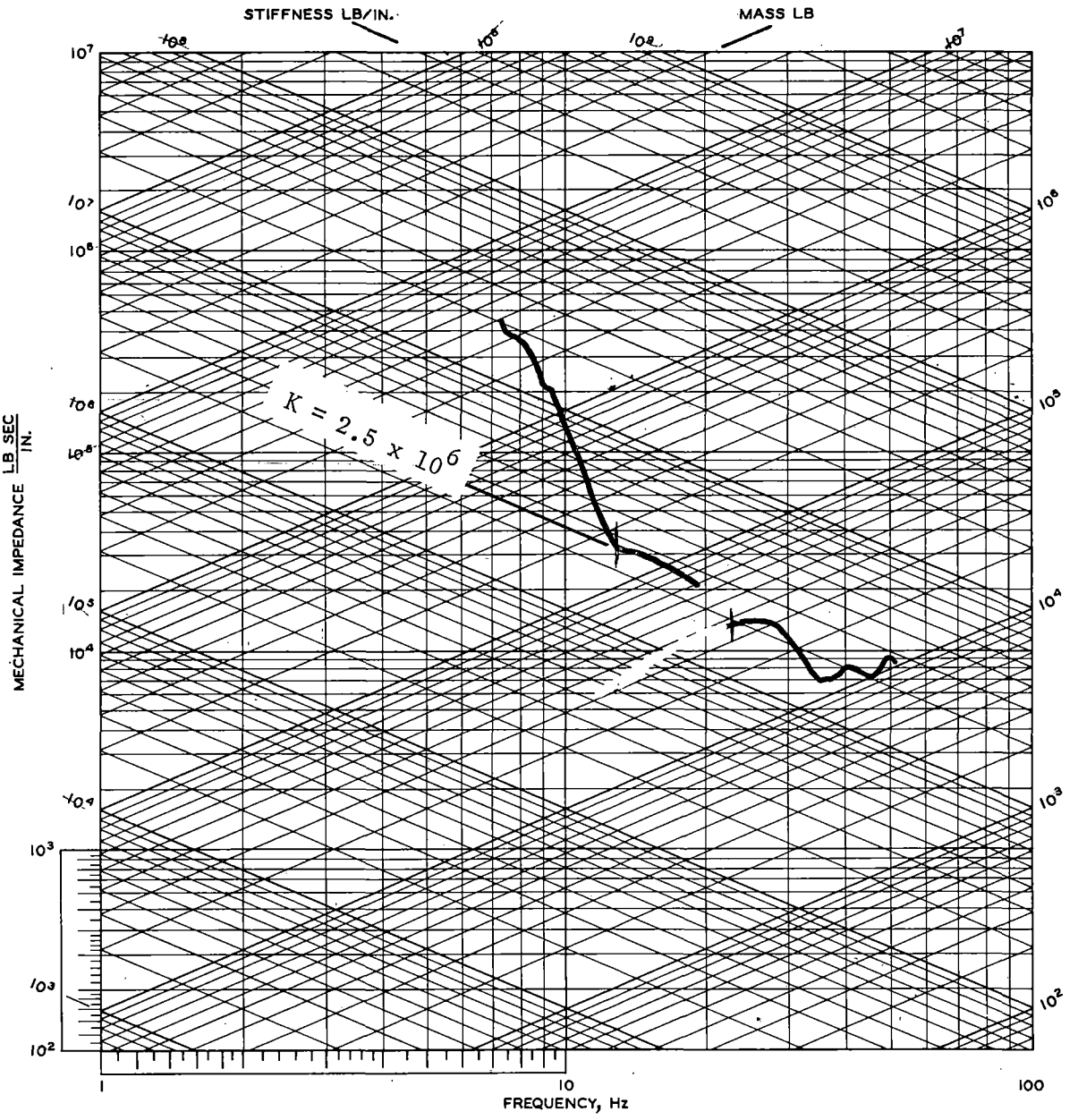

FIGURE 36. PRETRAFFIC MECHANICAL IMPEDANCE RESULTS, TRACK SECTION 5, ROCKING MODE, POINT 1

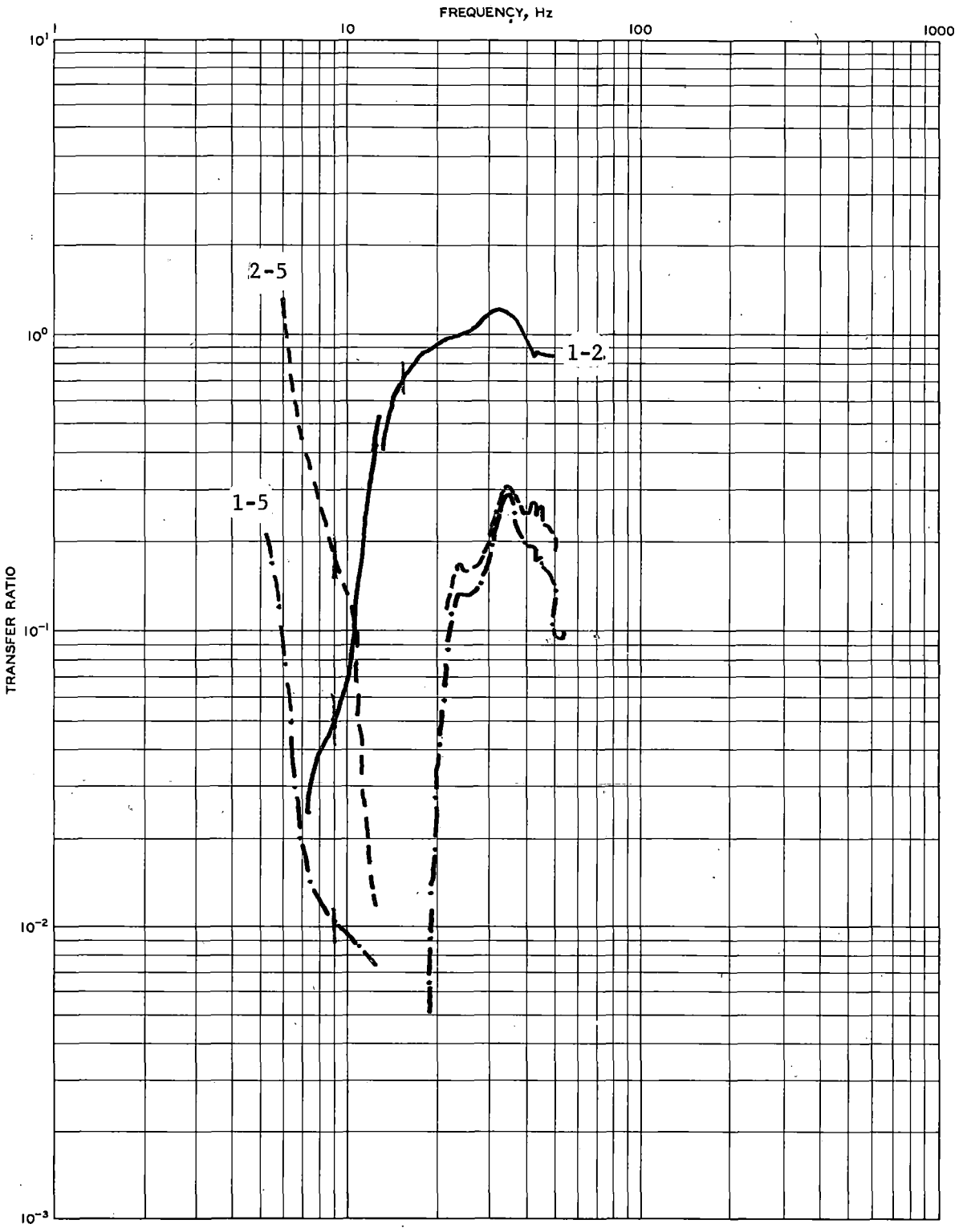

FIGURE 37. PRETRAFFIC TRANSFER RATIO RESULTS, TRACK SECTION 5, VERTICAL MODE, POINTS 1-2, 1-5, 2-5

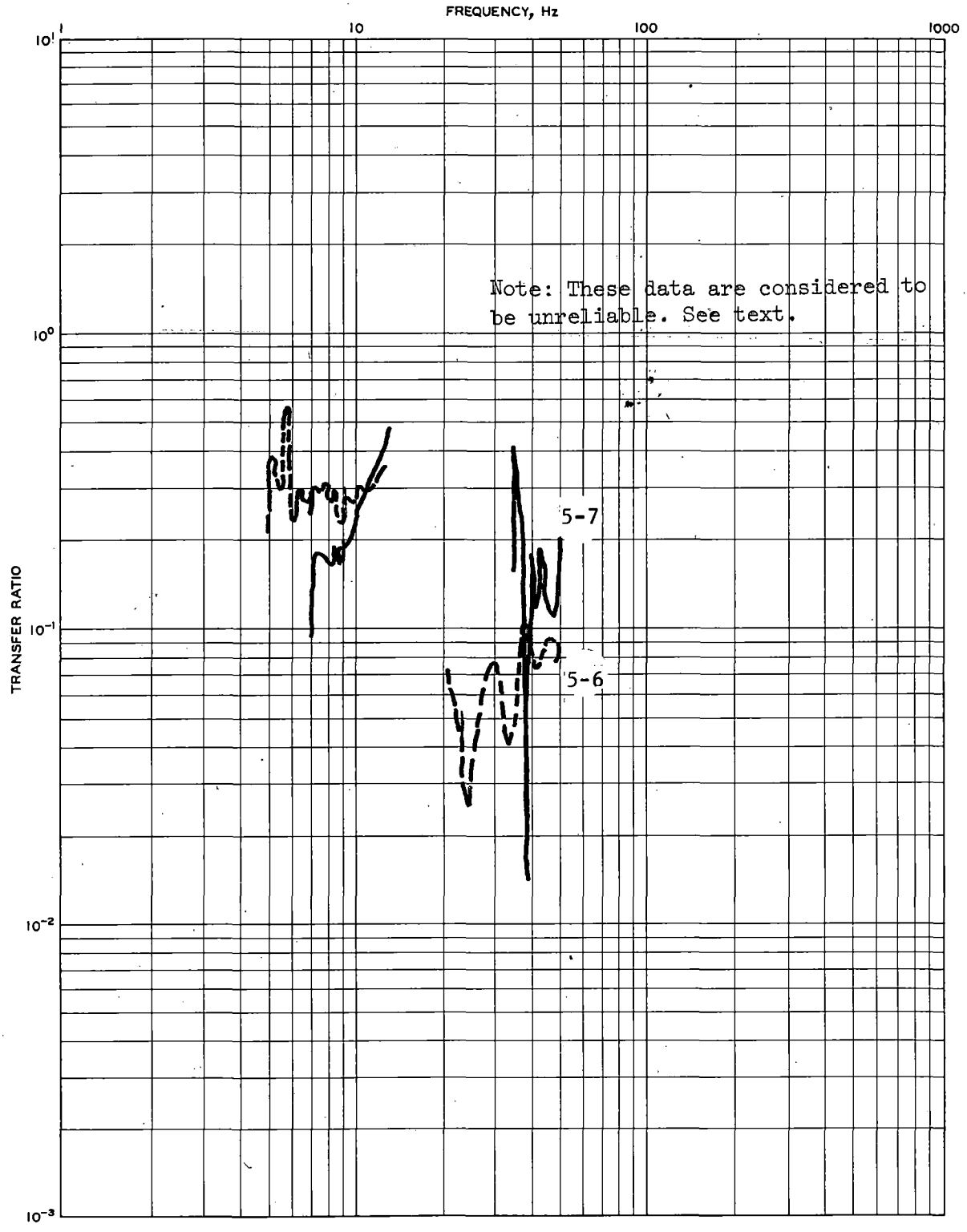

FIGURE 38. PRETRAFFIC TRANSFER RATIO RESULTS, TRACK SECTION 5, VERTICAL MODE, POINTS 5-6, 5-7

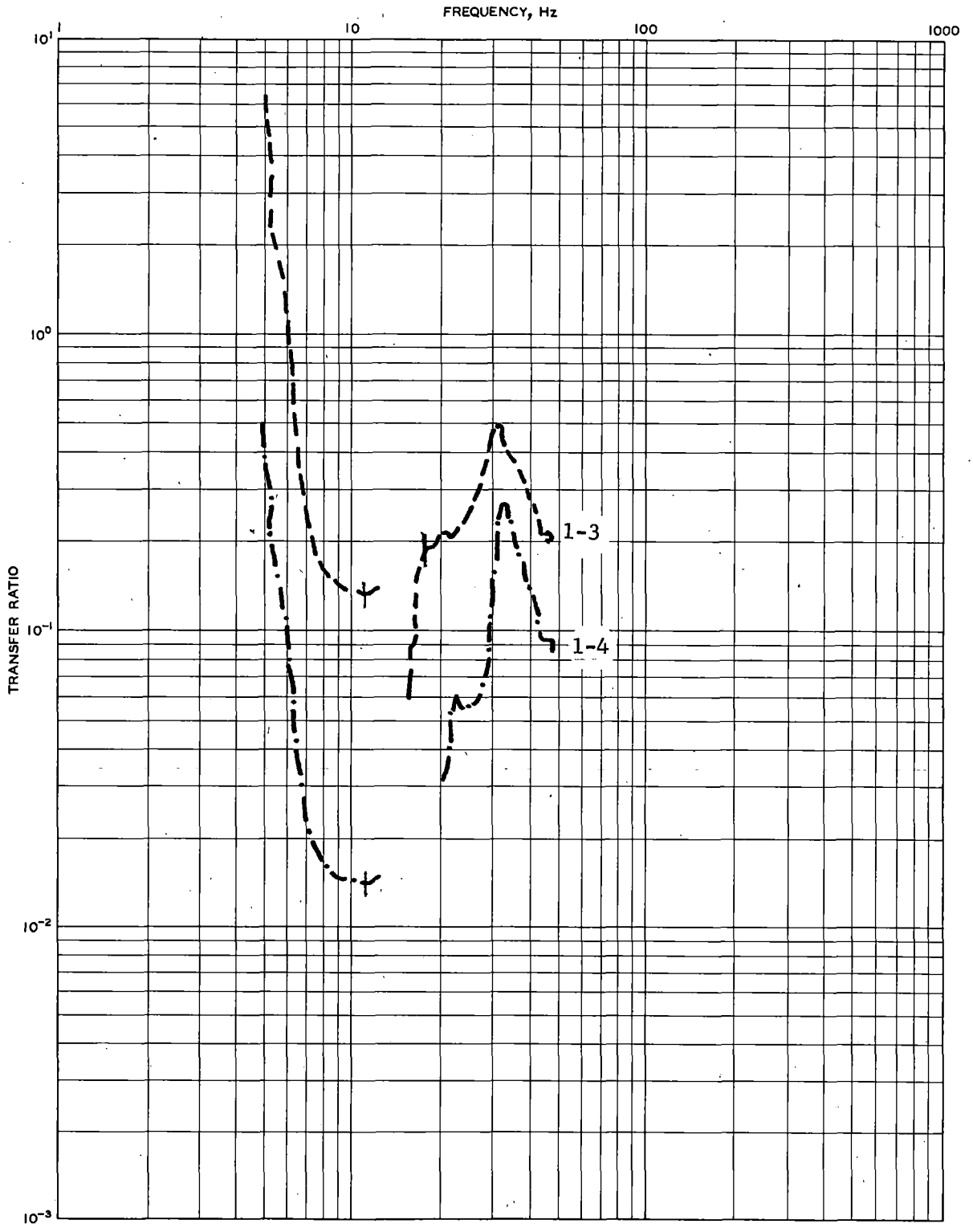

FIGURE 39. PRETRAFFIC TRANSFER RATIO RESULTS, TRACK SECTION 5, VERTICAL MODE, POINTS 1-3, 1-4

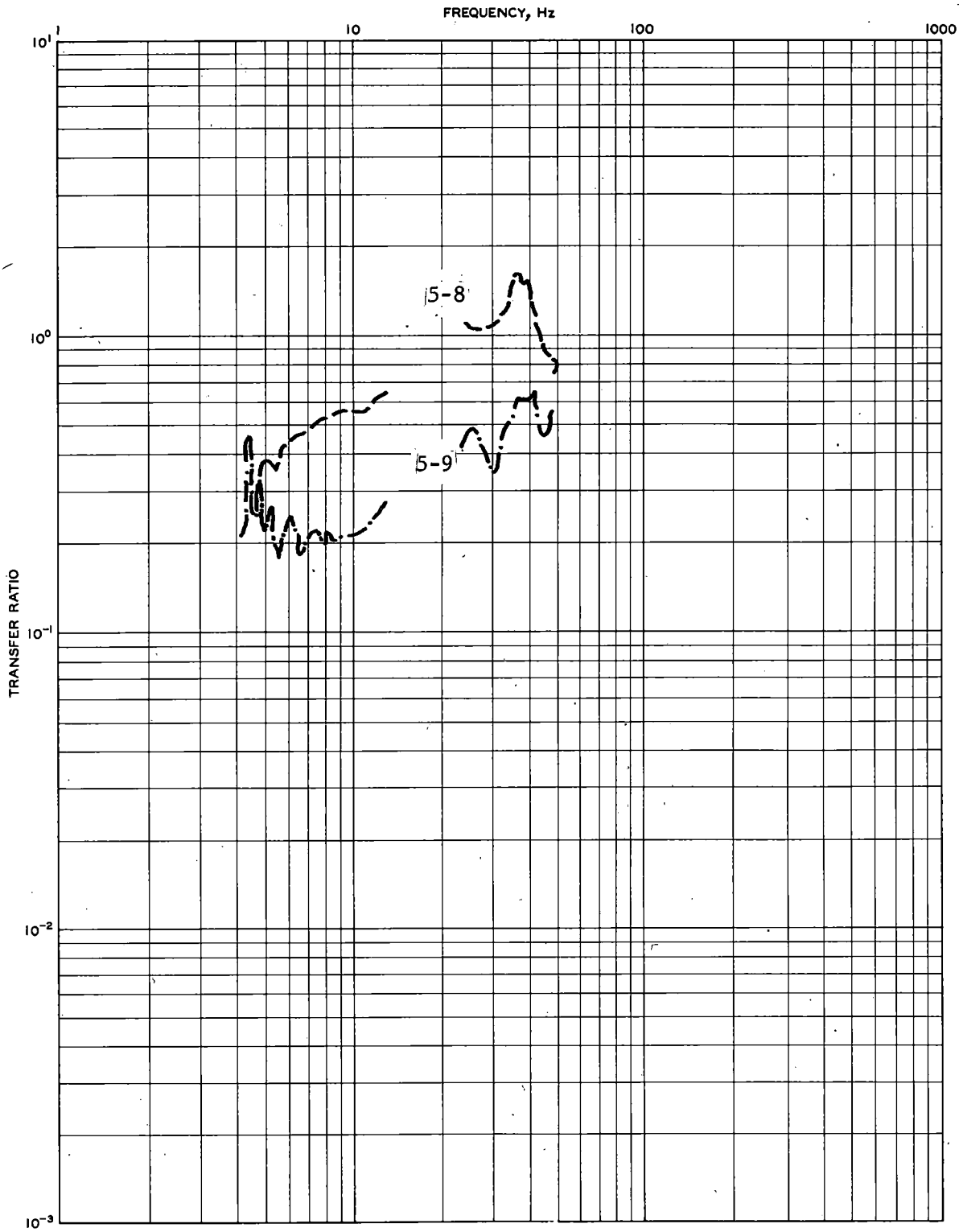

FIGURE 40. PRETRAFFIC TRANSFER RATIO RESULTS, TRACK SECTION 5, VERTICAL MODE, POINTS 5-8, 5-9

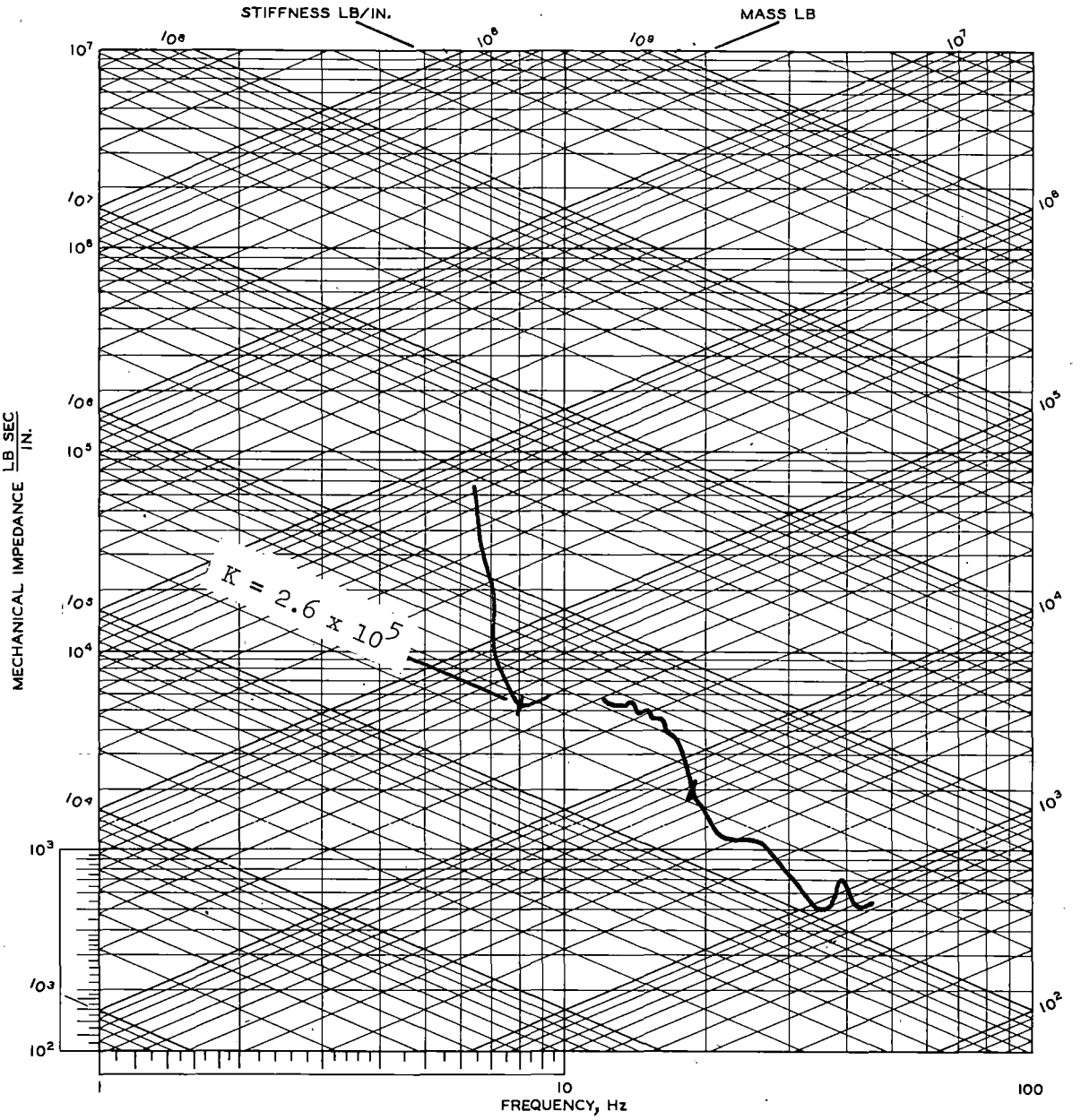

FIGURE 41. PRETRAFFIC MECHANICAL IMPEDANCE RESULTS, TRACK SECTION 6, VERTICAL MODE, POINT 1

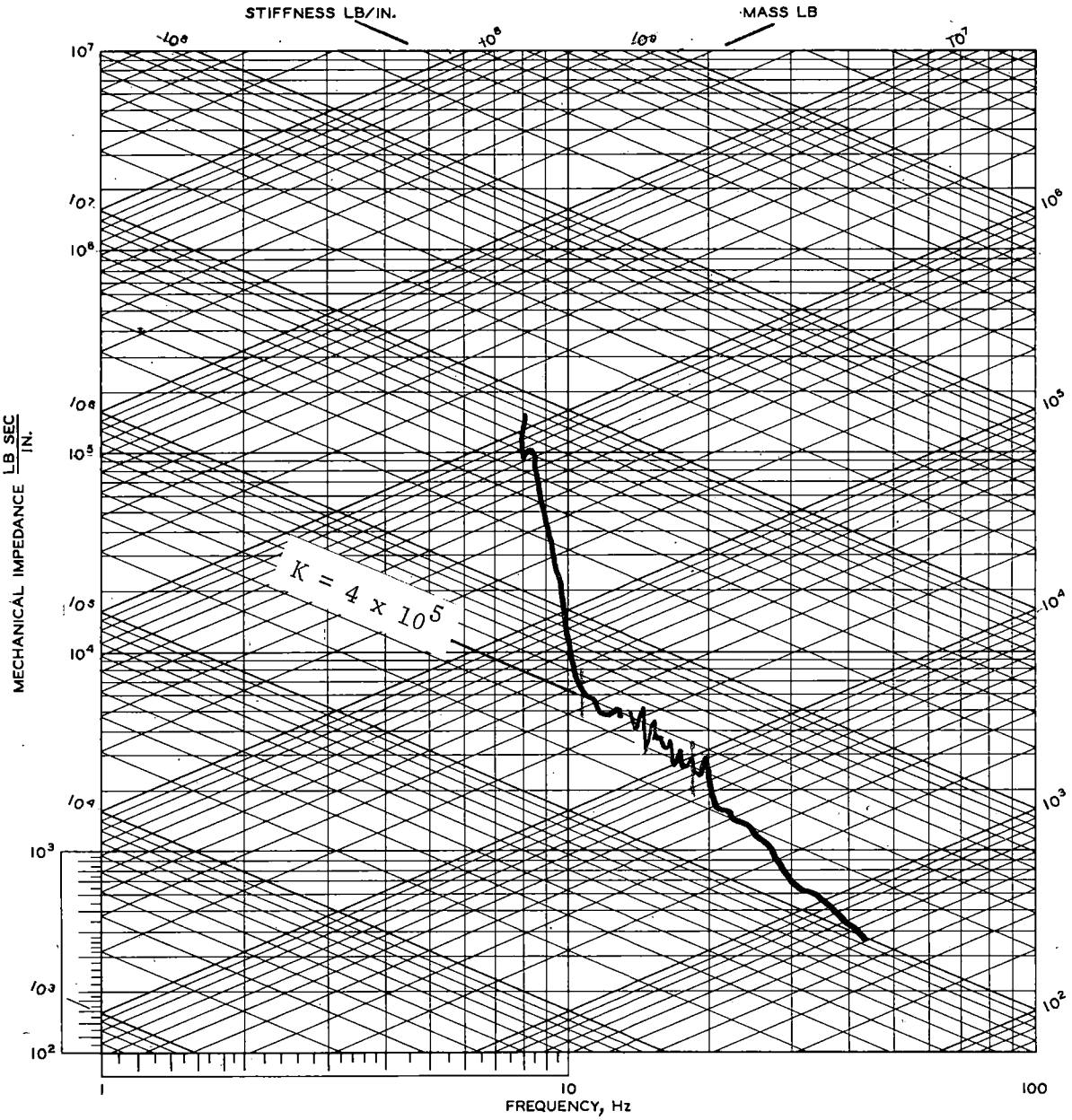

FIGURE 42. PRETRAFFIC MECHANICAL IMPEDANCE RESULTS, TRACK SECTION 6, ROCKING MODE, POINT 1

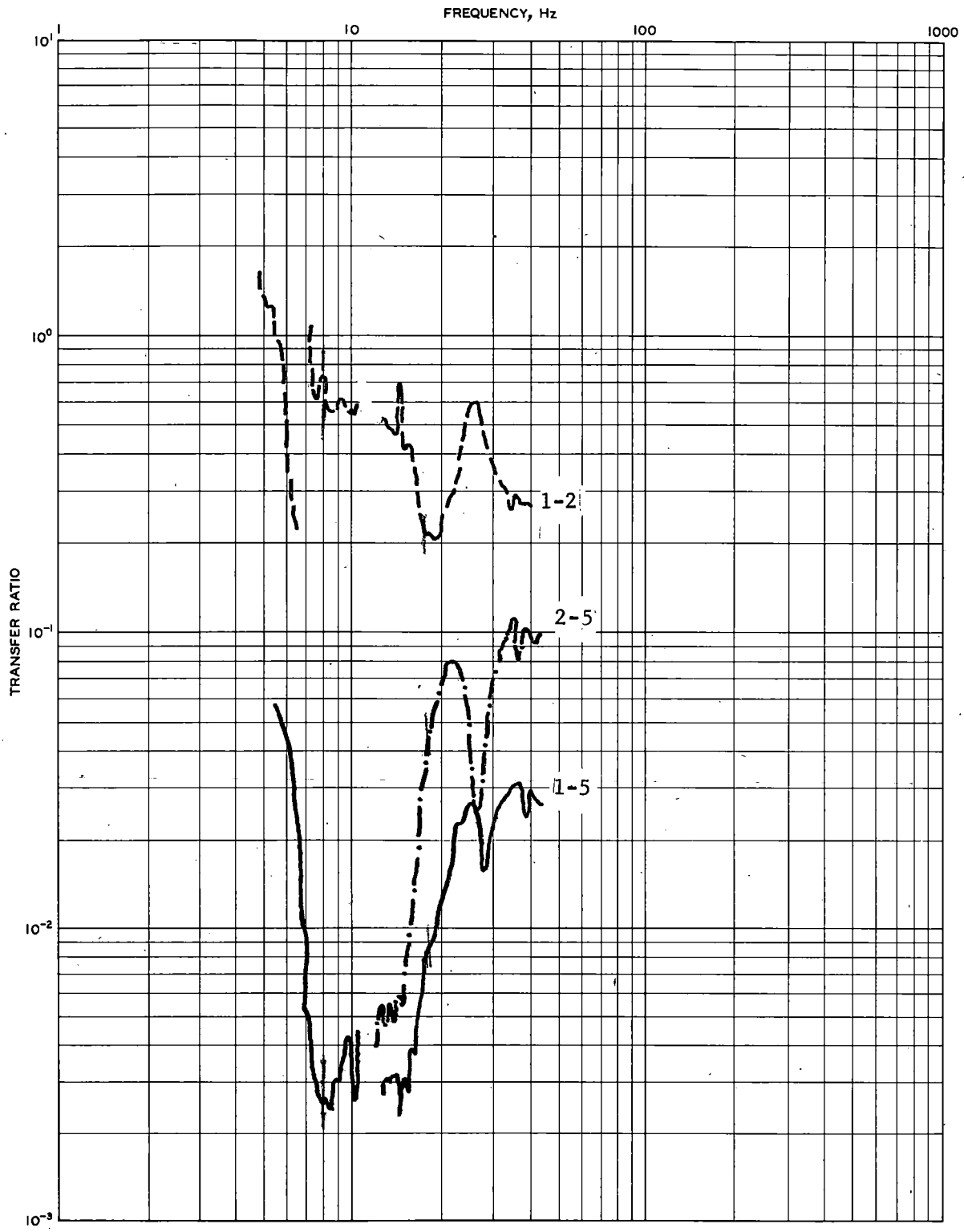

FIGURE 43. PRETRAFFIC TRANSFER RATIO RESULTS, TRACK SECTION 6, VERTICAL MODE, POINTS 1-2, 2-5, 1-5

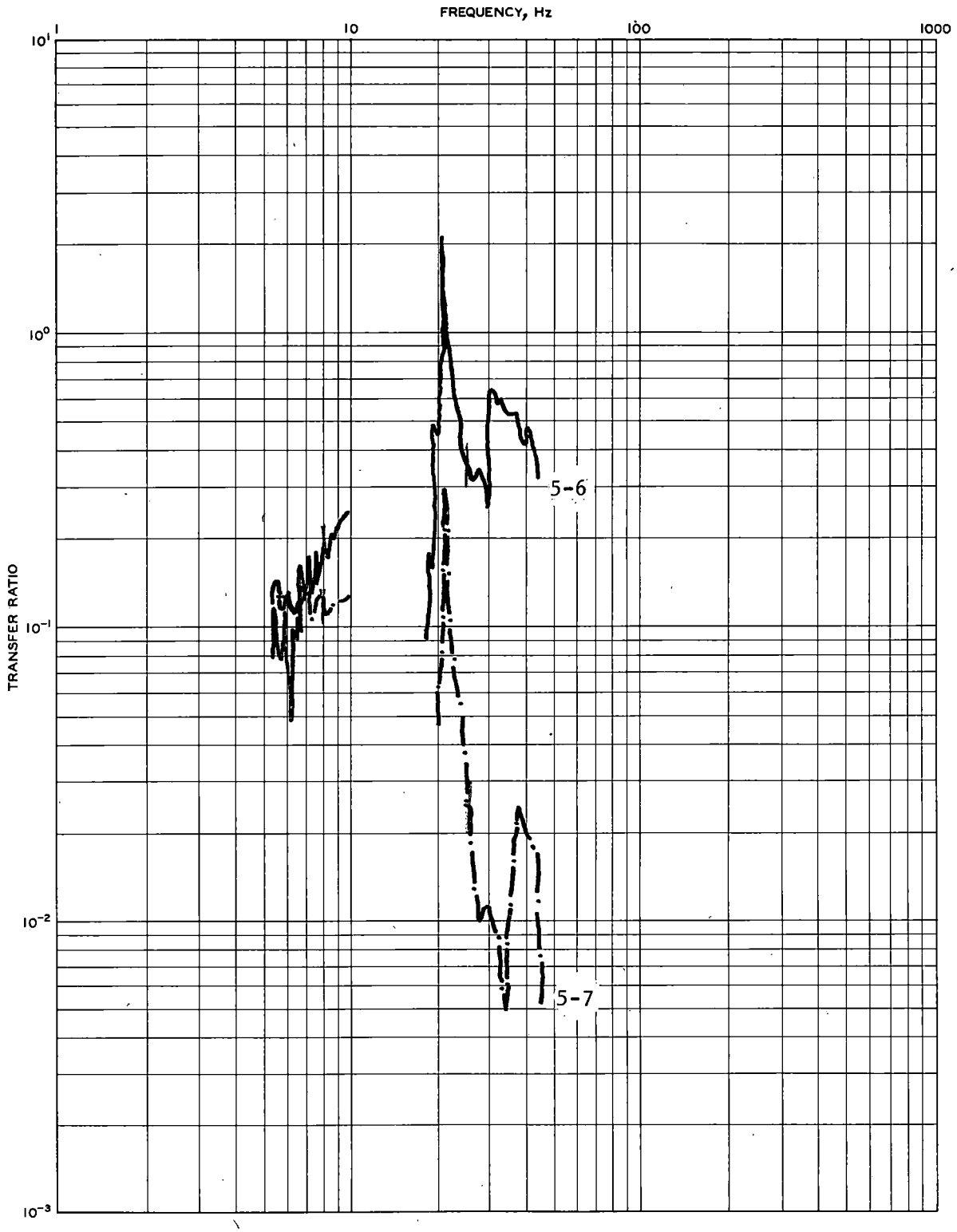

FIGURE 44. PRETRAFFIC TRANSFER RATIO RESULTS, TRACK SECTION 6, VERTICAL MODE, POINTS 5-6, 5-7

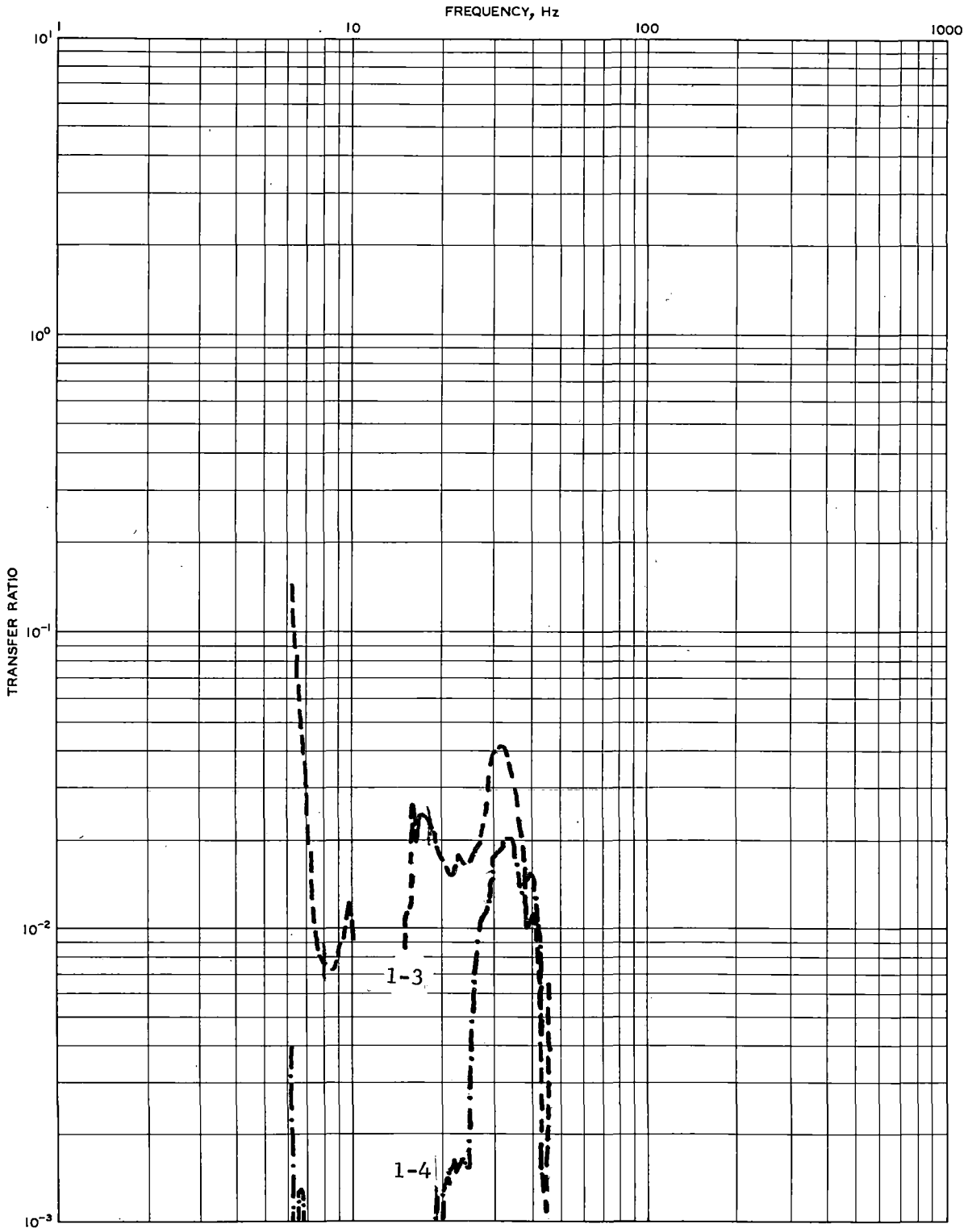

FIGURE 45. PRETRAFFIC TRANSFER RATIO RESULTS, TRACK SECTION 6, VERTICAL MODE, POINTS 1-3, 1-4

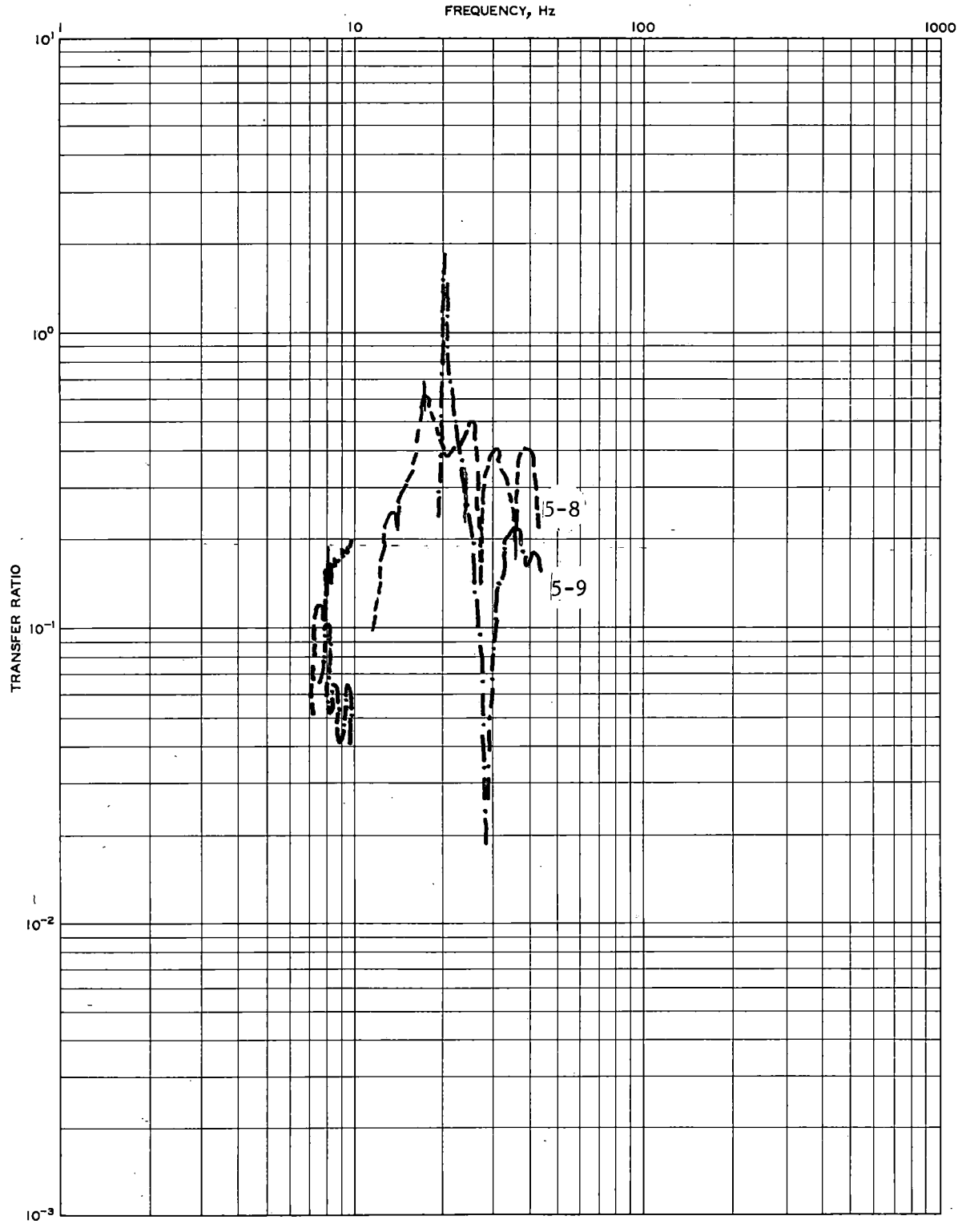

FIGURE 46. PRETRAFFIC TRANSFER RATIO RESULTS, TRACK SECTION 6, VERTICAL MODE, POINTS 5-8, 5-9

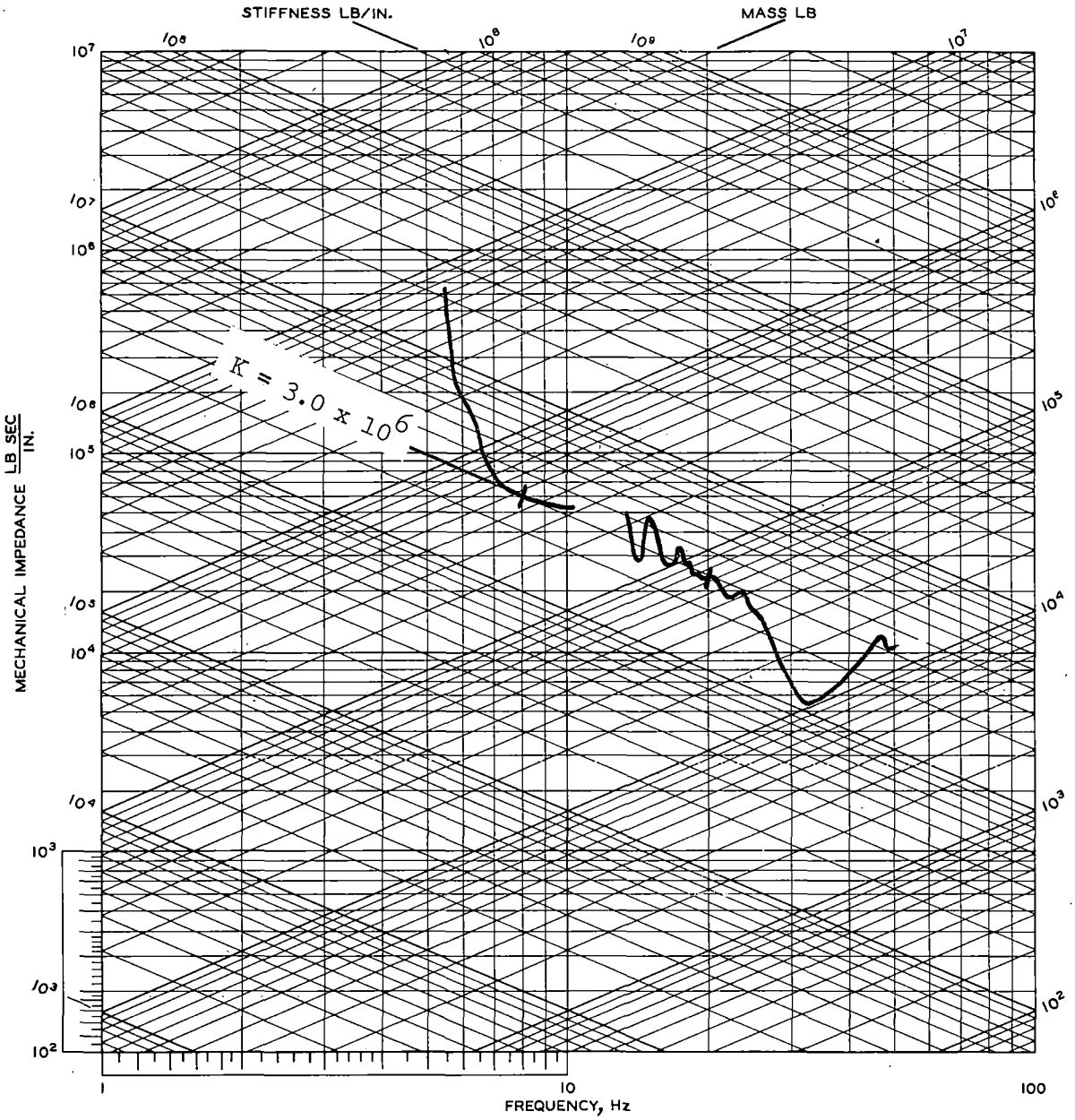

FIGURE 47. PRETRAFFIC MECHANICAL IMPEDANCE RESULTS, TRACK SECTION 7, VERTICAL MODE, POINT 1

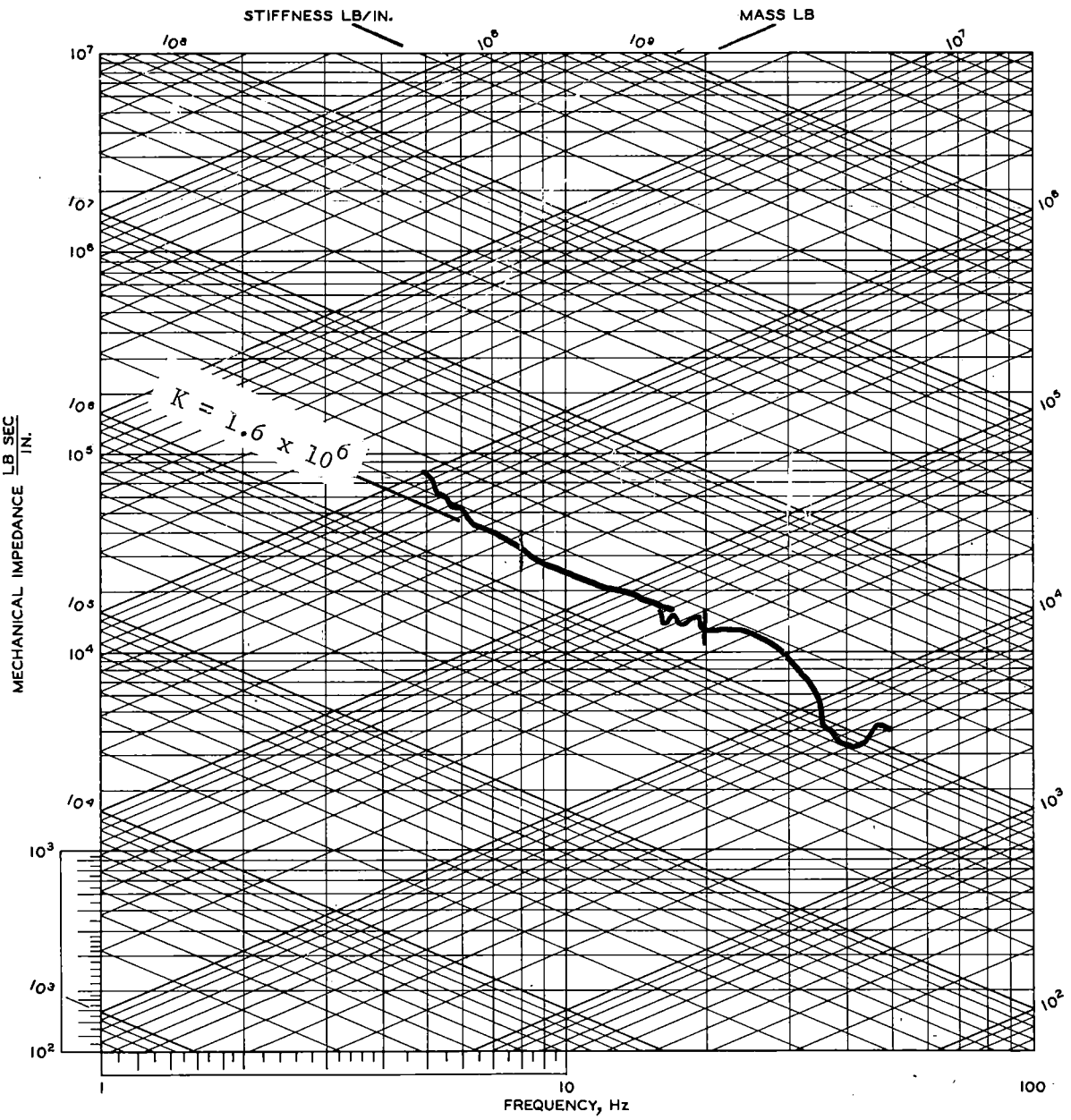

FIGURE 48. PRETRAFFIC MECHANICAL IMPEDANCE RESULTS, TRACK SECTION 7, ROCKING MODE, POINT 1

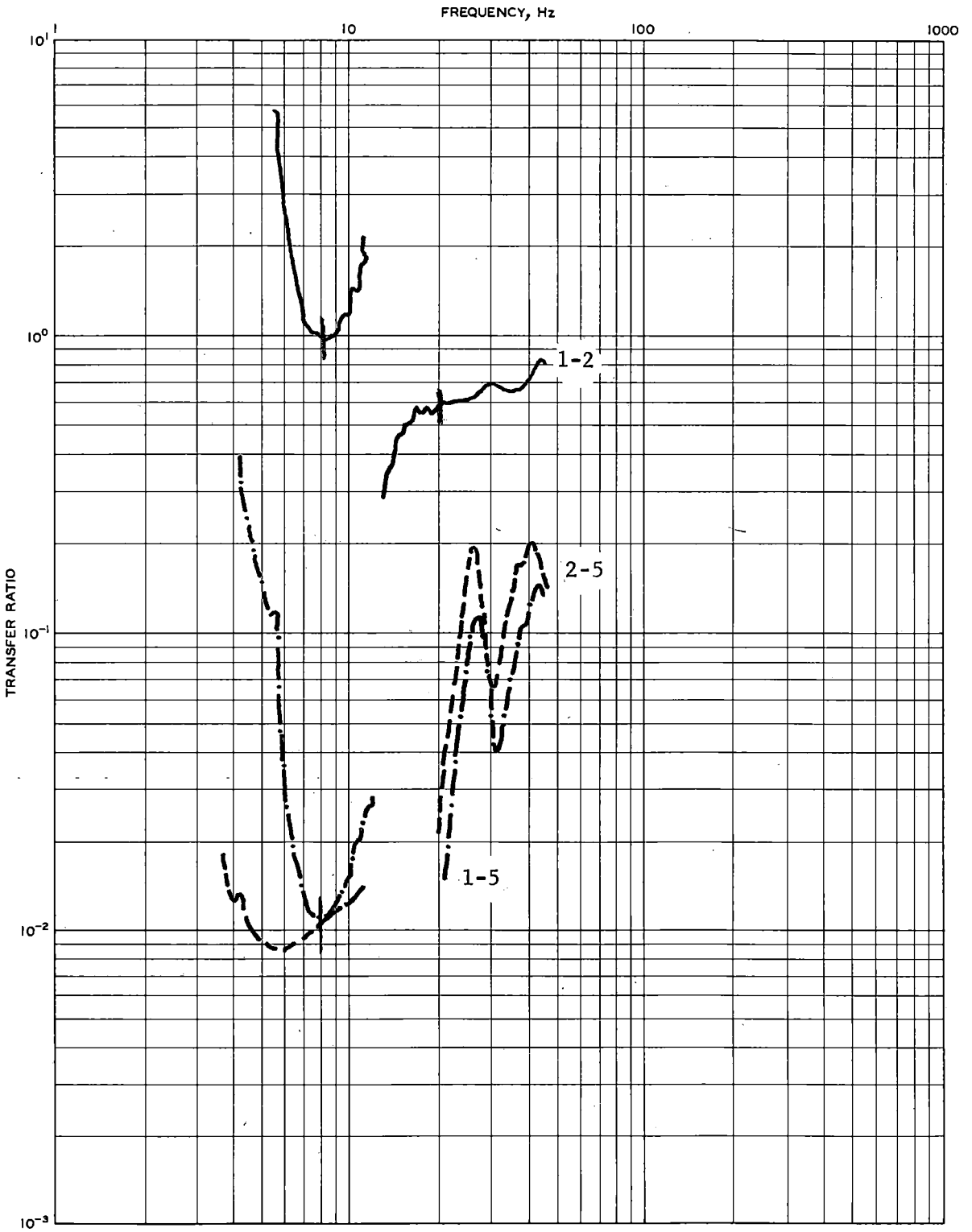

FIGURE 49. PRETRAFFIC TRANSFER RATIO RESULTS, TRACK SECTION 7, VERTICAL MODE, POINTS 1-2, 2-5, 1-5

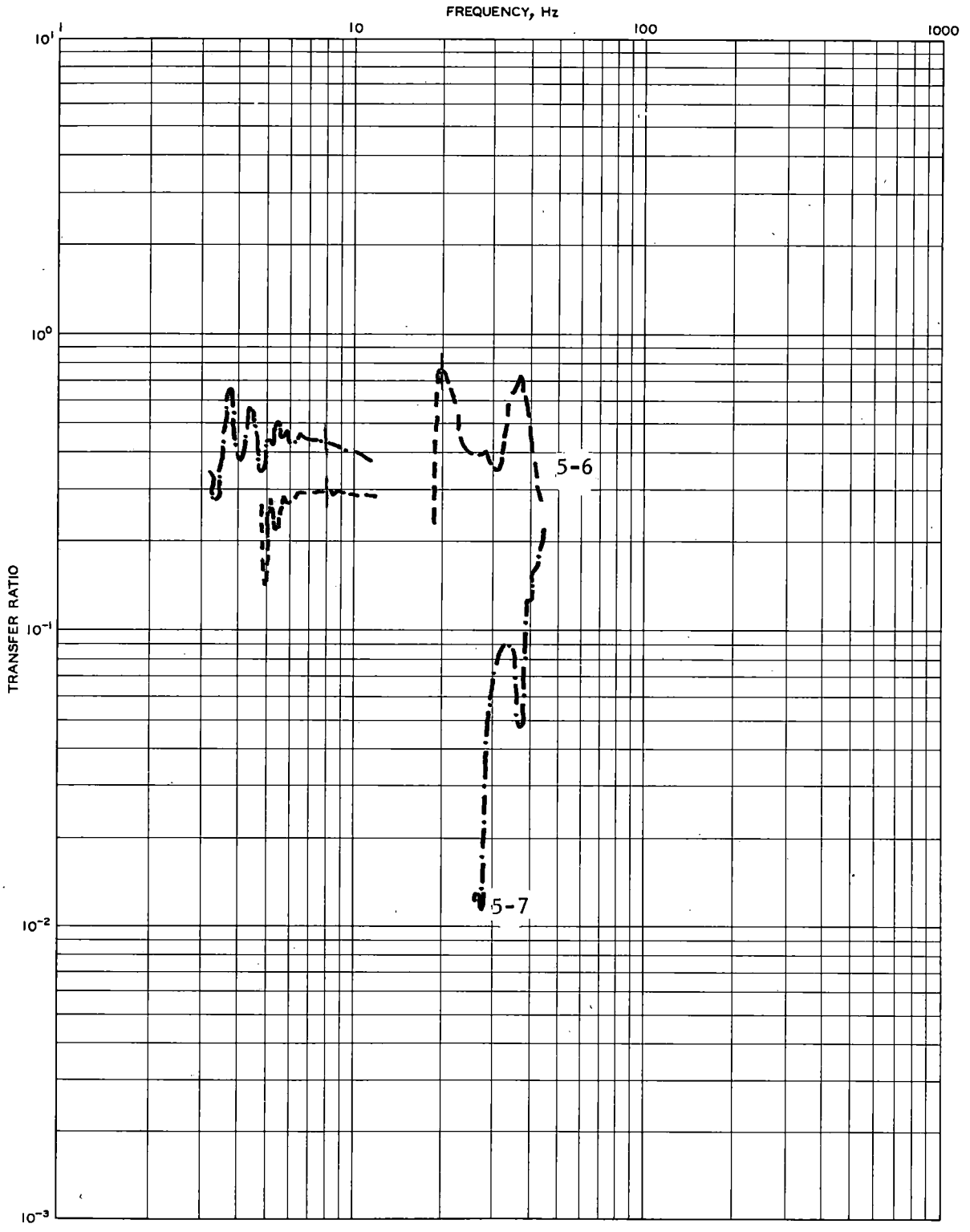

FIGURE 50. PRETRAFFIC TRANSFER RATIO RESULTS, TRACK SECTION 7, VERTICAL MODE, POINTS 5-6, 5-7

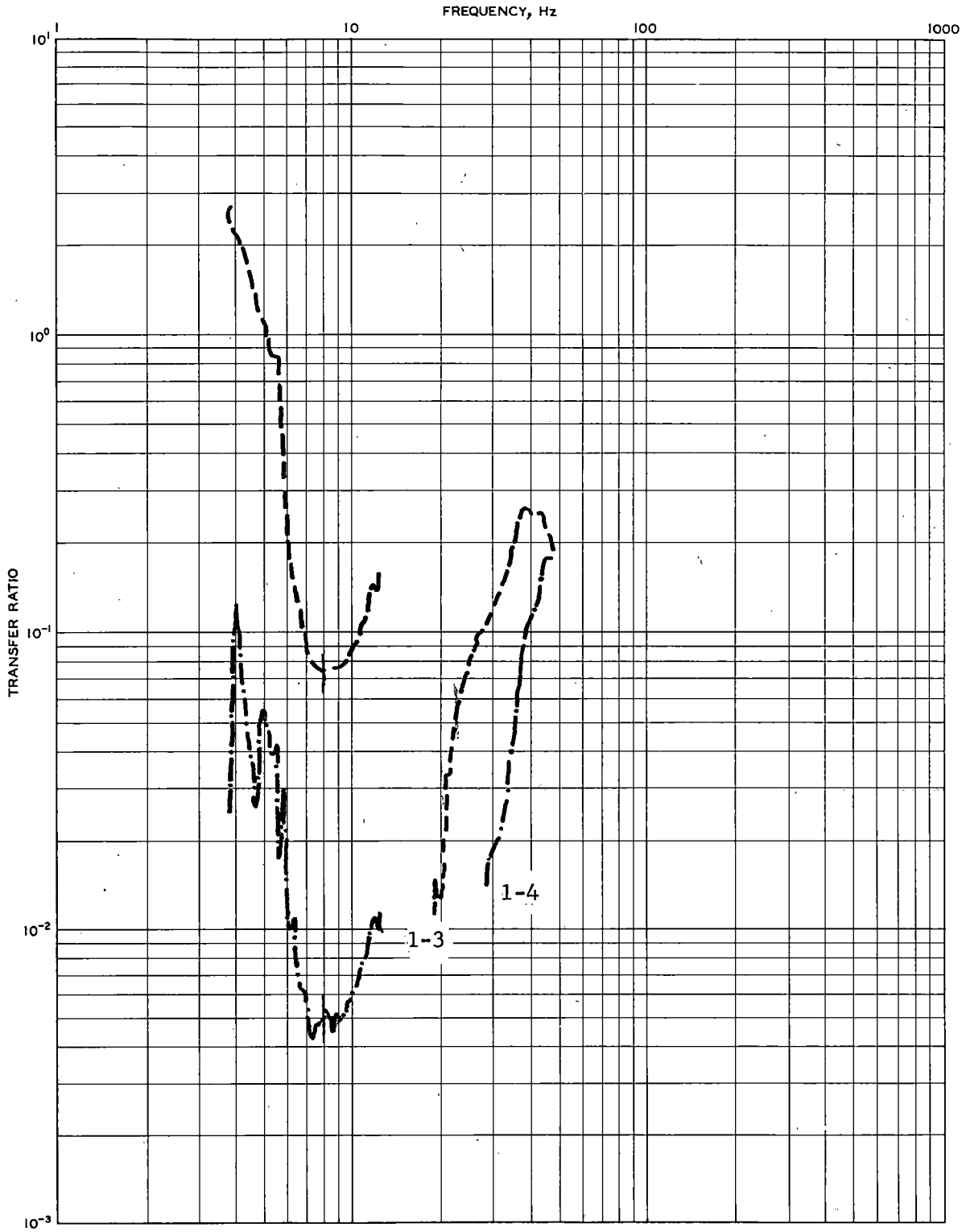

FIGURE 51. PRETRAFFIC TRANSFER RATIO RESULTS, TRACK SECTION 7, VERTICAL MODE, POINTS 1-3, 1-4

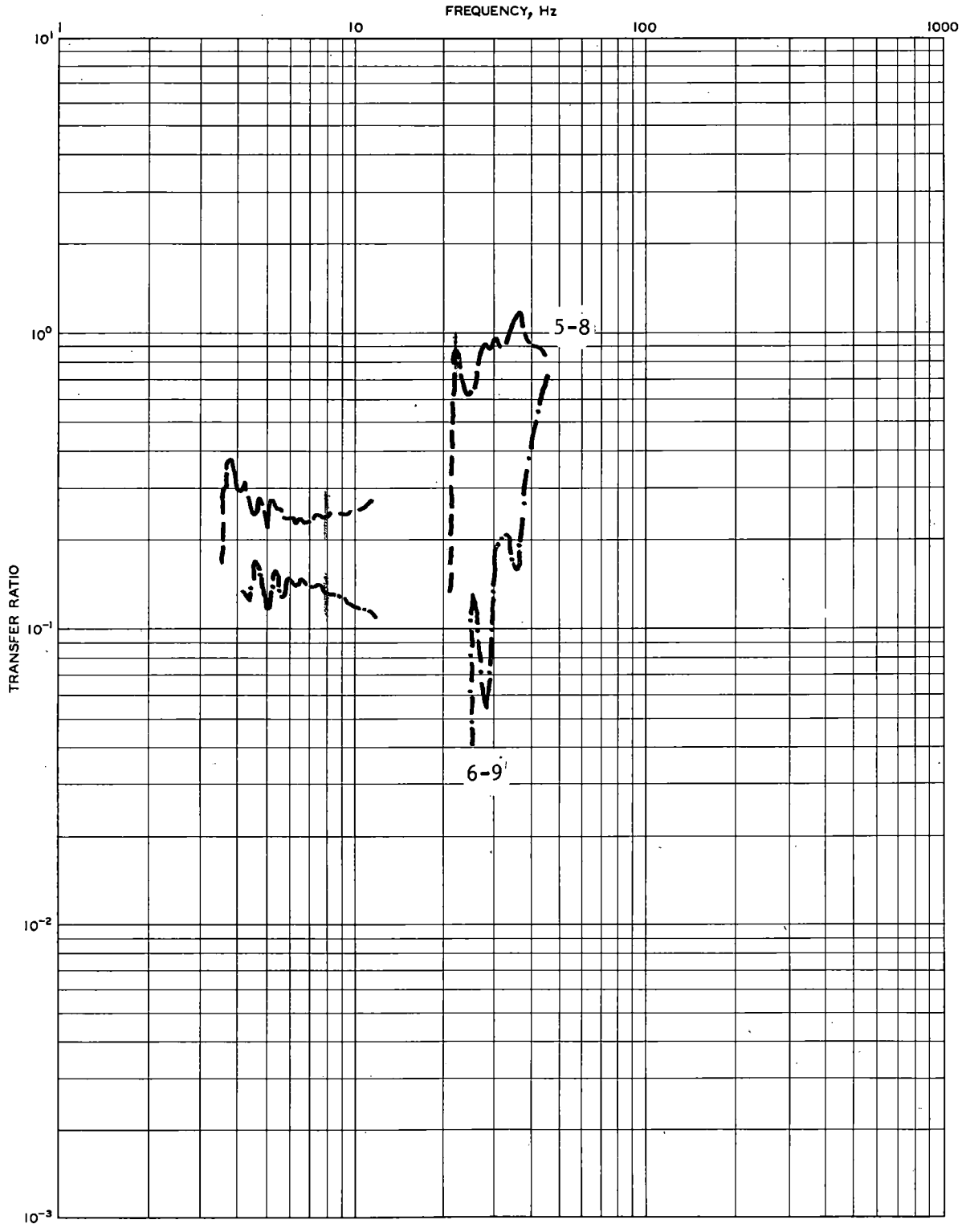

FIGURE 52. PRETRAFFIC TRANSFER RATIO RESULTS, TRACK SECTION 7, VERTICAL MODE, POINTS 5-8, 6-9

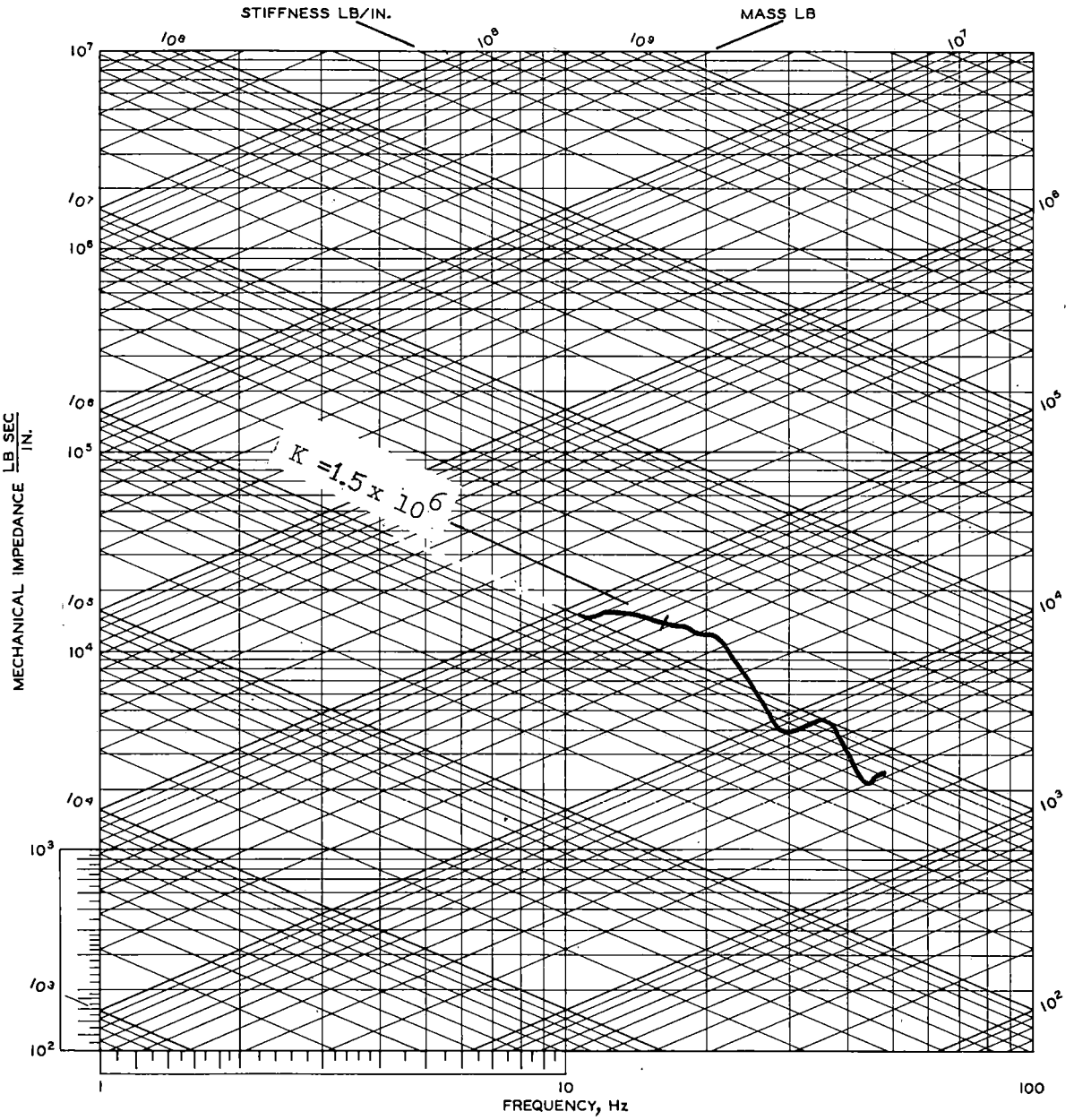

FIGURE 53. PRETRAFFIC MECHANICAL IMPEDANCE RESULTS, TRACK SECTION 8, VERTICAL MODE, POINT 1.

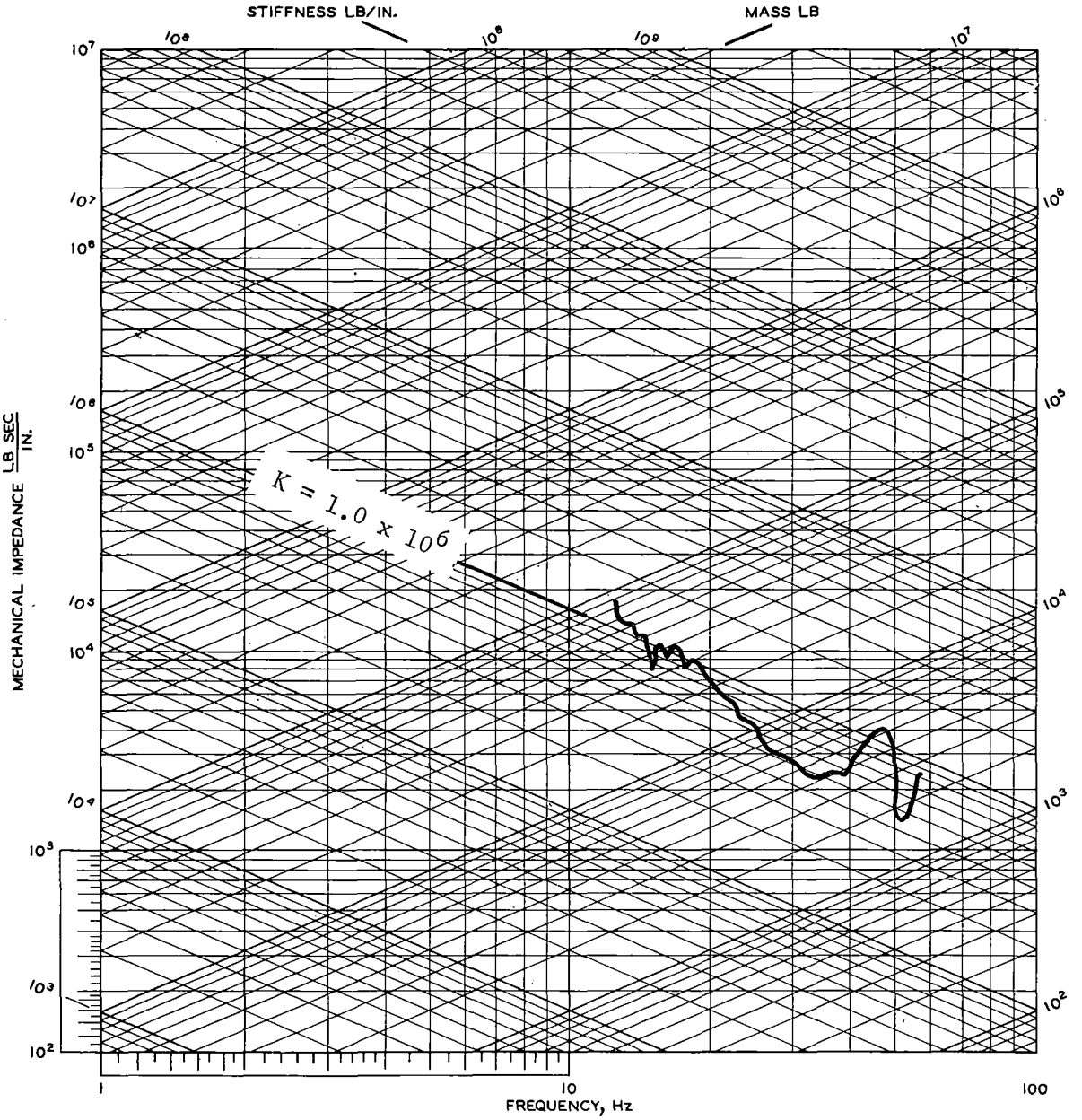

FIGURE 54. PRETRAFFIC MECHANICAL IMPEDANCE RESULTS, TRACK SECTION 8, ROCKING MODE, POINT 1

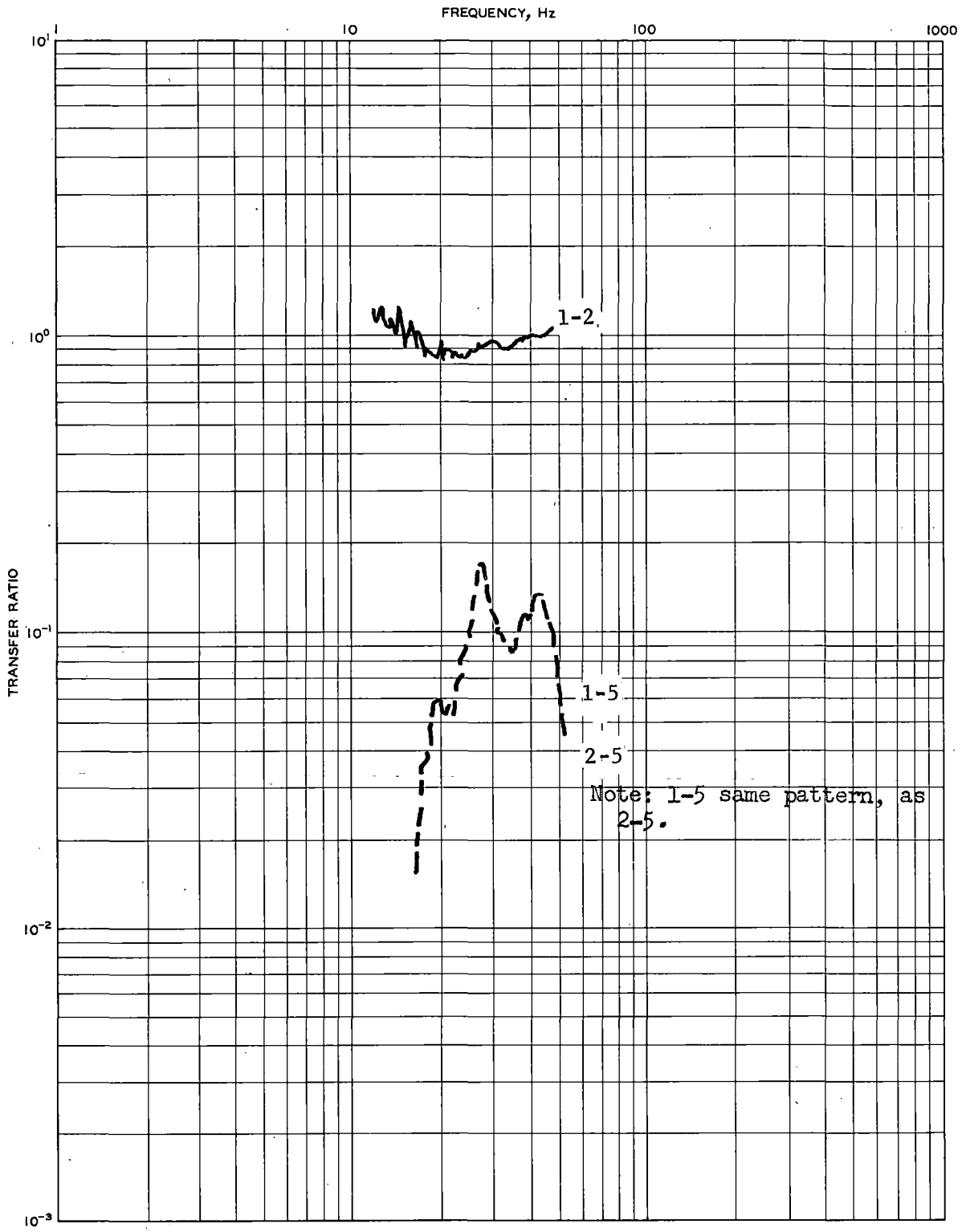

FIGURE 55. PRETRAFFIC TRANSFER RATIO RESULTS, TRACK SECTION 8, VERTICAL MODE, POINTS 1-2, 1-5, 2-5

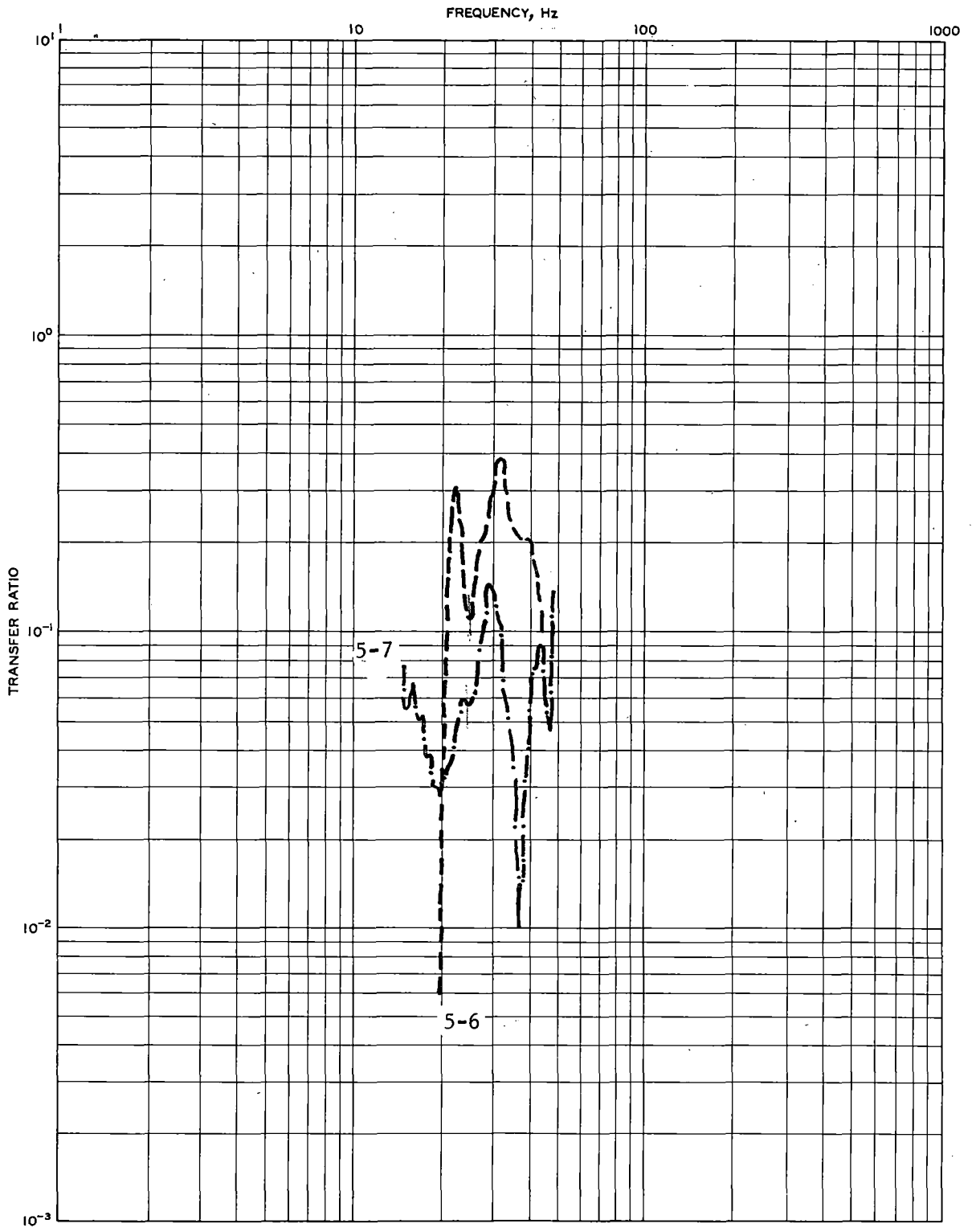

FIGURE 56. PRETRAFFIC TRANSFER RATIO RESULTS, TRACK SECTION 8, VERTICAL MODE, POINTS 5-6, 5-7

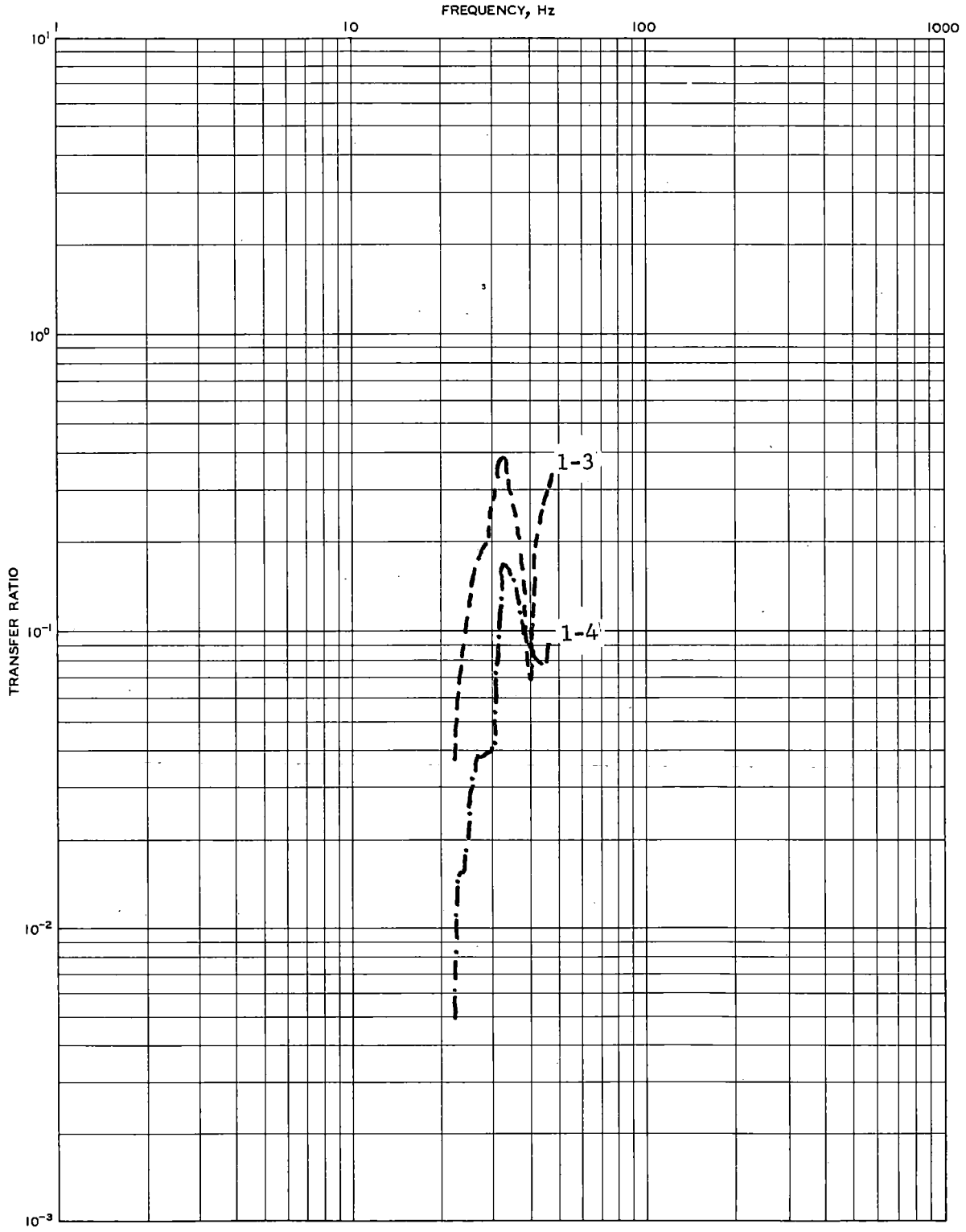

FIGURE 57. PRETRAFFIC TRANSFER RATIO RESULTS, TRACK SECTION 8, VERTICAL MODE, POINTS 1-3, 1-4

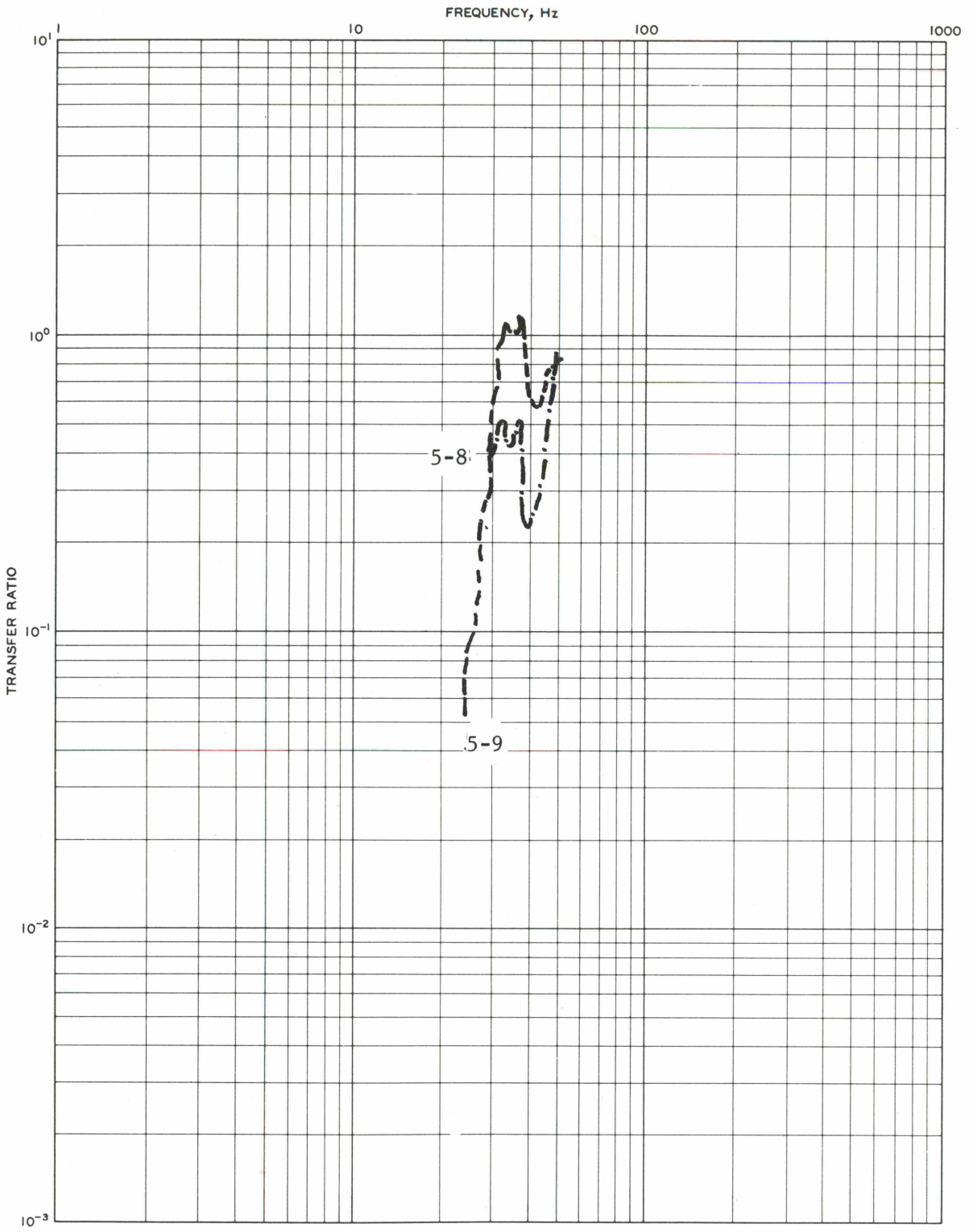

FIGURE 58. PRETRAFFIC TRANSFER RATIO RESULTS, TRACK SECTION 8, VERTICAL MODE, POINTS 5-8, 5-9

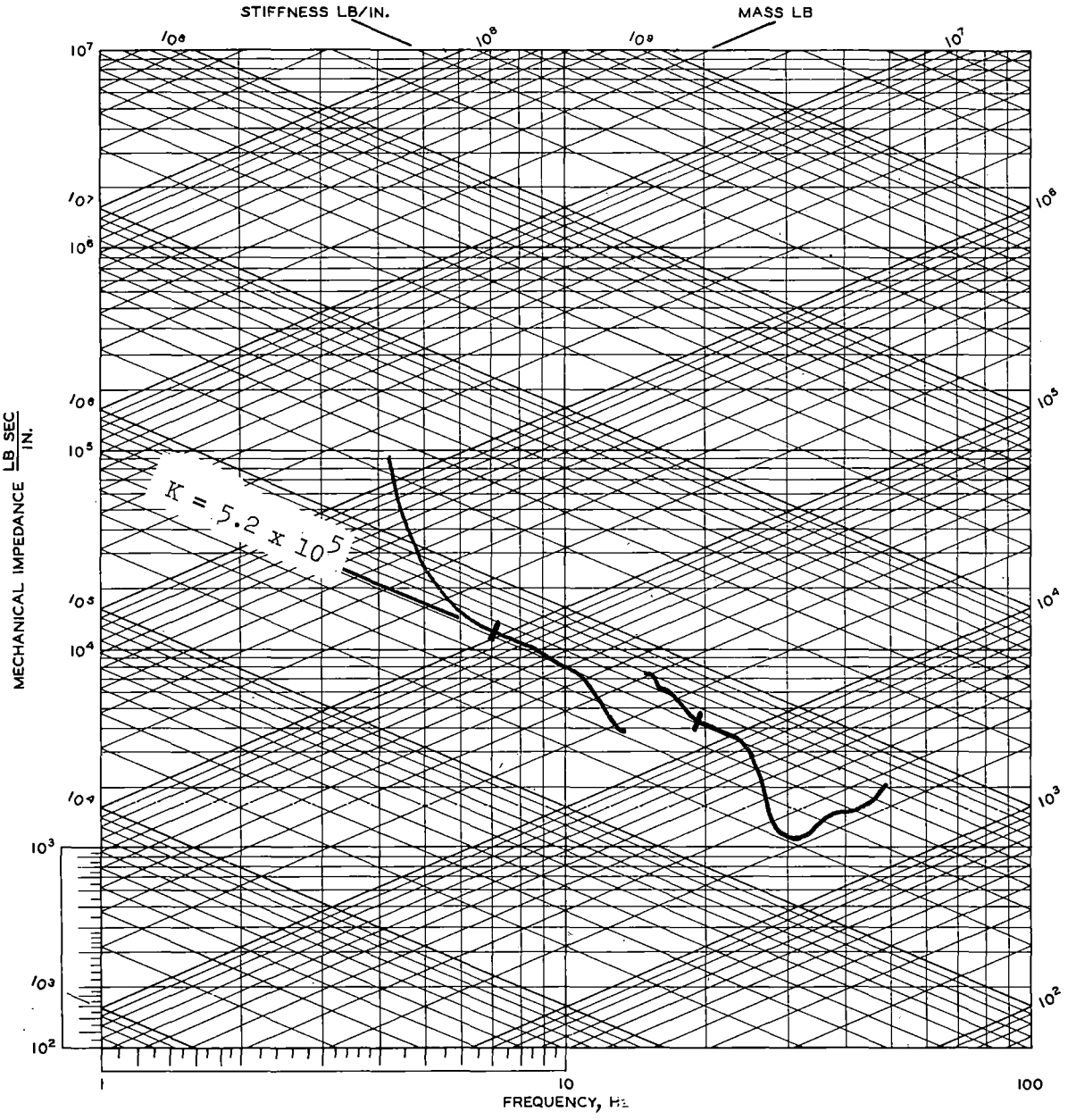

FIGURE 59. PRETRAFFIC MECHANICAL IMPEDANCE RESULTS, TRACK SECTION 9, VERTICAL MODE, POINT 1

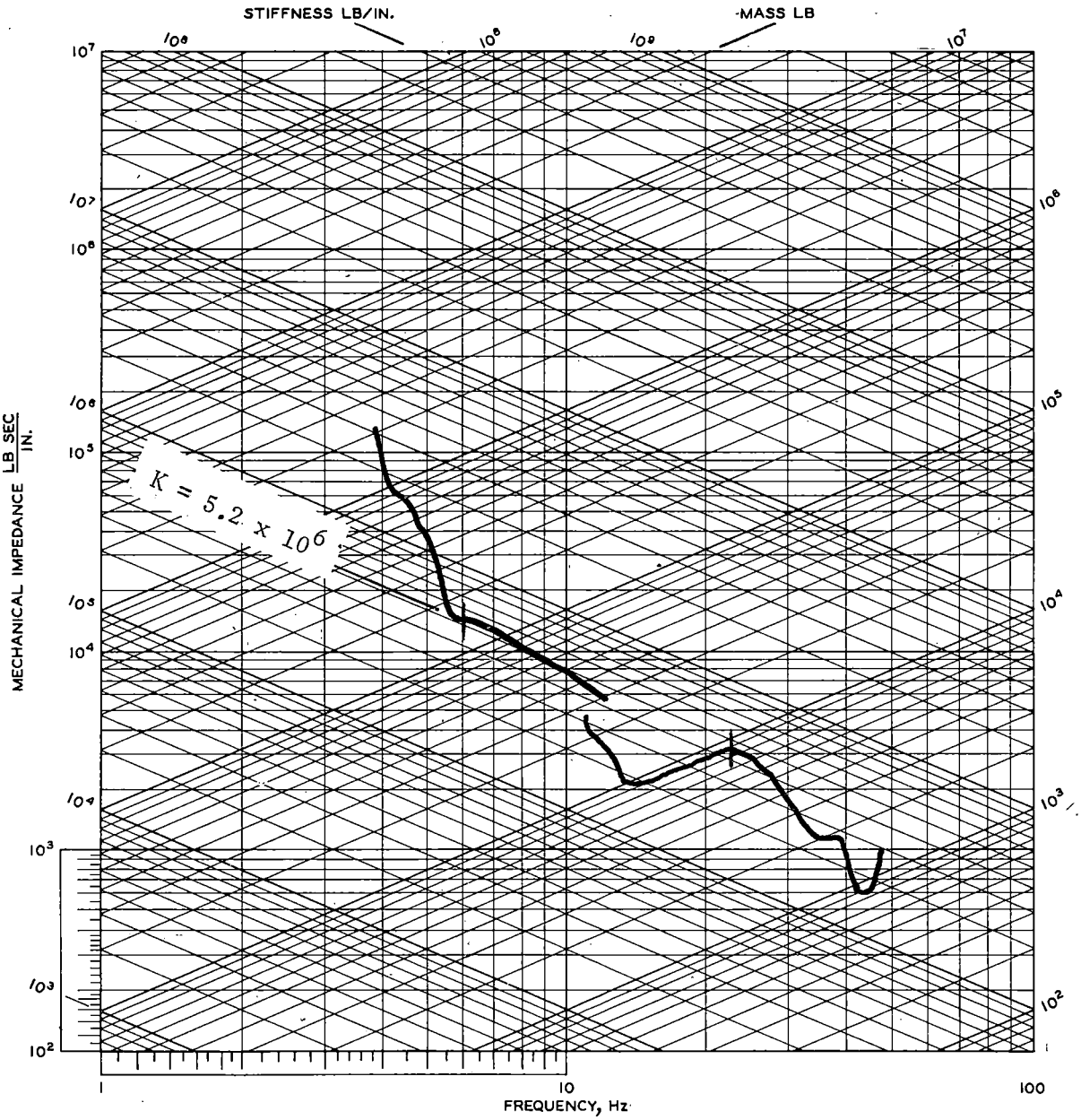

FIGURE 60. PRETRAFFIC MECHANICAL IMPEDANCE RESULTS, TRACK SECTION 9, ROCKING MODE, POINT 1

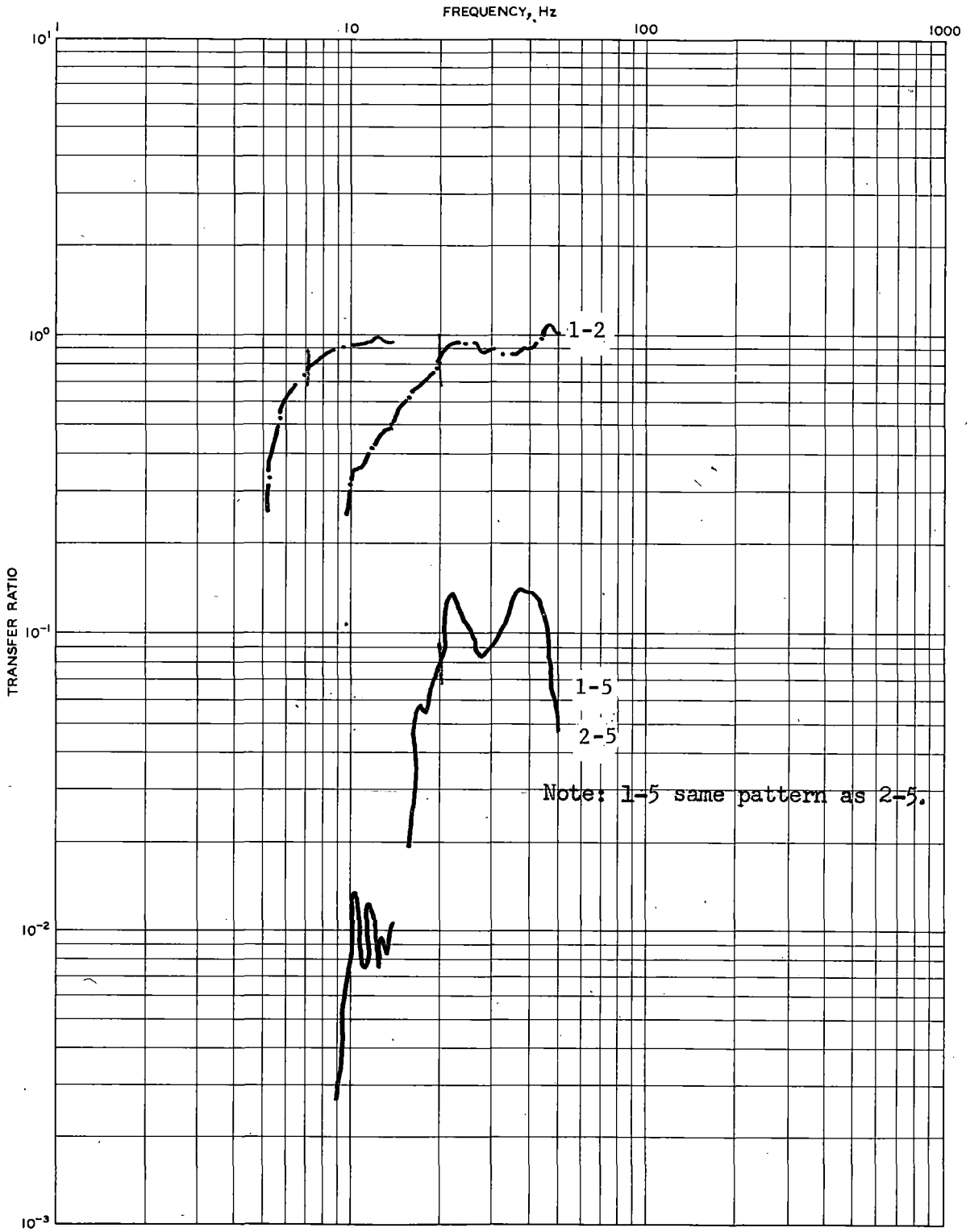

FIGURE 61. PRETRAFFIC TRANSFER RATIO RESULTS, TRACK SECTION 9, VERTICAL MODE, POINTS 1-2, 1-5, 2-5

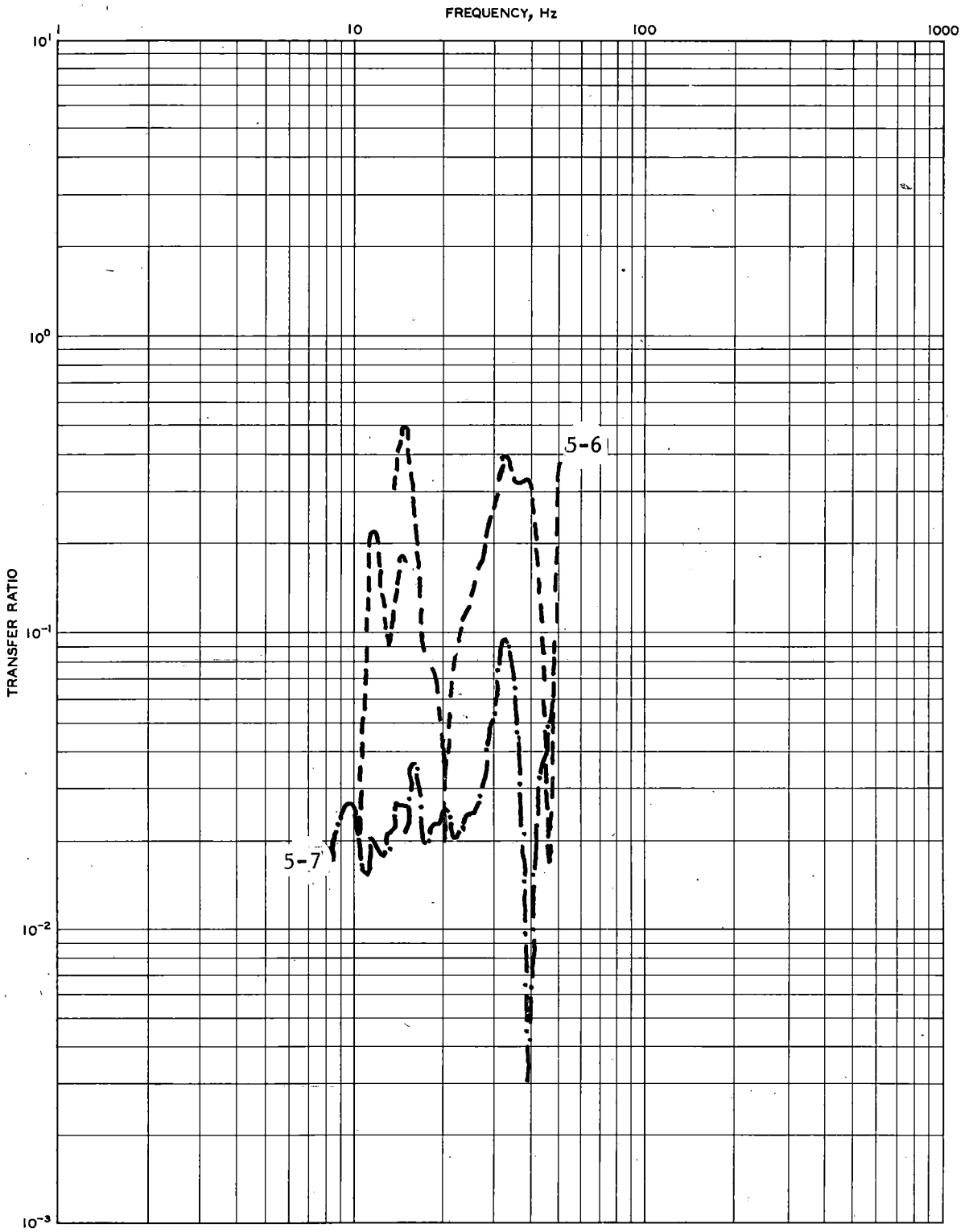

FIGURE 62. PRETRAFFIC TRANSFER RATIO RESULTS, TRACK SECTION 9, VERTICAL MODE, POINTS 5-6, 5-7

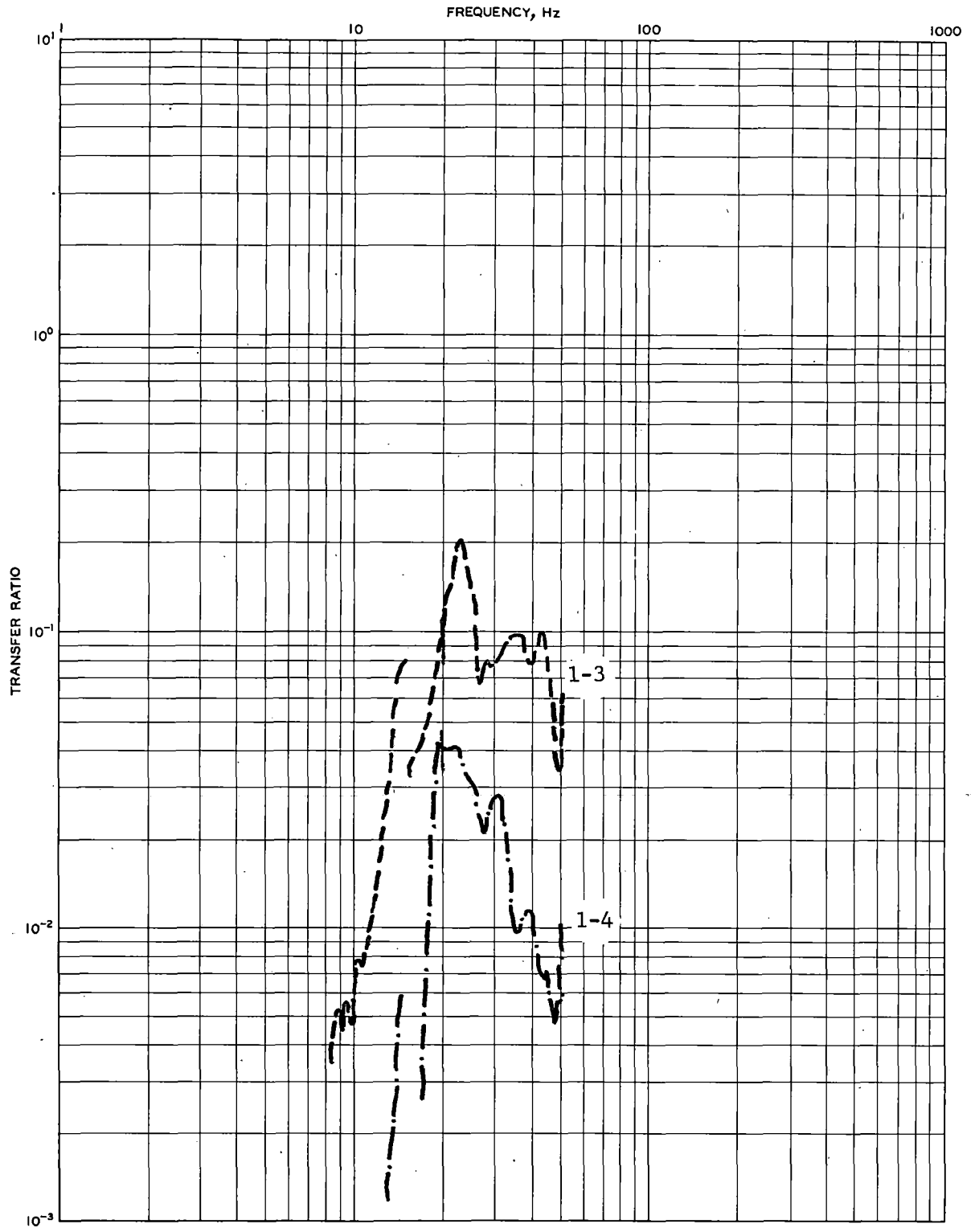

FIGURE 63. PRETRAFFIC TRANSFER RATIO RESULTS, TRACK SECTION 9, VERTICAL MODE, POINTS 1-3, 1-4

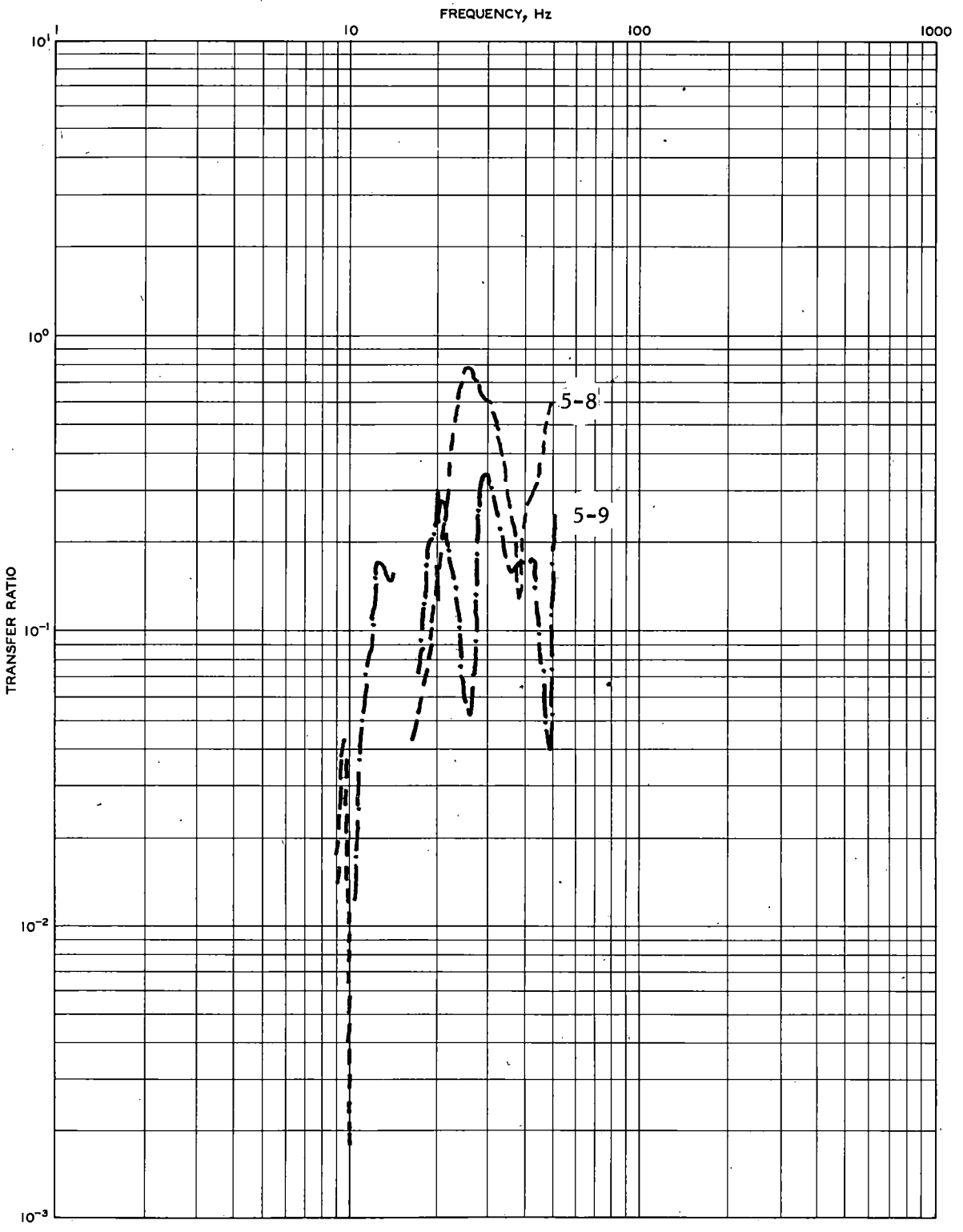

FIGURE 64. PRETRAFFIC TRANSFER RATIO RESULTS, TRACK SECTION 9, VERTICAL MODE, POINTS 5-8, 5-9

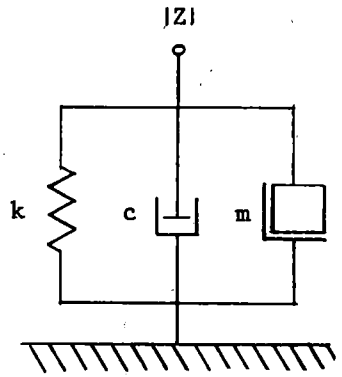

(a) Parallel three-element linear system

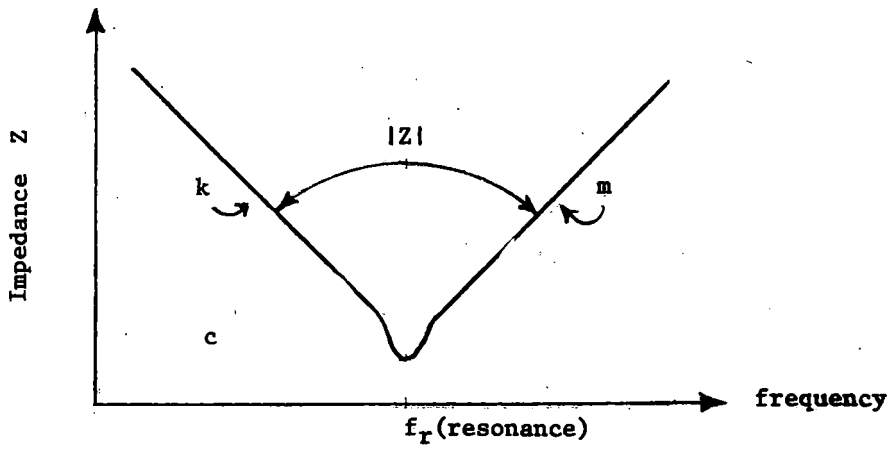

(b) Impedance versus frequency (log-log plot)

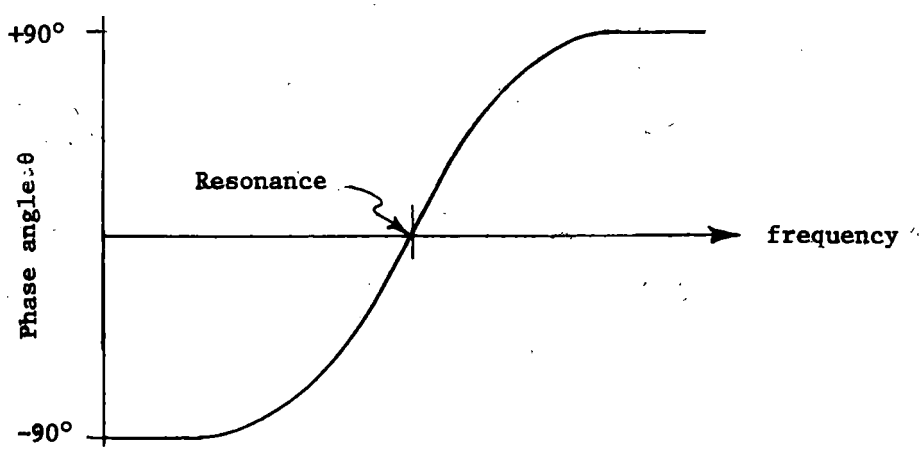

(c) Phase angle θ versus frequency

FIGURE 65. IDEALIZED REPRESENTATION OF A PARALLEL THREE-ELEMENT LINEAR SYSTEM

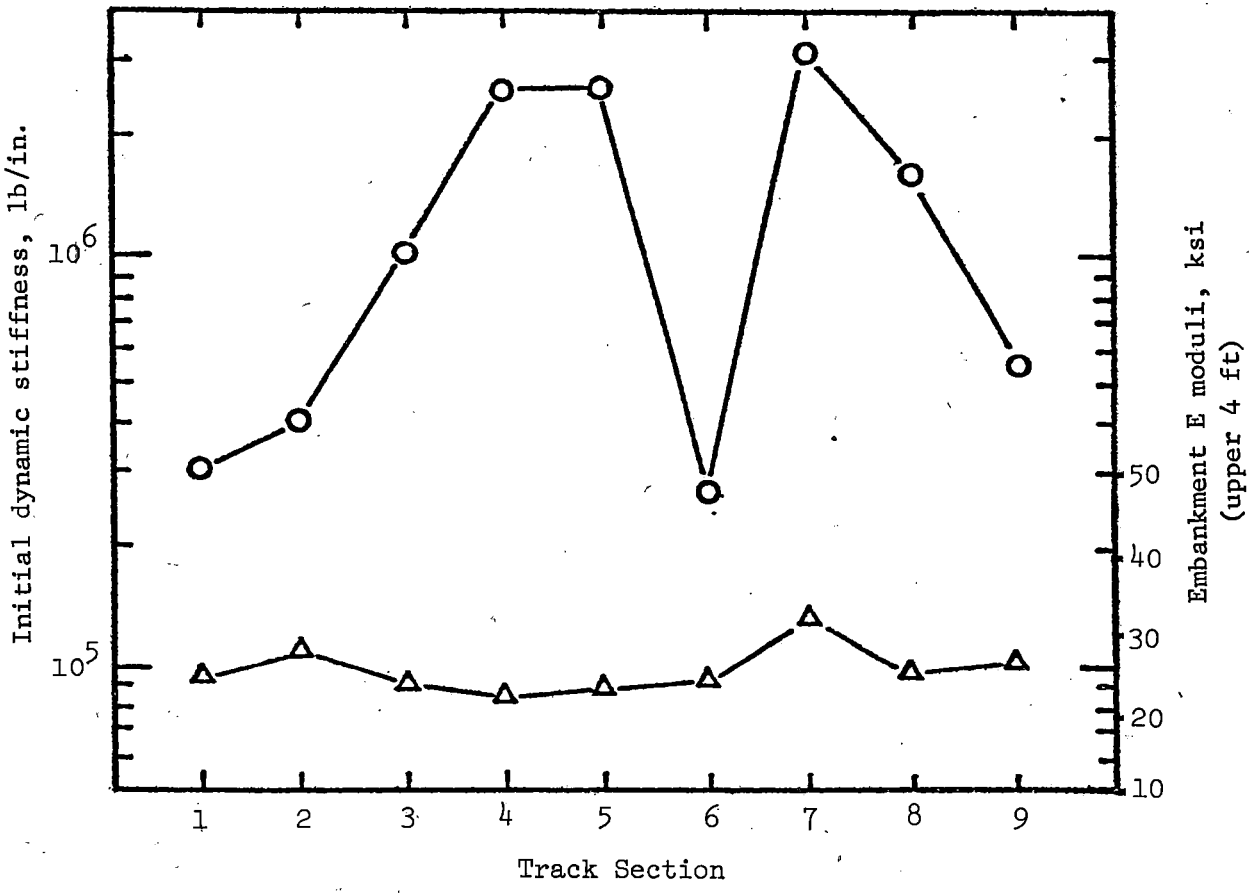

FIGURE 66. INITIAL DYNAMIC STIFFNESS RESULTS FROM PRETRAFFIC TESTING AND EMBANKMENT ELASTIC MODULI FROM EARLIER TESTING

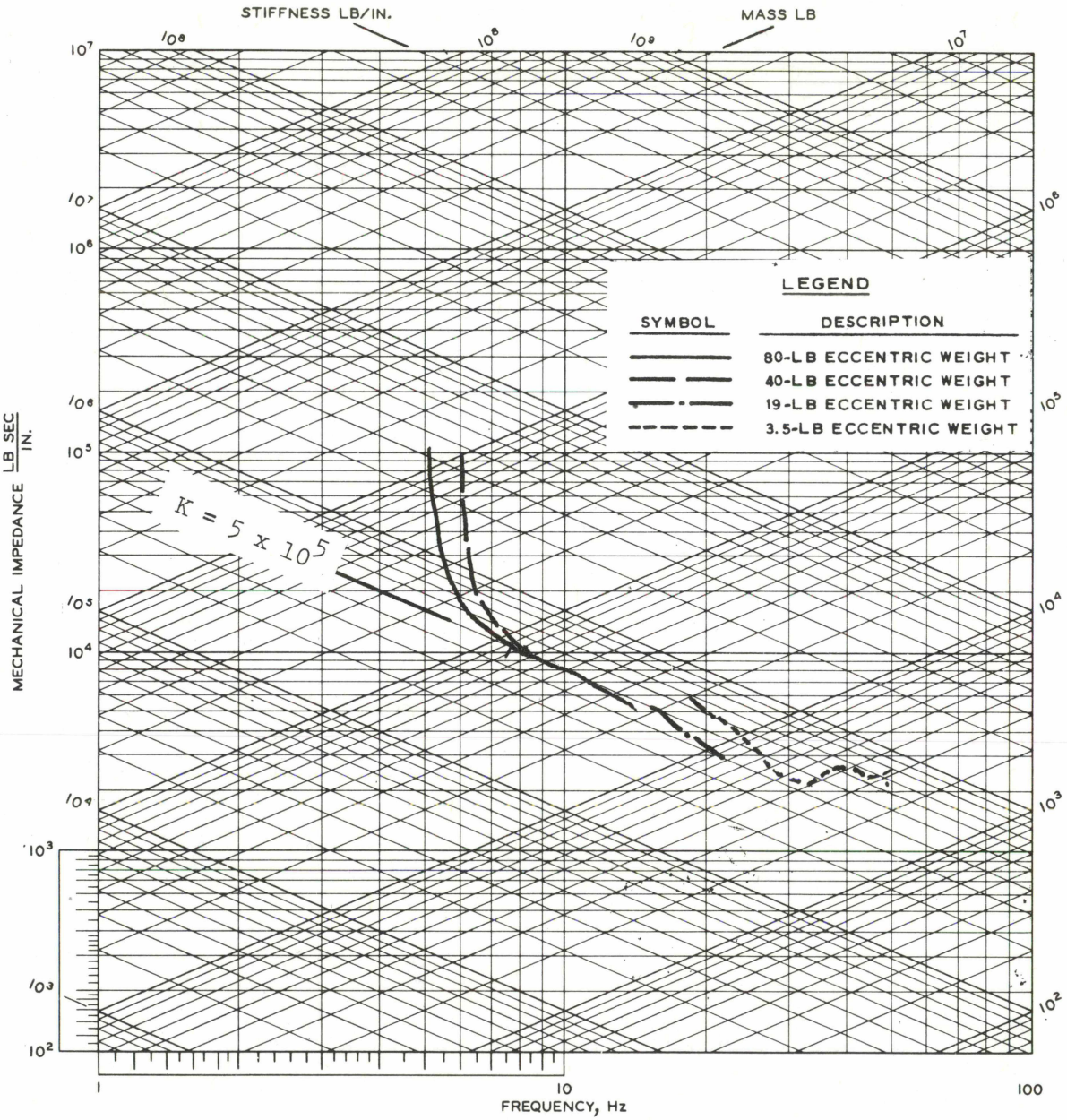

FIGURE 67. POSTTRAFFIC MECHANICAL IMPEDANCE RESULTS, TRACK SECTION 1, VERTICAL MODE, POINT 1

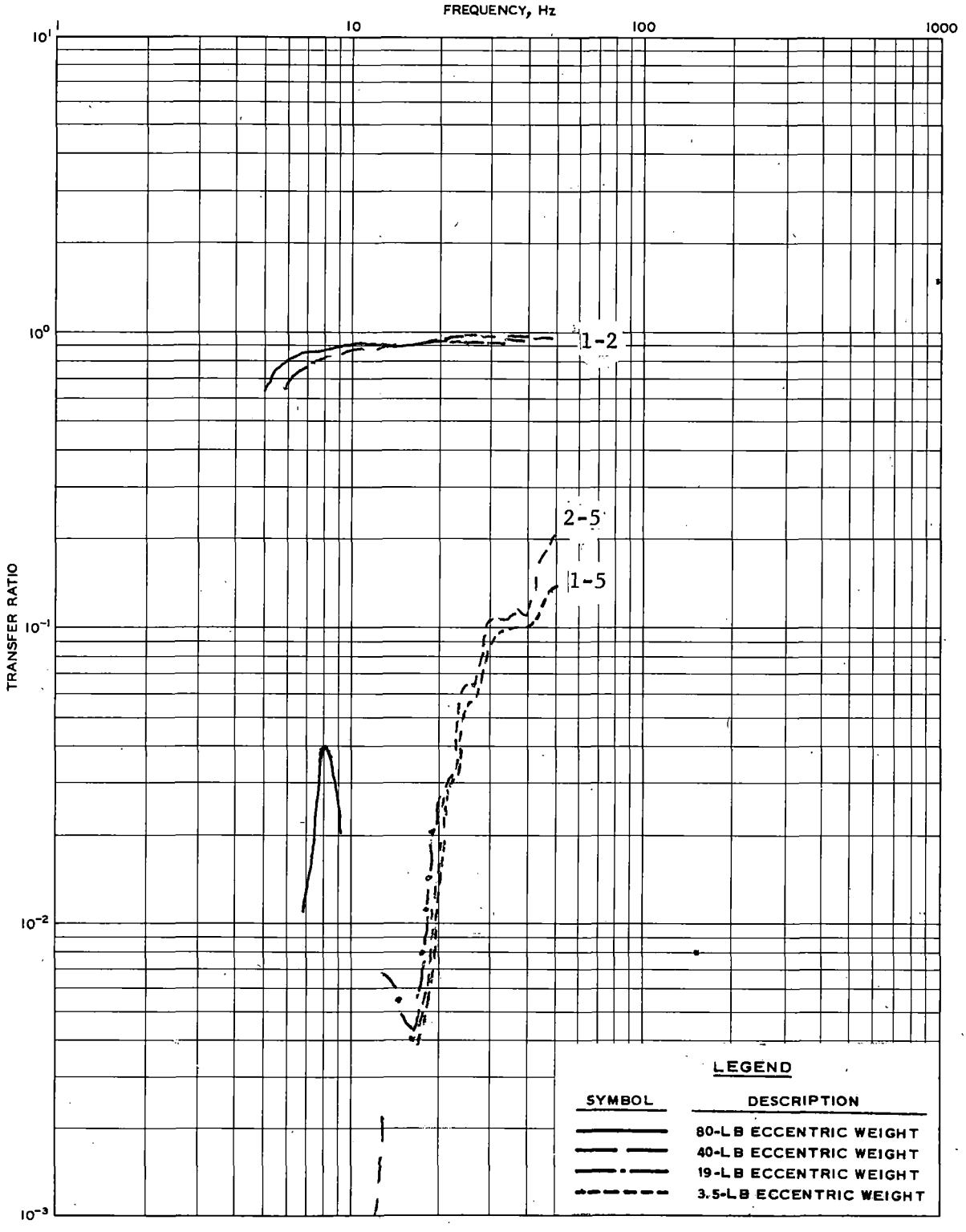

FIGURE 68. POSTTRAFFIC TRANSFER RATIO RESULTS, TRACK SECTION 1, VERTICAL MODE, POINTS 1-2, 1-5, 2-5

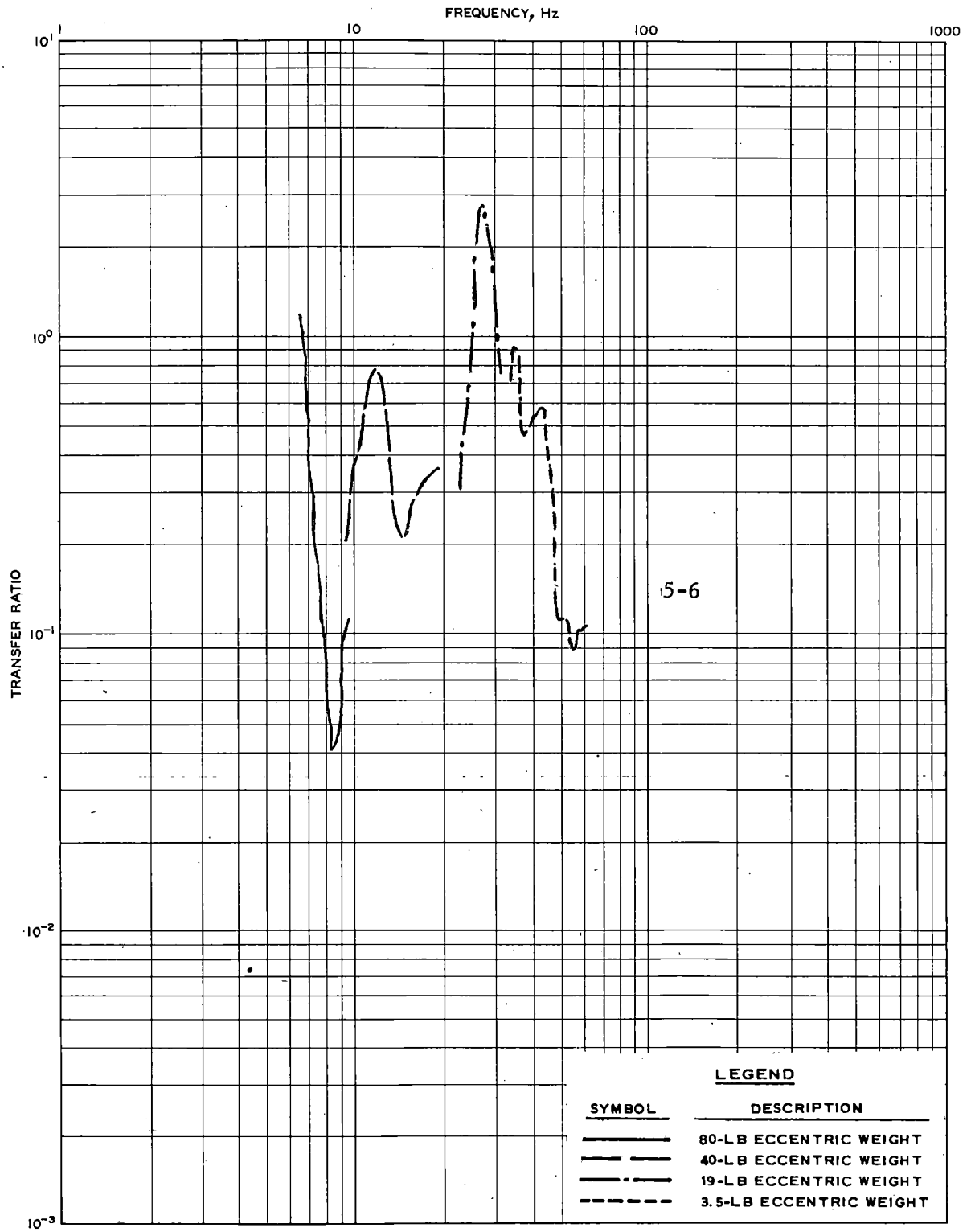

FIGURE 69. POSTTRAFFIC TRANSFER RATIO RESULTS, TRACK SECTION 1, VERTICAL MODE, POINTS 5-6

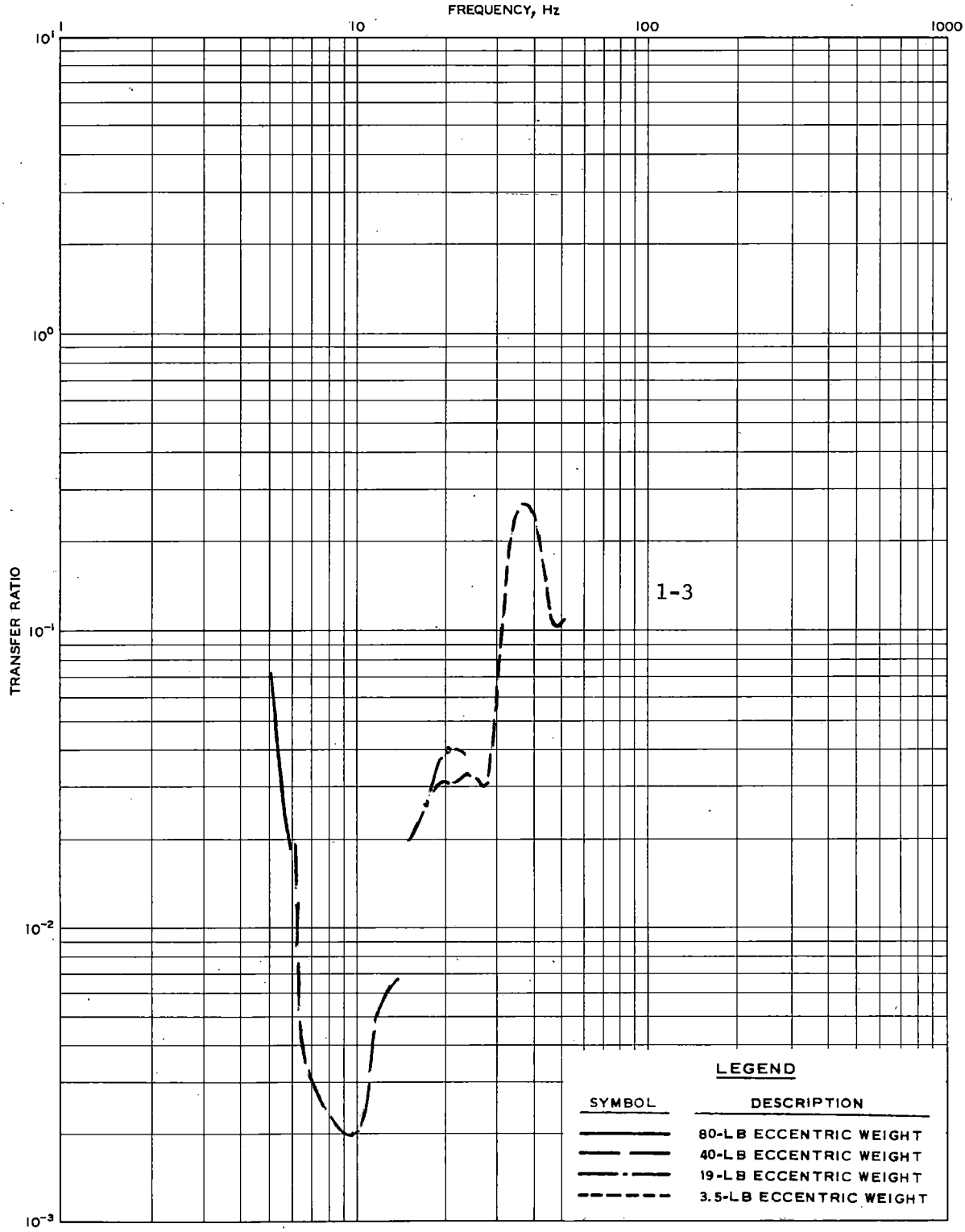

FIGURE 70. POSTTRAFFIC TRANSFER RATIO RESULTS, TRACK SECTION 1, VERTICAL MODE, POINTS 1-3

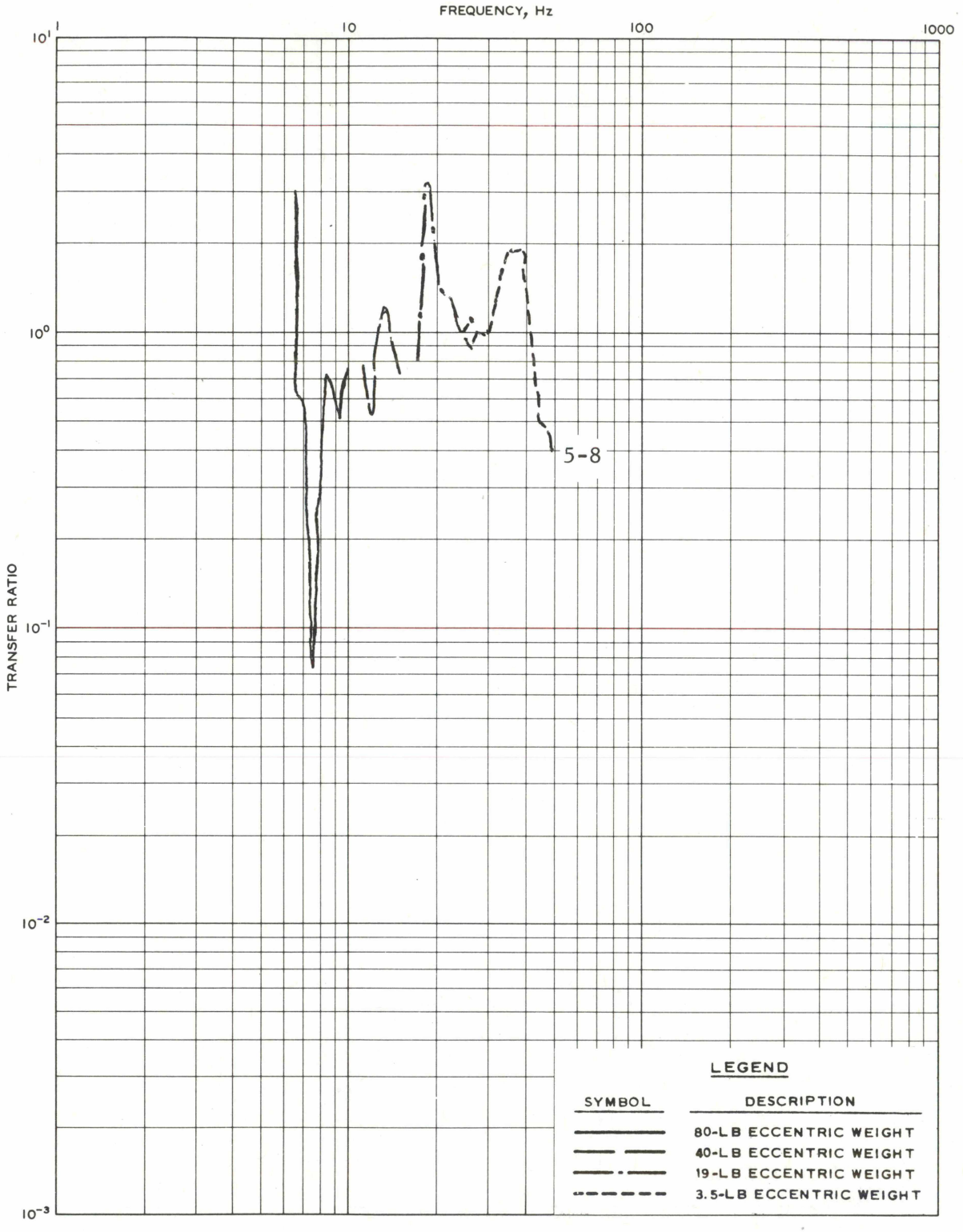

FIGURE 71. POSTTRAFFIC TRANSFER RATIO RESULTS, TRACK SECTION 1, VERTICAL MODE, POINTS 5-8

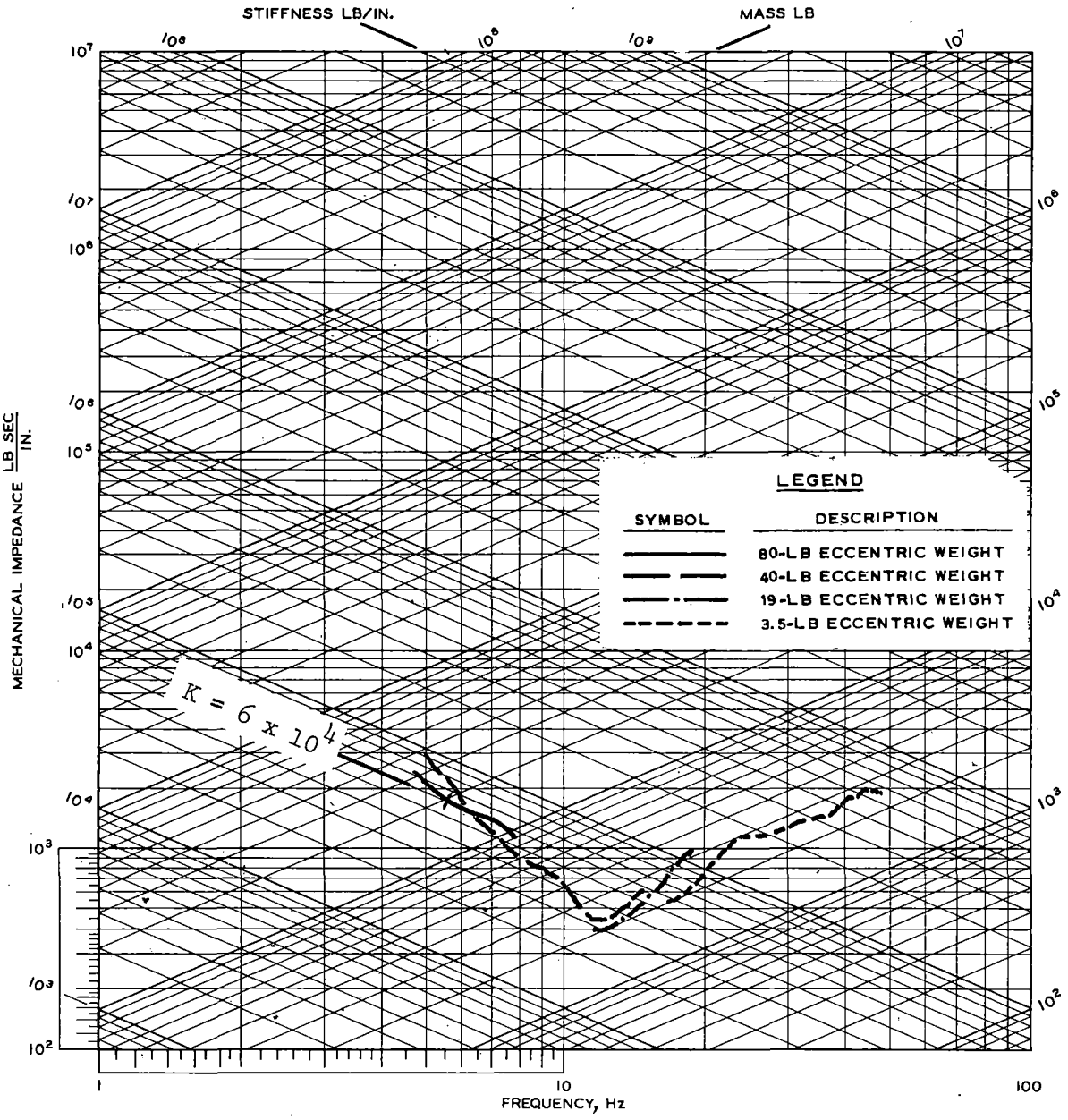

FIGURE 72. POSTTRAFFIC MECHANICAL IMPEDANCE RESULTS, LOCATION 2A, TRACK SECTION 2, VERTICAL MODE, POINT 1

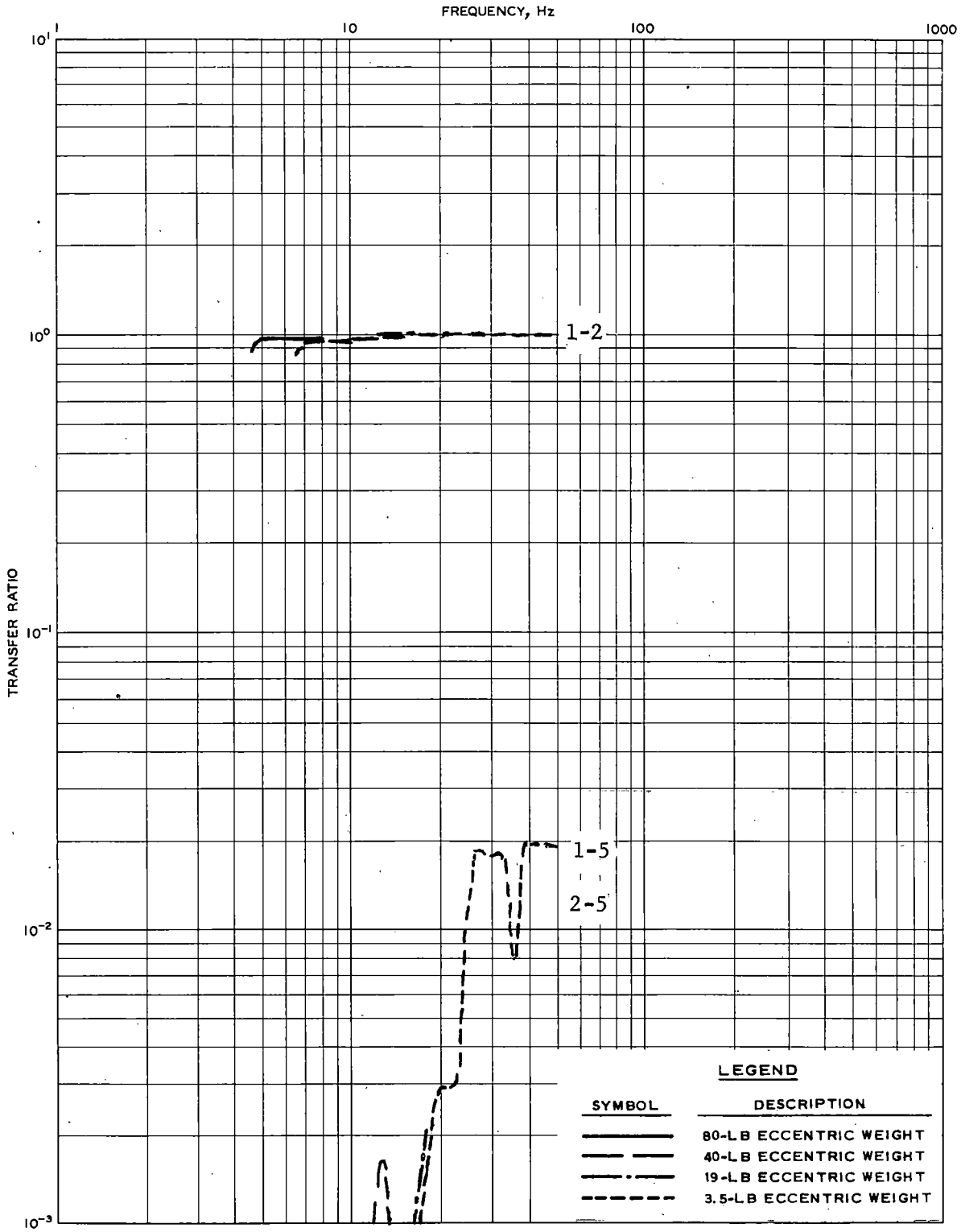

FIGURE 73. POSTTRAFFIC TRANSFER RATIO RESULTS, LOCATION 2A, TRACK SECTION 2, VERTICAL MODE, POINTS 1-2, 1-5, 2-5

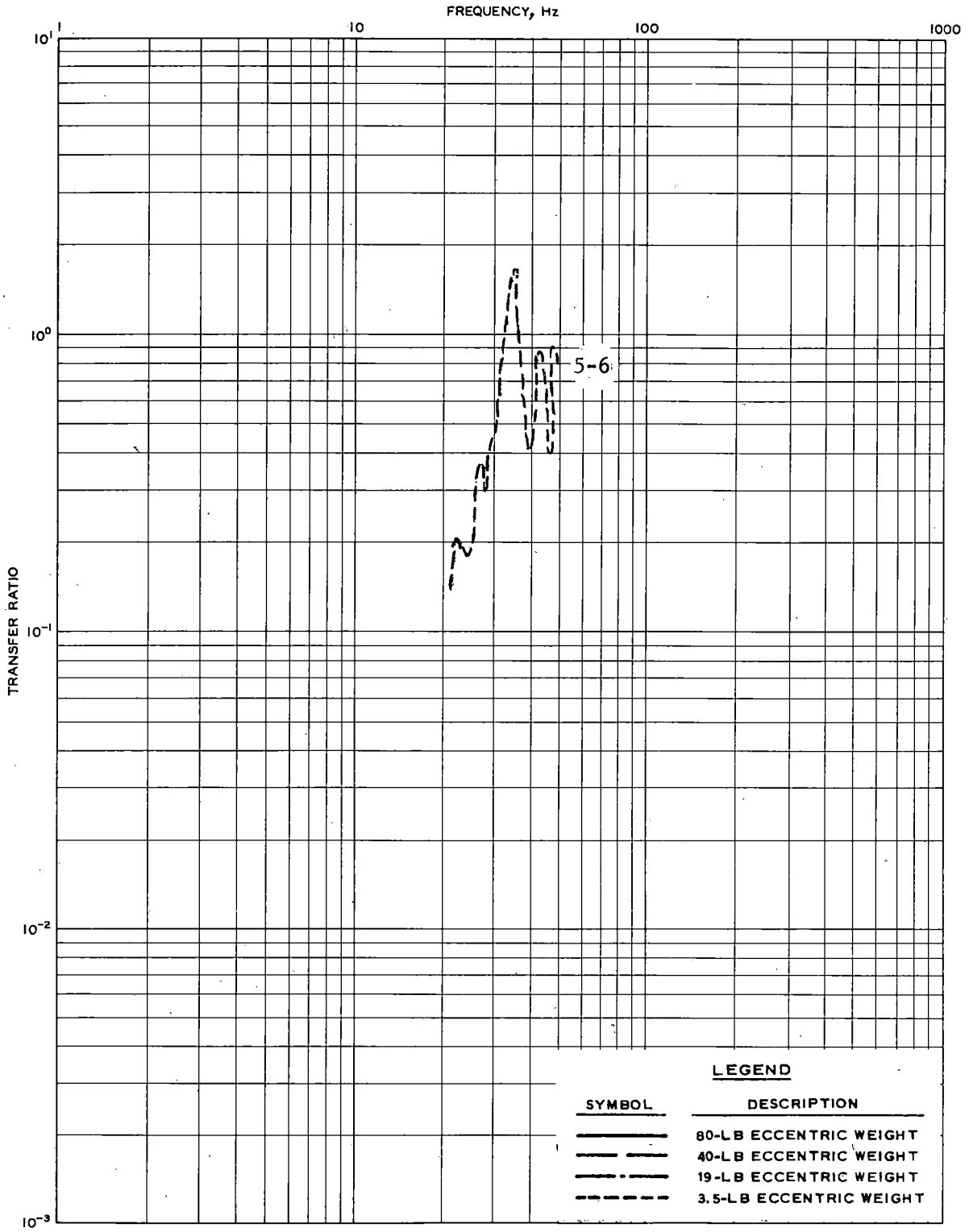

FIGURE 74. POSTTRAFFIC TRANSFER RATIO RESULTS, LOCATION 2A, TRACK SECTION 2, VERTICAL MODE, POINTS 5-6

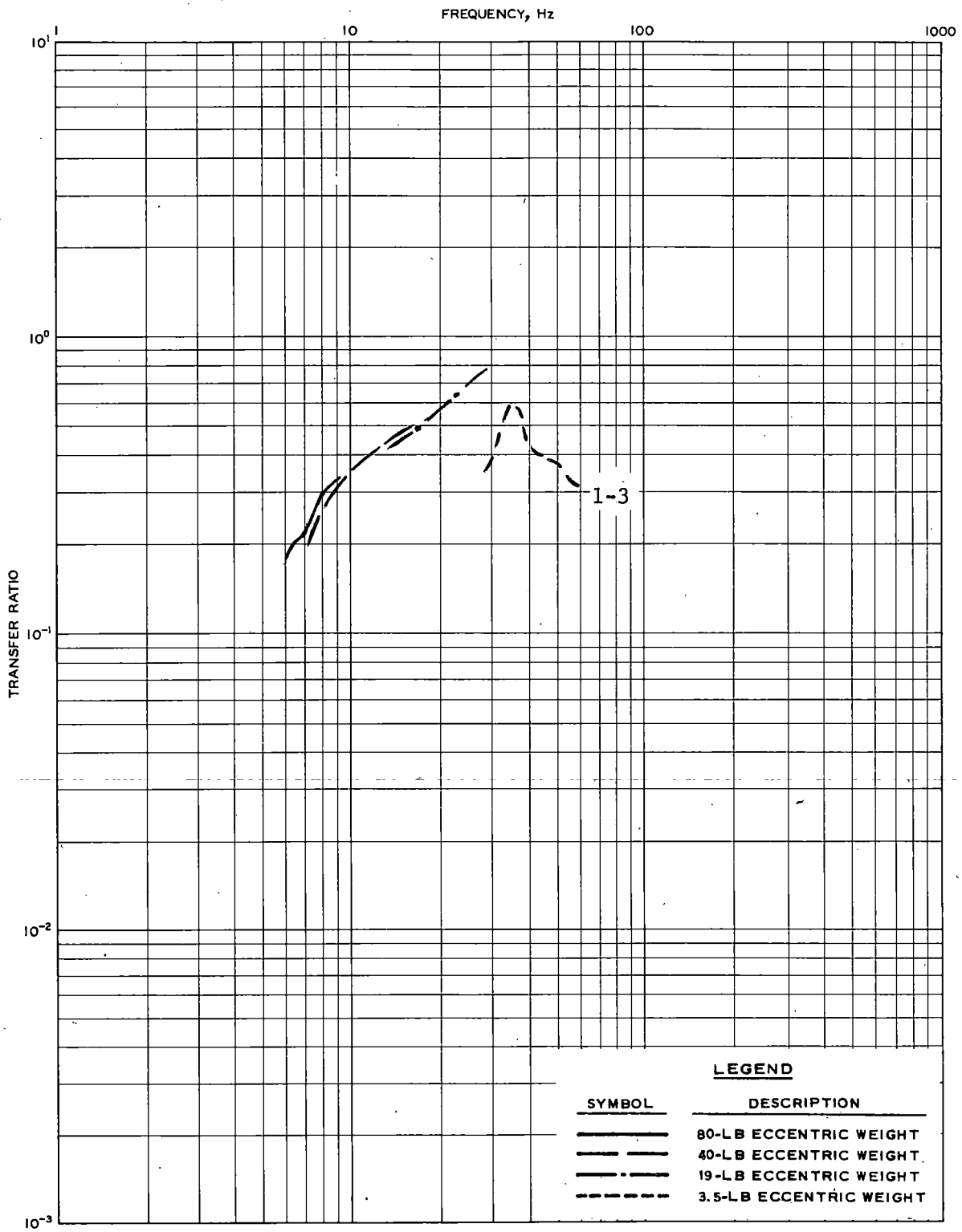

FIGURE 75. POSTTRAFFIC TRANSFER RATIO RESULTS, LOCATION 2A, TRACK SECTION 2, VERTICAL MODE, POINTS 1-3

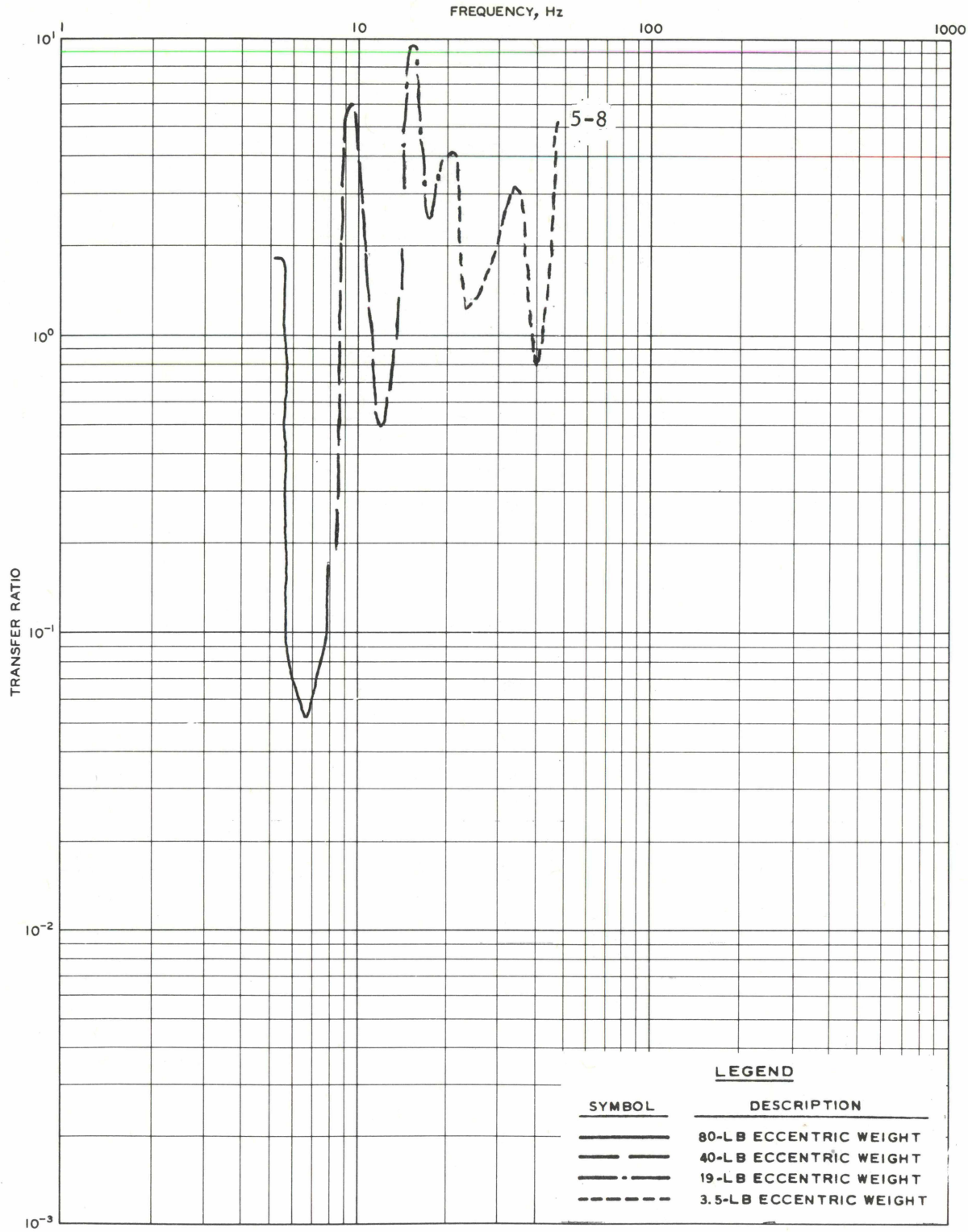

FIGURE 76. POSTTRAFFIC TRANSFER RATIO RESULTS, LOCATION 2A, TRACK SECTION 2, VERTICAL MODE, POINTS 5-8

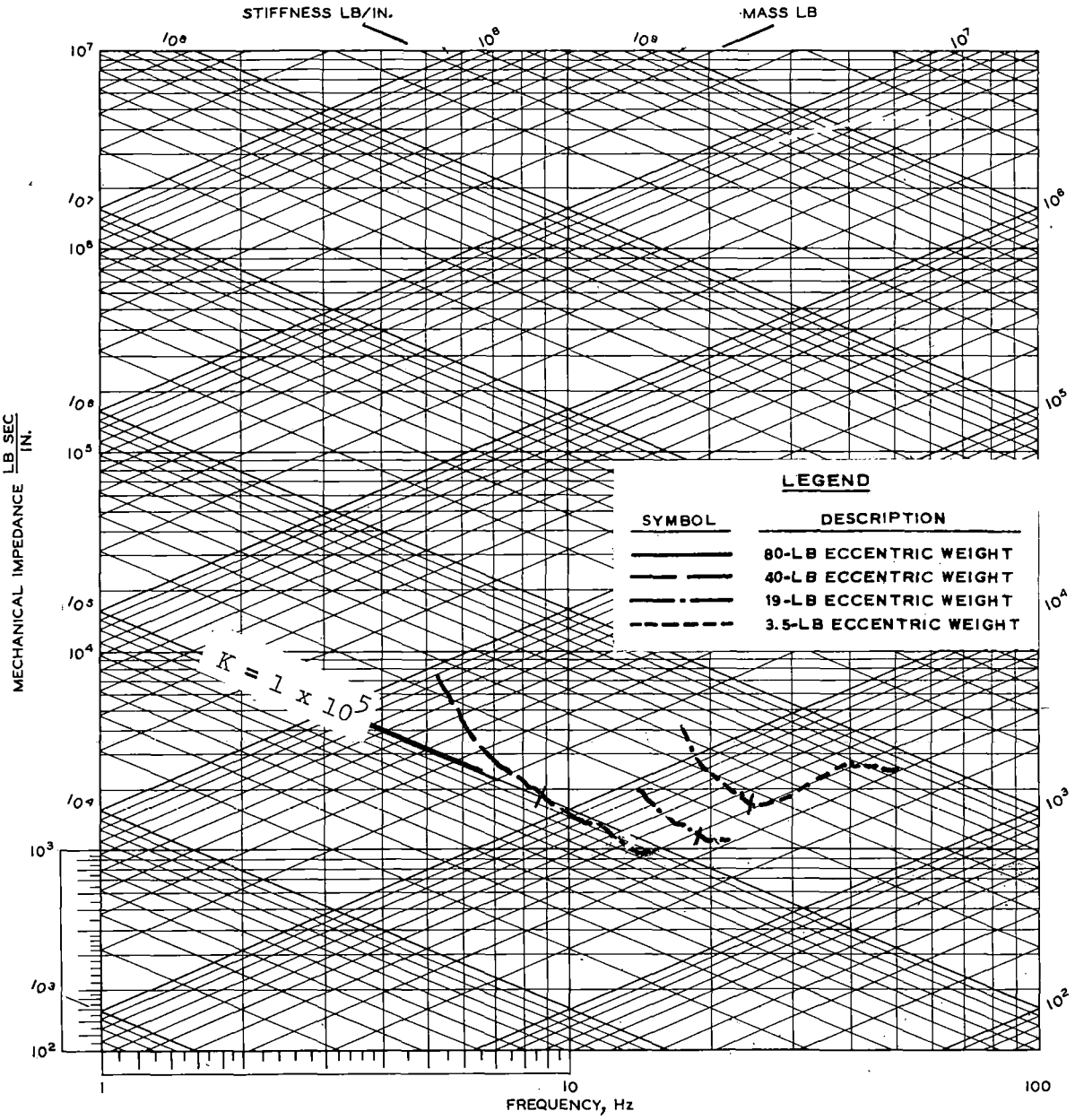

FIGURE 77. POSTTRAFFIC MECHANICAL IMPEDANCE RESULTS, LOCATION 2B, TRACK SECTION 2, VERTICAL MODE, POINT 1

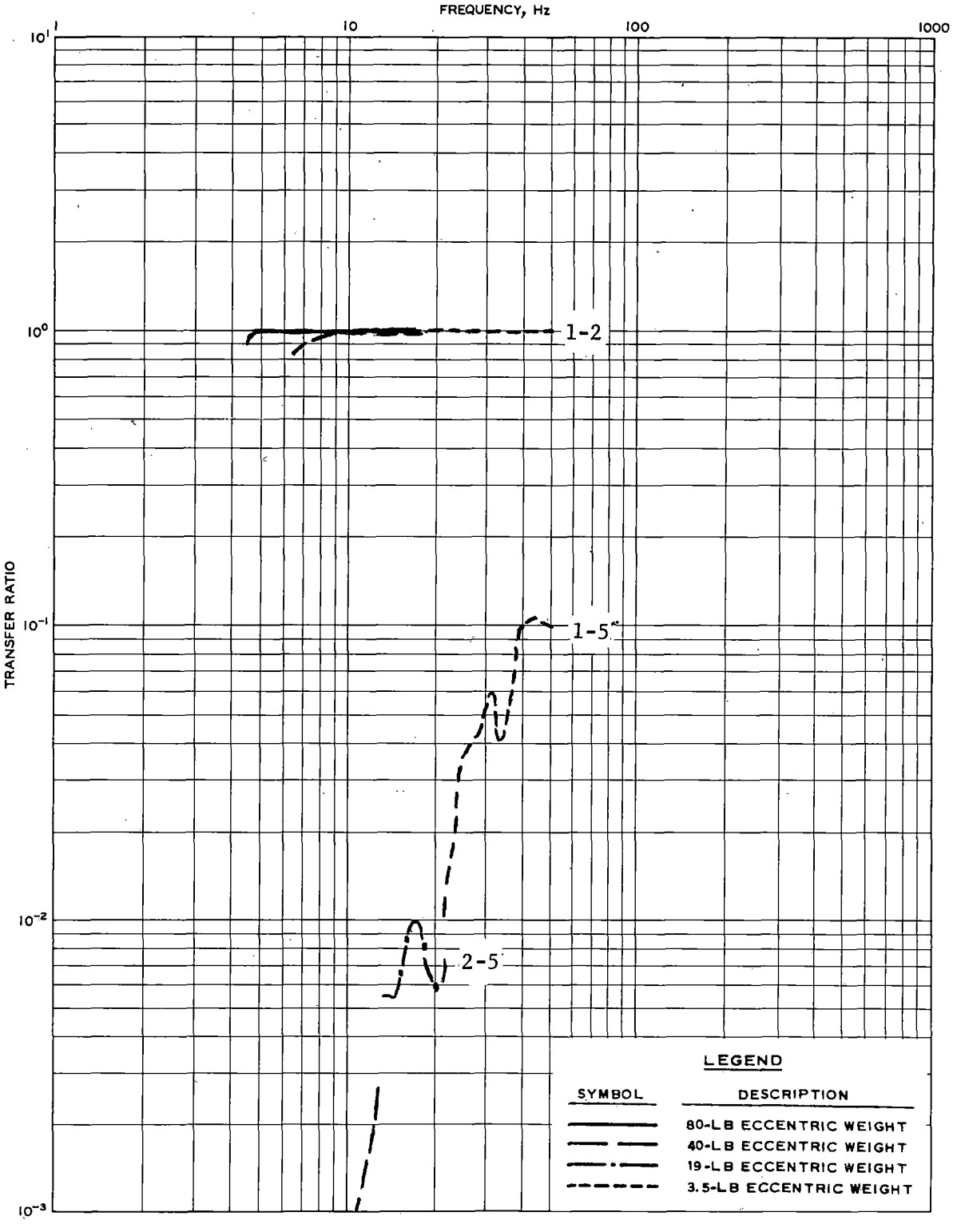

FIGURE 78. POSTTRAFFIC TRANSFER RATIO RESULTS, LOCATION 2B, TRACK SECTION 2, VERTICAL MODE, POINTS 1-2, 1-5, 2-5

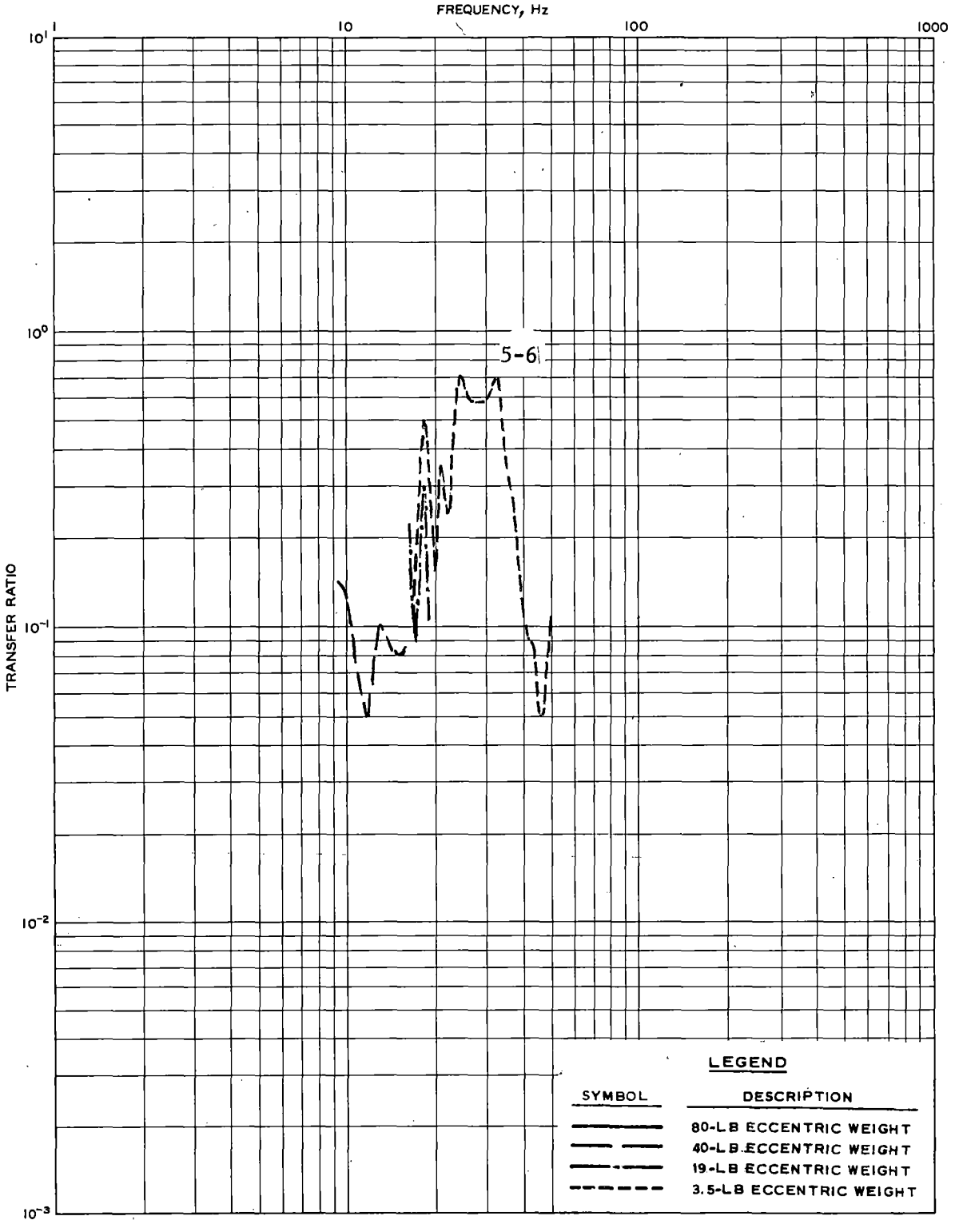

FIGURE 79. POSTTRAFFIC TRANSFER RATIO RESULTS, LOCATION 2B, TRACK SECTION 2, VERTICAL MODE, POINTS 5-6

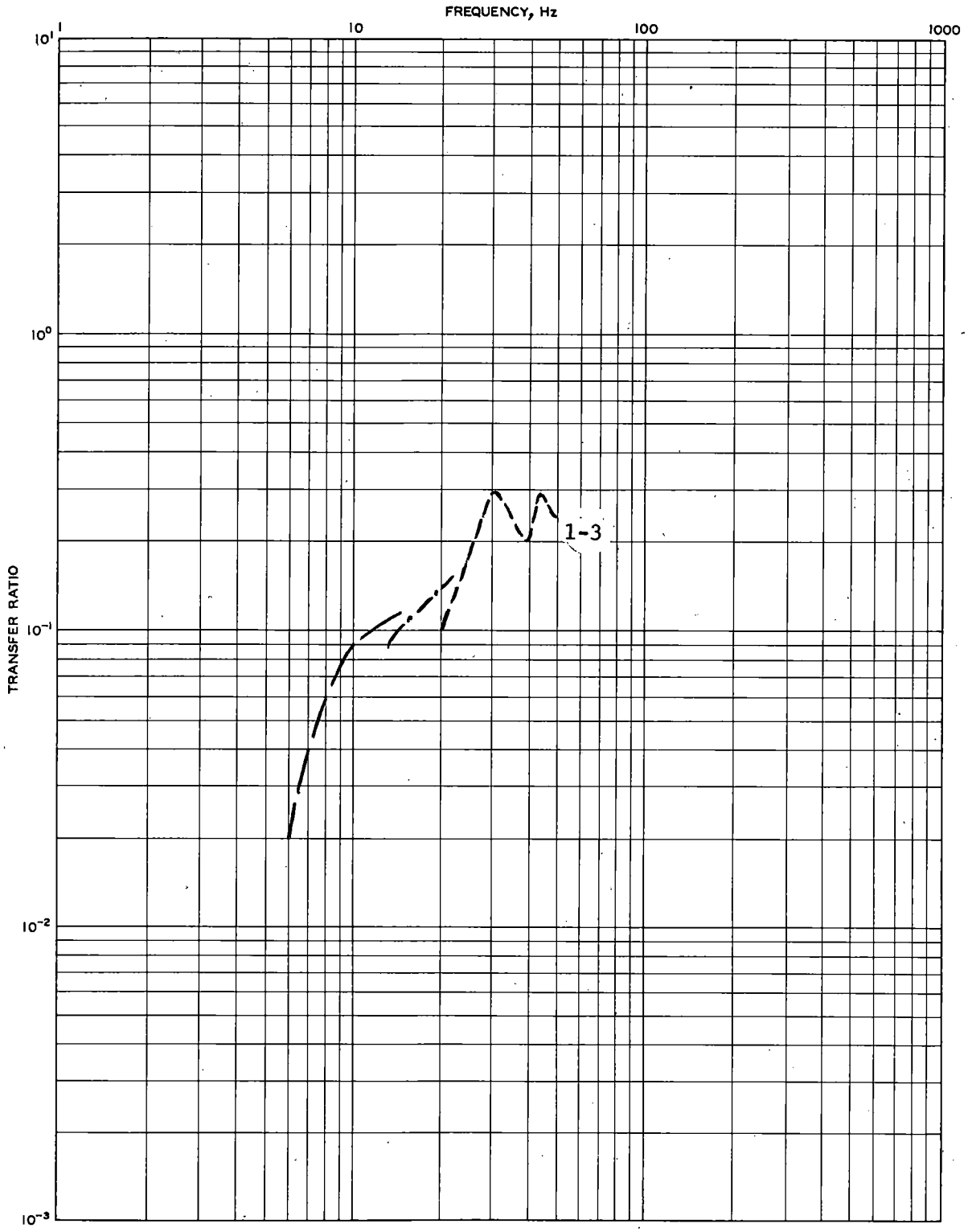

FIGURE 80. POSTTRAFFIC TRANSFER RATIO RESULTS, LOCATION 2B, TRACK SECTION 2, VERTICAL MODE, POINTS 1-3

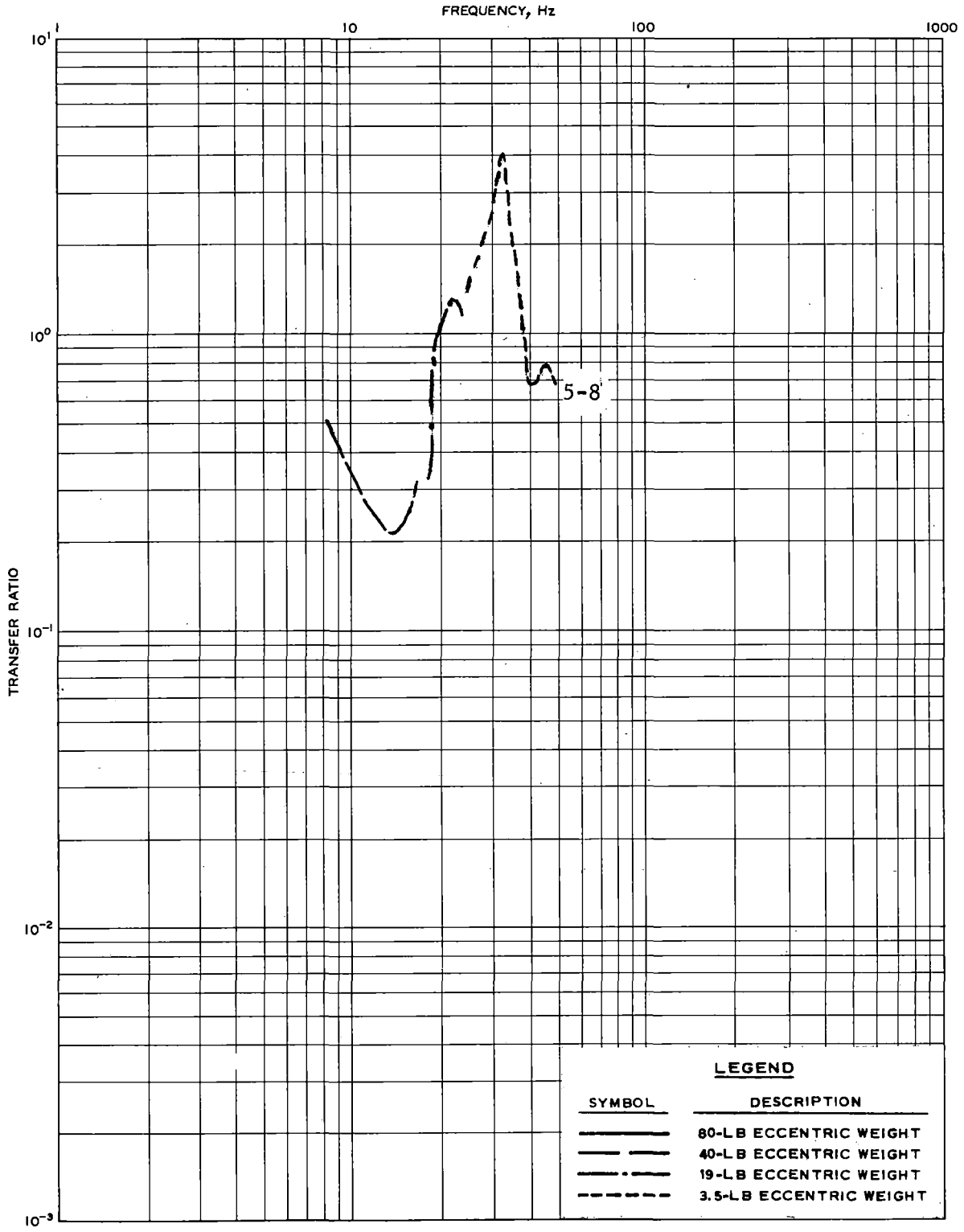

FIGURE 81. POSTTRAFFIC TRANSFER RATIO RESULTS, LOCATION 2B, TRACK SECTION 2, VERTICAL MODE, POINTS 5-8

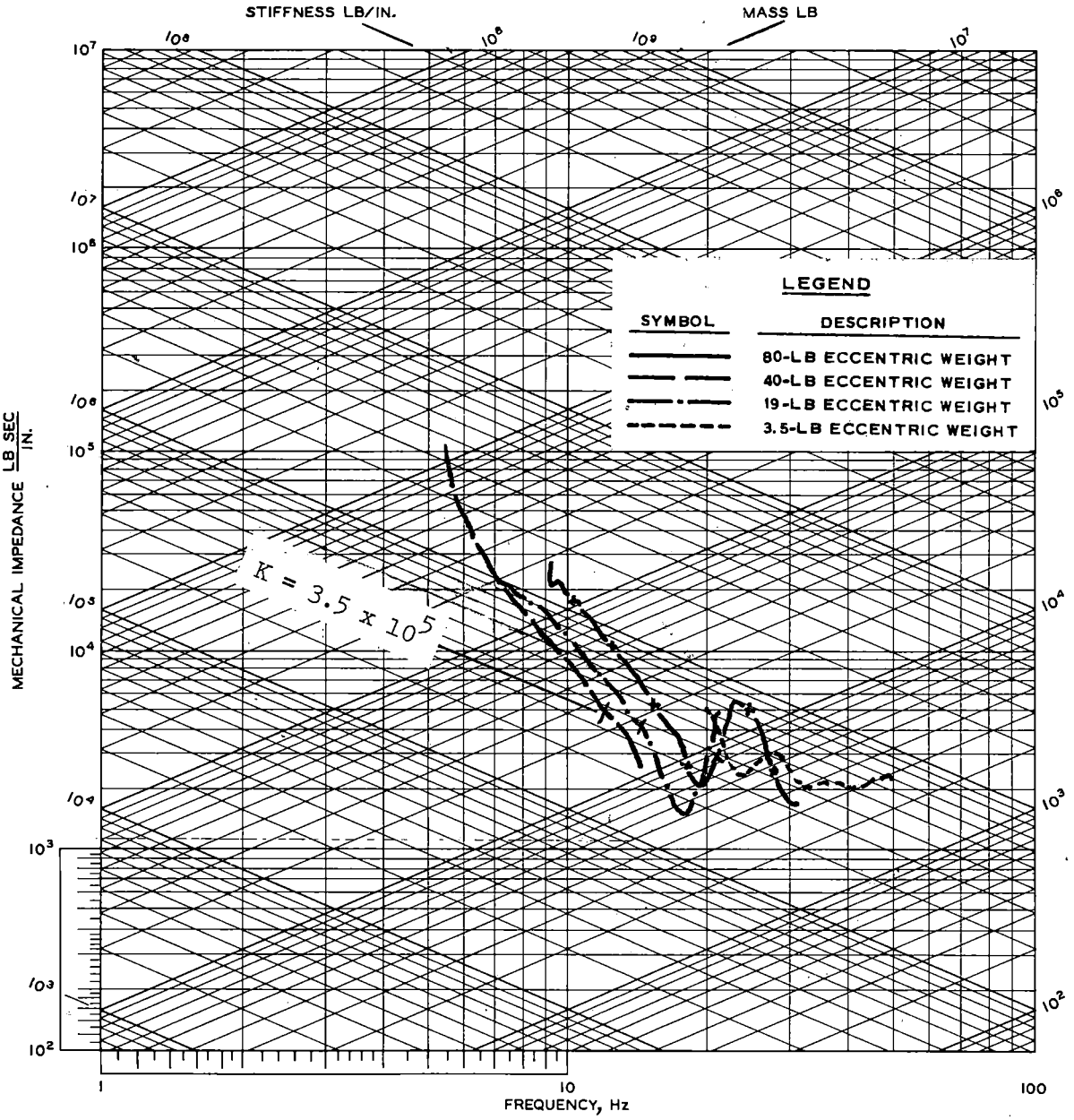

FIGURE 82. POSTTRAFFIC MECHANICAL IMPEDANCE RESULTS, LOCATION 3A, TRACK SECTION 3, VERTICAL MODE, POINT 1

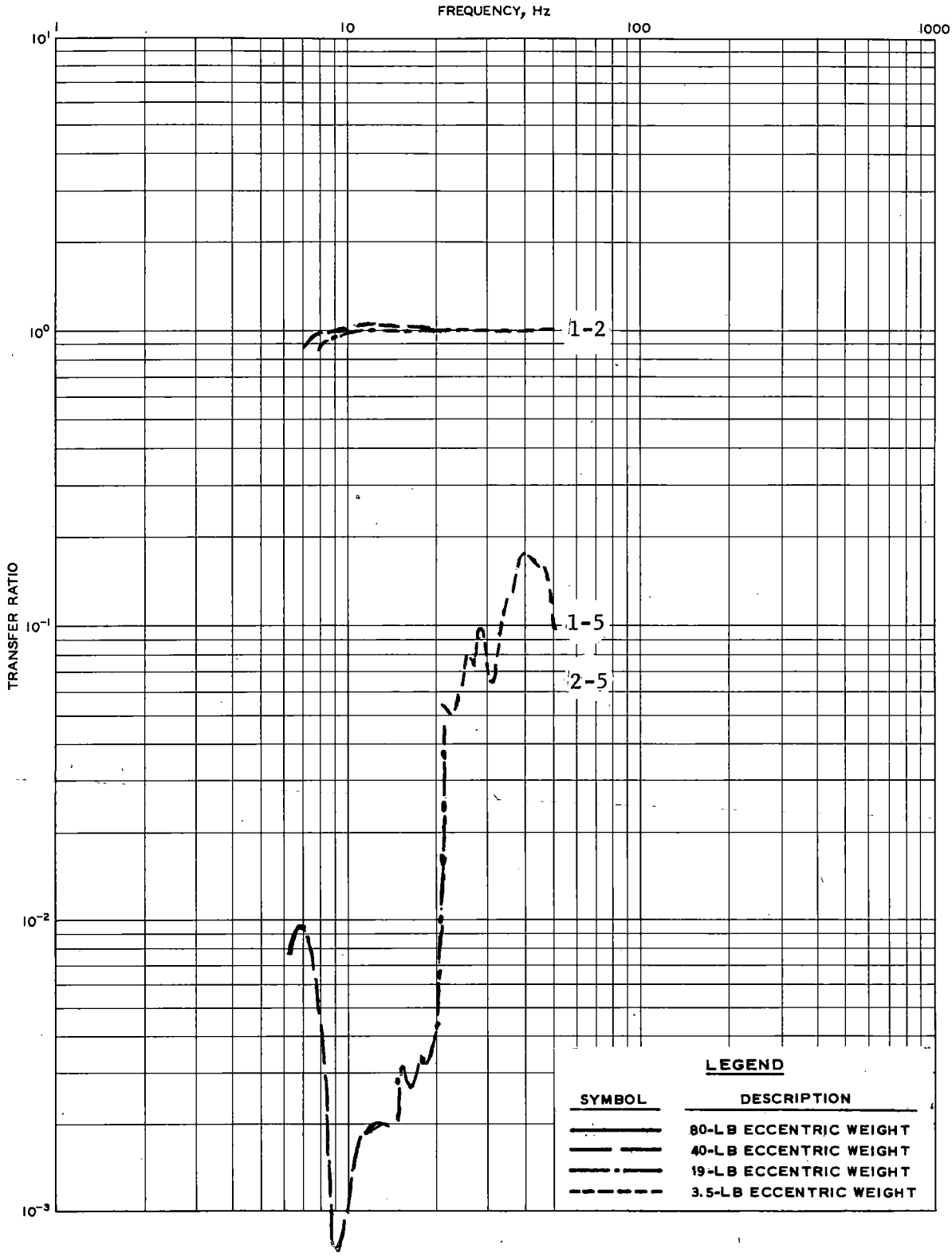

FIGURE 83. POSTTRAFFIC TRANSFER RATIO RESULTS, LOCATION 3A, TRACK SECTION 3, VERTICAL MODE, POINTS 1-2, 1-5, 2-5

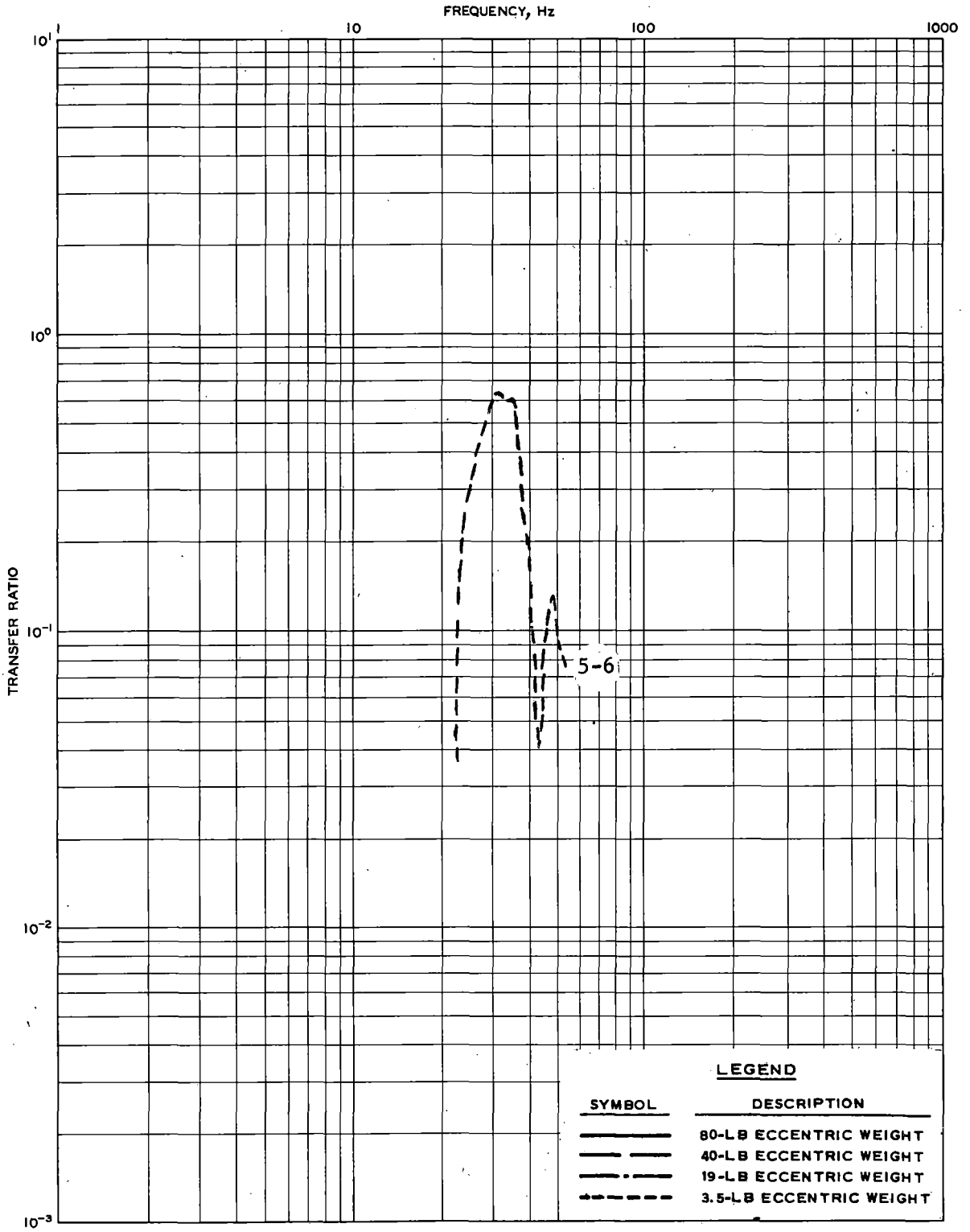

FIGURE 84. POSTTRAFFIC TRANSFER RATIO RESULTS, LOCATION 3A, TRACK SECTION 3, VERTICAL MODE, POINTS 5-6

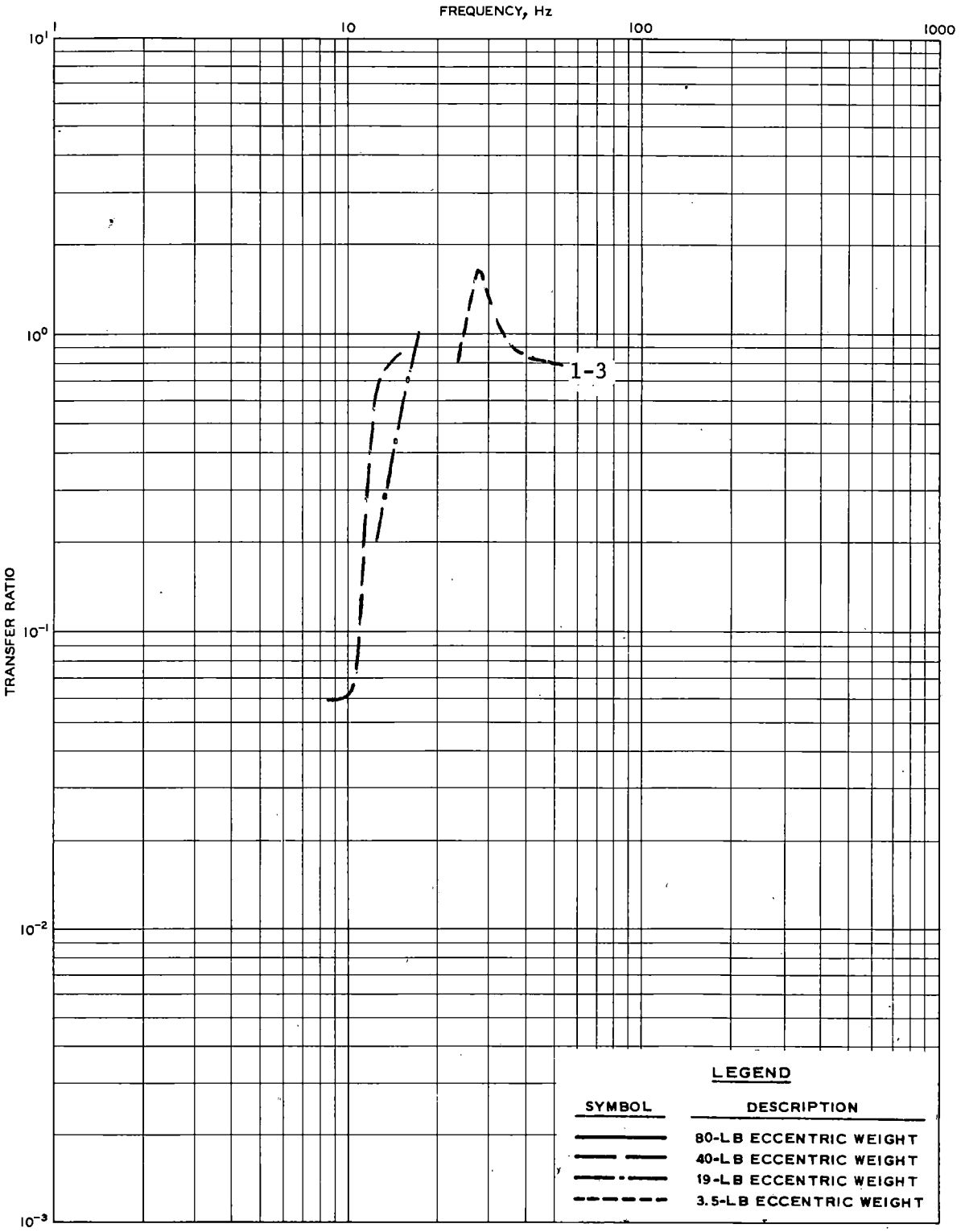

FIGURE 85. POSTTRAFFIC TRANSFER RATIO RESULTS, LOCATION 3A, TRACK SECTION 3, VERTICAL MODE, POINTS 1-3

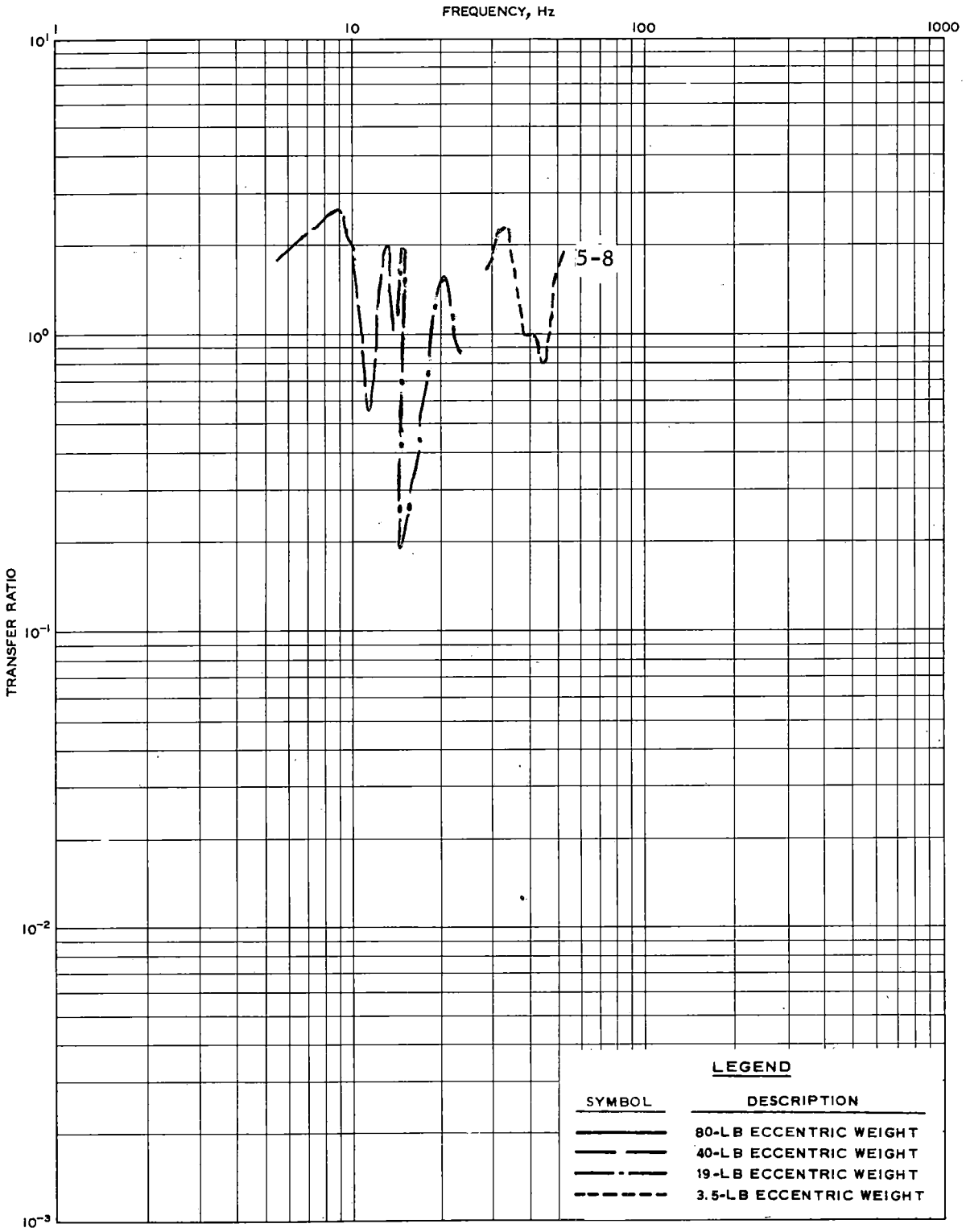

FIGURE 86. POSTTRAFFIC TRANSFER RATIO RESULTS, LOCATION 3A, TRACK SECTION 3, VERTICAL MODE, POINTS 5-8

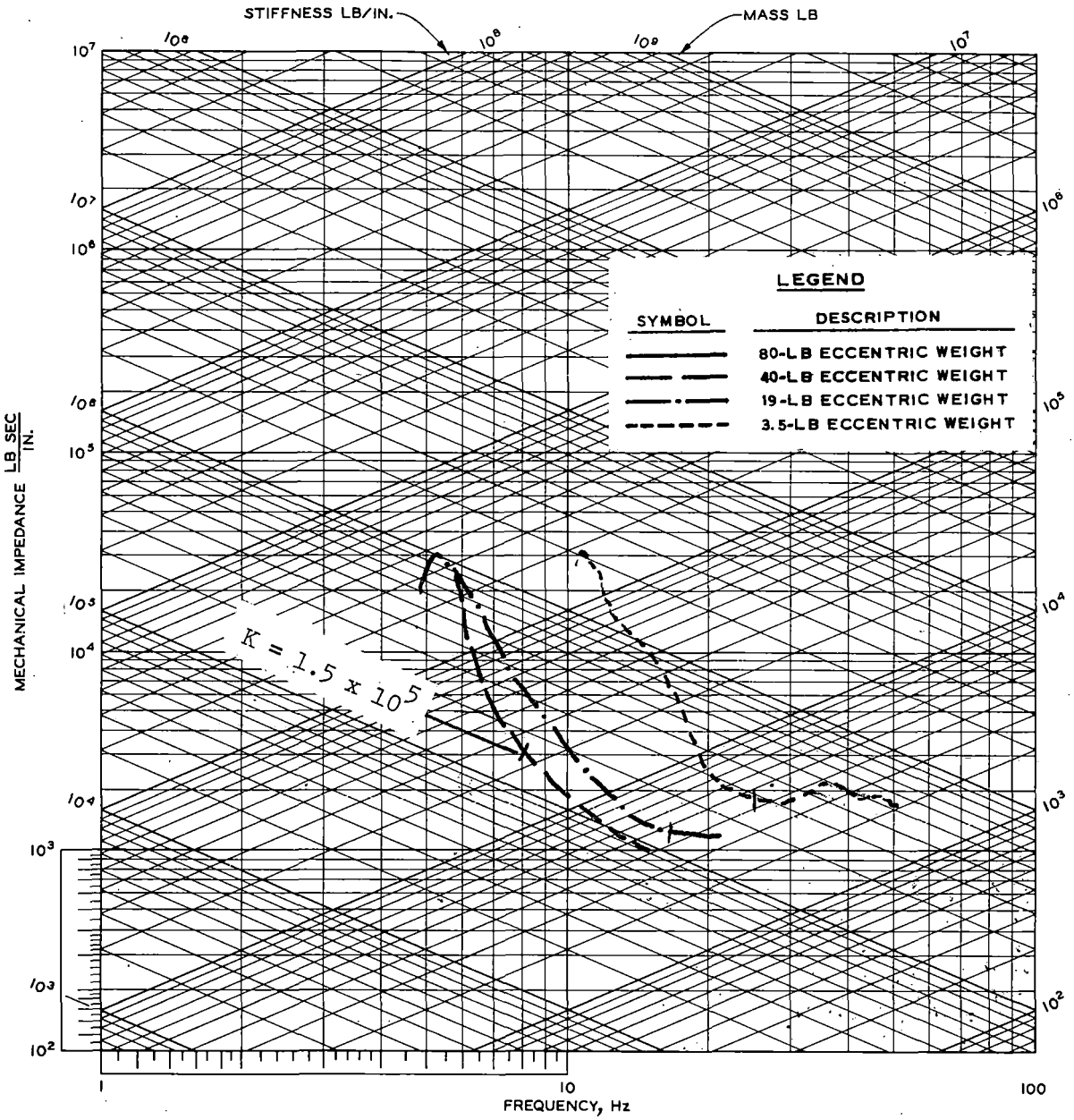

FIGURE 87. POSTTRAFFIC MECHANICAL IMPEDANCE RESULTS, LOCATION 3B, TRACK SECTION 3, VERTICAL MODE, POINT 1

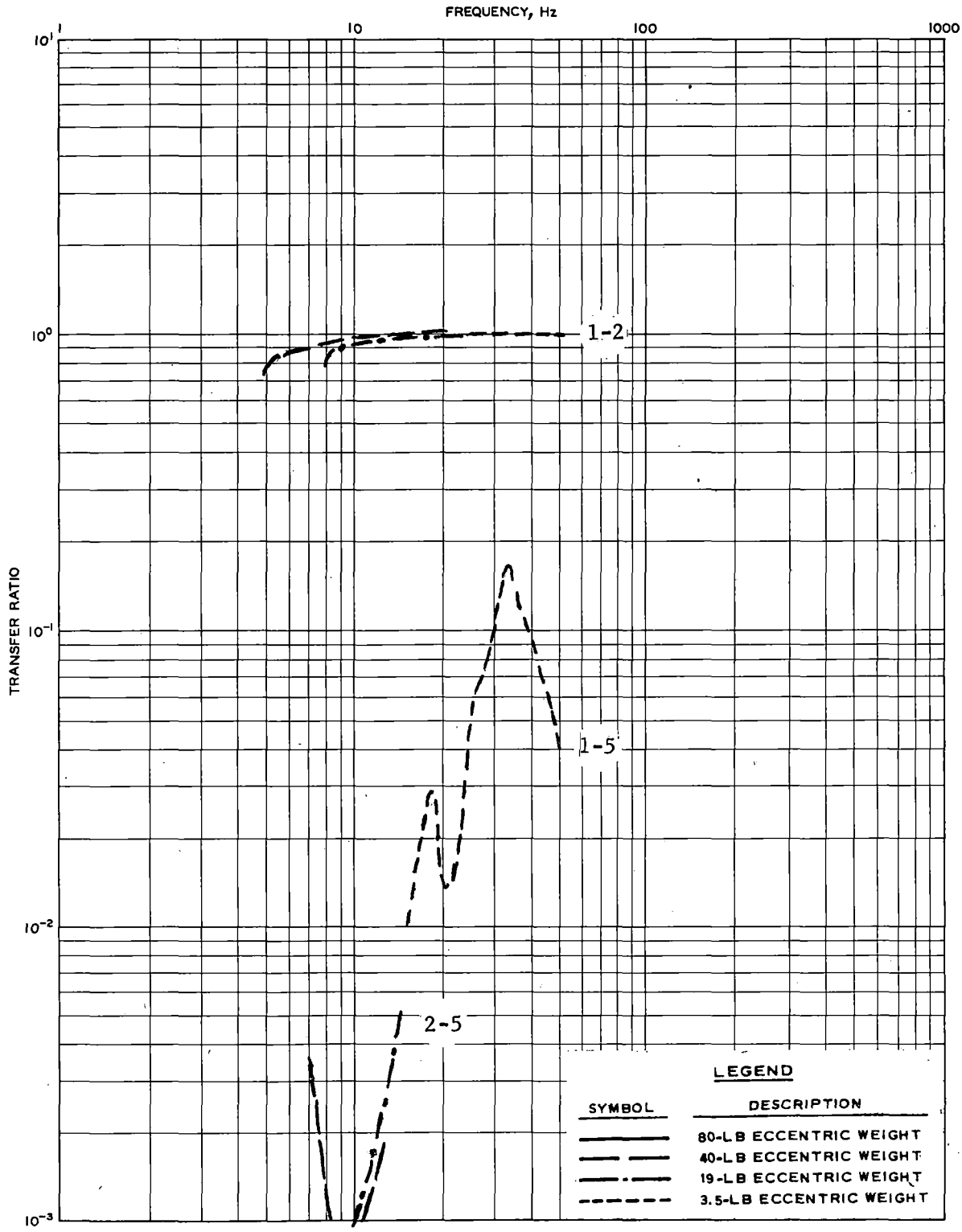

FIGURE 88. POSTTRAFFIC TRANSFER RATIO RESULTS, LOCATION 3B, TRACK SECTION 3, VERTICAL MODE, POINTS 1-2, 1-5, 2-5.

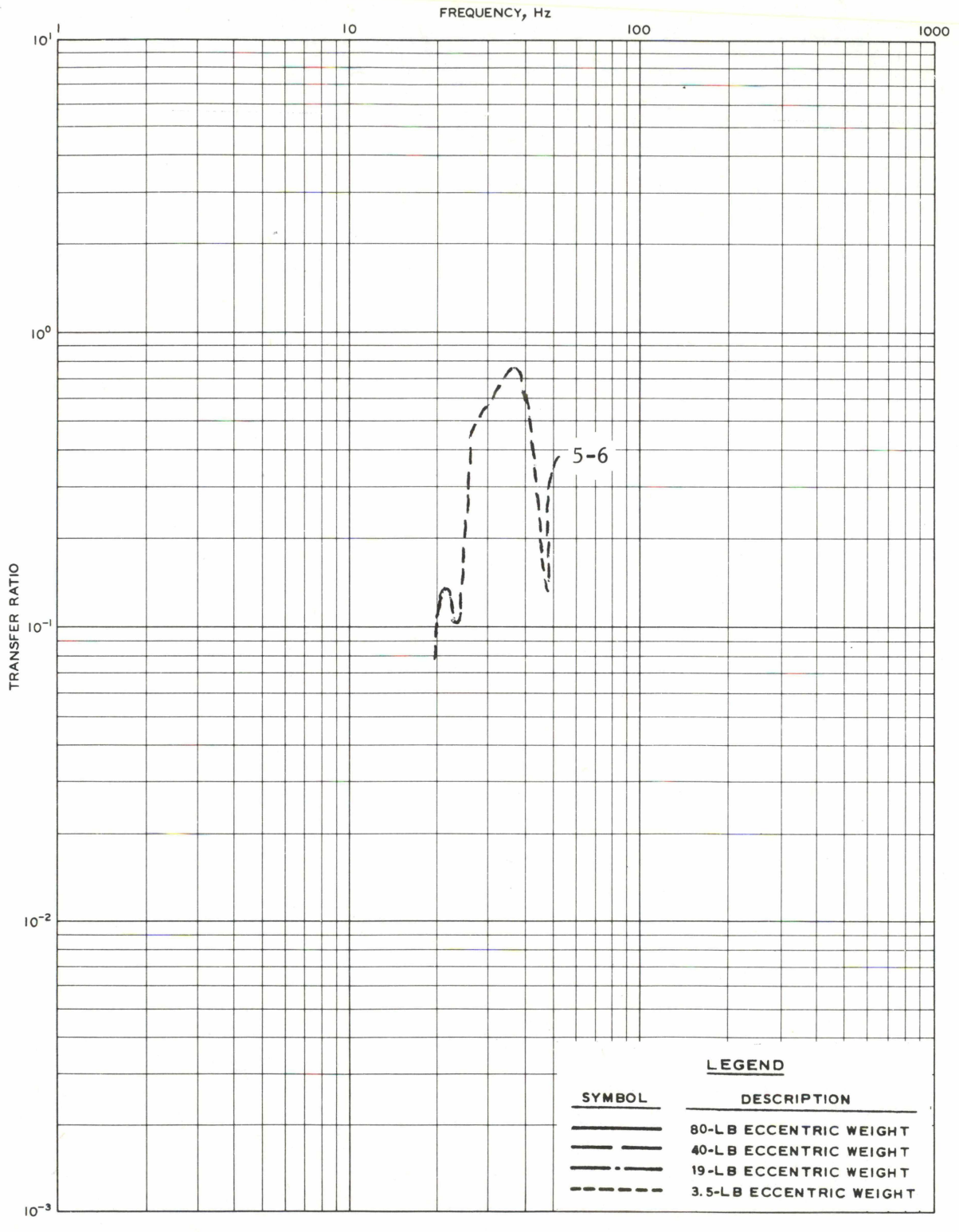

FIGURE 89. POSTTRAFFIC TRANSFER RATIO RESULTS, LOCATION 3B, TRACK SECTION 3, VERTICAL MODE, POINTS 5-6

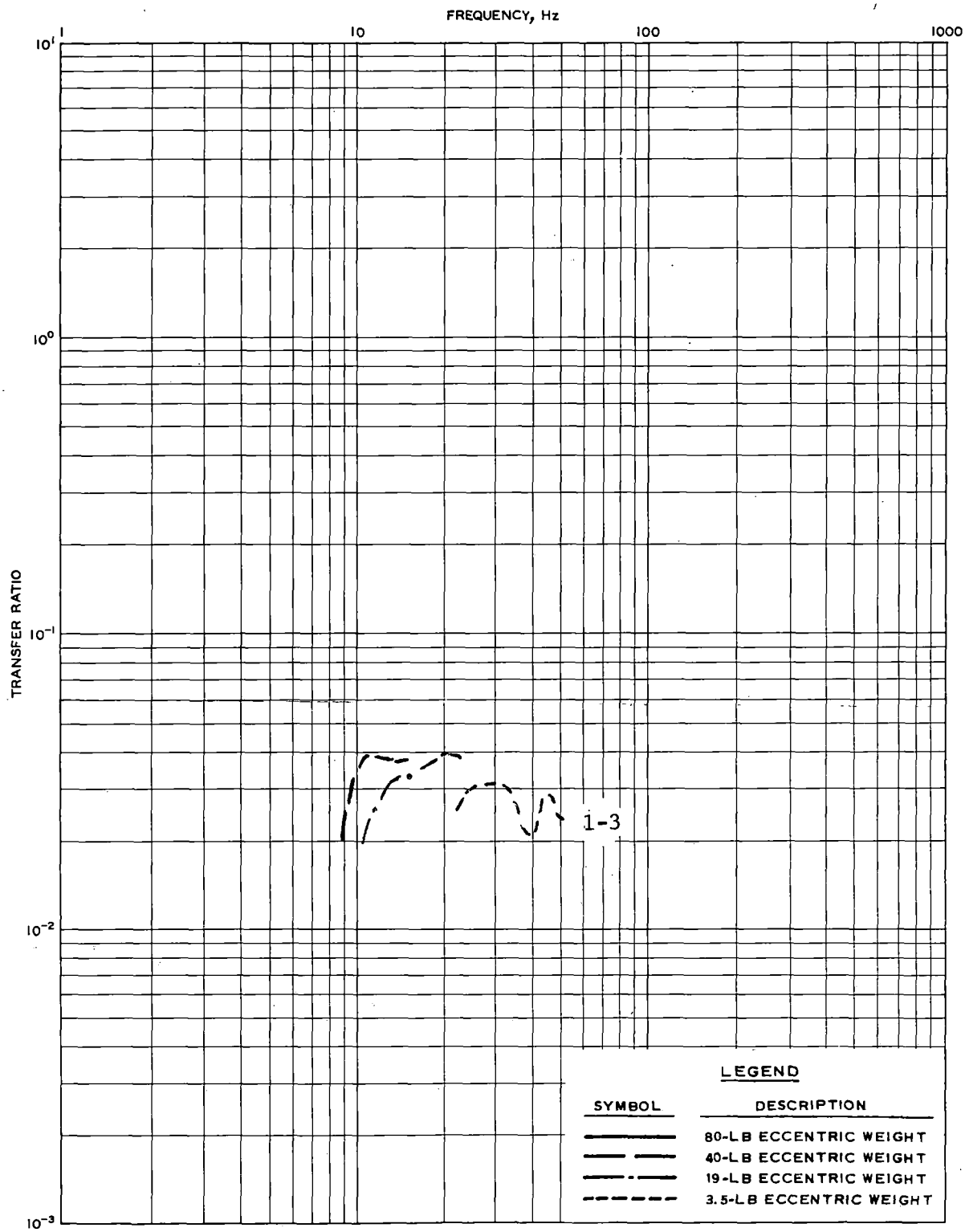

FIGURE 90. POSTTRAFFIC TRANSFER RATIO RESULTS, LOCATION 3B, TRACK SECTION 3, VERTICAL MODE, POINTS 1-3

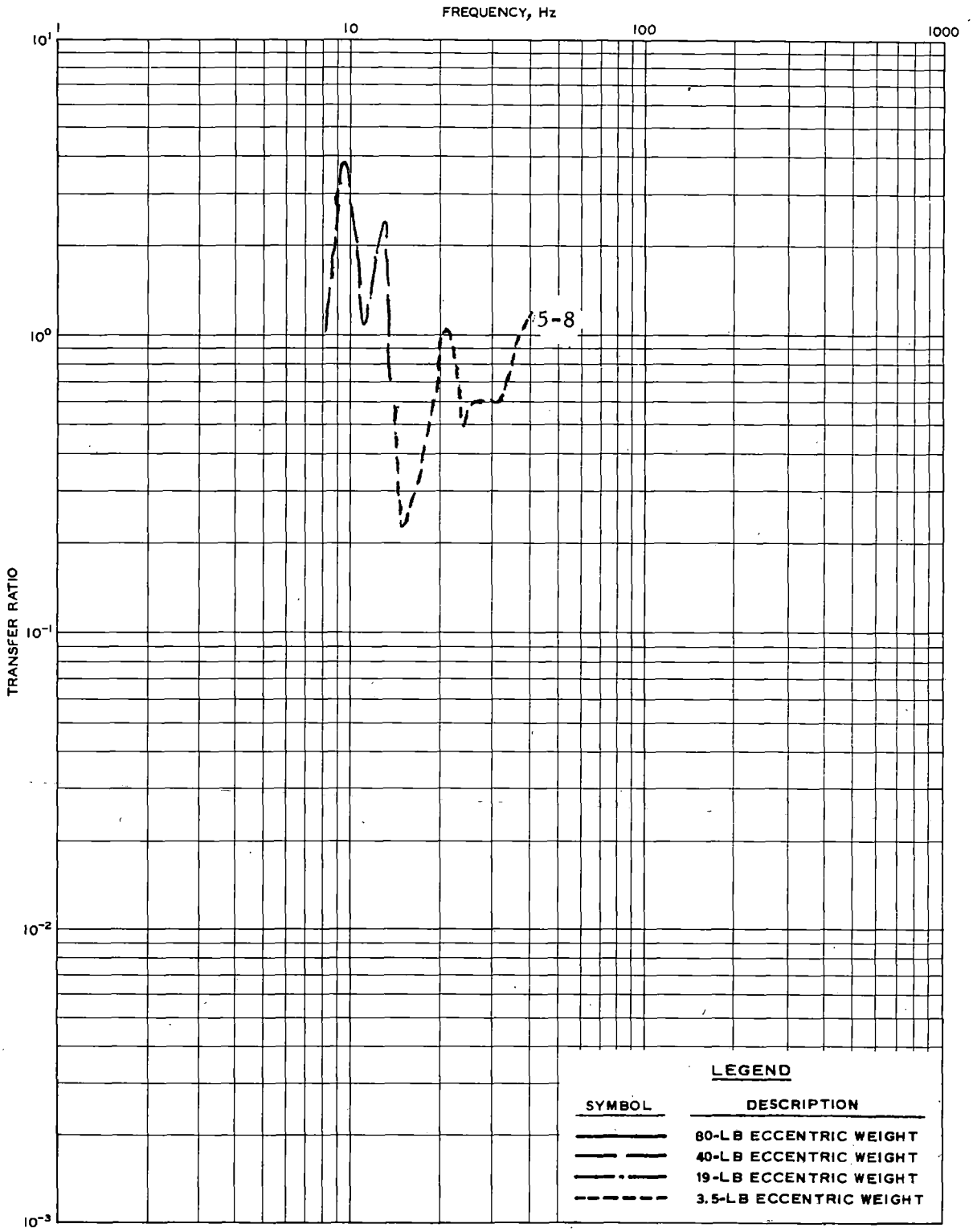

FIGURE 91. POSTTRAFFIC TRANSFER RATIO RESULTS, LOCATION 3B, TRACK SECTION 3, VERTICAL MODE, POINTS 5-8

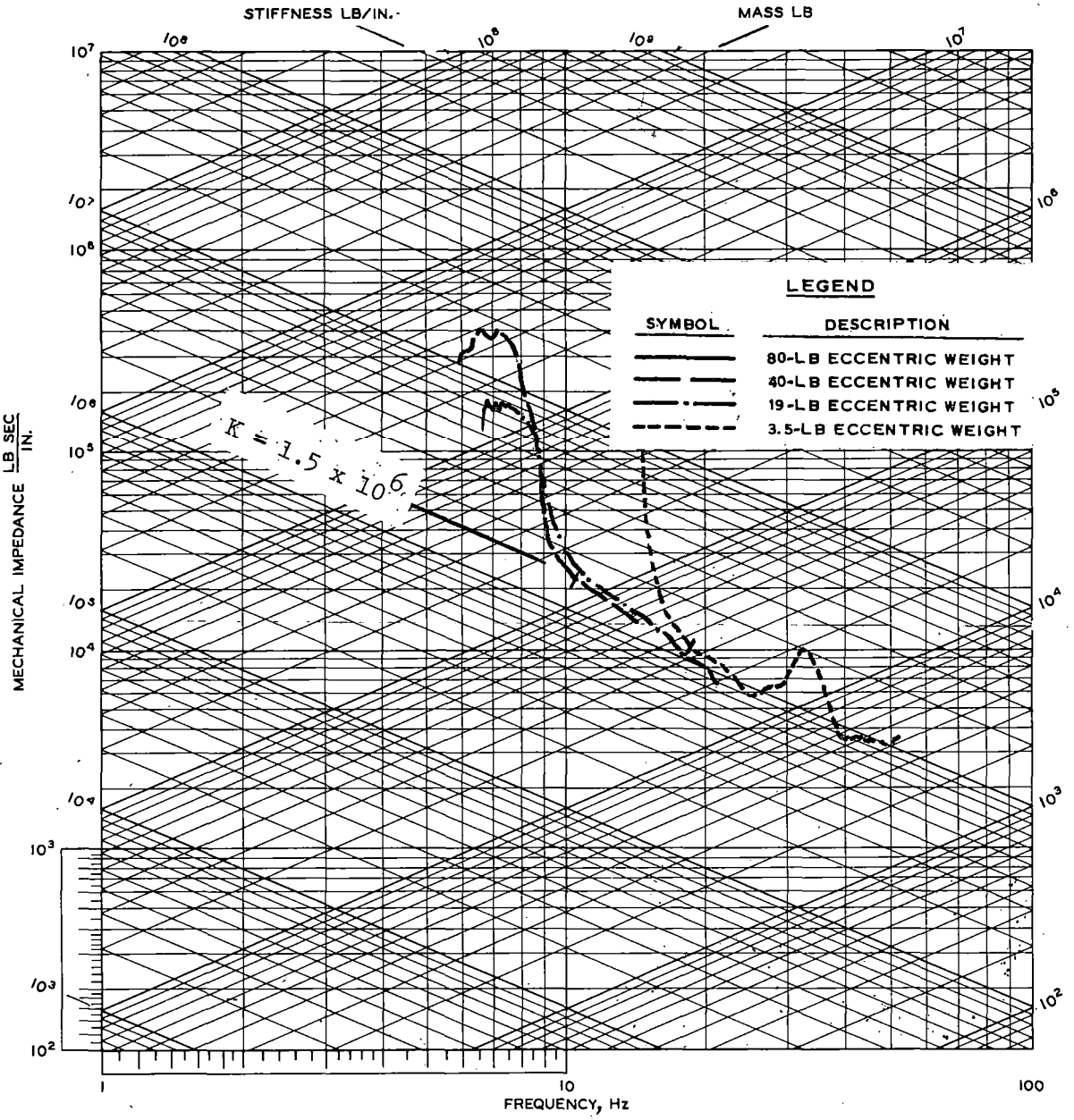

FIGURE 92. POSTTRAFFIC MECHANICAL IMPEDANCE RESULTS, TRACK SECTION 4, VERTICAL MODE, POINT 1

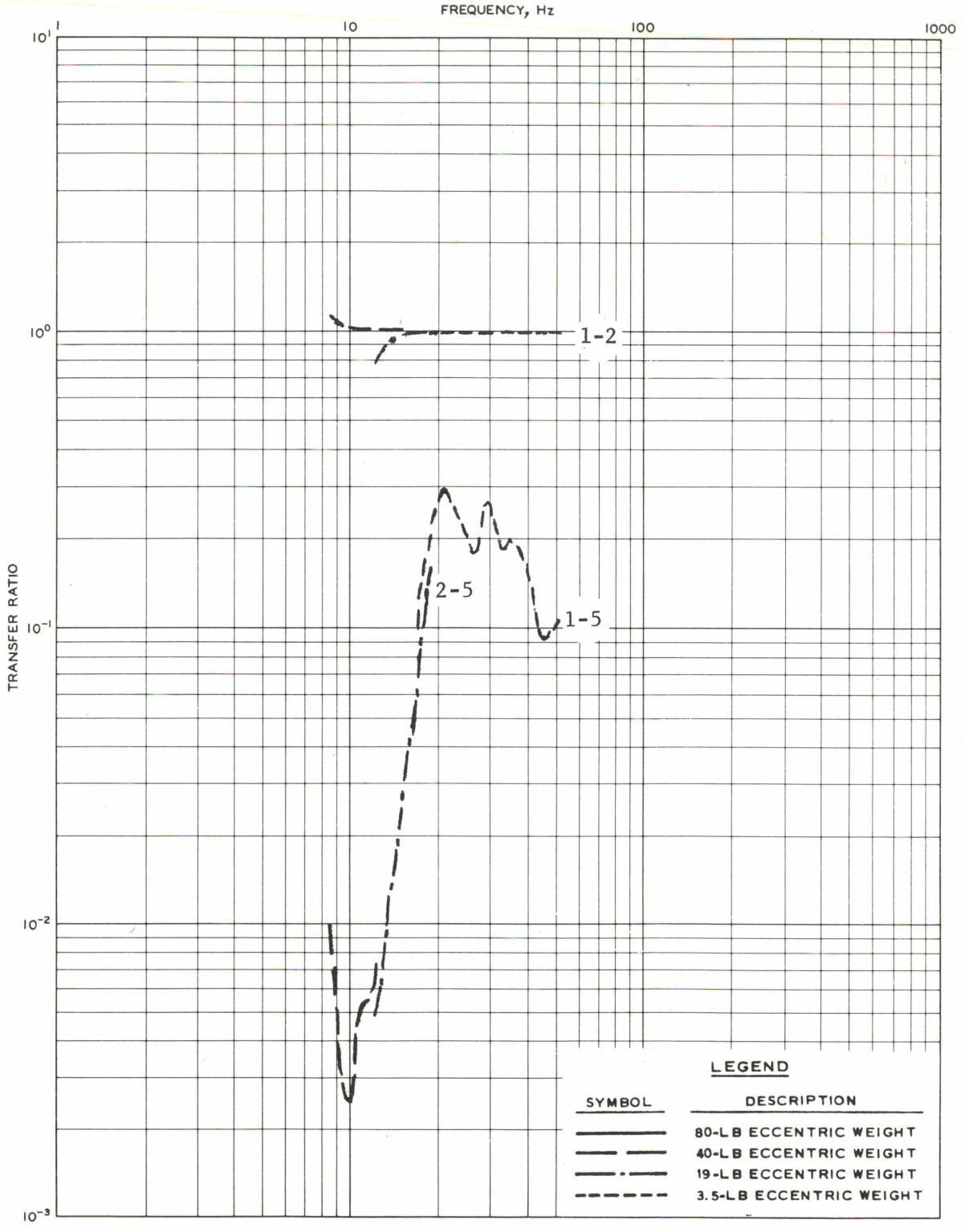

FIGURE 93. POSTTRAFFIC TRANSFER RATIO RESULTS, TRACK SECTION 4, VERTICAL MODE, POINTS 1-2, 1-5, 2-5

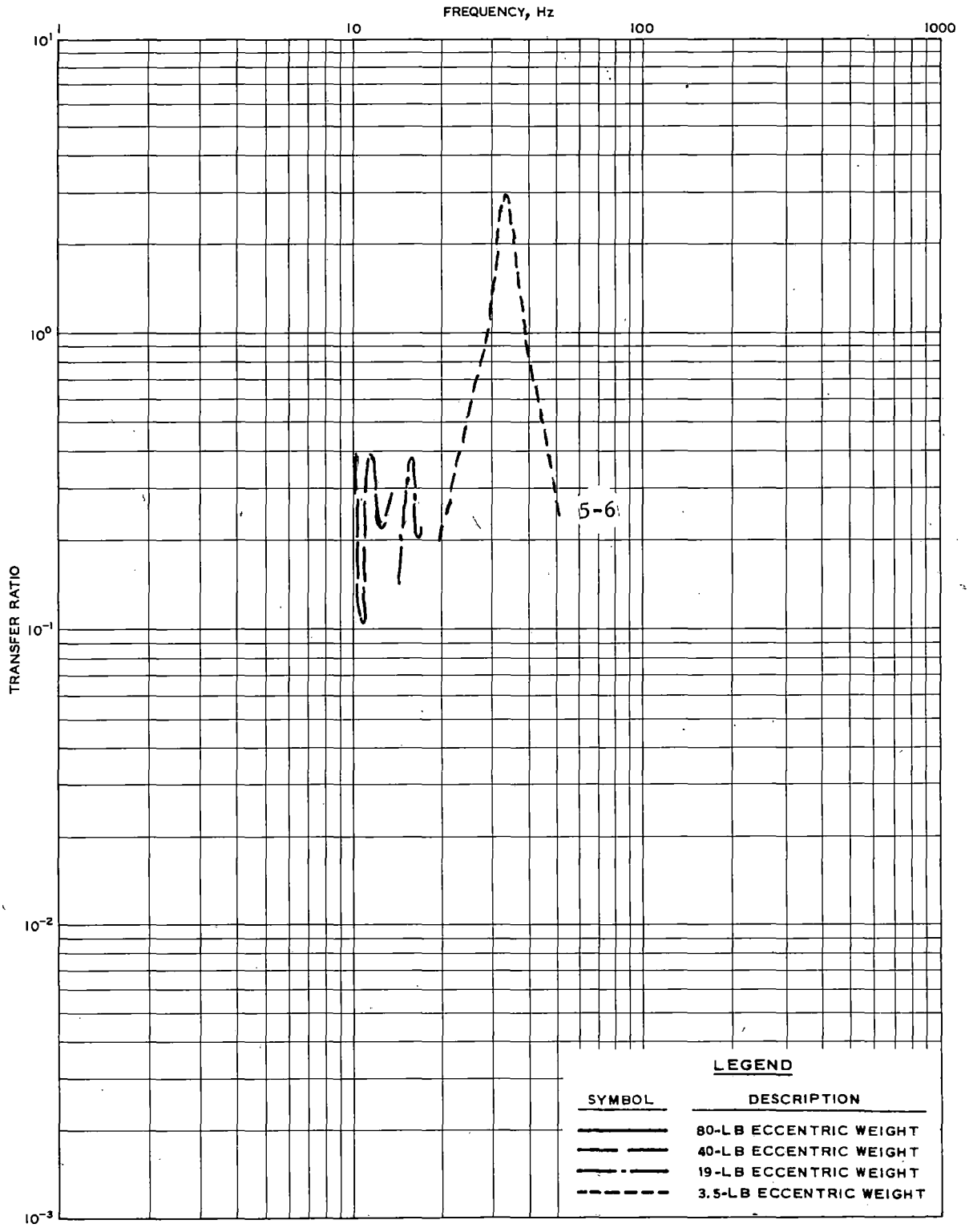

FIGURE 94. POSTTRAFFIC TRANSFER RATIO RESULTS, TRACK SECTION 4, VERTICAL MODE, POINTS 5-6

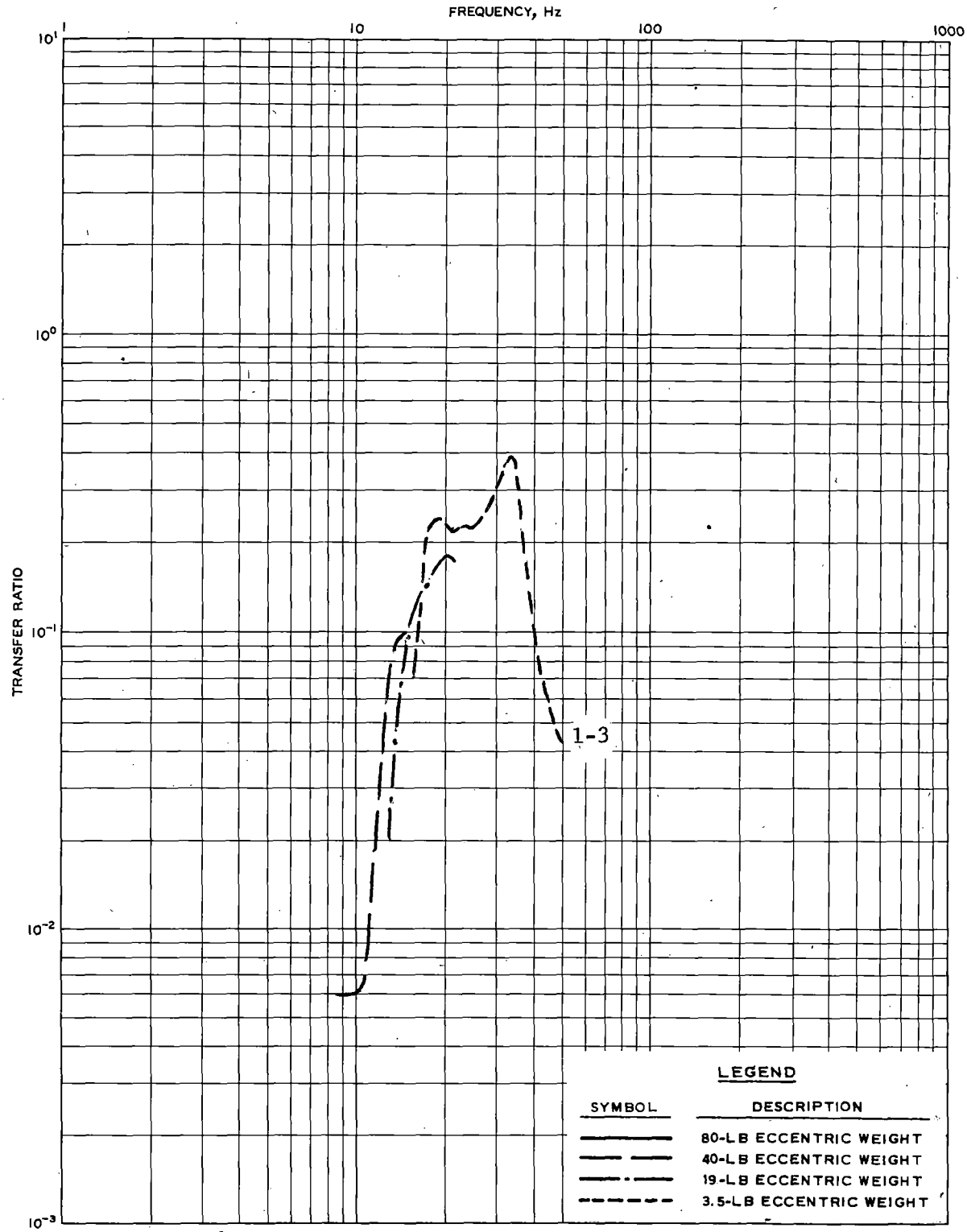

FIGURE 95. POSTTRAFFIC TRANSFER RATIO RESULTS, TRACK SECTION 4, VERTICAL MODE, POINTS 1-3

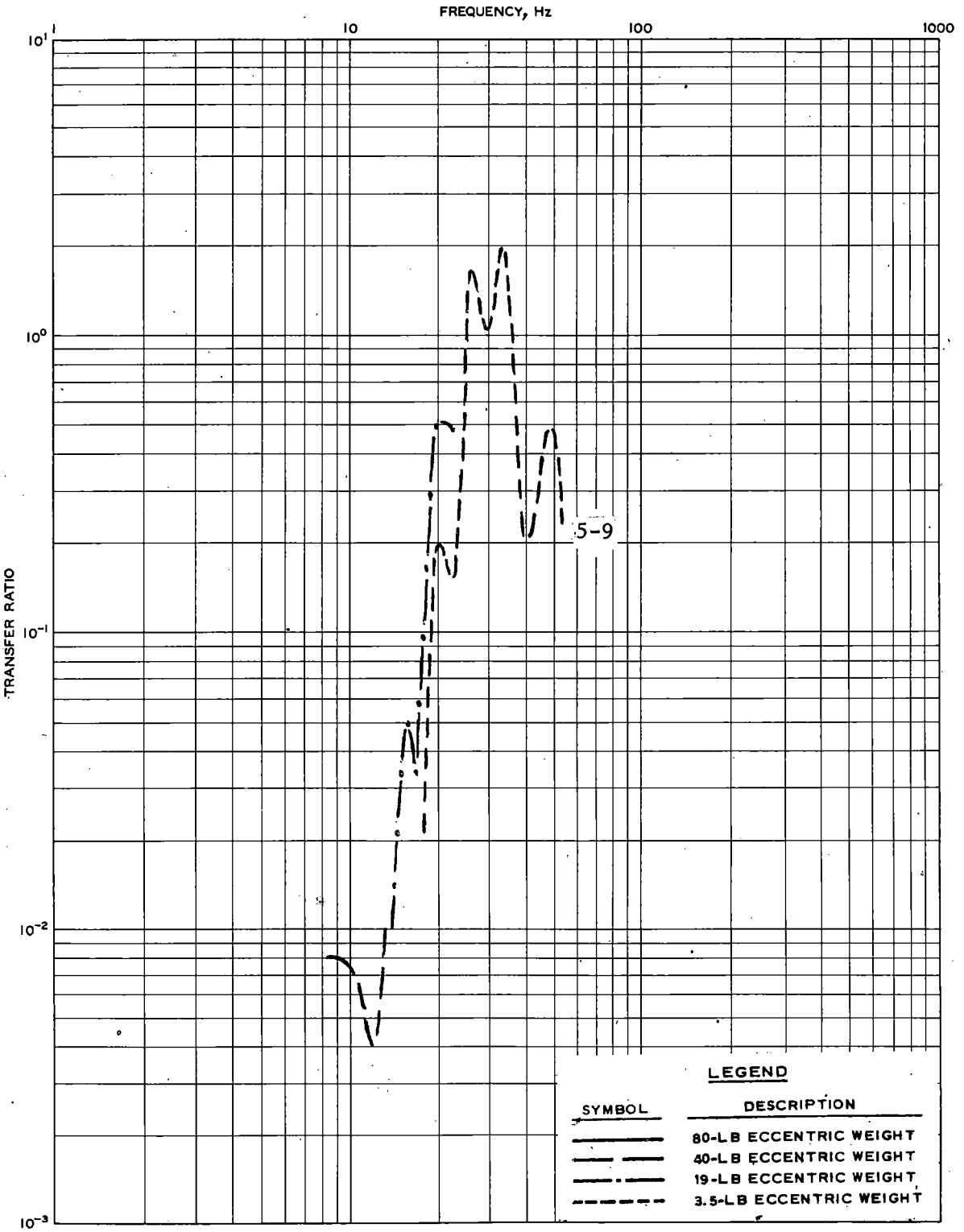

FIGURE 96. POSTTRAFFIC TRANSFER RATIO RESULTS, TRACK SECTION 4, VERTICAL MODE, POINTS 5-9

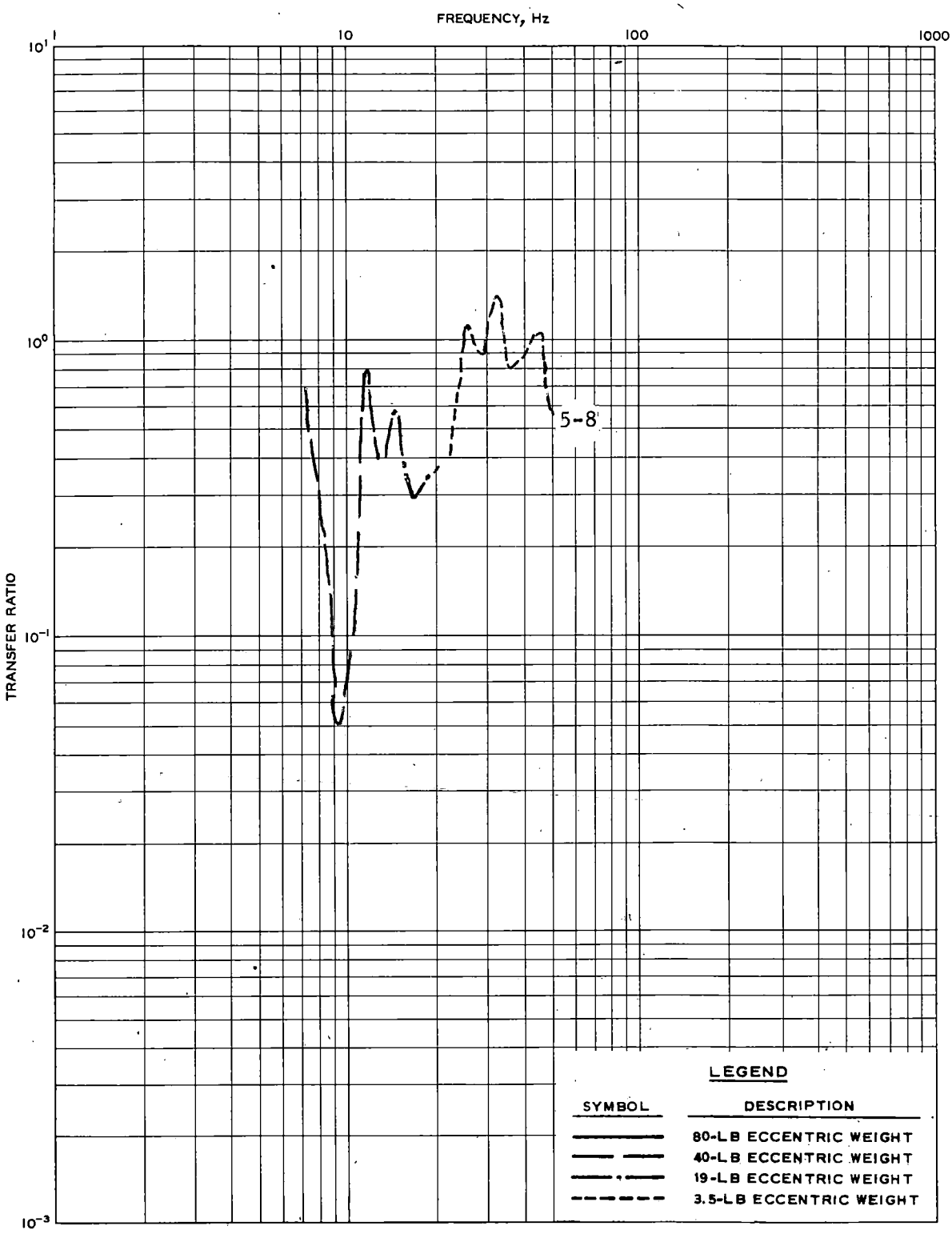

FIGURE 97. POSTTRAFFIC TRANSFER RATIO RESULTS, TRACK SECTION 4, VERTICAL MODE, POINTS 5-8

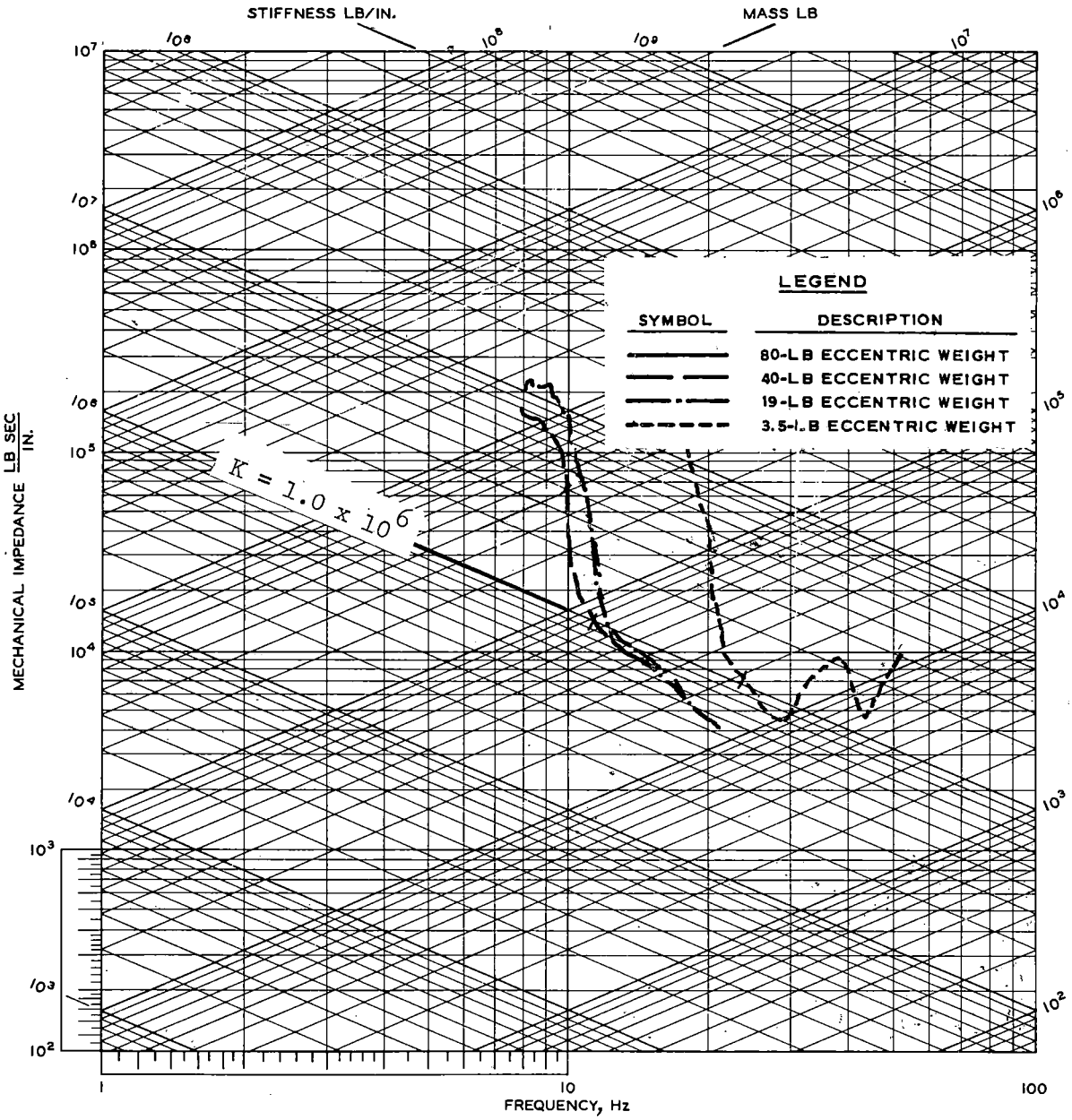

FIGURE 98. POSTTRAFFIC MECHANICAL IMPEDANCE RESULTS, TRACK SECTION 5, VERTICAL MODE, POINT 1

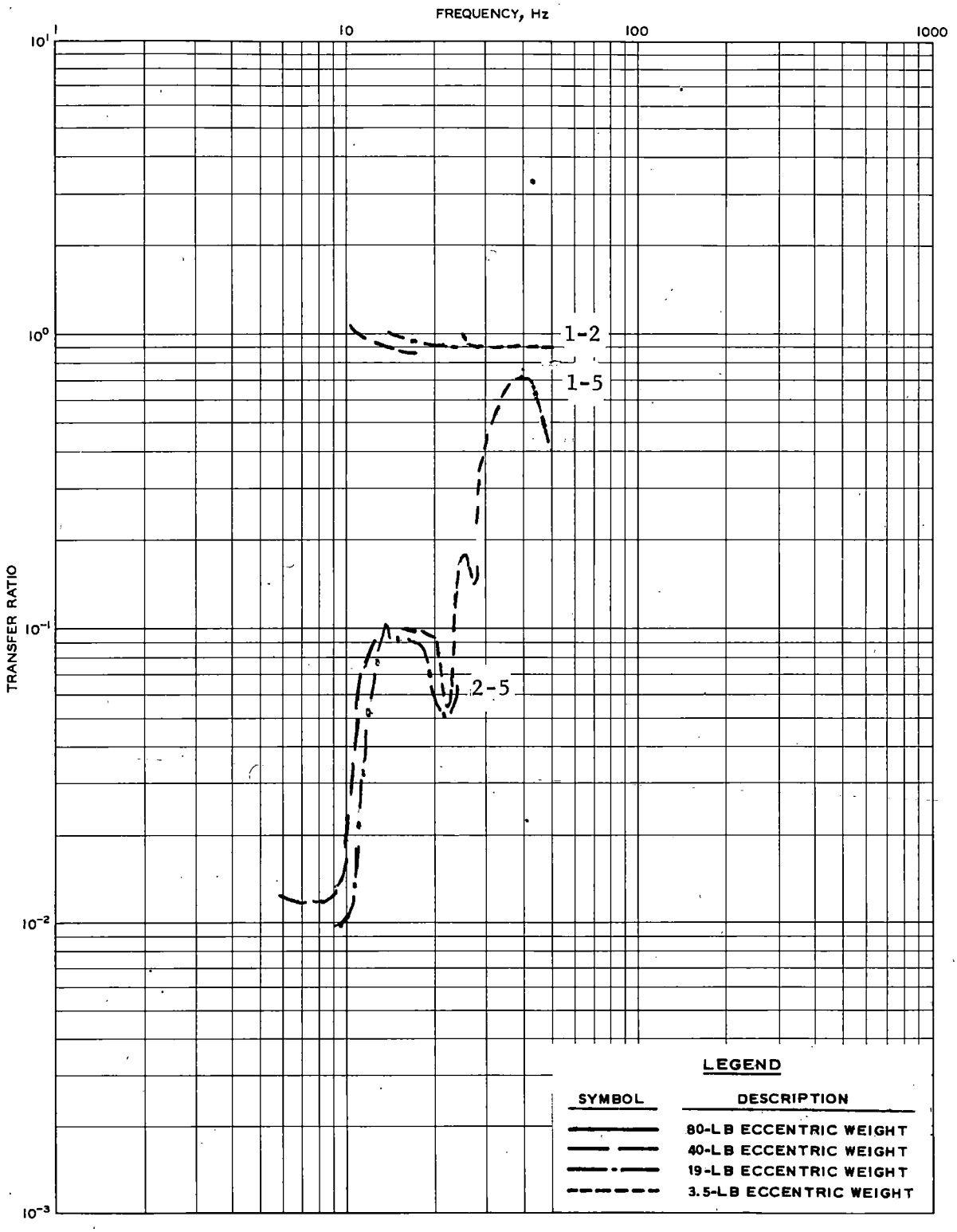

FIGURE 99. POSTTRAFFIC TRANSFER RATIO RESULTS, TRACK SECTION 5, VERTICAL MODE, POINTS 1-2, 1-5, 2-5

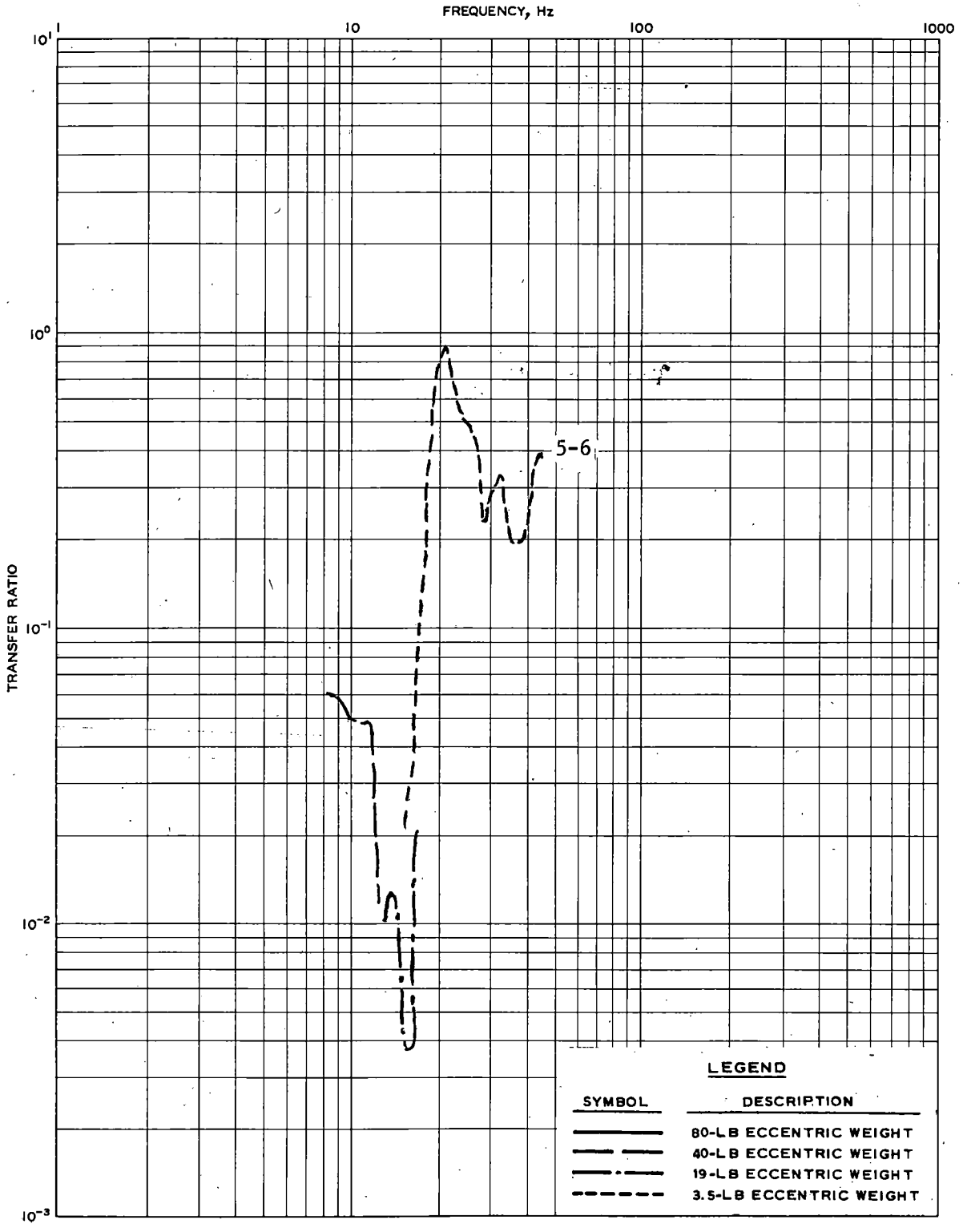

FIGURE 100. POSTTRAFFIC TRANSFER RATIO RESULTS, TRACK SECTION 5, VERTICAL MODE, POINTS 5-6

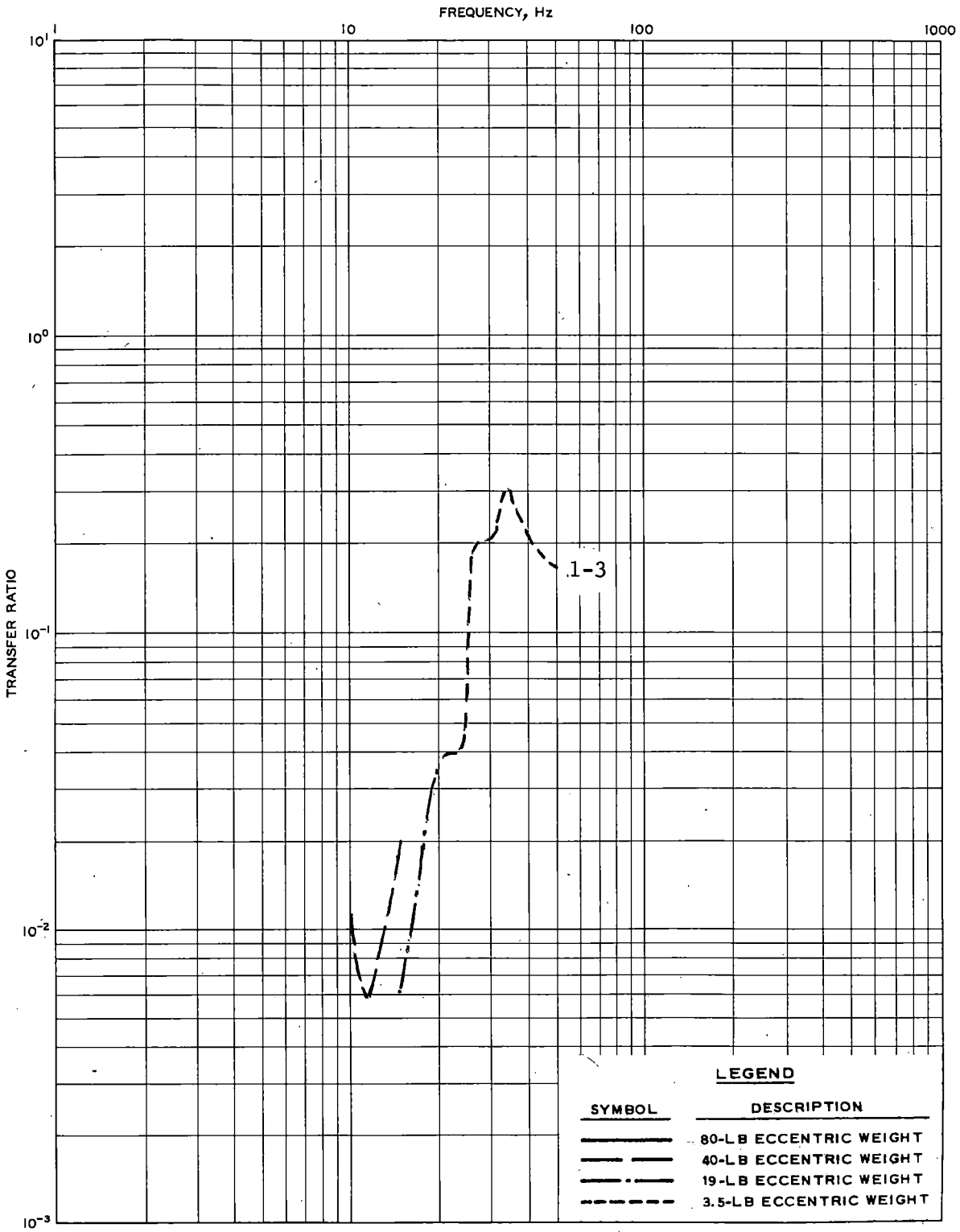

FIGURE 101. POSTTRAFFIC TRANSFER RATIO RESULTS, TRACK SECTION 5, VERTICAL MODE, POINTS 1-3

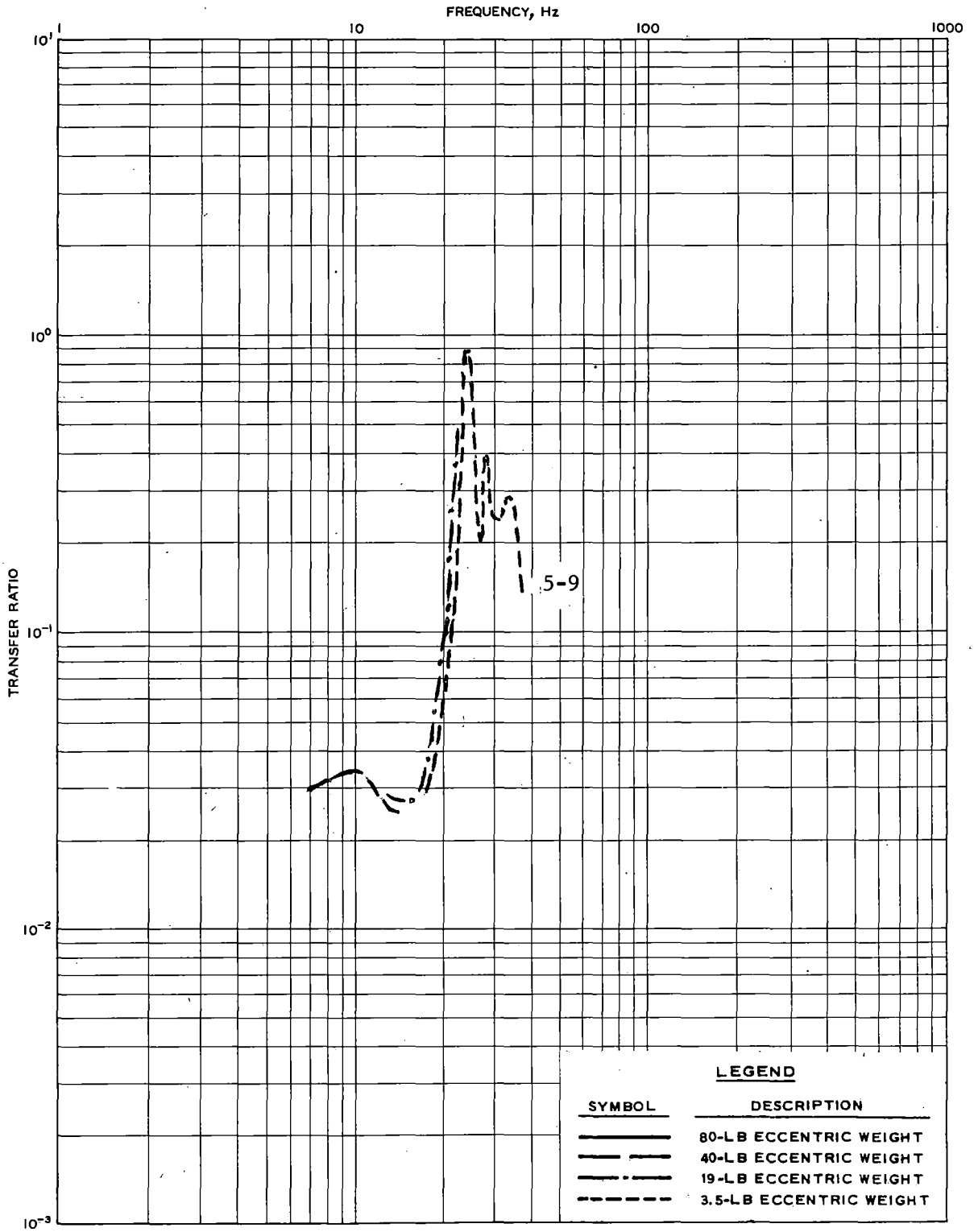

FIGURE 102. POSTTRAFFIC TRANSFER RATIO RESULTS, TRACK SECTION 5, VERTICAL MODE, POINTS 5-9

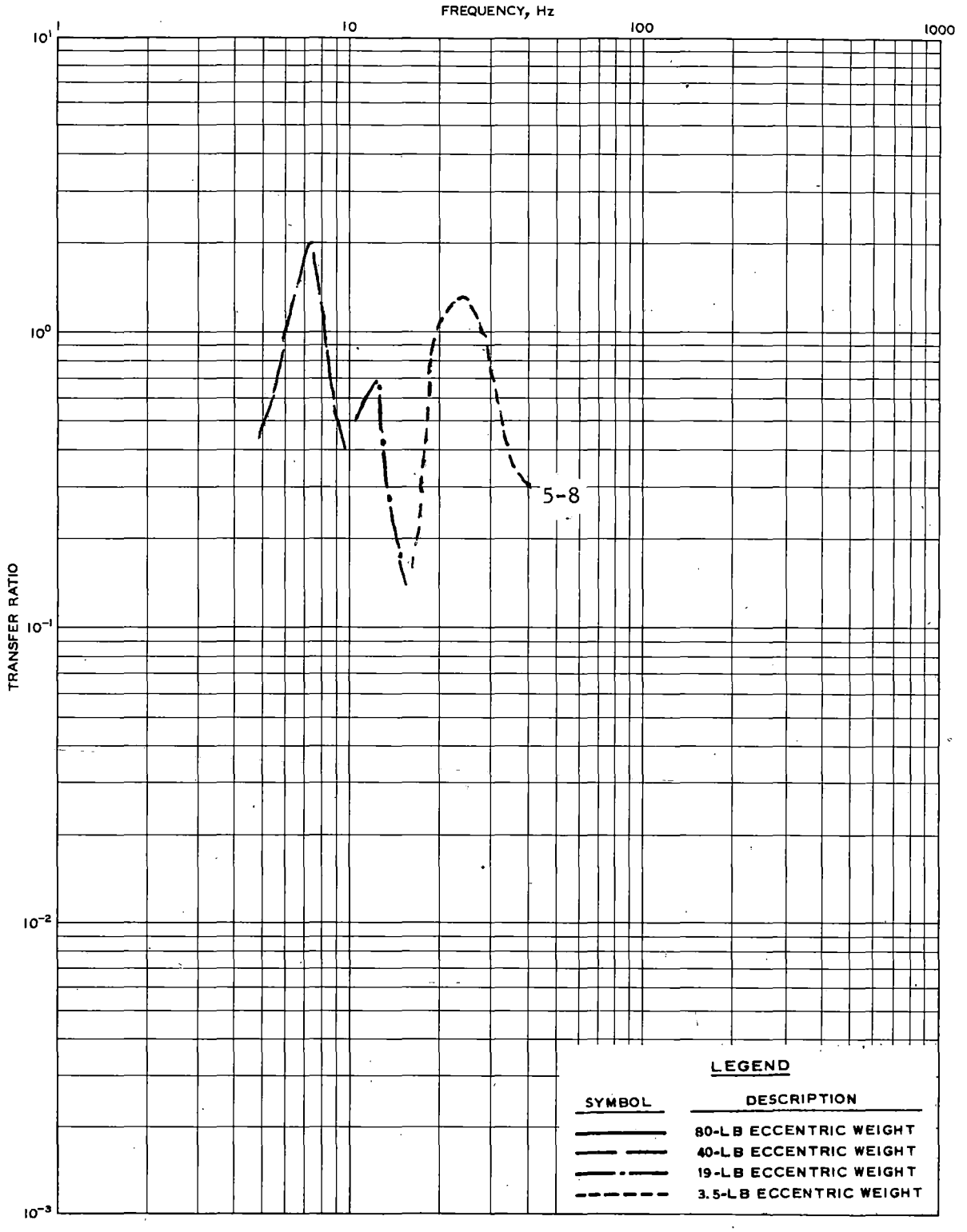

FIGURE 103. POSTTRAFFIC TRANSFER RATIO RESULTS, TRACK SECTION 5, VERTICAL MODE, POINTS 5-8

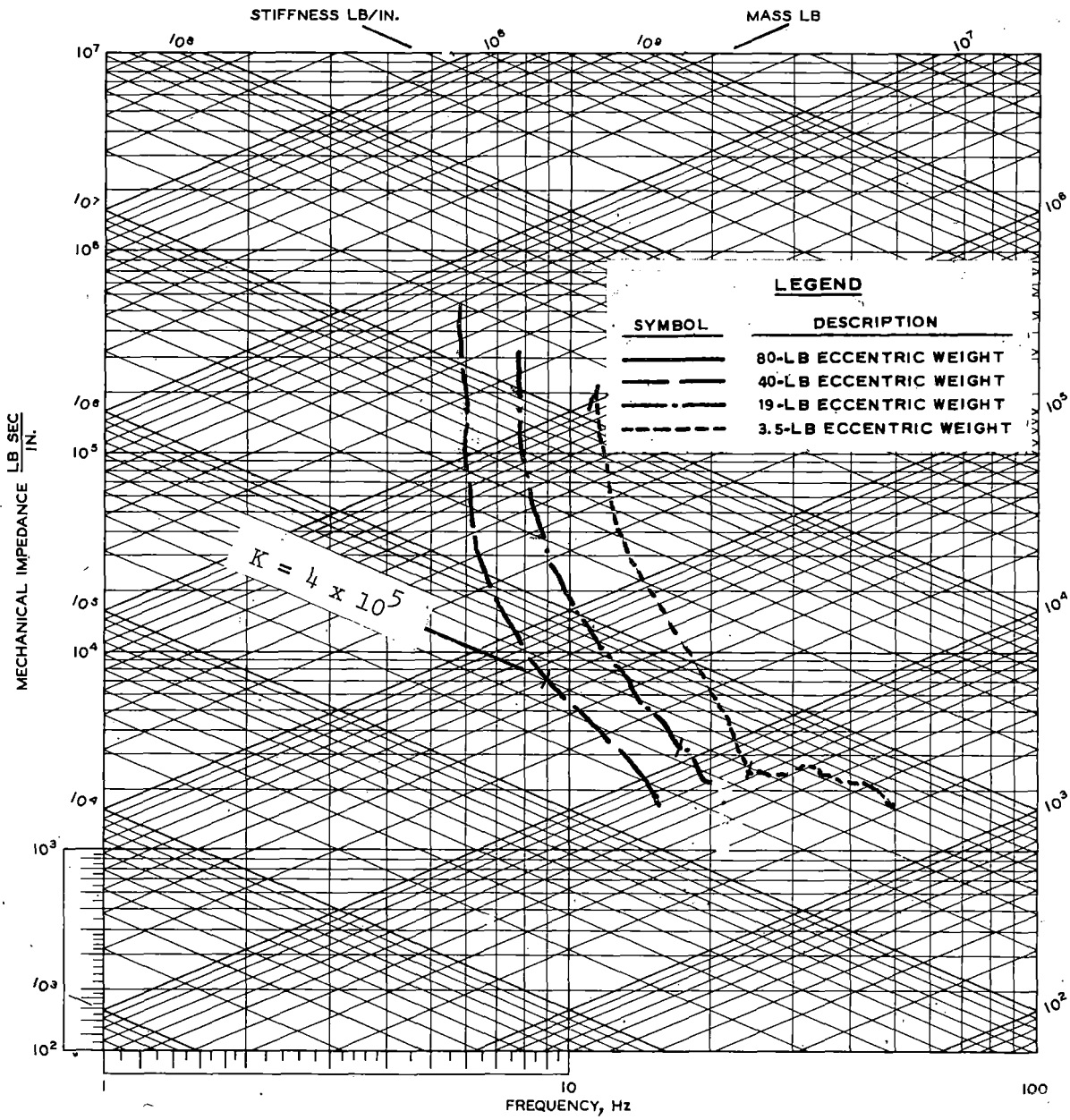

FIGURE 104. POSTTRAFFIC MECHANICAL IMPEDANCE RESULTS, TRACK SECTION 8, VERTICAL MODE, POINT 1

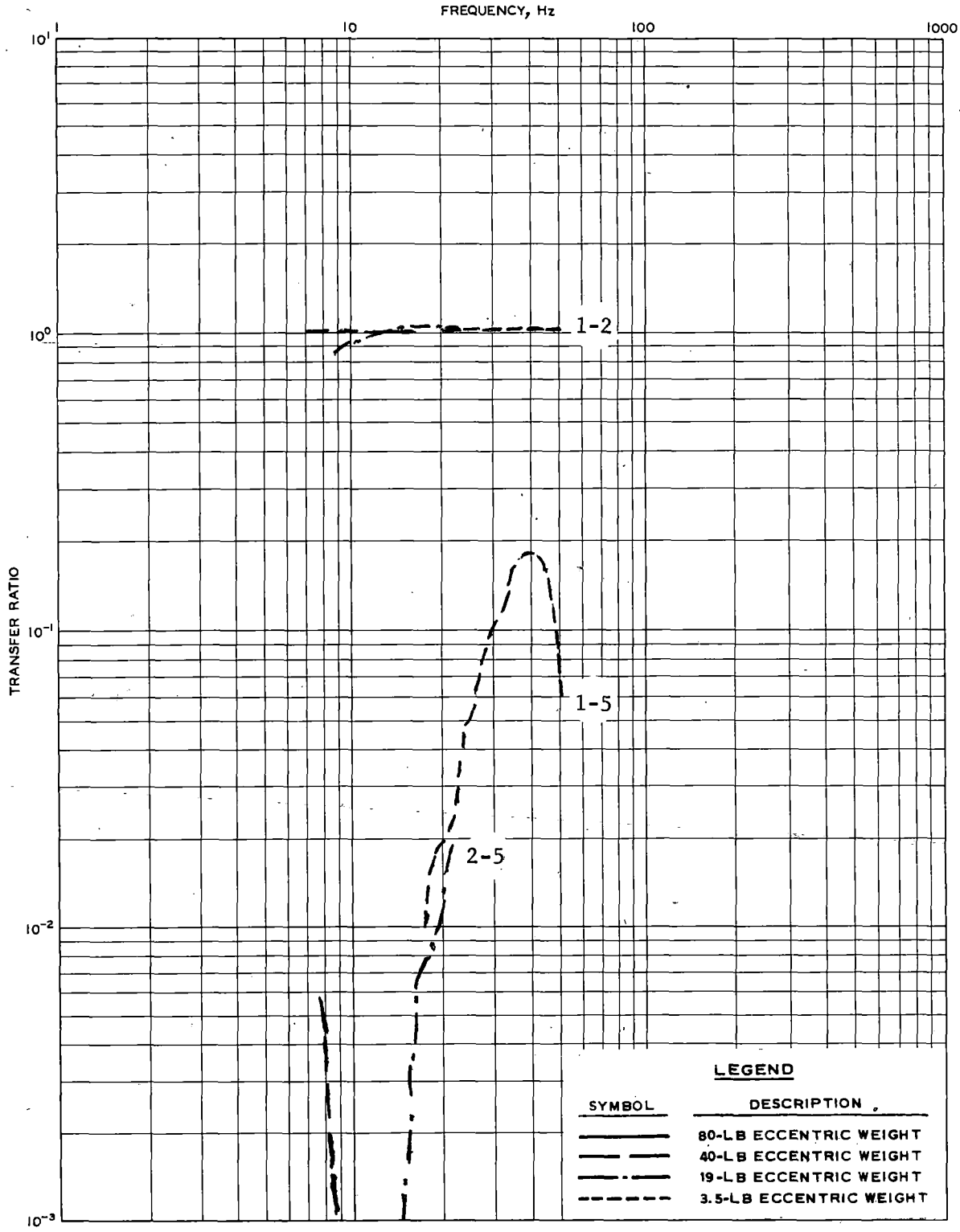

FIGURE 105. POSTTRAFFIC TRANSFER RATIO RESULTS, TRACK SECTION 8, VERTICAL MODE, POINTS 1-2, 1-5, 2-5

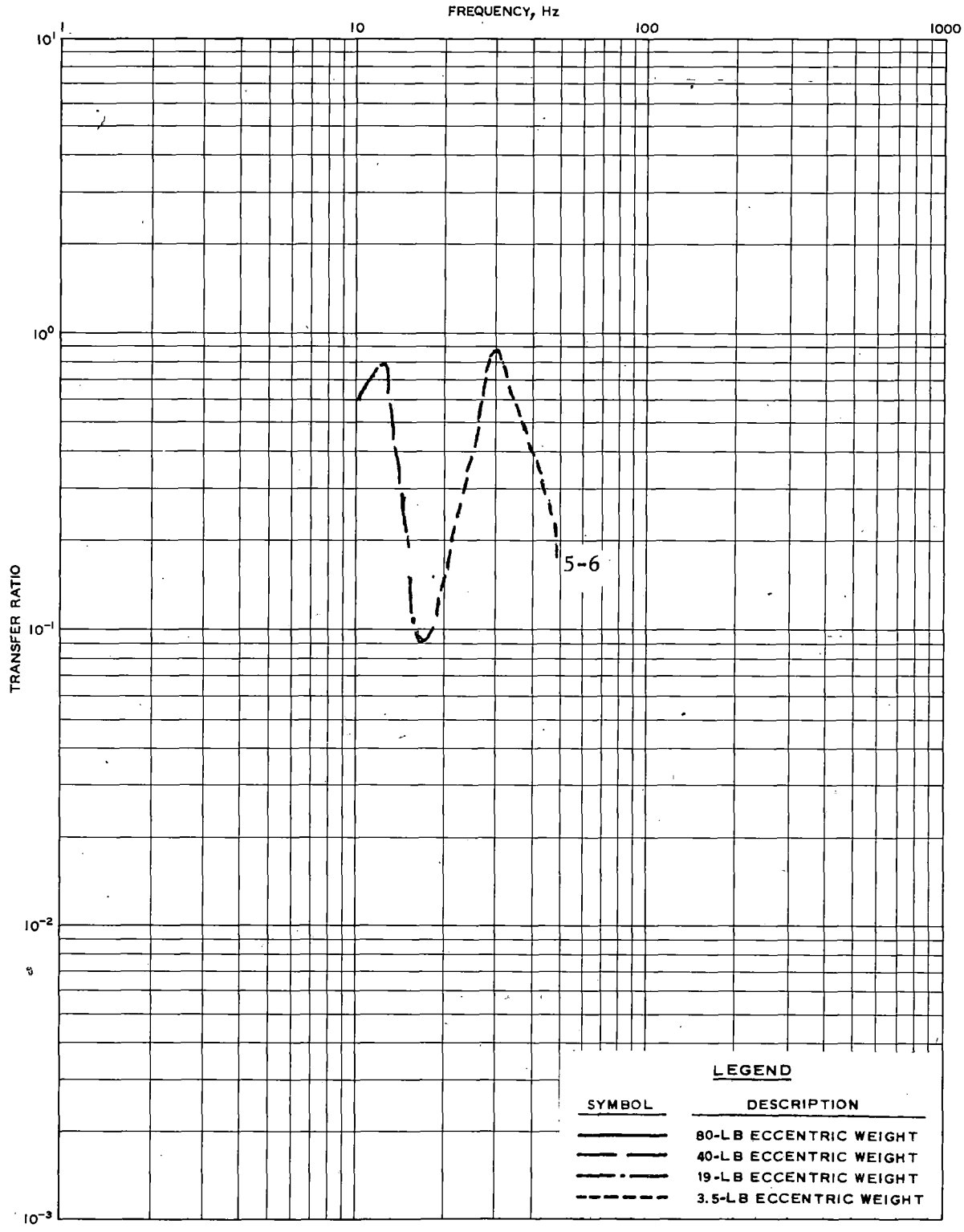

FIGURE 106. POSTTRAFFIC TRANSFER RATIO RESULTS, TRACK SECTION 8, VERTICAL MODE, POINTS 5-6

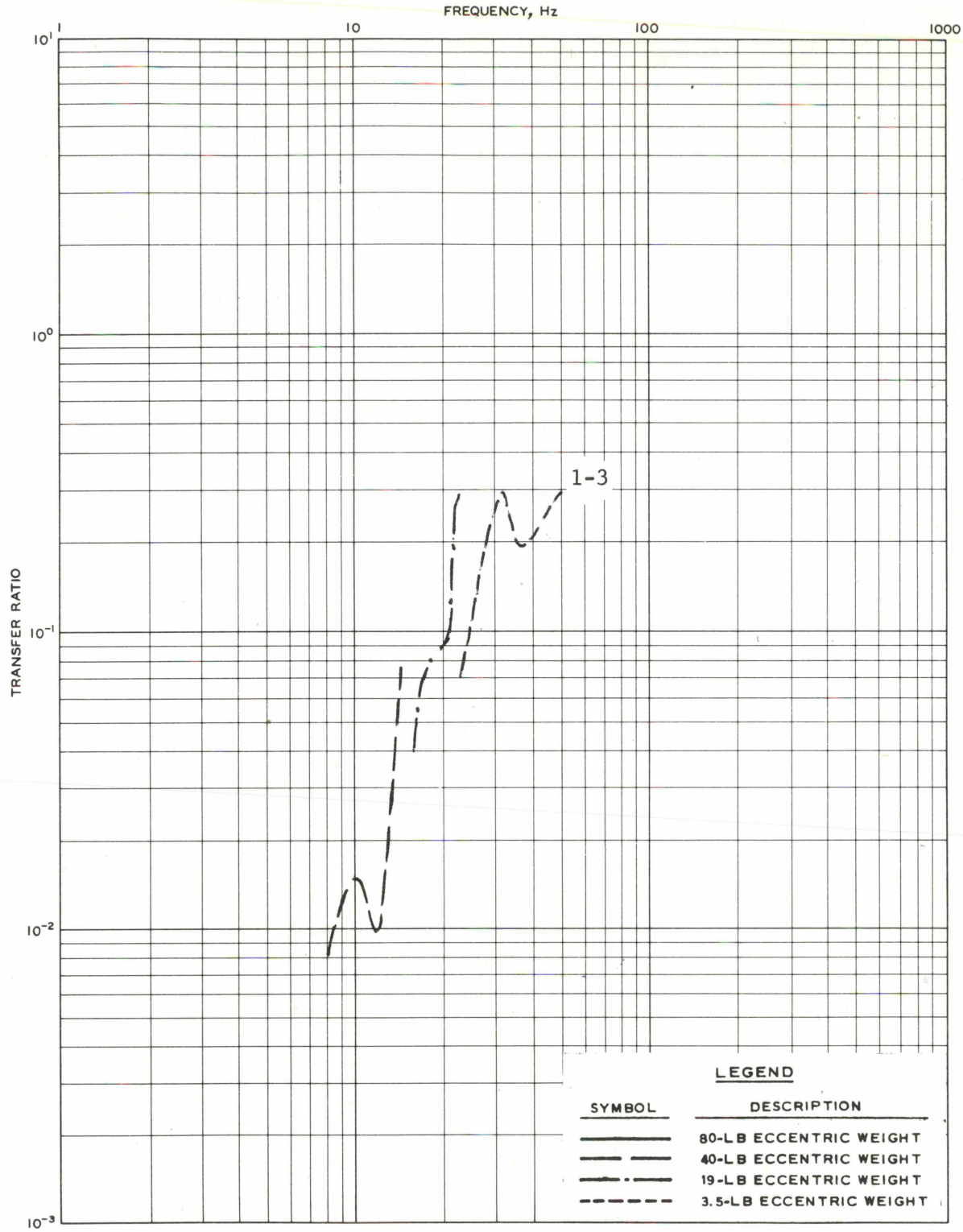

FIGURE 107. POSTTRAFFIC TRANSFER RATIO RESULTS, TRACK SECTION 8, VERTICAL MODE, POINTS 1-3

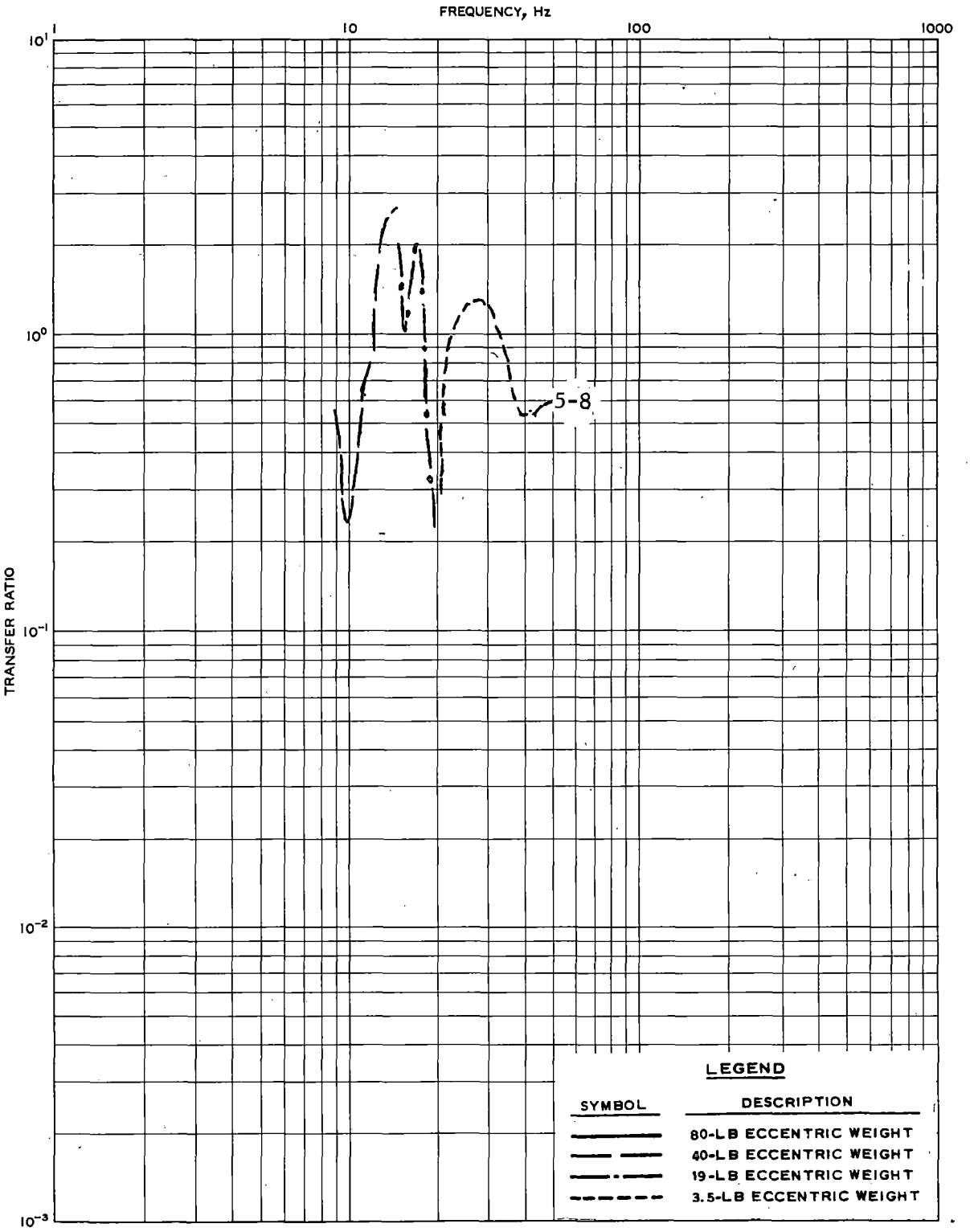

FIGURE 108. POSTTRAFFIC TRANSFER RATIO RESULTS, TRACK SECTION 8, VERTICAL MODE, POINTS 5-8

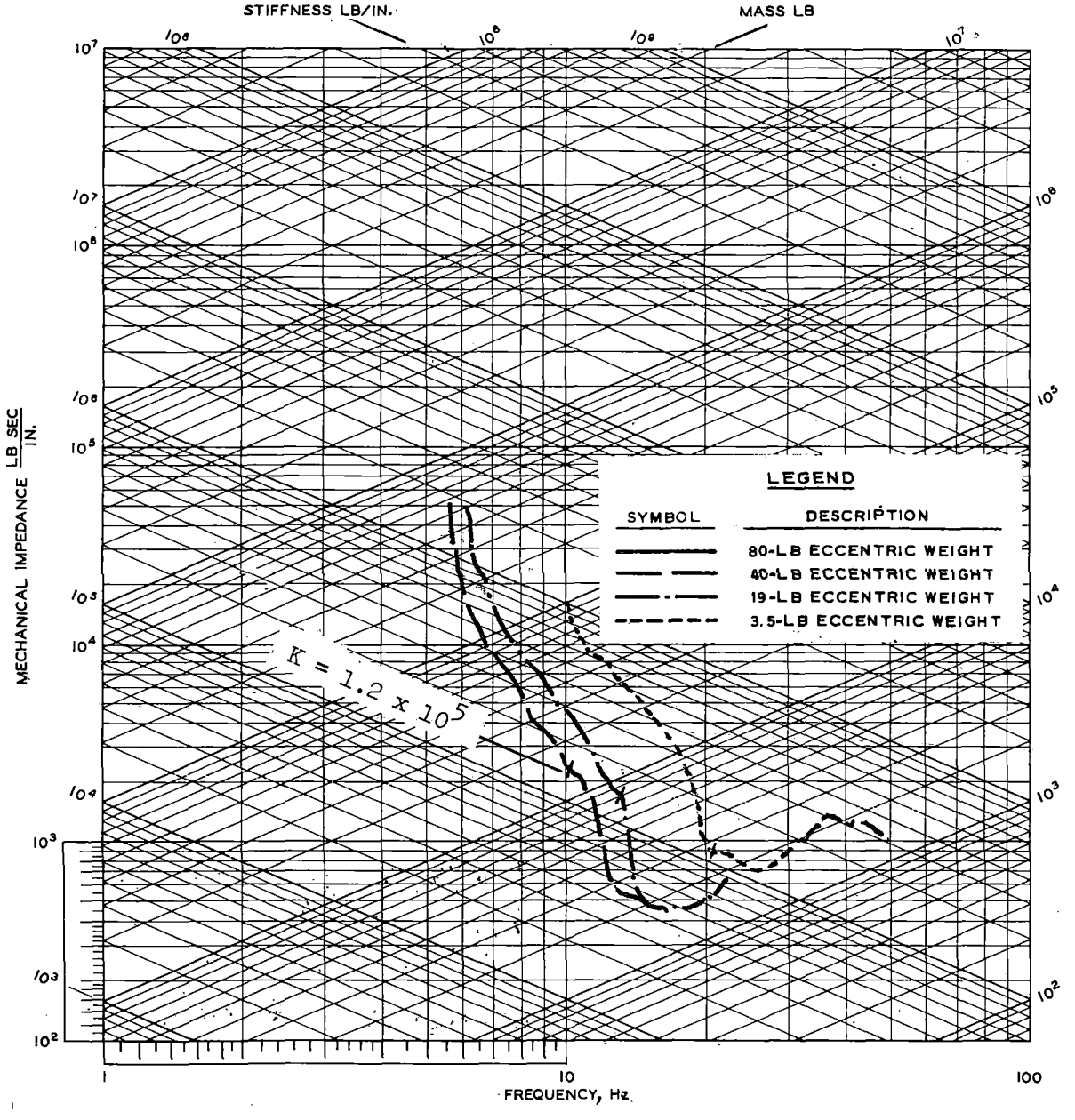

FIGURE 109. POSTTRAFFIC MECHANICAL IMPEDANCE RESULTS, TRACK SECTION 9, VERTICAL MODE, POINT 1

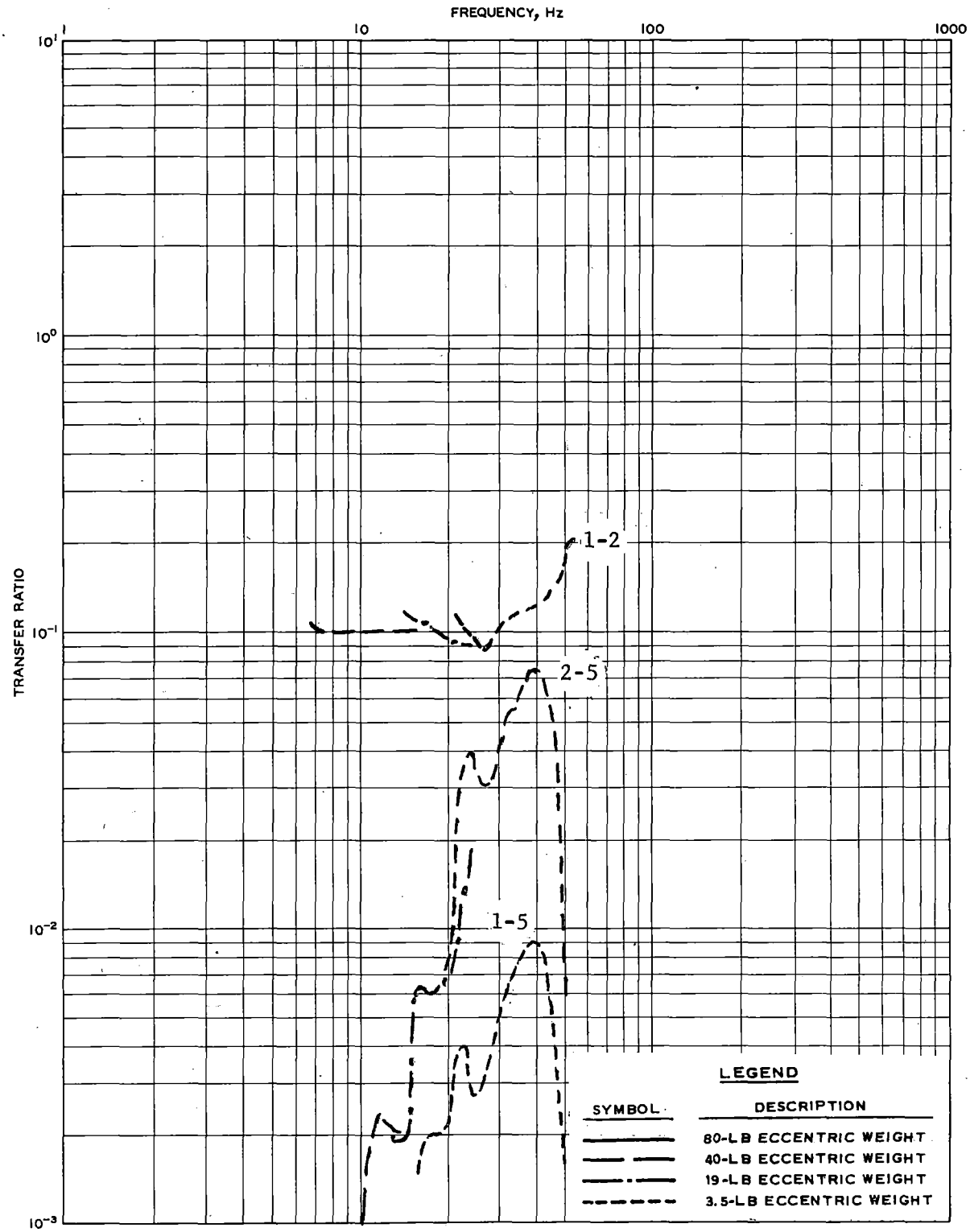

FIGURE 110. POSTTRAFFIC TRANSFER RATIO RESULTS, TRACK SECTION 9, VERTICAL MODE, POINTS 1-2, 1-5, 2-5

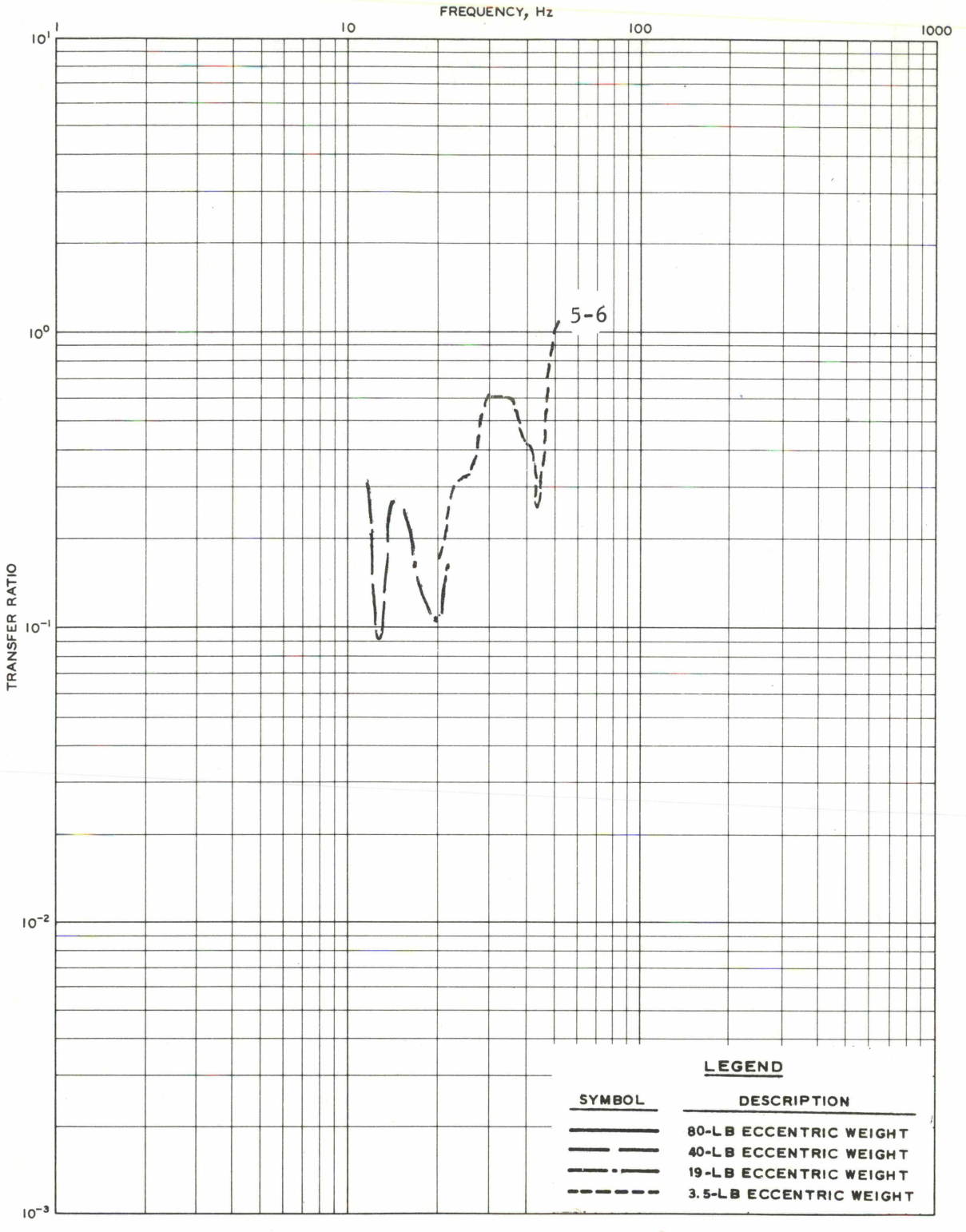

FIGURE 111. POSTTRAFFIC TRANSFER RATIO RESULTS, TRACK SECTION 9, VERTICAL MODE, POINTS 5-6

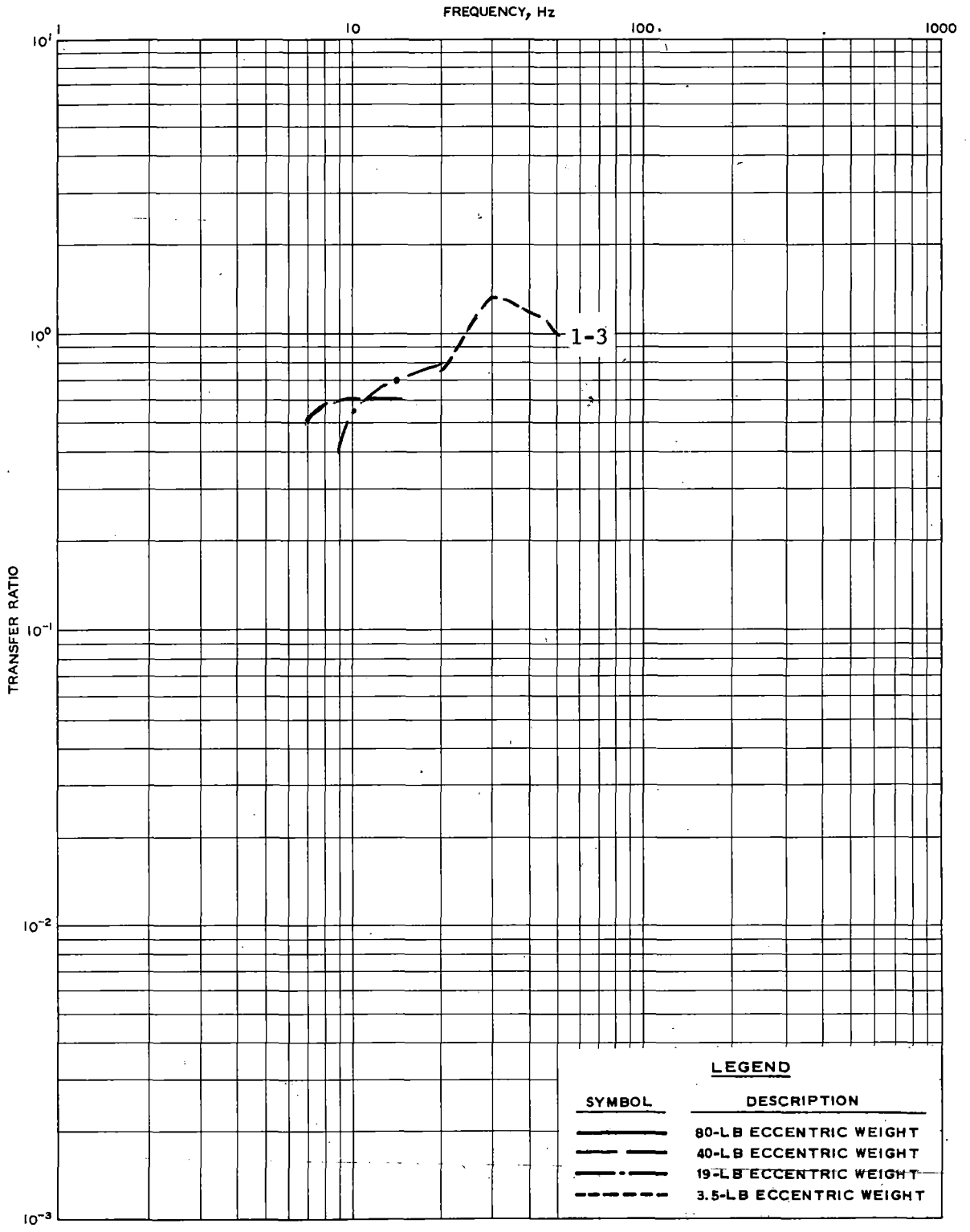

FIGURE 112. POSTTRAFFIC TRANSFER RATIO RESULTS, TRACK SECTION 9, VERTICAL MODE, POINTS 1-3

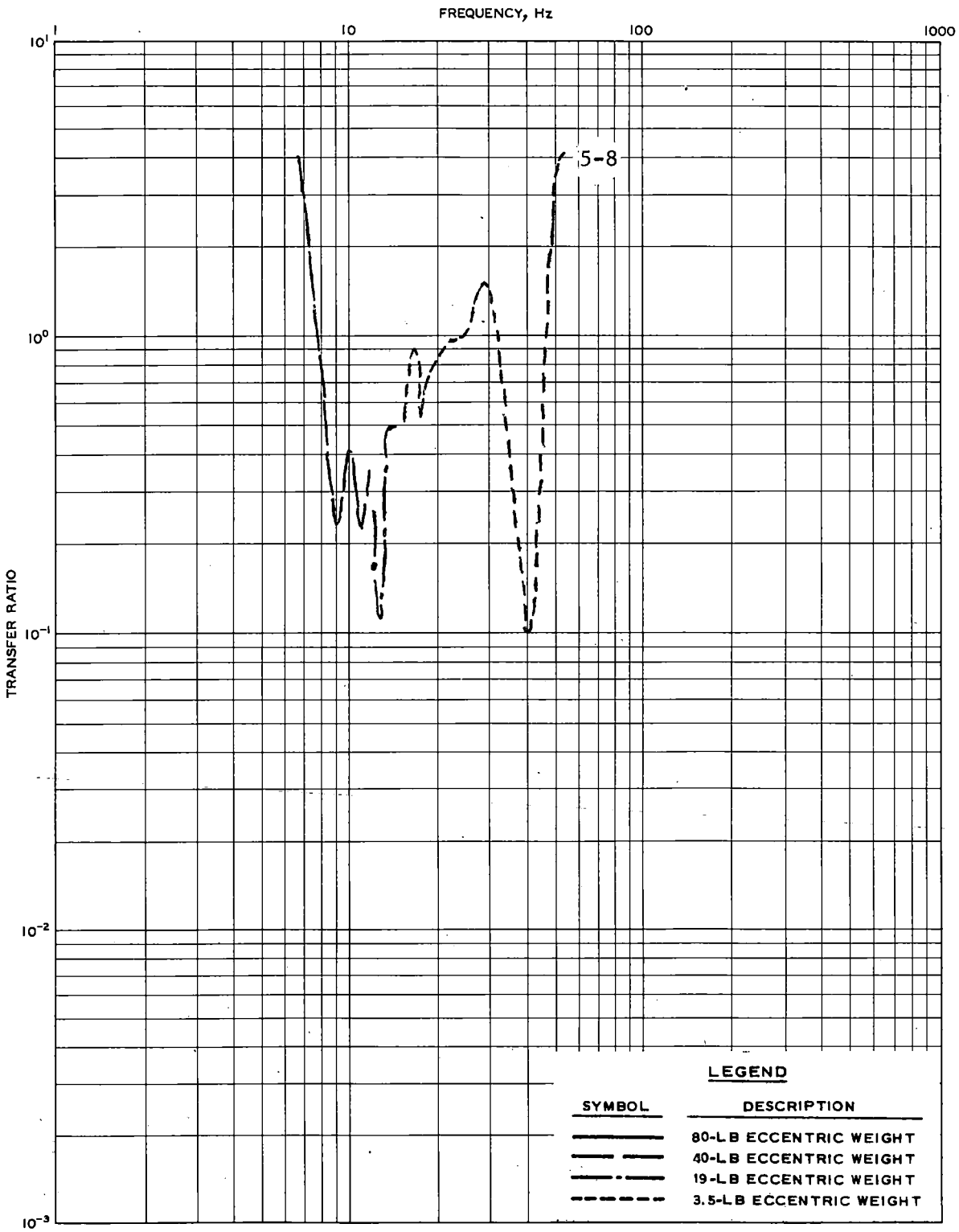

FIGURE 113. POSTTRAFFIC TRANSFER RATIO RESULTS, TRACK SECTION 9, VERTICAL MODE, POINTS 5-8

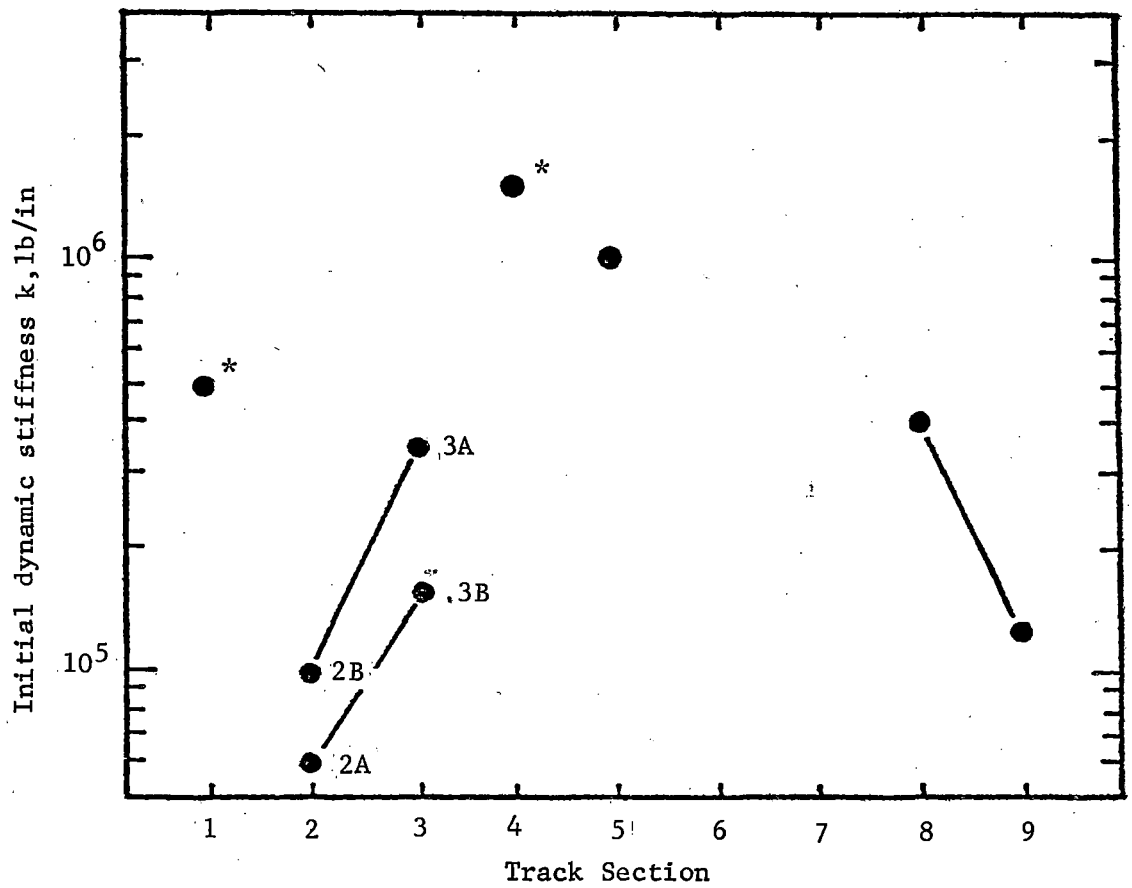

*Not considered to be representative of performance under traffic

FIGURE 114. INITIAL DYNAMIC STIFFNESS RESULTS FROM POSTTRAFFIC TESTING

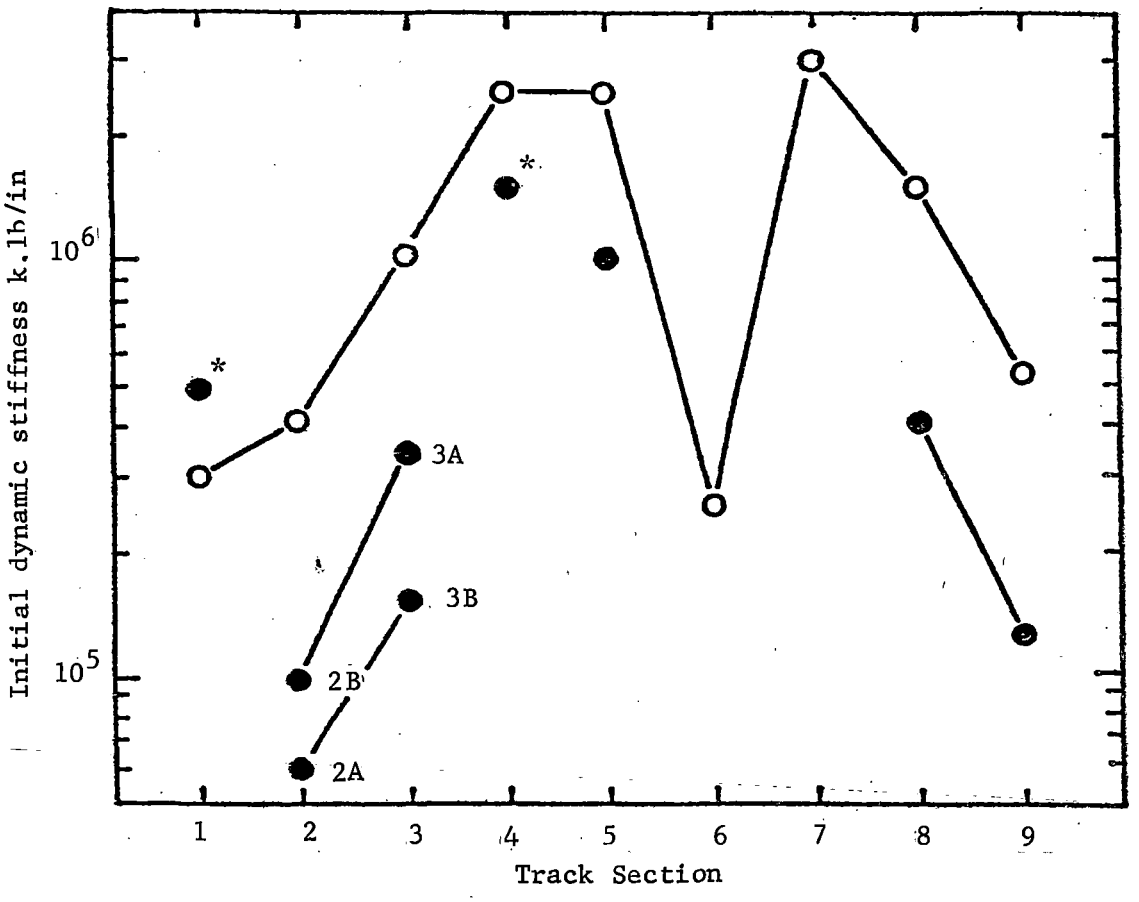

○ Pretraffic results (1973)

● Posttraffic results (1975)

* Not considered to be representative of performance under traffic

FIGURE 115. COMPARISON OF PRETRAFFIC AND POSTTRAFFIC INITIAL DYNAMIC STIFFNESS RESULTS

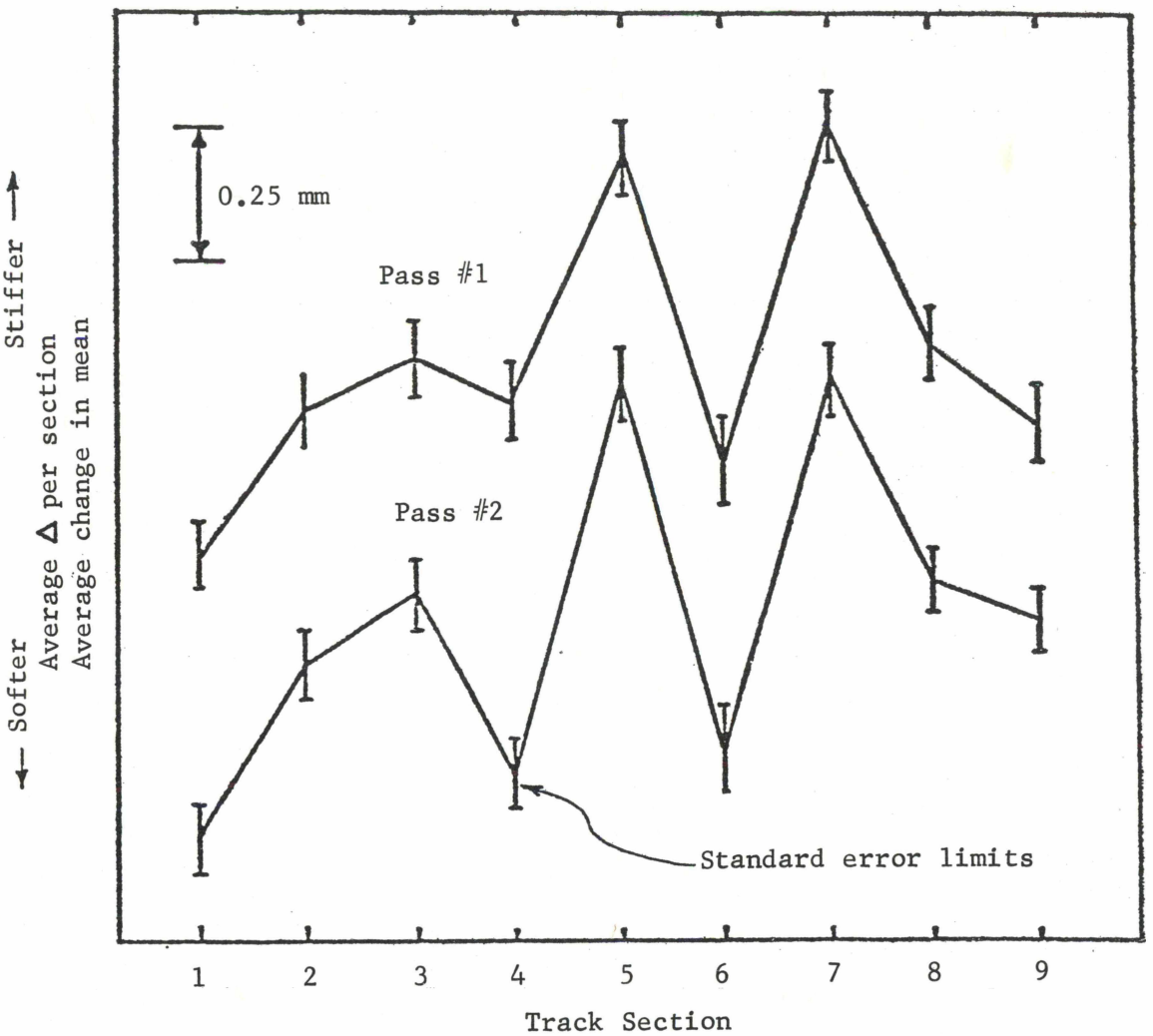

FIGURE 116. RELATIVE STIFFNESS RESULTS OF ENSCO TESTS CONDUCTED IN DEC 1974 *

* Reprinted, with permission, from IEEE INDUSTRY APPLICATIONS SOCIETY TENTH ANNUAL MEETING CONFERENCE RECORD (Reference 10).

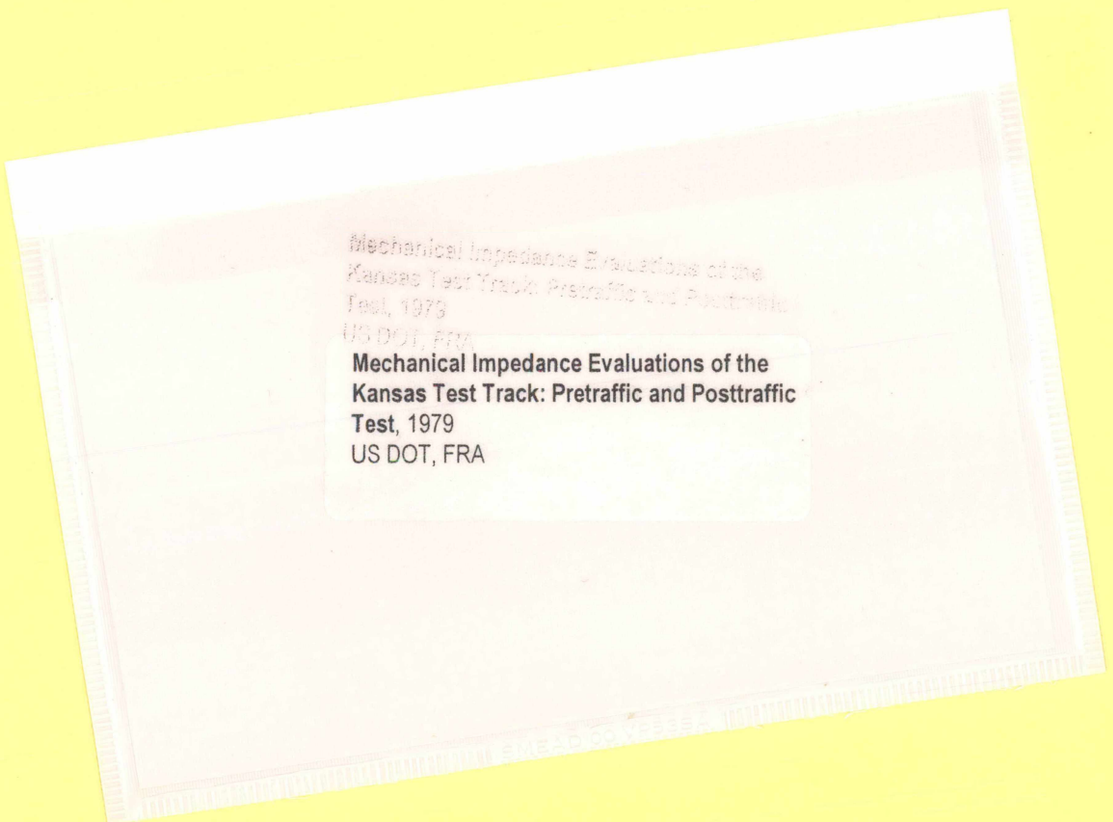
Mechanical Impedance Evaluations of the
Kansas Test Track: Pretraffic and Posttraffic
Test, 1979
US DOT, FRA